The Role of Gli3 in the Developing Mouse Forebrain

By

Tian Yu

Thesis submitted for the degree of doctor of philosophy at the University of Edinburgh

2007

DISCLAIMER

I (Tian Yu) performed all of the experiments presented in this thesis unless otherwise clearly stated in the text. No part of this work has been or is being submitted for any other degree or qualification.

Signed:

Date:

ACKNOWLEDGEMENTS

I would like to thank my supervisors David Price, John Mason, Vassiliki Fotaki and Paulette Zaki for their endless help and advice throughout the course of this study. The Gli3 team member Vassiliki and Paulette, have been perfect in guiding, supporting and taking care of me. My dear grannies, you surely deserve a big piece of this.

I am also grateful to Katy Gillies and Tom Pratt for making the lab work smooth and easy, Ben Martynoga for providing *Foxg1*$^{-/-}$ mutant embryos and sharing precious antibodies, Catherine Carr for supplying *Pax6*$^{Sey/Sey}$ mutant embryos, Natasha Tian for her support, especially during our writing up period (and good luck for your thesis!), Ian Simpson, Jane Quinn, Martine Manuel, Petrina Georgala, Shariza Nordin and Vlad Ivaniutsin for offering their time and help.

I would also like to thank Linda Wilson, Angela McDonald and Trudi Gillespie for their helping with confocal imaging, Laura Lettice for providing *Shh*$^{-/-}$ mutant embryos, Martin Collinson for sharing the Shh immuno protocol.

And finally, my biggest thanks will go to my Dad and Mum for giving me this chance to come to Edinburgh and offering me endless love and support over these years. I love you very very much. I would also like to thank all the other people in my big family, especially my grandparents. Without trips back home and a constant supply of food and medicine, this piece of work would never have been produced.

我是一只幽谷里的夜蝶;
在草丛间成形，在黑暗里飞行，
我献致我翅羽上美丽的金粉，
我爱恋万万里外闪亮的明星——
沙扬那拉！

我是一只酣醉了的花蜂;
我饱啜了芬芳，我不讳我的猖狂。
如今，在归途上嘤嗡着我的小嗓，
想赞美那别样的花酿，我曾经恣尝——
沙扬那拉！

最是那一低头的温柔，
像一朵水莲花不胜凉风的娇羞，
道一声珍重，道一声珍重，
那一声珍重里有蜜甜的忧愁——
沙扬那拉！

徐志摩

TABLE OF CONTENTS

ABBREVIATIONS

AP--Anterior to Posterior

ANR--Anterior neural ridge

BMP--Bone morphogenetic proteins

BrdU--Bromodeoxyuridine

CNS--Central Nervous System

CPe-- choroid plexus epithelium

C-terminal--Carboxy-terminal

Dhh--Desert hedgehog

DNA--Deoxyribonucleic acid

DV--Dorsal to Ventral

E--Embryonic day

EmT--eminentia thalami

Fgf--Fibroblast growth factor

GE--ganglionic eminences

Gli3-C--cleaved Gli3 isoform

Gli3-F--full length Gli3 isoform

Hh--Hedgehog

IddU--Iododeoxyuridine

Ihh--Indian hedgehog

LGE--lateral ganglionic eminence

MGE--medial ganglionic eminence

mRNA--messenger RNA

N-terminal--Amino-terminal

OPT--optical projection tomography

O.D.--optical density

PCR--polymerase chain reaction

PSB--pallial-subpallial boundary

Ptc1--Patched1

RA--Retinoic acid

RNA--Ribonucleic acid

Sey--Small eye

Shh--Sonic hedgehog

Smo--Smoothened

TUNEL--terminal deoxynucleotidyl transferase (TDT)-mediated dUTP-biotin nick end labelling

Wnt--Wingless-type MMTV integration site

Wt--wild types

Xt--extra-toes

ZLI--zona limitans intrathalamica

ABSTRACT

The mammalian forebrain, which consists of the telencephalon and the diencephalon, is responsible for many higher cognitive functions such as thinking, learning and memory. The cerebral cortex, which is important for language and processing information, is located in the dorsal portion of the telencephalon. The basal ganglia, which are important for movement, are located in the ventral telencephalon. Many genes are involved in patterning and the development of the forebrain. One gene that appears to be crucial for forebrain development is *Gli3*. Gli3 has been shown to work as both a transcriptional activator and a repressor of the Sonic Hedgehog (Shh) signalling pathway in the developing spinal cord and limb buds. In the telencephalon, Shh has been shown to be important for induction of ventral cell fate, but the exact function of Gli3 in the forebrain and the interactions between Gli3 and Shh are still obscure.

Previous studies have shown that Gli3 is required for the formation of the cortical hem area of the telencephalon, which does not form in $Gli3^{Xt/Xt}$ mutant mice lacking functional Gli3. The residual dorsal telencephalon of the $Gli3^{Xt/Xt}$ mutants is partially 'ventralized'.

The main aim of this study was to re-examine the developing forebrain of $Gli3^{Xt/Xt}$ mouse mutants to gain insight into the function of Gli3 during forebrain development.

In this thesis, the expression of Gli3 mRNA and protein was examined in the E12.5 and E14.5 wild type telencephalon. The ^{high}dorsal-to-^{low}ventral expression pattern of Gli3 corresponds to ^{severe}dorsal-to-^{mild}ventral defects observed in the $Gli3^{Xt/Xt}$ mutants. The ratios between the levels of the cleaved and full length isoforms of Gli3 in dorsal

and ventral telencephalon resemble those described in dorsal and ventral spinal cord and in the anterior and posterior limb bud, respectively, suggesting Gli3 in the dorsal telencephalon may act as a repressor of the Shh signalling pathway. The total amount and the ratios of the two isoforms of Gli3 protein were examined in Shh and Foxg1 null mice, which lack ventral telencephalon. The results obtained agree with a role of Gli3 as a repressor of the Shh pathway in the dorsal telencephalon.

The forebrains of *Gli3*$^{Xt/Xt}$ mutants were analysed systematically both anatomically and by molecular markers in this thesis. The border between the telencephalon and the diencephalon was delineated in the *Gli3*$^{Xt/Xt}$ mutants by using a combination of markers expressed in different areas within the forebrain. This lead to the observation that the previously reported 'ventralization' only occurred in the very rostral telencephalic sections of the *Gli3*$^{Xt/Xt}$ mutant embryos, suggesting a possible shape change of the *Gli3*$^{Xt/Xt}$ telencephalon. To examine the possible causes of the significant size reduction of *Gli3*$^{Xt/Xt}$ mutant telencephalon compared to wild type telencephalon from E10.5, cell proliferation and cell death properties studies were undertaken. The changes observed were not sufficient to explain the phenotypic differences between the *Gli3*$^{Xt/Xt}$ mutant and the wild type embryos indicating that they might be the result of an early patterning defect.

The dorsal telencephalon is severely reduced in volume at both E12.5 and E10.5, containing cells from adjacent eminentia thalami, probably due to the loss of the dorso-medial telencephalon. Large clusters of eminentia thalami cells were observed at later developmental stages, when the neocortex becomes highly disorganized, forming rosettes comprising mainly neural progenitors. These results suggest Gli3 is important for the formation of an intact telencephalic-diencephalic boundary and for preventing the abnormal location of diencephalic cells in the dorsal telencephalon.

The volume of *Gli3*$^{Xt/Xt}$ ventral telencephalon was increased compared to that of the wild types at E10.5, but became smaller than that of the wild type littermates at E12.5. This might have been the result of a combination of more cells exiting the cell cycle and increased cell death observed in the *Gli3*$^{Xt/Xt}$ ventral telencephalon at E10.5, suggesting Gli3 regulates cell differentiation and cell death properties at this age and brain region. The significant expansion of rostro-ventral telencephalon observed in the *Gli3*$^{Xt/Xt}$ mutant might correlate with the expansion of *Fgf8* expression and this hypothesis has been tested in this thesis.

Chapter 1: Introduction

1.1 THE PATTERNING OF THE MAMMALIAN FOREBRAIN

The forebrain, which consists of the telencephalon and the diencephalon, is important for learning, memory and movement. The mammalian telencephalon, which contains the cerebral cortex (including the hippocampus and the neocortex), basal ganglia and olfactory bulbs, is the largest, most complex part of the central nervous system (CNS). Telencephalic function is dependent on its connections with other neural structures including the thalamus, hypothalamus, olfactory epithelium, etc. Together, these structures are essential for transmission of sensory information, integration of new sensory information with established memories, and then formulating and effecting behavioural responses (Bear et al., 2001). The telencephalon is derived from the anterior margin of the neural plate, which is known as the anterior neural ridge (ANR) (Rubenstein et al., 1998; Varga et al., 1999; Tomioka et al., 2000; Whitlock and Westerfield, 2000). During development, different parts of the telencephalon express different sets of genes that instruct the development of each area in a region-specific manner, and control processes including cell proliferation, cell fate determination and migration. The mechanisms that drive regional patterning become more and more complex as the telencephalon develops, but their origins can be traced back to interactions between the embryonic germ layers and between the embryo and the extra-embryonic tissue before the closure of the neural tube (Sasai and De Robertis, 1997).

1.1.1 Mouse early embryogenesis

During the period of early embryogenesis, cells proliferate rapidly from the one cell stage, and form the blastocyst (Fig. 1.1A-D). The blastocyst consists of the inner cell

mass, which gives rise to the extraembryonic structures and the embryo, and the trophectoderm, which becomes the placenta and the extraembryonic membrane. The blastocyst continues to form the three primary germ layers of the embryo, the endoderm, mesoderm and ectoderm (Fig. 1.1G-I). The endoderm gives rise to the inner organs. The mesoderm forms the mesenchyme, the notochord and muscles. The ectoderm forms the spinal cord and the outer epithelium of the body and the neural tube, which later forms the forebrain (telencephalon and diencephalon), midbrain (mesencephalon) and hindbrain (rhombencephalon). The telencephalon arises from the most rostral part of the neural tube, and gives rise to the adult neocortex, hippocampus, olfactory bulbs and basal ganglia (Fig. 1.2).

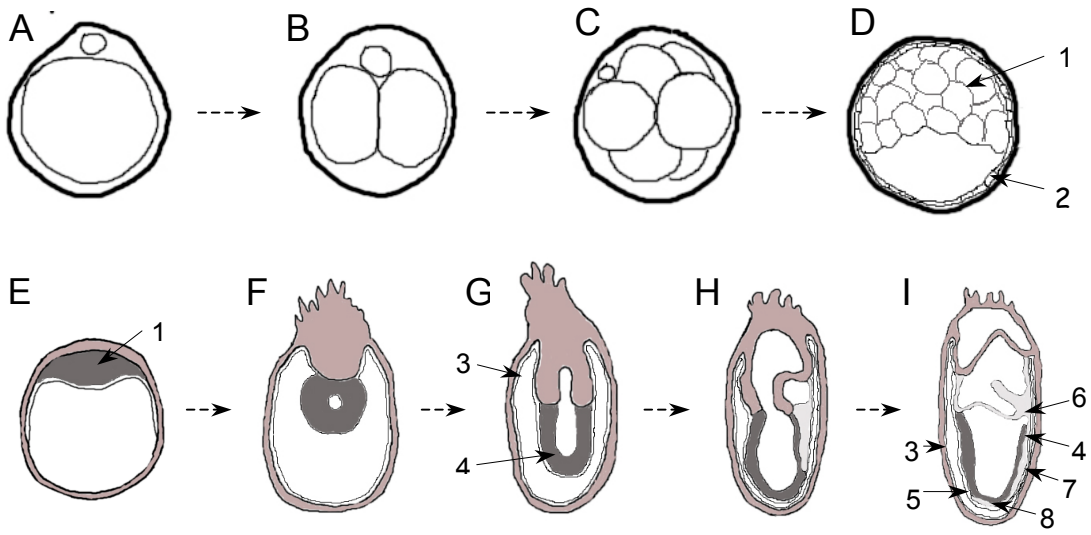

Figure 1.1 During mouse early embryogenesis, the fertilized egg (**A**) keeps dividing (**B**) to form first the morula (**C**) and then the blastocyst (**D**). The blastocyst implants (**E**) forms the egg cylinder (**F**). Gastrulation begins at late egg cylinder stage (**G**). At about embryonic day 7 (**H**), the embryonic mesoderm first emerges. During the primitive streak stage (**I**), the neural plate is defined anteriorly and the head process is developing. 1. inner cell mass; 2. trophectoderm; 3. anterior visceral endoderm; 4. embryonic ectoderm; 5. embryonic mesoderm; 6. amnion; 7. primitive streak; 8. node. (from 3D digital atlas, Edinburgh mouse atlas project, MRC, Human Genetics Unit, Edinburgh, UK)

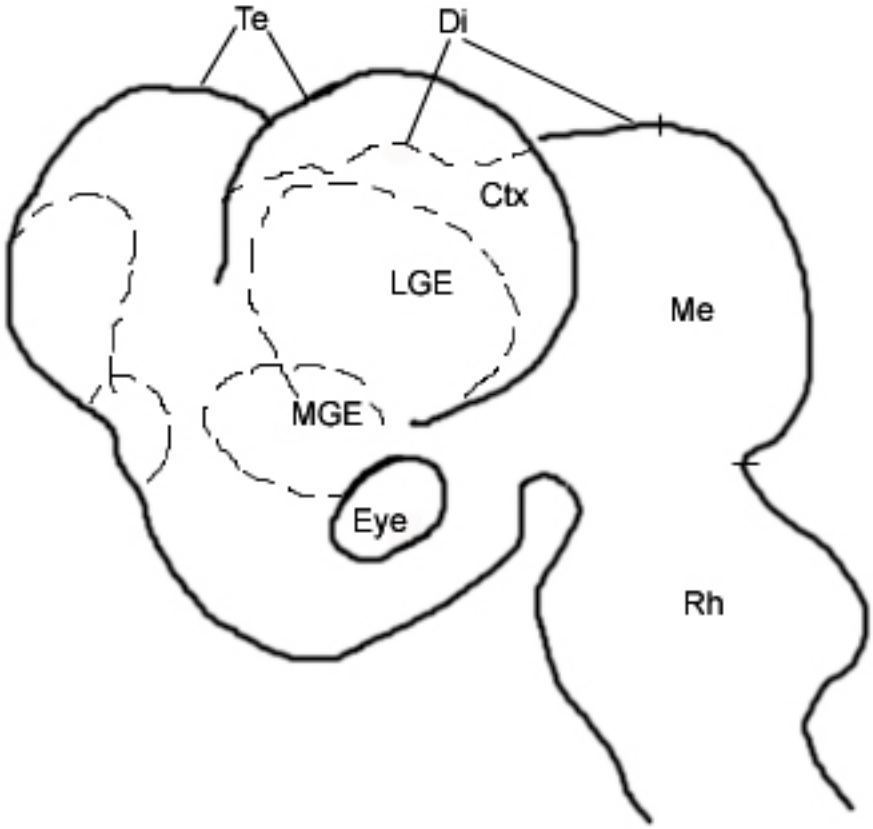

Figure 1.2 Schematic represantation of an E12.5 mouse brain. The forebrain consists of the telencephalon (Te) and the diencephalon (Di), which are located in the anterior part of the brain. The telencephalon is comprised dorsally, the cerebral cortex (ctx), and ventrally, the lateral (LGE) and medial (MGE) ganglionic eminences. The mesencephalon (Me) and the rhombencephalon (Rh) are located in the posterior part of the brain (boundaries are indicated by lines).

1.1.2 Induction of the telencephalon

The forebrain is patterned by many transcription factors and signalling molecules, which both regulate antero-posterior (AP) and dorso-ventral (DV) patterning of the neural tissue. Signalling molecules, both surrounding and within the telencephalon, send signals to regulate expression of transcription factors, which bind to DNA and control the transcription of their downstream genes.

Previous studies in fish and frogs support a model in which the induced neural tissue will develop anterior character, unless it is exposed to posteriorizing signals (Fekany et al., 1999; Koos and Ho, 1999; Fekany-Lee et al., 2000; Hashimoto et al., 2000). The primary role for signals that promote forebrain development may be to antagonize or negatively regulate factors that would posteriorize the anterior neural plate. In mammals, there appears to be two signalling centres, one in the node and one in the anterior visceral endoderm (AVE) (Fig. 1.1I), which are responsible for forming the anterior region of the embryo (Bachiller et al., 2000). When genes required for development of the AVE and the node are mutated or lost, embryos lose anterior structures including the telencephalon (Knoetgen et al., 1999; Bachiller et al., 2000). Although it is still unclear how exactly they regulate brain development, they may produce signals including antagonists of Wingless-type MMTV integration site (Wnt), bone morphogenetic proteins (Bmp) (including Noggin and Chordin) and Nodal signalling (Glinka et al., 1998; Niehrs, 1999; Piccolo et al., 1999; Bachiller et al., 2000; Foley et al., 2000), which are required for the induction and/or maintenance of the adjacent neural plate.

Houart and colleagues (Houart et al., 2002) showed that the local antagonism of Wnt signalling within the anterior neural plate can result in ectopic induction of

telencephalon in wild type embryos. Furthermore, they provided evidence that the posterior diencephalon is a likely source of Wnt ligands, including Wnt8b, which antagonize telencephalic specification. Thus, telencephalic identity is established through local suppression of Wnt signalling in the anterior neural plate during gastrulation.

The inhibition of BMP activity through the action of Bmp antagonists from the node has also been shown to be crucial in establishing all anterior neural plate fates, including the telencephalon, the diencephalon, and the eye (Wilson and Edlund, 2001). Mice lacking activity of extracellular Bmp antagonists Chordin and Noggin lack forebrain (Bachiller et al., 2000).

1.1.3 Antero-posterior (AP) patterning of the telencephalon

Subsequent to the initial subdivision of the neural plate, each territory undergoes further regional patterning. The earliest step in telencephalic induction is mediated by an organizer at the rostral-most end of the neural plate known as the anterior neural ridge (ANR), which is a specialised tissue found at the junction between the anterior neural plate and the non-neural ectoderm (Fig. 1.3) (Shimamura and Rubenstein, 1997; Houart et al., 1998). Removal of the ANR from explants results in a failure to express the winged-helix transcription factor *Foxg1* (previous known as *Bf1*) (Xuan et al., 1995), which marks the future telencephalon (Shimamura and Rubenstein, 1997) and is required for neural telencephalic and cortical morphogenesis (Xuan et al., 1995; Dou et al., 1999; Hanashima et al., 2004; Martynoga et al., 2005).

Fibroblast growth factors (Fgfs) have been suggested to be crucial in patterning the AP axis of the telencephalon. Several members, including *Fgf8*, *Fgf17* and *Fgf18* are

expressed in the anterior end of the telencephalon, the commissural plate (also known as ANR) (Fig. 1.3) (Maruoka et al., 1998). Among them, Fgf8 has been demonstrated to be particularly important (Lee et al., 1997; Shimamura and Rubenstein, 1997; Meyers et al., 1998; Martinez et al., 1999; Crossley et al., 2001; Fukuchi-Shimogori and Grove, 2001). *Fgf8* expression in the commissural plate instructs cells along the AP axis to express different levels of regulatory genes that in turn result in the adoption of different fates. Fgf8 has been suggested to regulate *Foxg1* expression (Shimamura and Rubenstein, 1997; Ye et al., 1998; Erter et al., 2001), and *Fgf8* expression is reduced in the *Foxg1*$^{-/-}$ mutants (Martynoga et al., 2005). *Fgf8* expression is probably initiated too late (around E6) in embryonic development (Crossley and Martin, 1995) to be the primary inducer of the telencephalon, and indeed much of the telencephalon is still present in mice mutant for *Foxg1* (Meyers et al., 1998; Martynoga et al., 2005), suggesting there must be other signalling pathways that help induce the telencephalon.

Another signalling pathway that might influence early AP patterning is the Wnt pathway, which is suggested to be critical for the establishment of the earliest subdivision of the neural plate (Yamaguchi, 2001; Houart et al., 2002). For instance, Wnt8 and the extracellular Wnt antagonists Dikkopf-1 (Dkk-1) are important for the establishment of the vertebrate head. Forebrain is absent in mice lacking the function of Dkk-1 (Mukhopadhyay et al., 2001), and the loss of *Wnt8* expression in zebrafish results in an enlarged forebrain, while more caudal neural tissue is reduced in size or absent (Erter et al., 2001; Lekven et al., 2001).

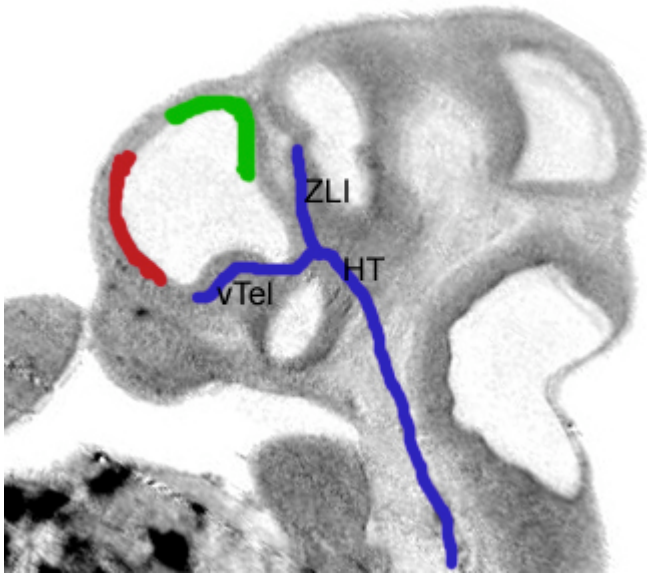

Figure 1.3 Mid-sagittal view of an E12.5 wild type embryo showing the signalling centres within the forebrain. Several Fgf family members, including *Fgf8*, *Fgf17* and *Fgf18*, are expressed in the anterior neural ridge (ANR, red). A cocktail of Wnt and Bmp genes are expressed in the cortical hem and the surrounding dorso-medial telencephalon (green). Shh is expressed in the ventral telencephalon (vTel), the hypothalamus (HT) and the zona limitans intrathalamica (ZLI) (blue).

1.1.4 Dorso-ventral (DV) patterning of the telencephalon

Dorso-ventral patterning mainly occurs later than antero-posterior patterning (Zaki et al., 2003), and the telencephalon becomes specified into dorsal (pallial) and ventral (subpallial) regions. The pallium gives rise to the cerebral cortex, while the subpallium consists of the medial (MGE) and lateral (LGE) ganglionic eminences, which later form the globus pallidus and the striatum of the basal ganglia.

1.1.4.1 Regional subdivisions along the DV axis of the telencephalon

The boundary between the dorsal and ventral telencephalon does not lie at the morphological angle of the pallium and LGE, but is slightly more ventral in the dorsal-most portion of the LGE (Puelles et al., 2000; Campbell, 2003). The expression of many transcription factors abuts the pallial-subpallial boundary (PSB); for example, *Pax6* is expressed on the dorsal side and *Gsh2* is expressed on the ventral side (Toresson et al., 2000; Yun et al., 2001).

The dorsal telencephalon (pallium) can be subdivided into ventral, lateral, dorsal and medial components, which give rise to neurons of the claustroamygdaloid complex, lateral cortex, neocortex and hippocampus, respectively (Puelles et al., 1999; Puelles et al., 2000; Stoykova et al., 2000; Yun et al., 2001). The ventral pallium is defined both by its expression of *Pax6* in the ventricular zone and *Tbr1* in the mantle region, and lacks *Emx1* expression (Puelles et al., 1999; Puelles et al., 2000). The boundaries of the other dorsal domains are not as easily marked by distinct gene expression as the ventral pallium. These regions show gradients of gene expression. For example, *Emx1*, *Emx2* (Simeone et al., 1992; Gulisano et al., 1996) and *Lhx2* (Monuki et al.,

2001) show their highest expression in the medial pallium, and progressive reduction of expression in more ventral regions. In contrast, *Pax6* and *Tbr2* show the opposite pattern with their highest expression in the ventricular zone of the ventral and lateral pallium (Stoykova et al., 2000; Toresson et al., 2000; Yun et al., 2001).

In the ventral telencephalon, many genes are expressed in both the LGE and MGE, including *Gsh2* in the ventricular zone (Hsieh-Li et al., 1995), and members of the Dlx gene family in both the ventricular zone and the subventricular zone (Eisenstat et al., 1999). The LGE has been divided into a small dorsal domain (dorsal LGE) and a lateral ventral domain (ventral LGE) (Yun et al., 2001). The dorsal LGE expresses the Ets gene *Er81*, which has been suggested to give rise to interneurons that migrate in the rostral migratory stream to populate the olfactory bulb (Stenman et al., 2003). The mantle zone of the ventral LGE uniquely expresses the LIM homeobox protein Islet1 and generates striatal projection neurons (Toresson et al., 2000; Stenman et al., 2003).

1.1.4.2 Patterning of the dorsal telencephalon

Dorsal structures such as the roof plate and cortical hem are important for the dorso-ventral identities of early neurectodermal cells (Lee and Jessell, 1999; Monuki et al., 2001). The roof plate has been suggested to be an organizing centre of the telencephalon, and to have an essential role in patterning the dorsal telencephalon (Monuki et al., 2001; Chizhikov and Millen, 2004). Many members of the Bmp family are expressed in the roof plate (Fig. 1.3) (Monuki and Walsh, 2001; Ragsdale and Grove, 2001). *In vitro* studies showed that Bmp2 and Bmp4 from the roof plate regulate the dorsal telencephalic development, and, in particular, the expression of the homeobox transcription factor *Lhx2* (Monuki et al., 2001). *In vivo* studies also showed that when the Bmp receptor in the telencephalon is removed, the choroid

plexus is missing, while the dorso-lateral and the ventral telencephalon are normal (Hebert et al., 2002), which suggests Bmp signalling has an essential role in patterning the dorsal midline (Campbell, 2003). Members of the Wnt protein family are also expressed in the dorsal midline region. When *Wnt2b* is lost from the dorsal midline, the roof plate of the telencephalon disappears (Monuki et al., 2001). These results suggest that the telencephalic roof plate is a crucial organizing centre of the dorsal telencephalon.

Another important dorsal signalling centre within the telencephalon is the cortical hem, which is the medial margin of the embryonic cerebral cortex. The cortical hem provides patterning signals and gives rise dorsally to the hippocampus and ventrally to the choroid plexus, and expresses several Bmp and Wnt genes (Fig. 1.3) (Furuta et al., 1997; Grove et al., 1998; Ragsdale and Grove, 2001). Mice mutant for *Wnt3a* show a deletion of the hippocampus, which is represented by tiny populations of residual cells or is missing completely, whereas the rest of the neocortical areas appear relatively normal (Lee et al., 2000). Mice mutant for *Lef1* show a similar defect in the hippocampus. *Lef1* interferes with the function of several members of the TCF/LEF family (Galceran et al., 2000). The TCF/LEF transcription factors mediate Wnt signalling via β-catenin (Patapoutian and Reichardt, 2000). Both *Wnt3a* and *Lef1* mutants have a reduction in cell proliferation in the hippocampal anlage (Galceran et al., 2000; Lee et al., 2000), suggesting that Wnt signalling is required for expansion of this structure. Furthermore, certain Wnts are also expressed throughout the ventricular zone of the cortex at early stages of telencephalic development (Parr et al., 1993; Grove et al., 1998). They may have a broader role in patterning the dorsal telencephalon.

It is still poorly understood how signalling molecules influence morphogenesis. One of the possibilities is that transcription factors respond to the signalling molecules

regionally and activate downstream targets (Monuki and Walsh, 2001; Ragsdale and Grove, 2001; Rallu et al., 2002a; Schuurmans and Guillemot, 2002). For instance, the downstream genes of Bmp and/or Wnt signalling in the dorsal telencephalon interrupt the functions of transcription factors, such as *Emx1*, *Emx2* (Simeone et al., 1992; Gulisano et al., 1996) and *Lhx2* (Monuki et al., 2001). *Lhx2* is selectively expressed in the cortical ventricular zone, but not in the dorsal midline area (Fig. 1.4). *Lhx2*$^{-/-}$ mutant mice lose almost all cortical progenitor cells and cortical plate neurons, while they have a massive excess of cortical hem tissue and choroid plexus in the lateral ventricle (Monuki et al., 2001). The expression of *Foxg1* and *Ngn2* can still be found in the remaining cells of the *Lhx2*$^{-/-}$ mutants, indicating that the specification of the cortex is still happening at some level in these mutants. This suggests that *Lhx2* is not essential for the specification of telencephalic or dorsal identity, but acts instead to select a specific cortical fate. In addition, the telencephalic enhancer of the *Emx2* gene has been shown to be expressed at its highest levels in the medial and dorsal pallium (Theil et al., 2002a). This enhancer contains binding sites for both Smad and Tcf proteins, which are transcriptional mediators of Bmp and Wnt signalling, respectively. In addition, Bmps and Wnts can activate this DNA enhancer in midbrain explants (Theil et al., 2002a). This leads to the possibility that Bmp signalling from the dorsal midline is functionally redundant with Wnt signalling in specifying certain aspects of dorsal telencephalic fate (Campbell, 2003).

The transcription factors *Emx2* and *Pax6* are expressed in the cortical ventricular zone in the dorsal telencephalon (Fig. 1.4), and they are suggested to be necessary both for the development of dorsal structures such as cortex, and for repressing ventral structures such as striatum (Bishop et al., 2000; Stoykova et al., 2000; Tole et al., 2000b; Toresson et al., 2000; Yun et al., 2001). *Emx2* and *Pax6* are expressed in graded and opposing fashions within the cortical ventricular zone. The *Emx2* gradient is ^{high}posterior-to-^{low}anterior, ^{high}medial-to-^{low}lateral, whereas the *Pax6*

expression has a ^{high}anterior-to-^{low}posterior, ^{high}lateral-to-^{low}medial profile (Bishop et al., 2000). Loss of *Emx2* function in mice results in size reductions in posterior cortical areas (including hippocampus and visual neocortical areas), whereas anterior neocortical regions (including motor areas) are either shifted or expanded (Bishop et al., 2000). Correspondingly, loss of *Pax6* function (*Small eye* mutations) results in a decreased anterior neocortical size (Bishop et al., 2000). Importantly, these defects correspond well to the normal expression gradient of *Emx2* and *Pax6*, suggesting *Emx2* and *Pax6* countergradients within the cortical ventricular zone provide an intrinsic code that directly regulates the size of the cortical area (Monuki et al., 2001).

1.1.4.3 Patterning of the ventral telencephalon

The Fgf signalling pathway also appears to regulate patterning along the DV axis, in addition to the AP axis. Previous work in fish (Shanmugalingam et al., 2000) showed *Nkx2.1* expression is reduced and ventral telencephalic midline tissue is disrupted in *ace* mutant embryos that lack Fgf8 function. Indeed, more severe reduction of ventral telencephalic markers confirms a role of Fgf signalling in promoting ventral telencephalic identity or growth (Wilson and Rubenstein, 2000). Fgf8 hypomorphic and conditional null mutants show a loss of rostro-ventral structures, including the septum, LGE and MGE (Storm et al., 2006). A recent study has shown that mice carrying mutations in Fgf receptors fail to develop ventral telencephalon from very early stages, and cells along the DV axis adopt a dorsal fate (Gutin et al., 2006). More importantly, an *in vitro* study provides evidence that ectopic Fgf8 can induce ventral markers expression in dorsal telencephalic explants (Kuschel et al., 2003).

Sonic hedgehog (Shh) is a member of the hedgehog (Hh) family of secreted signalling proteins implicated in a wide variety of developmental processes (Fig. 1.3).

The role of Shh signalling in neural development has been extensively studied in the developing mammalian spinal cord (Ericson et al., 1995a; Roelink et al., 1995), and it is now clear that Shh and the downstream zinc finger transcription factor Gli3 are essential for the patterning of the DV axis, including the telencephalon (Chapter 1.2 and 1.3).

Retinoic acid (RA) signalling has been suggested to be important for neuronal progenitors and neuronal differentiation (Maden et al., 1998; LaMantia, 1999; Pierani et al., 1999; Schneider et al., 2001; Diez del Corral et al., 2003). In the spinal cord, evidence has led to a model that RA signalling establishes the intermediate region of the caudal neural tube, partially by antagonizing Fgf signalling (Diez del Corral et al., 2003; Novitch et al., 2003). In the telencephalon, evidence has suggested that RA influences anterior forebrain development (Toresson et al., 1999; Schneider et al., 2001; Smith et al., 2001; Marklund et al., 2004). Studies in chick embryos showed that RA signalling is crucial in specifying telencephalic cells to an intermediate fate (including the striatum, the olfactory bulb and parts of the amygdala), opposing Fgf functions (Marklund et al., 2004). At later stages of telencephalic development, radial glial cells in the LGE serve as a source of RA, and retinoid signalling appears to enhance neuronal differentiation (Toresson et al., 1999).

Several transcription factors such as Pax6, Gsh2 and Nkx2.1 are involved in the DV patterning of the telencephalon. *Pax6*$^{sey/sey}$ mutants show a progressive dorsal spread of ventrally-expressed genes, such as *Dlx1* and *Vax1* (Stoykova et al., 1996). Conversely, *Gsh2*$^{-/-}$ mutants show a reduction in size of LGE and expression of *Dlx2* (Szucsik et al., 1997). Mice carrying both *Pax6* and *Gsh2* deletions show milder phenotypes than single mutants (Toresson et al., 2000; Yun et al., 2001), indicating that the interactions between *Pax6* and *Gsh2* regulate DV patterning on either side of

the PSB (Toresson et al., 2000; Yun et al., 2001). In addition, the expression of Pax6 and Gsh2 is not expanded in the *Nkx2.1*$^{-/-}$ mutants, and Nkx2.1 expression is not expanded in either *Pax6*$^{Sey/Sey}$ or *Gsh2*$^{-/-}$ mutants, suggesting neither *Pax6* nor *Gsh2* are cross repressive with *Nkx2.1* (Corbin et al., 2003). Furthermore, *Gsh2;Nkx2.1* double mutants show combined phenotypes of both *Nkx2.1* and *Gsh2* single mutants, suggesting that *Gsh2* and *Nkx2.1* cooperate in patterning the LGE and MGE (Corbin et al., 2003). Together, these results suggest that homeobox genes function to mediate DV patterning of the telencephalon and establish boundaries between regional subdivisions.

Pax6 and *Gsh2* are also suggested to control telencephalic patterning by regulating *Mash1*, *Neurogenin1* (*Ngn1*) and *Neurogenin2* (*Ngn2*) expression (Yun et al., 2001). Ngn1, Ngn2 and Mash1 encode basic helix-loop-helix (bHLH) transcription factors that are implicated in regulating telencephalic DV fates (Fode et al., 2000). *Ngn1* and *Ngn2* are expressed in the ventricular zone of the dorsal pallium, lateral pallium, and ventral pallium while *Mash1* is expressed in the ventricular zone of the LGE and MGE as well as the medial pallium (Gradwohl et al., 1996; Sommer et al., 1996; Ma et al., 1997). Studies on *Ngn1* and *Ngn2* mutants show that they function to specify, or at least maintain, the dorsal and repress ventral properties including *Mash1* expression (Fode et al., 2000). In contrast, *Mash1* is necessary for the development of some early-born subpallial neurons (Casarosa et al., 1999; Horton et al., 1999; Marin et al., 2000), but it is not necessary for the repression of dorsal properties including the expression of *Ngn1* and *Ngn2* (Casarosa et al., 1999; Yun et al., 2001).

Pax6 mutants show ectopic expression of *Mash1* and reduction of *Ngn1* and *Ngn2* expression at E10.5. Subpallial markers are present in the pallium of *Pax6* mutants (Stoykova et al., 1996), which is similar to what happens in the *Ngn1* and *Ngn2* mutants (Fode et al., 2000). Toresson et al. (2000) suggested that *Pax6* represses

ventral genes via *Ngn1* and *Ngn2*. In contrast, *Gsh2* mutants show ectopic expression of *Ngn1* and *Ngn2*, and the reduction of *Mash1* expression in the dLGE at E10.5 (Yun et al., 2001). However, evidences have shown that *Gsh2* is not required for the expression of *Mash1* and the repression of *Ngn1* and *Ngn2* directly. The role of *Gsh2* in the telencephalic development is to repress *Pax6* and its dorsalizing function and the LGE (Toresson et al., 2000; Yun et al., 2000).

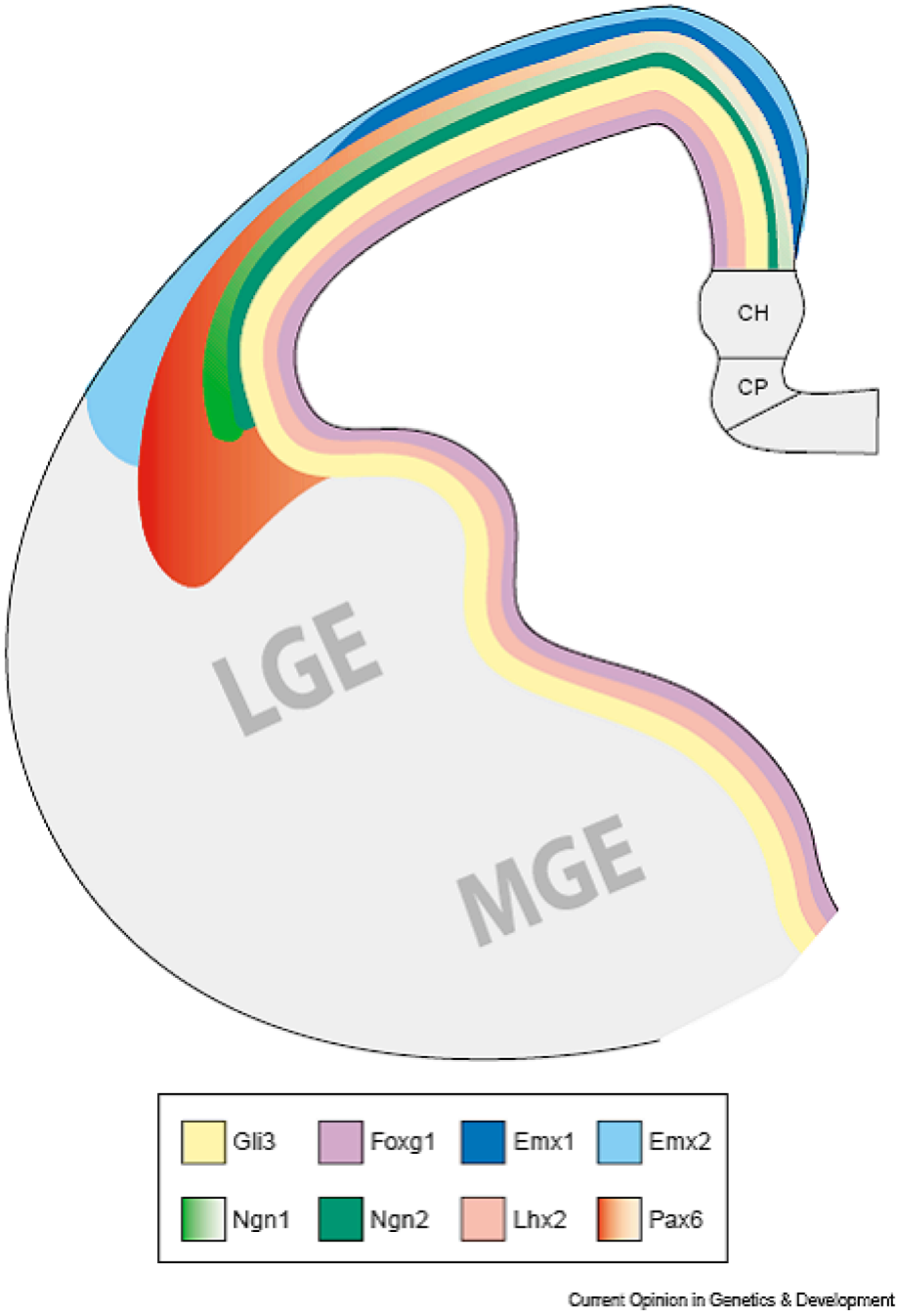

Figure 1.4 Coronal section of E12.5 mouse telencephalon, and the expression patterns of transcription factors that are involved in the development of telencephalon. Dorsally expressed transcription factors include Emx1, Emx2, Ngn1, Ngn2 and Pax6. Gli3, Foxg1 and Lhx2 are expressed in both dorsal and ventral telencephalon (Zaki et al., 2003).

1.1.5 Summary

The development of functional and morphological subdivisions of the telencephalon is incredibly complex. More and more evidence shows that the interaction between secreted signalling molecules and transcription factors controls the process of telencephalic development. However, there are still critical questions that need to be answered. Which signalling centres are involved in the early cortical patterning? What is the link between these early signals and the differential expression of the transcription factors which appear to be involved in the patterning of the telencephalon? How do these and other transcription factors function in patterning the telencephalon? To fully understand these processes, we need to identify the genetic targets of the signalling molecules and transcription factors that regulate regional and neuronal specification, differentiation and migration.

1.2 SONIC HEDGEHOG (SHH) AND FOREBRAIN DEVELOPMENT

1.2.1 Introduction

Sonic hedgehog (Shh) along with Desert hedgehog (Dhh) and Indian hedgehog (Ihh) are the mammalian homologues of the *Drosophila* Hedgehog (Hh) family of signalling molecules (Riddle et al., 1993; Fietz et al., 1994). Among the three, Shh is the only one which has been shown to be expressed in the forebrain (Echelard et al., 1993; Riddle et al., 1993). The *Hh* gene was first identified in *Drosophila* because of its role in embryonic segment polarity (Nusslein-Volhard and Wieschaus, 1980) and the patterning of the imaginal discs (Mohler, 1988; Tabata et al., 1992; Basler and Struhl, 1994). *Shh* was identified in chick and mouse afterwards, and it was shown to be important in patterning the limb and the neural tube (Echelard et al., 1993; Riddle et al., 1993; Roelink et al., 1994).

1.2.1.1 Hh signalling pathway in *Drosophila* and vertebrates

Hh signalling has been studied in greatest depth in *Drosophila* (Hooper and Scott, 2005). The Shh signalling pathway in vertebrates is very similar to the Hh pathway (Fig. 1.5). At the cell surface, Shh binds to its receptor Patched 1 (Ptc1), a twelve-transmembrane protein (Fig. 1.5a) (Goodrich et al., 1997). Unlike other receptors, in the absence of Shh, Ptc1 blocks the downstream signalling pathway, and the binding of Shh relieves this repression. A seven-transmembrane protein Smoothened (Smo) acts downstream of Ptc1. Smo is an essential positive mediator of the Hh signalling pathway (Zhang et al., 2001), by regulating the Gli family of transcription factors, Gli1, Gli2 and Gli3 (Murone et al., 1999). Gli responds to Shh and functions as a transcriptional activator. In the absence of Shh, Gli3 protein binds to Fused (Fu), Supressor of Fused (Sufu), microtubules and is phosphorylated by Protein Kinase A (PKA) to form a short cleaved form of Gli3, which acts as a transcriptional repressor (Fig. 1.5b) (Ruiz i Altaba, 1999; Sasaki et al., 1999; Shin et al., 1999). Several studies in the vertebrate spinal cord and limb development have shown that expression of Gli1 and Gli2 results in activation of Shh target genes (Ruiz i Altaba, 1999; Sasaki et al., 1999), while expression of Gli3 results in repression of Shh target genes (Ruiz i Altaba, 1999; Persson et al., 2002). These suggested that Gli1 and Gli2 act primarily as activators, while Gli3 acts both as an activator and repressor of the Shh pathway (Ruiz i Altaba, 1998, 1999; von Mering and Basler, 1999; Aza-Blanc et al., 2000). In the developing forebrain, Gli1 is expressed in the ventral forebrain near Shh expression, and Gli1 has been suggested to be a direct readout of the Shh signalling pathway (Goodrich et al., 1996; Lee et al., 1997). Gli1 has been suggested to be redundant with other Gli proteins, because *Gli1* knock out mice seem to be normal (Park et al., 2000). Studies on *Gli2*$^{-/-}$ mutants have suggested that Gli2 is important for the induction of floor plate cells (Ding et al., 1998),

however the role of Gli2 in the developing forebrain is still unknown. Gli2 and Gli3 might have partially overlapping functions in skeleton formation, but the loss of Gli3 affects dorsal brain development can not be compensated for by Gli2 (Theil et al., 1999; Tole et al., 2000). Thus it appears that Gli3 is the major factor in the Shh signalling pathway during forebrain development.

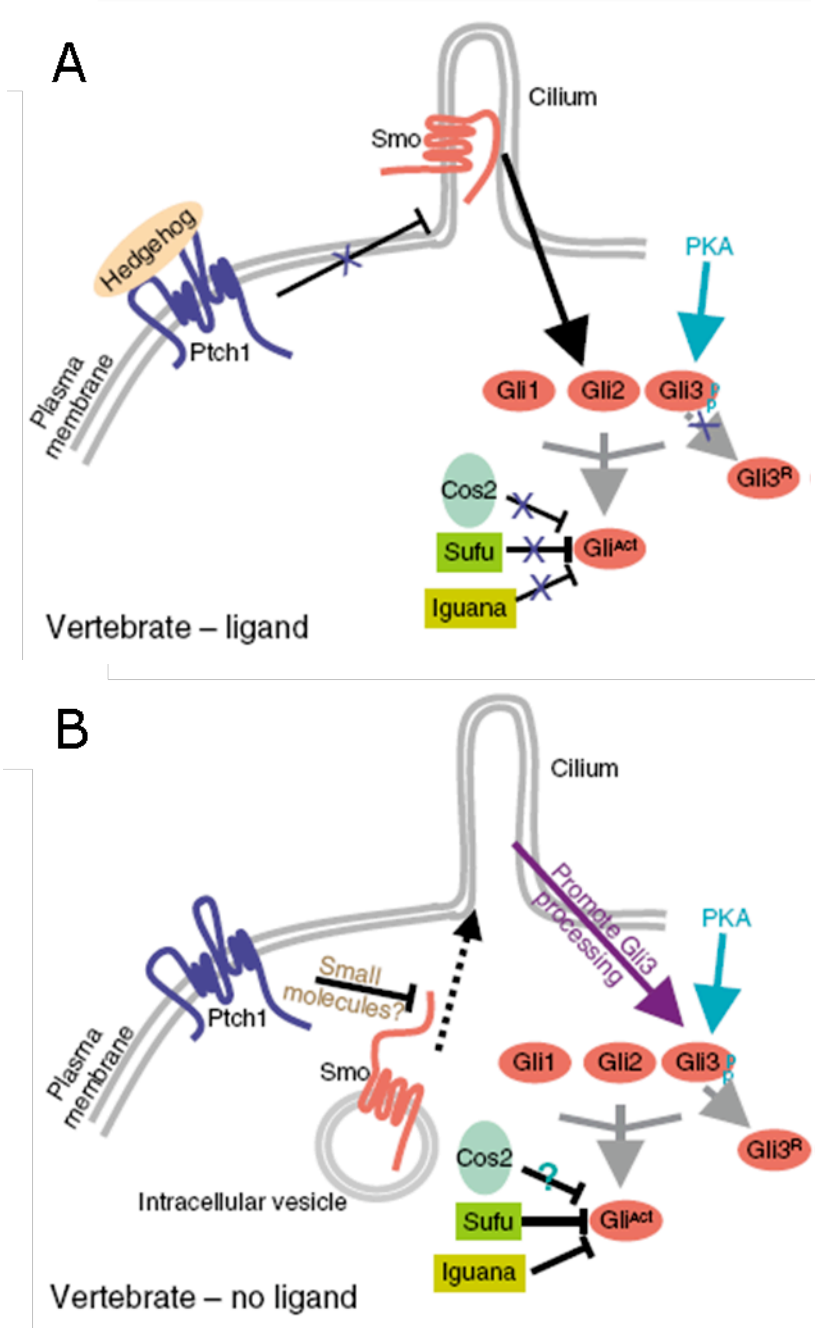

Figure 1.5 Shh signalling pathway in vertebrates. **A.** When Shh is present, it binds to Patch1 (Ptch1), which relieves Smoothened (Smo). The activation of Smo leads to the formation of a macromolecular complex with Su(fu) (Supressor of fused) , PKA, and the Gli proteins. These are imported into the nucleus and activate target genes. The processing of Gli3 is inhibited. **B.** In the absence of Sonic hedgehog, Patched (Ptch1) inhibits (Smo), blocking the downstream transduction cascade. Gli3 is phosphorylated by protein kinase A (PKA), cleaved to form the repressor Gli3 (Huangfu and Anderson, 2005).

1.2.1.2 The phenotype of *Shh*$^{-/-}$ mutant mice

When humans lose one copy of the *Shh* gene, they suffer from holoprosencephaly (HPE), which made people propose that Shh might be one of the important molecules in the development of the CNS. The holoprosencephalic patient has a single unpaired telencephalic vesicle and a single eye (Ericson et al., 1996; Roessler et al., 1996; Roessler et al., 1997). Ventral structures, such as striatum, are lost in some extreme cases (Roessler et al., 1997).

There are many studies about Shh in mammals up to date. *Shh*$^{-/-}$ mouse mutants die at or just before birth. They have fused optic vesicles; they have neither optic stalk nor olfactory bulbs (Chiang et al., 1996). Ventral structures are absent from very early stages along the neural tube (Ishibashi and McMahon, 2002; Ishibashi et al., 2005). The telencephalon is severely hypoplastic and ventral structures are not identifiable. The expression of ventral telencephalic markers, such as Nkx2.1, Gsh1, Olig2 and Lhx6, is absent due to the loss of the ventral telencephalon (Corbin et al., 2000; Lu et al., 2000; Corbin et al., 2003). In contrast, dorsal telencephalic markers, including Emx1 and Pax6, are expressed throughout most of the remaining telencephalic tissue in the *Shh*$^{-/-}$ mutants (Chiang et al., 1996; Ohkubo et al., 2002). Recent studies have shown a small expression of the ventral markers Gsh2, Dlx2 and ER81, indicating that not all the ventral structures are lost. At least the most dorsal part of the lateral ganglionic eminence (dLGE) is still present (Corbin et al., 2003; Fuccillo et al., 2006).

1.2.2 The function of Shh

Shh acts on many different aspects of CNS development, including induction of different classes of neurons in the ventral brain (Echelard et al., 1993; Roelink et al.,

1994; Ericson et al., 1996), early regionalization (Shimamura et al., 1997), generation of oligodendrocyte precursors in both spinal cord and brain (Orentas et al., 1999; Tekki-Kessaris et al., 2001), proliferation of specific neuron progenitor populations (Rowitch et al., 1999; Tekki-Kessaris et al., 2001; Ishibashi and McMahon, 2002), eye patterning (Ekker et al., 1995; Chiang et al., 1996; Huh et al., 1999) and modulation of growth cone movements (Trousse et al., 2001).

1.2.2.1 Shh functions as a morphogen

Shh protein is cleaved to yield two secreted proteins (Bumcrot et al., 1995), a 25 kDa C-terminal protein (C-Shh), which has protease activity (Porter et al., 1995), and a 19 kDa N-terminal protein (N-Shh), which mediates all signalling activities, including the control of left-right asymmetry, and dorso-ventral patterning of the CNS and antero-posterior patterning of the limbs (Hammerschmidt et al., 1997).

Shh signalling has been studied in detail in the mouse neural tube, where different concentrations of Shh appear to specify a series of cell fates (Jacob and Briscoe, 2003). Shh can regulate the fate of immediately adjacent cells. Alternatively, Shh can function as a short-range morphogen (over 10-15 cell diameters) that controls three alternative fates depending on its concentration. Shh can also work as a long range morphogen that controls several cell fates, for example in the neural tube, a field that spans many cell diameters (Briscoe and Ericson, 1999). There is evidence in zebrafish showing that Shh could act directly over a distance of up to 200 μm (Lewis et al., 2001). Shh is produced by two ventral midline signalling centres: the notochord, an important part of the mesoderm, which lies beneath the ventral neural plate and the floor plate, at the ventral midline of the central nervous system (Marti et al., 1995a). Mutants that lack all Shh signalling fail to specify correctly different cell types in the ventral half of the neural tube (Wijgerde et al., 2002). Gli3 repressor

is essential for the fates of cells that are exposed to low concentrations of Shh (lateral neural cell types) (Persson et al., 2002) and Gli2 activator is essential for the ventral neural cells that respond to highest levels of Shh in the floor plate (Ding et al., 1998; Matise et al., 1998). The intervening neural cell types can be specified by different levels of Gli activator (Stamataki et al., 2005), suggesting that different levels of Shh are directly translated into different ratios of Gli activator/Gli repressor, which control cell fate.

1.2.2.2 Shh and the patterning of forebrain

The phenotype of *Shh*$^{-/-}$ mutants provides good evidence that Shh is important for the formation of ventral telencephalic structures. Several studies have suggested that *Shh* is required for the induction of ventral telencephalic cell fate during a specific time frame. Machold et al. (2003) removed *Smo* gene function by using Cre recombinase under the control of Nestin promoter in the CNS. Nestin is expressed by all neural progenitors (Dahlstrand et al., 1995), and this recombination starts ventrally around E9.5 and removes Hh signalling completely by E12.5. In these mutants (*Smo*$^{c/-}$*;Nestin*^{Cre}), both medial and lateral ganglionic eminences are morphologically present, and the expression of ventral markers is largely restored (Machold et al., 2003). Fuccillo et al. (2004) used another floxed allele of *Smo* to ablate Shh signalling using Cre recombinase under the control of the Foxg1 promoter. *Foxg1* expression starts in the prospective ventral telencephalon as early as E8.5 (Xuan et al., 1995), and the ablation of *Smo* is completed at around E9.5. Surprisingly, the expression of ventral markers is totally absent in these mutants (*Smo*$^{c/-}$*;Foxg1*^{Cre}), whereas dorsal markers are expanded (Fuccillo et al., 2004). These findings suggest that the period between E9 and E12 is crucial for the induction of ventral cell fate by Hh signalling. Gunhaga et al. (2000) showed that exposure of prospective forebrain cells to Shh signalling at grastrula stage is sufficient to generate both progenitor cells

and post mitotic neurons with ventral telencephalic character in chick, suggesting that it is also possible that the induction of ventral telencephalon by Shh signalling happens as early as gastrulation (Gunhaga et al., 2000). It is interesting that not all ventral gene expression is lost in the *Shh*$^{-/-}$ mutants. It is possible that other Hh homologues can pattern the telencephalon or can partially compensate for the absence of Shh. In fact, mice mutant for both *Shh* and *Ihh* appear to lack all ventral characters throughout the CNS (Zhang et al., 2001). This phenotype is very similar to that of the *Smo*$^{-/-}$ mutants, which are unable to transduce any Hh signal and die around E9.5 (Zhang et al., 2001). In addition, although *Shh* has been shown to be crucial in ventral telencephalic patterning, ventral telencephalon is largely restored when *Gli3* is removed from the *Shh*$^{-/-}$ mutants (Rallu et al., 2002b). This suggests that there might be other factors besides Shh that may induce ventral telencephalic fate.

The role of Shh in patterning the dorso-medial telencephalon is still obscure. The dorsal midline is lost in both *Shh*$^{-/-}$ and *Gli3*$^{-/-}$ mutants and also in *Shh*$^{-/-}$*;Gli3*$^{-/-}$ double mutants (Chiang et al., 1996; Grove et al., 1998; Theil et al., 1999; Rallu et al., 2002b), suggesting that Shh and Gli3 might co-operate in patterning this region. Fuccillo et al. (2004) showed that the dorso-cortical midline seems to be unaffected in the *Smo*$^{c/-}$*;Foxg1*^{Cre} mutants, which suggests that Shh signalling is required to pattern this region earlier than E9 (Fuccillo et al., 2004). Another interesting result has been shown very recently by the same group (Fuccillo et al., 2006). When they removed *Pax6* from the *Shh*$^{-/-}$ mutant, the expression of *Wnt8b* and *Bmp4* was partially rescued in the *Shh*$^{-/-}$*;Pax6*$^{-/-}$ compound mutant, which suggests that increased levels of Pax6 might be partially responsible for the defective dorsal midline of *Shh*$^{-/-}$ mutants (Fuccillo et al., 2006).

The Shh source outside the telencephalon might also affect its patterning. For

example, Shh from the anterior part of the primitive streak and Henson's node at gastrula stages might be crucial for the specification of the MGE (Gunhaga et al., 2000). Shh from the prechordal plate also plays an important role in specification of the ventral telencephalon. The prechordal plate is part of the mesoderm which lies under the rostral diencephalon (Dale et al., 1997; Dale et al., 1999). Also, Shh from the adjacent zona limitans intrathalamica (ZLI) of the diencephalon might influence the specification of the ventral telencephalon. The ZLI is a neuroepithelial domain in the alar plate of the diencephalon which separates the ventral thalamus from the dorsal thalamus (Rubenstein et al., 1998; Vieira et al., 2005). The ZLI functions as a diencephalic signalling centre, and Shh derived from the ZLI has been shown to affect the induction of the ZLI itself, and give morphogenetic information to the thalamus (Kiecker and Lumsden, 2004; Zeltser, 2005).

1.2.2.3 Shh and the specification of Oligodendrocytes

Another important role of Shh is the specification of oligodendrocytes in ventral CNS development (Tekki-Kessaris et al., 2001). Oligodendrocyte precursors (OLPs) in the spinal cord and caudal forebrain arise from specific regions of the ventral neuroepithelium at either side of the floor plate and then disperse throughout the developing gray matter and populate white matter tracts (Miller, 1996; Miller et al., 1999; Richardson et al., 2000; Spassky et al., 2000). In the anterior forebrain, OLPs emerge from the anterior entopeduncular area and probably from the ZLI (Olivier et al., 2001). OLPs in the spinal cord express a number of markers including the basic helix-loop-helix transcription factors Olig1 and Olig2 (Lu et al., 2000; Zhou et al., 2000). Neuroepithelial cells in the ventral spinal cord of the *Olig2*$^{-/-}$ mouse mutants fail to differentiate into oligodendrocytes (Takebayashi et al., 2002). The generation of OLPs appears to require Shh signalling, since all OLPs originate in areas of the CNS that either express *Shh* themselves or are in close proximity to *Shh* expressing

cells (Davies and Miller, 2001), which at least partially explains their ventral origin within the spinal cord. There is evidence that oligodendrocyte lineage genes (*Olig1*, *Olig2*) are lost in the *Shh*$^{-/-}$ mutants (Lu et al., 2000), which also suggests that *Shh* is required for the induction of OLPs. Several studies showed that *Shh* can initially induce oligodendrocyte differentiation (Poncet et al., 1996; Pringle et al., 1996; Orentas et al., 1999), and many gain- and loss-of-function experiments in mouse embryos have shown that *Shh* is both necessary and sufficient for the specification of OLPs in the spinal cord (Orentas et al., 1999) and the forebrain (Nery et al., 2001; Tekki-Kessaris et al., 2001).

1.2.2.4 Shh and cell growth and survival

Shh is also suggested to regulate cell growth and survival in the CNS. First of all, the reduction in the overall brain size of the *Shh*$^{-/-}$ mutant suggested that cell cycle or cell death parameters might be altered in these mutants. It has been shown that ectopic expression of *Shh* or ectopic activation of the Shh signalling pathway through the removal of *Ptc1* activity results in massive proliferation in brain and spinal cord (Goodrich et al., 1997; Rowitch et al., 1999; Dahmane et al., 2001). Several studies in diencephalon and mesencephalon (Ishibashi and McMahon, 2002) and cerebellum (Kenney and Rowitch, 2000) have suggested that G1-phase cyclins, including Cyclin D1 (Sherr and Roberts, 1999), are transcriptional targets of Shh signalling. Ptc1 is suggested to regulate directly the G2-phase Cyclin B (Barnes et al., 2001). These all suggest that Shh possibly plays a direct role in regulating cell proliferation.

Shh is also suggested to be involved in cell death. Ectopic cell death was detected in the developing spinal cord (Chiang et al., 1996; Litingtung and Chiang, 2000), the diencephalon and the anterior midbrain (Ishibashi and McMahon, 2002) of *Shh*$^{-/-}$ mutants. Also *Shh*$^{-/-}$ mutants exhibit an increased Bmp and Msx expression (Ohkubo

et al., 2002). These suggested that Shh might regulate cell death in many places of the developing embryo, including the brain and the spinal cord.

1.3 GLI3 AND FOREBRAIN DEVELOPMENT

1.3.1 Introduction

The zinc finger transcription factor Gli3 is a mammalian homologue of *Drosophila* cubitus interruptus (ci), which is an important mediator of the Hh signalling pathway (Ruppert et al., 1990; Ingham and McMahon, 2001). *Gli3* is important in development because it has been observed that strains of mice mutant for *Gli3* have many malformations. They are called '*extra-toes*' *(Xt)* mice because the heterozygous mutants ($Gli3^{Xt/+}$) have extra digits on both forelimbs and hindlimbs (Johnson, 1967). The heterozygous mutant mice have one or two extra digits on the limbs, while the homozygous mutant mice ($Gli3^{Xt/Xt}$) can have as many as ten digits on one limb. These mutants do not survive beyond birth and are severely abnormal.

1.3.1.1 Gli3 expression

The expression of the *Gli3* gene is first detected at around E7.0-E7.5 and is found throughout embryogenesis in derivatives of both the ectoderm and the mesoderm (Hui et al., 1994). The *Gli3* gene is normally expressed in the telencephalon, the roof of the diencephalon, midbrain and the hindbrain during gestation of wild type embryos (Schimmang et al., 1992). The onset of expression in the neural ectoderm begins at the primitive streak stage. *Gli3* is first expressed in rather broad domains; in general, the expression domains become more restricted at later stages of development (Schimmang et al., 1992; Hui and Joyner, 1993; Hui et al., 1994).

1.3.1.2 The general brain phenotype of *extra-toes* mutant mice

Johnson (1967) first described extra-toes mutant mice from Harwell and several other *Xt* alleles have been reported since. Among them, the allele from Jackson Laboratory, Xt^J, is one of the most widely studied allelic variants (Hui and Joyner, 1993). The Xt^J mutant contains a 51.5 Kb intragenic deletion of *Gli3*, which removes all *Gli3* sequence 3' of the second zinc finger (Maynard et al., 2002). The *Gli3* gene transcript is absent in the Xt^J homozygotes. Thus, the Xt^J mice have a deficiency of *Gli3* expression (Hui and Joyner, 1993). The heterozygous Xt^J mouse has been shown to be the mouse model for Greig Cephalopolysyndactyly Syndrome (GCPS), a human genetic condition that results in skeletal defects, including the formation of a duplicated, fused fifth digit and craniofacial anomalies (Hui and Joyner, 1993). Mutations in human *GLI3* can also cause Pallister-Hall syndrome (Kang et al., 1997), Postaxial Polydactyly type A/B (Radhakrishna et al., 1997; Zhao et al., 2002) or Acrocallosal syndrome (Elson et al., 2002)

Xt^J homozygous embryos are classified into two groups based on overall brain morphology. Some embryos show severe exencephaly, probably as a result of a delay in neural tube closure (Hui and Joyner, 1993). They have an overgrowth of neural tissue in the mesencephalon, as Johnson (1967) described in the Harwell mice. Recent research focuses mostly on the non-exencephalic Xt^J homozygous mutant mice ($Gli3^{Xt/Xt}$). The telencephalic vesicles of the non-exencephalic $Gli3^{Xt/Xt}$ embryos are smaller than those of the wild type embryos, but their cerebral cortex is relatively thicker (Tole et al., 2000a). The dorsal medial wall of the telencephalic vesicles fails to invaginate, and these mutants do not have medial structures, such as the hippocampus and choroid plexus (Grove et al., 1998; Theil et al., 1999). The conjunction between the telencephalon and the diencephalon does not form normally, and the olfactory structures are absent (Johnson, 1967; Hui and Joyner, 1993; Franz,

1994; Theil et al., 1999; Fotaki et al., 2006). There are variable defects of the eyes. The eye of mice homozygous for the Harwell mutation may be just half of the normal diameter. In some extreme cases, the eye may be represented by a pigmented hollow ball with a lens rudiment, by a pigment mass, or may have disappeared without trace (Johnson, 1967; Franz, 1994). The eyes of *Gli3*$^{Xt/Xt}$ mice are poorly developed as well (Hui and Joyner, 1993). The optic stalk is thicker than in the wild types (Aoto et al., 2002).

1.3.2 Analysis of the forebrain of *Gli3*$^{Xt/Xt}$ mutant embryos

Previous studies have shown that the expression of many transcription factors and signalling molecules that are involved in forebrain patterning have changed in the *Gli3*$^{Xt/Xt}$ mutant mice (Table 1.1).

1.3.2.1 The dorso-medial telencephalon of the *Gli3*$^{Xt/Xt}$ mutant embryos

The cortical hem is lost in *Gli3*$^{Xt/Xt}$ mutant embryos, and as a consequence the choroid plexus in the lateral ventricle and the hippocampus are missing (Franz, 1994). The cortical hem is derived from the dorsal midline of the telencephalic vesicle and is marked by the expression of multiple *Wnt* and *Bmp* genes, including *Wnt2b*, *3a*, *5a*, and *7a* (Grove et al., 1998). Among them, *Wnt2b*, *3a* and *5a* show a strikingly similar pattern of expression in the telencephalon. In the *Gli3*$^{Xt/Xt}$ embryos at E12.5, no expression of *Wnt2b*, *3a* or *5a* is detected in adjacent tissue that might correspond to the cortical hem. Expression of these three *Wnt* genes elsewhere in the telencephalon is either undetectable or weak and diffuse. Nonetheless, *Wnt2b*, *3a* and *5a* are strongly expressed at other appropriate sites (Grove et al., 1998). *Wnt8b*, which is expressed in a broader region in the dorso-medial telencephalon, is reported to be unaltered in the *Gli3*$^{Xt/Xt}$ mutants at E12.5 (Tole et al., 2000a; Theil, 2005).

The choroid plexus and cortical hem are linked by shared expression of the members of the *Bmp* and *Msx* families (Furuta et al., 1997; Grove et al., 1998). Tole et al. (2000a) showed that at E12.5, *Bmp2*, *4*, *6* and *7* are strongly expressed in the cortical hem and the developing choroid plexus in the wild types. *Gli3*$^{Xt/Xt}$ mutants are deficient in the dorsal telencephalic expression of all four *Bmp* genes (Theil et al., 1999; Tole et al., 2000a). By contrast, a small region of *Bmp7* expression in the ventral telencephalon appears unaltered in the mutants (Tole et al., 2000a). The homeobox gene *Msx1*, which can be induced by Bmp2 and Bmp4 (Furuta et al., 1997), starts to be expressed in the dorsal midline and the surface ectoderm at E9.5 and reaches a higher level at E11.5. *Msx1* expression is lost specifically from the dorsal midline, consistent with the loss of *Bmp4* expression in the *Gli3*$^{Xt/Xt}$ embryos. In the dorsal midline of the more posterior neural tube and in the surface ectoderm of the mutants, *Msx1* expression is unaffected (Theil et al., 1999). Noggin, a negative regulator of the Bmp signalling pathway, is normally expressed in the dorsal midline along the entire neuraxis (Shimamura et al., 1995). The expression is reported unaltered in *Gli3*$^{Xt/Xt}$ embryos (Theil et al., 1999).

The telencephalic hippocampus also appears to be missing from the *Gli3*$^{Xt/Xt}$ mutants, as assessed by both morphology (Franz, 1994) and molecular markers (Tole et al., 2000a). In wild type mice at E12.5, a marker of the embryonic hippocampus *Ephb1* is expressed along the medial face of the telencephalic hemisphere (Donoghue and Rakic, 1999). In the dorsal telencephalon of *Gli3*$^{Xt/Xt}$ mutants, no *Ephb1* expression is detected (Tole et al., 2000a). At E15.5, expression of the glutamate receptor subunit, KA1, marks the major hippocampal field CA3 in wild type mice (Tole et al., 1997). In *Gli3*$^{Xt/Xt}$ mutants at the same age, KA1 expression appears normally in the thalamus, but no KA1 expression is detected in the medial telencephalon (Tole et al., 2000a), confirming loss of the hippocampal structures.

1.3.2.2 Analysis of dorsal telencephalic markers in the *Gli3*$^{Xt/Xt}$ mutant telencephalon

Members of the *Emx* gene family, which are involved in the development of dorsal structures, are reduced or lost in some sites of the *Gli3*$^{Xt/Xt}$ telencephalon (Theil et al., 1999; Tole et al., 2000a). *Emx1* expression is normally restricted in the dorsal telencephalon, and *Emx2* is expressed in a broader domain than *Emx1* in wild type embryos (Simeone et al., 1992; Theil et al., 1999; Tole et al., 2000a). Emx1 expression is shown to be completely lost at E10.5 (Theil et al., 1999) and E12.5 (Tole et al., 2000a). *Emx2* expression is shown to be absent from the rostral forebrain at E8.5, E9.5 and E11 (Theil et al., 1999). However, at E12.5, *Emx2* expression is detected in the *Gli3*$^{Xt/Xt}$ mutant dorsal telencephalon by another group (Tole et al., 2000a), although at a lower level compared to the wild types. The differences between these studies might be due to the differences among ages they studied.

The expression of the transcription factor *Pax6*, which also might be involved in the development of the dorsal structures, is reported to be reduced greatly in the *Gli3*$^{Xt/Xt}$ mutant telencephalon (Aoto et al., 2002). Based on *Pax6* and *Engrailed2* (*En2*) expression, Aoto et al. (2002) proposed that the ventral thalamus, the posterior midbrain and the anterior hindbrain are significantly expanded, while the dorsal telencephalon and the anterior midbrain are reduced in size in the *Gli3*$^{Xt/Xt}$ mutants.

The expression of *Otx1* and *Otx2*, which are both involved in the AP patterning of the rostral telencephalon, are expressed normally in E8.5 to E10.5 *Gli3*$^{Xt/X}$ mutant dorsal telencephalon, but are reported to be reduced slightly at E12.5 (Theil et al., 1999).

1.3.2.3 Analysis of ventral telencephalic markers in the *Gli3*$^{Xt/Xt}$ mutant telencephalon

The dorsal telencephalon is partially ventralized in *Gli3*$^{Xt/Xt}$ mutants (Tole et al., 2000a; Kuschel et al., 2003). In E12.5 wild types, the mantle zone of the MGE and LGE are marked by the expression of the homeobox gene *Islet1*, with no expression detected in the dorsal telencephalon. Strong expression of another homeobox gene *Dlx2* and the proneural gene *Mash1* also distinguish the ventral from the dorsal telencephalon at this age. By contrast, in *Gli3*$^{Xt/Xt}$ mutants, *Islet1*, *Dlx2* and *Mash1* expression are reported to be extended in a dramatic manner into the dorsal telencephalon along the rostro-caudal axis (Tole et al., 2000a; Aoto et al., 2002; Kuschel et al., 2003). This ectopic expression is most striking in the rostral telencephalon. Another ventral specific marker, *Dlx5*, is found to be upregulated in *Gli3*$^{Xt/Xt}$ dorsal telencephalon, with a similar but slightly delayed expression profile as compared to the ventral progenitor markers *Dlx2* and *Mash1* (Kuschel et al., 2003).

Gli3 has been reported to repress expression of *Shh* in the anterior limb regions and in the dorsal spinal cord. The expression of Shh has been analyzed in the *Gli3*$^{Xt/Xt}$ mutant telencephalon by whole mount *in situ* hybridization. *Shh* expression can normally be found throughout the ventral neuroaxis in wild types (Echelard et al., 1993). Theil and colleagues (1999) showed that *Shh* transcripts are confined exclusively to the ventral neural tube at all axis levels of *Gli3*$^{Xt/Xt}$ mutants at E8.5 and E10.5. This was confirmed by Aoto et al. (2002) at E11.5 and Tole et al. (2000a) at E12.5. In both wild type and *Gli3*$^{Xt/Xt}$ E9.5 embryos, expression of the *Shh* target genes *Patched1* (*Ptc1*) and *Gli1* is confined to the ventral region of the neural tube and excluded from the dorsal brain (Theil et al., 1999; Tole et al., 2000a). The expression of *Nkx2.1* was reported to be confined to the ventral telencephalon at

E10.5 by Theil et al. (1999) and at E12.5 by Tole et al. (2000a), but was shown to be expanded by Aoto et al. (2002) in E11.5 *Gli3*$^{Xt/Xt}$ mutant embryos.

Aoto et al. (2002) indicated that not only the DV patterning but also the AP patterning of the forebrain is affected in *Gli3*$^{Xt/Xt}$ mutants. Starting at E8.5, *Fgf8* and its downstream target, *Sprouty2*, are expressed in a restricted region of the rostral end of the telencephalon, corresponding to the ANR (Aoto et al., 2002). In contrast, *Gli3*$^{Xt/Xt}$ mutant embryos show a huge expansion of *Fgf8* and *Sprouty2* expression into more caudal regions. In extreme cases, this domain covers the entire telencephalic roof (Aoto et al., 2002).

Table 1.1 The expression of maker genes analyzed in the wild type and *Gli3*$^{Xt/Xt}$ mutant embryos.

Markers	Age	Expression in wild type embryos	Expression in *Gli3*$^{Xt/Xt}$ mutants	Refs
Wnt2b,3a, 5a	E12.5	Along the medial telencephalic wall	Undetectable or weak and diffuse in the telencephalon	Grove et al. 1998
Wnt7a	E11.5, E12.5	In the lateral and dorsal cerebral cortex	Persists	Grove et al. 1998
			Ectopic, striped expression	Theil 2005
Wnt8b	E12.5	In the hippocampus, cortical hem, the choroid plexus epithelium (CPe), eminentia thalami	Persists in the dorsal part of the telencephalon, but marks a smaller domain	Tole et al. 2000a
			Restricted to the dorso-medial telencephalon	Theil 2005
Bmp4	E9.5, E10.5	In the junction of the telencephalon and the diencephalon, and in the anterior most dorsal roof of the telencephalon	Undetectable in the di-telencephalic boundary	Theil et al. 1999
Bmp6	E12.5	In the cortical hem and the developing CPe	Lost in the dorsal telencephalon	Tole et al. 2000a
Bmp7	E12.5	In the cortical hem, in the ventral part of the telencephalon, and in the CPe	Lost in the dorsal part of the telencephalon, but unaltered in the ventral telencephalon	Tole et al. 2000a
Noggin	E9.5	In the dorsal midline throughout the entire neuraxis, with highest expression levels in the telencephalon	Unaltered	Theil et al. 1999
Msx1	E12.5	In the cortical hem, the CPe, the telencephalic roof, the head mesenchyme, the surface ectoderm	Lost specifically from the telencephalic roof	Theil et al. 1999

Table 1.1 The expression of maker genes analyzed in the wild type and *Gli3*$^{Xt/Xt}$ mutant embryos (continue).

Otx1,2	E8.5-E 11.5	In the dorsal telencephalon	Reduced in the telencephalon at E11.5	Theil et al. 1999
Emx1	E10.5	Confined to the dorsal telencephalon	Not detectable	Theil et al. 1999; Tole et al. 2000a; Aoto et al. 2002
Emx2	E8.5-E 11.5	In the dorsal telencephalon, expanding into the ventral telencephalon	Lost from the telencephalic vesicles	Theil et al. 1999
	E12.5		Readily detectable in the dorsal telencephalon	Tole et al. 2000a
Pax6	E11.5	Dorsal telencephalon, amygdala in the ventral telencephalon, dorsal and ventral diencephalon, and optic cup	Unaltered	Theil et al. 1999
			Greatly reduced in the telencephalon; but expanded in the ventral thalamus	Aoto et al. 2002
	E12.5		Pattern of protrusions of the ventricular zone	Theil 2005
Ngn2	E12.5	Throughout the dorsal telencephalon	Detectable in the dorsal telencephalon	Tole et al. 2000a
Shh	E8.5-E 10.5	Exclusively confined to the ventral neural tube	Unaltered	Theil et al. 1999; Tole et al. 2000a; Aoto et al. 2002
Gli1	E9.5, E12.5	Confined to the ventral region of the neural tube	Unaltered	Theil et al. 1999; Tole et al. 2000a
Ptc1	E9.5, E12.5	Ventral part of the neural tube	Unaltered	Theil et al. 1999; Tole et al. 2000a
Nkx2.1	E9.5, E12.5	Ventral telencephalon and diencephalon	Unaltered	Theil et al. 1999; Tole et al. 2000a
	E11.5		Expanded dorsally	Aoto et al. 2002

Table 1.1 The expression of maker genes analyzed in the wild type and *Gli3*$^{Xt/Xt}$ mutant embryos (continue).

Gsh2	E12.5	The PSB and the lateral ganglionic eminence	Expands into cortical areas	Rallu et al. 2002b
Islet1	E12.5	Postmitotic neurons of the ventral telencephalon	Expanded in the dorsal telencephalon	Tole et al. 2000a
Mash1	E12.5	Ventral telencephalon	Expanded into cortical area	Rallu et al. 2002b; Theil 2005
Dlx2	E12.5	Ventral telencephalon	Unaltered	Theil et al. 1999
			Extended into dorsal telencephalon, most striking in the rostral part	Tole et al. 2000a; Aoto et al. 2002; Theil, 2005
Fgf8	E8.5-E 11.5	In the anterior neural ridge (ANR) and the roof of telencephalon and diencephalon	Up-regulation	Aoto et al. 2002
	E11.5; E12.5		Shows an extension into more caudal regions	Theil et al. 1999; Kuschel et al. 2003
	E12.5		Partially maintained in the dorsal midline of the telencephalon	Grove et al. 1998
Sprouty2	E12.5	Confined to the ANR	Expanded throughout the dorsal telencephalic midline	Kuschel et al. 2003

1.3.2.4 The cortical lamination of the *Gli3*$^{Xt/Xt}$ mutant embryos

Histological analyses of *Gli3*$^{Xt/Xt}$ mutants have shown that cortical lamination is lost (Franz, 1994; Theil et al., 1999). A recent study has shown that the mantle zone, the cortical plate and the subplate fail to form, and the cortical progenitors lose their apical-basal cell polarity (Theil, 2005). The loss of early cortical layers in the mutants was suggested to be caused by several defects, including a reduction of reelin and p73 positive Cajal-Retzius cells (Yang et al., 2000; Meyer et al., 2002), whereas another marker for early born Cajal-Retzius cells, Calretinin (del Rio et al., 1995), is increased in the mutant neocortex. These results suggest the Cajal-Retzius cells are misspecified in the mutant embryos (Theil, 2005).

1.3.3 Loss of Gli3 partially rescues *Shh*$^{-/-}$ telencephalic phenotype

Work on spinal cord has demonstrated that many of the ventral spinal cord defects observed in the *Shh*$^{-/-}$ mutants are partially rescued by removing one copy of Gli3 (*Shh*$^{-/-}$;*Gli3*$^{Xt/+}$), and further rescued in *Shh*$^{-/-}$;*Gli3*$^{Xt/Xt}$ double mutants (Litingtung and Chiang, 2000; Persson et al., 2002). In addition, studies on limb showed a similar result (Litingtung et al., 2002). These findings suggest that Shh is required to specify the ventral fate in the spinal cord and Gli3 normally suppresses this. In the telencephalon, Gli3 has been shown to partially rescue the telencephalic phenotype of *Shh*$^{-/-}$ mutants (Rallu et al., 2002b). However, this has not been fully studied due to a high incidence of exencephaly in the double mutants. Nonetheless, these results suggest that there might be other pathways working in parallel to the Shh-Gli3 one to induce DV patterning in the telencephalon.

1.3.4 Gli3 and cell growth and survival

Not much is know about Gli3 function in the cell cycle. The only information available comes from the analysis of BrdU labelling index in the E12.5 *Gli3*$^{Xt/Xt}$ mutant telencephalon (Theil et al., 1999), which showed no changes compared to wild types. Gli3 is suggested to regulate cell survival via a negative control of *Fgf8* (Aoto et al., 2002). *In vitro* studies have shown that *Gli3*$^{Xt/Xt}$ mutant cells survive better in cultures and release more survival promoting factors than the control telencephalic cells (Zaki et al., 2005), suggesting a role for Gli3 in regulating cell death.

1.4 AIM OF THE STUDY

The main aim of this thesis is to analyse further the *Gli3*$^{Xt/Xt}$ mutant forebrain to gain insight into the function of Gli3, and specifically:

1. To investigate whether Gli3 may act as a transcriptional repressor of the Shh signalling pathway in the telencephalon,

2. To study the *Gli3*$^{Xt/Xt}$ mutant dorsal telencephalon, and examine to what extent the dorsal telencephalon is affected by the loss of Gli3,

3. To study the *Gli3*$^{Xt/Xt}$ mutant ventral telencephalon,

4. To investigate whether Gli3 may regulate cell proliferation, cell differentiation and cell death in the developing telencephalon.

Chapter 2: Materials and Methods

2.1 ANIMALS

Mice were housed and bred according to Home Office regulations in a dedicated facility. *Gli3*$^{Xt/+}$ mice were maintained on a CBA background. *Foxg1*$^{+/-}$ mice were maintained on a mixed CBA X C57/B16 background. *Pax6*$^{Sey/+}$ mice were maintained on a mixed Swiss/CD1 background. *Shh*$^{-/-}$ mutant embryos were kindly provided by Dr. Laura Lettice (MRC, Human Genetics Unit, Western General Hospital, Edinburgh). Embryonic day (E) 0.5 was defined as the morning of the vaginal plug discovery.

2.2 GENOTYPING OF MICE

DNA samples from embryonic tissues of embryos from the *Gli3*$^{Xt/+}$ heterozygous matings (yolk sac for E11.5 or younger embryos, tail tip or limb bud for E12.5 or older embryos) were used for genotyping mice and embryos by polymerase chain reaction (PCR). *Gli3*$^{Xt/+}$ were identified by the presence of at least one extra digit on the hindlimbs. *Shh*$^{-/-}$ mutants embryos were identified by the characteristic fused telencephalic vesicles. *Pax6*$^{Sey/Sey}$ embryos were identified by the lack of eyes. *Foxg1*$^{-/-}$ embryos were identified by a smaller telencephalon compared to the wild type littermates and confirmed by PCR genotyping by Ben Martynoga.

2.2.1 DNA extraction

DNA was extracted from embryonic tissue samples for Hot SHOT PCR genotyping (Truett et al., 2000). Samples were incubated with an alkaline lysis buffer (25 mM NaOH, 0.2 mM disodium EDTA, pH 12) to 96 ˚C for 1 hour. After heating, samples

were cooled at 4 ˚C, and 75 μl neutralizing reagent (4mM Tris-HCl, pH 5) were added to each sample. 5 μl of the final preparation were used per each PCR reaction for E11.5 or younger embryos, and 5 μl of 1:10 dilution of the final preparation were used for E12.5 or older embryos.

2.2.2 PCR reaction and visualization of product

The PRC reaction mix contained: 50-100 ng genomic DNA, 2 μl 10X reaction buffer (1X: 20 mM Tris-HCl (pH 8.4), 50 mM KCl), 30 μM Magnesium Chloride, 5 pM of each forward and reverse primer (Table 2.1), 4 μM dNTP, 1U Taq Polymerase and ddH_2O. The PCR conditions were as follows: initial denaturation at 95 ˚C for 2 minutes, followed by 35 cycles of denaturation at 94 ˚C for 1 minutes, annealing at 63 ˚C for 20 seconds and extension at 72 ˚C for 50 seconds (Maynard et al., 2002). The C3 Forward /C3 Reverse primers amplified a wild type band of 193 bp and the 580 Forward/580 Reverse primers amplified a mutant band of 580 bp.

PCR products were run on 1% agarose gels (LE Seakem) in 1X Tris-boric acid-EDTA (TBE, 89 mM Tris-Base, 89 mM boric acid, 2 mM EDTA) buffer with 0.1 μg/μl Ethidium bromide (10 μg/ml stock, SIGMA) at 60 mA for about 45 minutes. The bands were visualized in a transilluminator under UV. The expected sizes were 193 bp wild type and 580 bp mutant band.

Primer	Sequence
C3 Forward ($Gli3^{+/+}$)	5'-GGCCCAAACATCTACCAACACATAG-3'
C3 Reverse ($Gli3^{+/+}$)	5'-GTTGGCTGCTGCATGAAGACTGAC-3'
580 Forward ($Gli3^{Xt/Xt}$)	5'-TACCCCAGCAGGAGACTCAGATTAG-3'
580 Reverse ($Gli3^{Xt/Xt}$)	5'-AAACCCGTGGCTCAGGACAAG-3'

Table 2.1 Primers used in $Gli3^{Xt}$ PCR genotyping.

2.3 EMBRYONIC FIXATION AND HISTOLOGY

2.3.1 Semithin sections

For semithin sections, embryos were dissected in cold phosphate-buffered saline (PBS, pH 7.4), and fixed in 4% paraformaldehyde (PFA) and 2% glutaraldehyde in PBS overnight at 4 ˚C. After being dehydrated through a series of ascending ethanols (50%, 70%, 90% and 100%), embryos were infiltrated and embedded in plastic (Technovit 7100, Kulzer Histo-Technik, Heraeus Kulzer, Germany), according to the manufacturer's recommendations. Blocks were cut in a frontal plane using a microtome with disposal Kulzer knives at 4 μm thickness. Sections were placed on a hot water bath (40 ˚C) and collected on poly-L-lysine (Sigma) coated slides before drying in a 37 ˚C oven for at least 2 hours. After drying, sections were stained with cresyl violet for detection of pyknotic nuclei.

2.3.2 Paraffin sections for immunohistochemistry and immunofluorescence

For most of the immunohistochemistry and immunofluorescence reactions, embryos were dissected in cold PBS, and fixed in cold 4% PFA in PBS overnight at 4 ˚C. Embryos were washed in cold PBS for three times, and dehydrated through a series of ascending ethanols (70%, 90%, 95% and 100%) prior to xylene washes and embedding in paraffin in an automated tissue processor (Tissue-Tek VIP, Sakura, see Table 2.2 for program used). Embryos younger than E11.5 were pre-embedded in 2% agarose (Sigma) in PBS before being processed. Paraffin blocks were cut at 10 μm (E12.5 and older embryos) or 7 μm (E11.5 and younger embryos), and sections were collected serially on poly-L-lysine (Sigma) coated slides. For cresyl violet staining, sections were dewaxed in xylene and rehydrated through a descending ethanol series (100%, 95%, 90% and 70%) to ddH_2O. Sections were incubated in cresyl violet

(0.5% with 1.2% acetic acid) for 1 minute before washing in ddH_2O, and being passed through 70% ethanol, 95% ethanol with acetic acid to 100% ethanol, prior to being washed in xylene and mounted with DPX (BDP).

For immunofluorescence against Sonic hedgehog (Shh), embryos were dissected in cold PBS and fixed in cold 4% PFA in PBS for 2 hours at 4 ˚C. Embryos were washed in cold PBS, and cryoprotected through 5%, 10% and 15% sucrose in PBS until they submerged at 4 ˚C. Embryos were embedded in a mixture of 15% sucrose and 7.5% gelatine (Sigma) in PBS overnight at 4 ˚C. They were then frozen on dry ice, and kept at -70 ˚C until sectioning. Blocks were cut on a Leica cryostat at 10 μm, and sections were collected on superfrosted slides (Fisher).

Step	Solution	Time (h)	Temperature	P/V	Agitation
1	50% Ethanol	1:00	R/T	On	Yes
2	80% Ethanol	1:00	R/T	On	Yes
3	95% Ethanol	1:00	R/T	On	Yes
4	99% Ethanol	1:00	R/T	On	Yes
5	99% Ethanol	1:00	R/T	On	Yes
6	Absolute Ethanol	1:30	R/T	On	Yes
7	Absolute Ethanol	2:00	R/T	On	Yes
8	Xylene	1:00	R/T	On	Yes
9	Xylene	2:00	R/T	On	Yes
10	Xylene	2:00	R/T	On	Yes
11	Wax	1:00	60 ˚C	On	Yes
12	Wax	1:00	60 ˚C	On	Yes
13	Wax	1:00	60 ˚C	On	Yes
14	Wax	1:00	60 ˚C	On	Yes

Table 2.2 Steps of the Tissue-Tek tissue processor.
R/T: room temperature. P/V cycle: 30 seconds ambient, 90 seconds pressure, 30 seconds ambient, 90 seconds vacuum.

2.3.3 Preparations for *in situ* hybridization

E10.5 embryos for whole mount *in situ* hybridization were dissected in RNase free

PBS and fixed in 4% PFA in PBS overnight at 4 ˚C. After being washed in PBS with 0.1% Triton X-100 (Fisher) (PBT1), embryos were dehydrated through a series of descending methanols in PBT1 (25%, 50% and 75%) to 100% methanol for 10 minutes each, at room temperature. Embryos were kept at -20 ˚C prior to use.

Embryos for *in situ* hybridization on paraffin sections were collected and embedded as for immunohistochemistry in paraffin wax, except all the solutions used were made in RNase free conditions. Blocks were cut at 10 μm and sections were collected serially on TESPA (Sigma) coated slides.

2.4.1 IMMUNOHISTOCHEMISTRY

Sections were dewaxed in xylene and rehydrated through a series of descending ethanols to PBS. Endogenous peroxidases were blocked with 3% H_2O_2 (stock 30%, Sigma) and 10% methanol in PBS for 15 minutes in the dark. After washing in PBS with 0.2% Triton X-100 (PBT2), antigen retrieval was carried out by microwaving sections at full power in 10 mM sodium citrate buffer (pH 6.0) for four times of 5 minutes each. After cooling for 20 minutes, sections were blocked in 10% normal goat serum (NGS) and 0.2% gelatine in PBT2 for an hour at room temperature and incubated with the primary antibodies at 4 ˚C overnight. All primary antibodies were diluted in PBT2 with 5% NGS, 0.2% gelatine at optimal conditions (Table 2.3).

Slides were washed for three times, 10 minutes each, in PBT2 and then incubated with appropriate biotinylated secondary antibodies (goat anti-mouse IgG and goat anti-rabbit IgG, 1:200, Dako) in 5% NGS, 0.2% gelatine in PBT2 for 1 hour at room temperature. After washing in PBT2 for three times, 10 minutes each, slides were incubated for 1 hour with avidin-biotin-peroxidase reagent (1:200 of the A and B reagents in PBT2, Vectorlabs). They were then washed in PBT2, three times, 10

minutes each, and visualized with 0.03% diaminobenzidine (stock 30% in Tris-HCl, Sigma)/ 0.0003% hydrogen peroxide (stock 30%, Sigma). Some reactions were counterstained with cresyl violet (as above), and after staining, slides were dehydrated through a series of ascending ethanols and cleared in xylene before mounting with DPX mountant (BDP).

2.4.2 IMMUNOFLUORESCENCE

Immunofluorescence was carried out following a similar protocol as for the immunohistochemistry, except that the washes and the blocking reagent were made with 0.1% Triton-X in PBS (PBT1) instead of PTB2. Fluorescence double immunohistochemistry was carried out by selecting two primary antibodies (Table 2.3) from two different species. Slides were incubated with the appropriate secondary antibodies (Table 2.4) for 1 hour in the dark at room temperature. TO-PRO-3 iodide (Molecular Probes, Invitrogen) was used to counterstain the cell nuclei. Fluorescence immunoreacted slides were mounted with Mowiol (Calbiochem).

Cryostat sections for Shh fluorescent immunohistochemistry were post-fixed for 10 minutes in 4% PFA at 4 ˚C, prior to three washes in cold PBS of 5 minutes each. Sections were blocked in PBS containing 4% NGS and 0.3% albumin from bovine serum (BSA, Sigma) (blocking buffer) for 2 hours at room temperature before adding mouse anti-Shh antibody (1:25) in blocking buffer, and were incubated overnight at 4 ˚C. Sections were washed in PBS for three times, 5 minutes each, and were incubated with secondary antibody (1:200, Alexa488 conjugated goat anti-mouse IgG1, Molecular Probes, Invitrogen, A21121) for 45 minutes at room temperature in the dark. Excessive antibodies were removed by washing with PBS for 10 minutes before mounting with Mowiol (Calbiochem).

Antigen	Species	Clone name	Optimal dilution	Source
BrdU	Rat monoclonal	BU1/75	1:100	Abcam
BrdU/IddU	Mouse	B44	1:100	BD Bioscience
β-III-tubulin	Mouse	Tuj1	1:800	Sigma
β-actin	Rabbit		1:500	Sigma
Calbindin	Rabbit		1:2000	Swant
Calretinin	Rabbit		1:2000	Swant
Cyclin D1	Rabbit		1:400	Abcam
Pan-Dlx	Rabbit		1:100	J. Kohtz
Dlx2	Rabbit		1:500	Abcam
Foxg1	Rabbit		1:500	Abcam
Gli3	Rabbit		1:100	Santa Cruz
Gsh2	Rabbit		1:1500	K. Campbell
Islet1	Mouse	39.4D5	1:50	DSHB
Lhx2/9	Rabbit		1:1000	T. Jessell
Lim1/2	Mouse	4F2	1:100	DSHB
Mash1	Mouse	24B7.2D11	1:100	BD Pharmingen
Nestin	Mouse	RAT401	1:50	DSHB
Nkx2.1	Mouse	8G7G3/1	1:100	Abcam
Olig2	Rabbit		1:10000	D. Rowitch
Pax2	Rabbit		1:100	Covance
Pax6	Mouse	PAX6	1:400	DSHB
Reelin	Mouse	G10	1:400	Chemicon
Shh	Mouse	5E1 supernant	1:25	DSHB
Tbr2	Rabbit		1:500	R. Hevner

Table 2.3 Primary antibodies used in this thesis.
Several monoclonal antibodies were obtained from the Developmental Studies Hybridoma Bank (DSHB) developed under auspices of the NICHD and maintained by the University of Iowa, Development of Biological Sciences, Iowa City, IA 52242.

Antibody	Conjugate	Immunoglobulins	Catalogue No.	Optimal dilution	Source
Goat anti-mouse	Alexa Fluor 488	IgG (H+L)	A11001	1:200	Invitrogen
Goat anti-mouse	Alexa Fluor 488	IgG_1	A21121	1:200	Invitrogen
Goat anti-mouse	Alexa Fluor 488	IgG (H+L) highly absorbed	A11029	1:200	Invitrogen
Goat anti-mouse	Biotinylated	IgG	E 0433	1:200	Dako
Goat anti-mouse	HRP	IgG	P 0447	1:200	Dako
Goat anti-rabbit	Alexa Fluor 568	IgG (H+L)	A11011	1:200	Invitrogen
Goat anti-rabbit	Biotinylated	IgG	E 0432	1:200	Dako
Goat anti-rabbit	HRP	IgG	P 0448	1:200	Dako
Goat anti-rat	Alexa Fluor 568	IgG (H+L)	A11077	1:200	Invitrogen

Table 2.4 Secondary antibodies used in this thesis.
Goat anti-mouse Alexa Fluor 488 IgG_1 was used with anti Shh antibody.
Goat anti-mouse Alexa Fluor 488 IgG (H+L) highly absorbed was used with anti-BrdU/IddU antibody.
Goat anti-mouse Alexa Fluor 488 IgG (H+L) was used with other primary antibodies.

2.5 MORPHOMETRIC MEASUREMENTS

Areal and volumetric measurements were carried out on E10.5 and E12.5 wild type and *Gli3*$^{Xt/Xt}$ mutant embryos. Tissue was processed, sectioned and mounted serially at a frontal (E10.5, 7 μm thickness-4 series; every 3 consecutive sections) or a coronal plane (E12.5, 10 μm thickness-4 series; every 4 consecutive sections) throughout the telencephalon. Each series of sections was immunoreacted with either Foxg1 or double immunofluorescence with Pax6 and Olig2 at E10.5, and with Foxg1, Pax6, Mash1 or Olig2 at E12.5. Four embryos per genotype were analysed in all cases, except for E12.5 embryos immunoreacted with Olig2, where 2 embryos of each genotype were included in the analysis. Photos of immunoreacted sections were taken serially throughout the telencephalon, and the expression domain of each protein was traced by Image Tool (UTHSCSA) to get the area of expression. The total volume was calculated by summing up all the areas and multiplying the sum by the section thickness. The area of expression of each protein was also compared on defined rostral, middle and caudal sections of the telencephalon at both ages. The rostral and caudal sections were chosen at about 30 μm from where the most rostral and caudal tips of the telencephalic lobes appear, and the middle sections were selected as the sections in the centre of the rostro-caudal axis. For each marker, two sections at each level were measured and averaged for each embryo. Examples of E10.5 and E12.5 wild type and *Gli3*$^{Xt/Xt}$ mutant embryos and defined sections are shown in Figure 5.1 and Figure 2.1, respectively. These embryos were scanned and reconstructed with optical projection tomography (OPT) microscope at the MRC Human Genetics Unit, Edinburgh, UK.

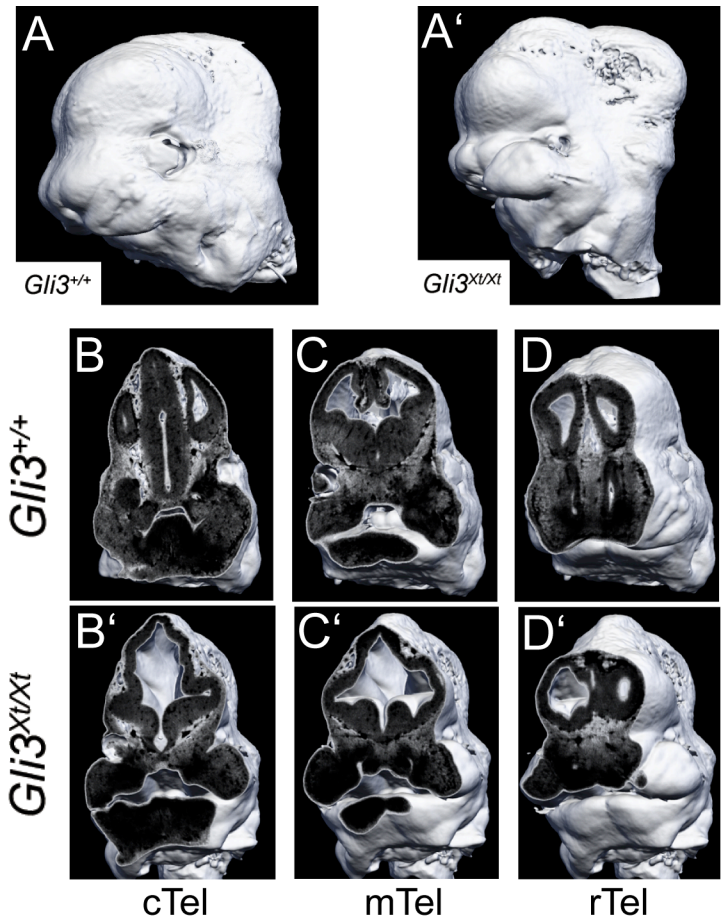

Figure 2.1 OPT images of E12.5 wild type (*Gli3*$^{+/+}$) and Gli3 mutant (*Gli3*$^{Xt/Xt}$) heads (A and A') and their defined caudal (cTel), middle (mTel) and rostral (rTel) telencephalic sections (B-D and B'-D').

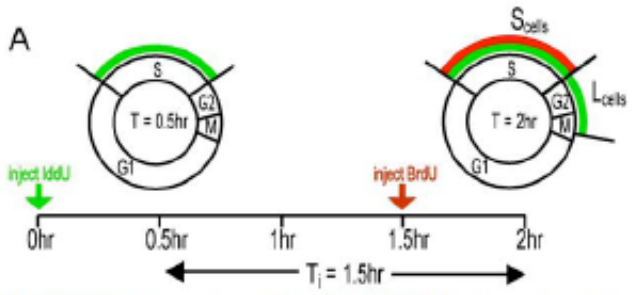

Figure 2.2 IddU/BrdU double labelling experiment allows the estimation of the duration of S-phase and cell cycle. Pregnant dams were injected with IddU at T=0 hr to label cells in S-phase at the beginning of the experiment. At T=1.5 hr, BrdU was given and the animals were sacrificed after 30 minutes, to label the cells in S-phase (S_{cells}) at the end of the experiment. During the interval (T_i=1.5 hr), some cells leave S-phase (L_{cells}), and they will be labelled with just IddU but not BrdU. (Martynoga et al., 2005)

2.6 CELL CYCLE STUDIES

2.6.1 Iododeoxyuridine (IddU) and bromodeoxyuridine (BrdU) injections

For double labelling experiments, pregnant females were intraperitonally injected with 200 μl (10 mg/ml) iododeoxyuridine (IddU, diluted in 0.9% NaCl) (50-70 mg per kilogram of body weight) (Sigma) and 1.5 hours later with the same amount of bromodeoxyuridine (BrdU) (Sigma). These animals were sacrificed after 30 minutes of the BrdU injection, and E10.5 and E12.5 embryos were collected. For BrdU labelling index experiments, a 30 minutes pulse of BrdU (as above) was given to pregnant dams, and E12.5 and E13.5 embryos were collected.

2.6.2 Measurements of cell cycle and S-phase duration

For IddU/BrdU double labelling, embryos were collected at E10.5 and processed as above (Chapter 2.4.2). This method allows the estimation of duration of S-phase (T_S) and cell cycle (T_C) (Fig. 2.2) (Shibui et al., 1989; Martynoga et al., 2005). IddU and BrdU are thymidine analogues that are incorporated into DNA synthesised during S-phase. Cells that are in S-phase at the beginning of this experiment are labelled with IddU and those in S-phase at the end of the experiment are labelled with both BrdU and IddU (S_{cells}). The interval during which cells are labelled with IddU but not BrdU is 1.5 hours. Thus, cells that leave the cell cycle (L_{cells}) will be labelled with IddU but not BrdU, and cells entering the cell cycle during the last 30 minutes will be labelled with only BrdU. By antibody staining, it is possible to distinguish BrdU positive cells from those that are positive for both IddU and BrdU, which allows the counting of the L_{cells} and S_{cells}. Counts of BrdU positive cells and BrdU and IddU positive cells were done in 60 μm wide sampling bins distributed in the dorsal and ventral telencephalon along the rostro-caudal axis of wild type and *Gli3*$^{Xt/Xt}$ mutant

embryos (2-4 bins in each area (dorsal and ventral telencephalon) per embryo, five embryos per genotype).

T_S and T_C are calculated using the two formulas below:

$$T_S = 1.5/(L_{cells}/S_{cells})$$

$$T_C = T_S/(S_{cells}/P_{cells})$$

P_{cells} is the total number of cells that are proliferating in the ventricular zone. Immunoreactivity to β-III-tubulin (Tuj1) was used to label the postmitotic neurons. Thus, P_{cells} is calculated as the number of cells that are negative for Tuj1 throughout the thickness of the dorsal and ventral telencephalon.

2.6.3 Calculation of labelling index

The labelling indices (LI) of BrdU and IddU in two hours at E10.5 were calculated as double labelled cells in proportion to total number of cells in the ventricular zone (counterstained by TO-PRO-3) in the wild type and mutant telencephalon (n=5 per genotype). Counts were done in bins as described above (Chapter 2.6.2).

A short pulse of BrdU was given to pregnant females, and E12.5 and E13.5 embryos were collected and processed as above (Chapter 2.4.2). BrdU-labelled and total number of cells (counterstained by TO-PRO-3) in the ventricular (proliferative) zone were counted in 125 μm wide strips through the thickness of the neocortex to give the labelling index (LI). In the wild type neocortex, samples were taken from the dorsal, dorso-lateral and lateral neocortex (box a, b and c in Fig 4.11A, respectively). Samples were taken throughout the neocortex in the mutant. The percentage of cells that were outside the ventricular zone in relation to the total number of cells throughout the thickness of the cortex was also calculated to estimate the size of the

postmitotic layer (PL). Four to twelve fields of view from control (n=4) and *Gli3*$^{Xt/Xt}$ (n=6) embryos were counted at each age.

2.7 *IN SITU* HYBRIDIZATION

2.7.1 RNA probe preparation

1) Riboprobes

The Shh plasmid for riboprobe synthesis was a gift from J. Rubenstein's lab, University of California, CA. The Wnt8b plasmid for riboprobe synthesis was a gift from J. O. Mason (University of Edinburgh, UK). A 669 bp fragment (nucleotides 560-1170) of Gli3 mouse cDNA was a gift from T. Theil, (University of Edinburgh, UK), and was PCR-amplified and subcloned into a pGEM-T Easy Vector (Promega) as described in (Zaki et al., 2005) (Table 2.5).

2) Transformation

About 1 ng of plasmid was added to 50 μl of chemically competent cells (One Shot TOP10, Invitrogen) and incubated for 10 minutes on ice before heating at 42 ˚C for 45 seconds. After cooling on ice for 20 minutes, bacteria were recovered in 500 μl SOC medium (Invitrogen) for 1 hour at 37 ˚C with shaking. 20 to 200 μl from each transformation were spread on separate LB (Luria broth) agar (Sigma l-2897) plates containing ampicillin (100 μg/ml, Roche 835242), and incubated at 37 ˚C overnight.

3) Bacterial cultures and extraction of plasmid DNA

Bacteria picked from a single colony were cultured in LB medium (Sigma) overnight at 37 ˚C with agitation. Plasmid DNA was extracted by using Qiagen midi or maxi-prep kits. DNA was incubated with a digestion mix, containing: 1-3 μg DNA, 1-3 units of appropriate restricted enzyme (Table 2.5), 10X reaction buffer, 0.1 mg/ml Bovine Serum Albumin (BSA) in ddH_2O, at 37 ˚C for 2 hours. A small amount was run on an agarose gel with DNA ladder of known concentration (1 kb DNA ladder, Roche) to quantify the yield and confirm plasmid linearization.

4) Labelling of probes

1 μg of linearized plasmid was transcribed by T3 or T7 RNA polymerase (Table 2.5) with a digoxigenin (DIG) labelled nucleotide mix (Roche Applied Science) at 37 ˚C for 2 hours. Labelled RNA probes were precipitated with 4M LiCl and cold ethanol and resuspended in 50 μl of sterile, RNase free ddH_2O, and stored at -80 ˚C. Probes were quantified by Boehringer DIG Quantification test strips (Roche Applied Science 1714755) and Boehringer DIG control test strips (Roche Applied Science 1714791), according to the manufacturer's instruction.

Probes	Plasmid Source	Restriction enzyme	Polymerase	Enzyme Source
Gli3	T. Theil	SpeI	T7	New England BioLabs
Shh	J. Rubenstein	HindIII	T3	New England BioLabs
Wnt8b	J. Mason	XbaI	T3	New England BioLabs

Table 2.5 RNA probes used in this thesis.

2.7.2 Whole mount *in situ* hybridization

Whole mount *in situ* hybridization was carried out following a published protocol (Theil et al., 2002b). Embryos were prepared as described in Chapter 2.3.3, and rehydrated through a series of descending methanols to PBT1 before treatment with proteinase K (10 mg/ml, Sigma) for 5-10 minutes. Small holes were made using fine needles (30G 1/2, Microlance) at the back of the heads of embryos for better probe penetration. Embryos were then post-fixed in 4% PFA, 0.1% glutaraldehyde in PBT1. After a few washes in PBT1, embryos were pre-hybridized in pre-hybridization mix (50% de-ionized formamide, 5X SSC (1X SSC: 0.15 M NaCl, 15 mM Trisodium citrate, pH 7.5), 0.1% Triton X-100, 50 μg/ml heparin, 0.1 mg/ml yeast tRNA and 5 mM EDTA) at hybridization temperature (65 ˚C in this study) for 1-2 hours. The pre-hybridization mix was replaced by pre-warmed pre-hybridization mix with 150-300 mg/ml of labelled probe, and embryos were hybridized at the same temperature overnight with rotation.

Embryos were washed twice for 30 minutes each in pre-hybridization mix and solution 1 (50% formamide in 1X SSC with 0.1% Triton X-100), 20 minutes in 1:1 solution 1 : MABT (100 mM Maleic acid (Sigma) pH 7.5, 150 mM NaCl, 0.1% Triton X-100) at 65 ˚C, and then with MABT twice for 10 minutes at room temperature. Embryos were then blocked with blocking solution (2% Boehringer blocking reagent (Roche Applied Science), 20% sheep serum (Sigma) in MABT) for 2-4 hours at room temperature before replacing with sheep anti-DIG antibody (1:2000, Roche Applied Science) diluted in blocking solution and incubating for 16 hours at 4 ˚C with agitation. After five one hour washes in MABT at room temperature, embryos were washed twice with freshly prepared NTMT (100 mM NaCl, 100 mM Tris-HCl, pH 9.5, 50 mM $MgCl_2$, 0.5% Tween-20, 0.2 mg/ml

Levamisole (Sigma)) prior to staining with NTMT containing 2% stock p-nitrotetrazolium blue chloride / 5-bromo-4-chloro-3-indolyl-phosphate (NBT/BCIP, Roche Applied Science) in the dark. After the colour had developed to a desired extent (approximately 2 hours), embryos were washed with PBS, fixed in 4% PFA, and kept in 60 % glycerol.

2.7.3 *In situ* hybridization on paraffin sections

In situ hybridization on paraffin sections was carried out following a published protocol with slight modification (Nieto et al., 1996). Sections were dewaxed in Histoclear (Fisher) and rehydrated through a descending series of ethanol to 2X SSC. After incubating in proteinase K for 7.5 minutes and washing in 2X SSC for 30 minutes at room temperature, slides were post-fixed in 4% PFA for 15 minutes. Samples were treated with 0.2 M HCl for 15 minutes, and 0.1 M Triethanolamine (TEA, Sigma) for 30 seconds and then with 3.125 μl/ml acetic anhydride in 0.1 M TEA for 10 minutes before being pre-hybridized in pre-hybridization mix (50% formamide (deionised, Sigma), 2X SSC, 5X Denhardt's (Sigma), 10% Dextran (Sigma), 0.2 mg/ml yeast tRNA, 0.5% SDS, DEPC (Diethyl pyrocarbonate, Sigma) treated ddH_2O) for 1-2 hours at 60 ˚C. Hybridization was carried out using approximately 150 mg/ml probe in pre-hybridization mix for each slide, overnight in a humidified chamber at 60 ˚C.

After hybridization, slides were washed in 2X SSC for 10 minutes at 50 ˚C, 50% formamide in 2X SSC for 45 minutes at 60 ˚C, 4X SSC for 5 minutes at 50 ˚C, 4X SSC plus 20 μg/ml RNase A for 30 minutes at 37 ˚C, 2X SSC for 30 minutes at 50 ˚C, PBST1 for 10 minutes and PBST1 with 1% BSA at room temperature prior to incubation with anti-DIG antibody diluted in 1% BSA, PBT1 at 4 ˚C overnight. Slides were then washed in PBT1 three times, 20 minutes each, and incubated in

buffer 3 (0.1 M Tris-HCl, 0.1 M NaCl, 0.05 M $MgCl_2$) for 5 minutes before the colour reaction in staining solution (1% NBT/BCIP stock in buffer 3) to obtain the desired colour. Slides were mounted with Aquamount (BD Bioscience) after brief washes with PBS.

2.8 TERMINAL DEOXYNUCLEOTIDYL TRANSFERASE (TDT) -MEDIATED DUTP-BIOTIN NICK END LABELLING (TUNEL)

2.8.1 Whole mount TUNEL

E10.5 embryos were dissected in cold PBS, fixed in cold 4% PFA in PBS overnight and washed in PBS the day before dehydration through an ascending ethanol series and kept at -20 ˚C in 100% ethanol until use. Whole mount TUNEL was performed following a published protocol (Smith and Cartwright, 1997) using ApopTag *in situ* apoptosis detection kit (Chemicon International). Briefly, embryos were rehydrated through a descending ethanol series to PBS, and incubated in equilibration buffer (supplied by the manufacturer) for 5 minutes at room temperature prior to adding working strength terminal deoxynucleotidyl transferase (TdT) enzyme solution (70% reaction buffer: 30% enzyme, supplied by the manufacturer) for 2 hours at 37 ˚C in a humidified chamber. The reaction was terminated by adding stop buffer (supplied by the manufacturer) at 37 ˚C for 20 minutes. After the reaction, embryos were washed in freshly prepared TBST (0.14 M NaCl, 10 mM KCl, 25 mM Tris-HCl pH 7.0, 0.1% Tween-20, 1 mM Levamisole) and NTMT (0.1 M NaCl, 0.1 M Tris-HCl pH 9.5, 50 mM $MgCl_2$, 0.1% Tween-20, 2mM Levamisole), for 15 minutes in each solution, before being blocked in TBST with 10% sheep serum for 30 minutes at room temperature. After incubating with anti-DIG antibody (1:3000, Roche Applied Science) in NTMT for 40 minutes at room temperature, samples were washed in TBST and NTMT respectively for three times, 10 minutes each. Staining was

visualized by incubating embryos with 2% NBT/BCIP (Roche Applied Science) in NTMT for about 10 minutes in the dark. The staining was stopped by adding PBS with 10 mM EDTA, and embryos were post-fixed in 4% PFA. After a few washes in PBS, embryos were cleared in a graded series of glycerols and stored in 60% glycerol at 4 ˚C.

2.8.2 TUNEL on paraffin sections

Embryos were collected and processed as for immunohistochemistry (Chapter 2.3.2). TUNEL on paraffin sections was performed by using the *In Situ* Cell Death Detection Kit Fluorescein (Roche Applied Science). Sections were dewaxed in xylene and dehydrated through a descending ethanol series to PBS before treating with proteinase K for 15 minutes at 37 ˚C. After washing in PBS for 10 minutes, antigen retrieval was carried out by microwaving sections in 10 mM sodium citrate buffer (pH 6.0) for 2 minutes in low power. Slides were incubated with reaction mix (10% enzyme solution: 90% label solution, supplied by the manufacturer) at 37 ˚C for an hour. After a few washes in PBS in the dark, samples were counterstained with TO-PRO-3 for 10 minutes, and slides were mounted with Mowiol (Calbiochem).

2.9 CULTURES OF EMBRYONIC TELENCEPHALON

Heads of E9.5 embryos were dissected and cut into two half hemispheres manually in cold EBSS medium, and cultured on poly-L-lysine (Fisher) coated 6 wells plates containing 2 ml of defined culture medium (see below) plus 10% foetal bovine serum (Sigma). After 1 hour incubation at 37 ˚C in a 5% CO_2 humidified chamber, 2 μg/ml of anti-Fgf8b antibody (R&D system) was added to one half of the heads. The other half was used as control. Both pieces of tissue were cultured for 16 hours. Explants were fixed in 4% PFA and washed in PBS with 0.25% Tween-20 (PBSTw) for 10

minutes prior to dehydration through an ascending series of methanols in PBSTw up to 100% methanol. Explants were stored at -20 ˚C in 100% methanol until whole mount immunofluorescence was performed.

EBSS medium was prepared by mixing the following reagents together under sterile conditions and stored at 4 ˚C until use.

100 ml Earle's balanced salt solution 10X (EBSS) (Sigma E7510)

0.22 g Na_2HCO_3 (Sigma S5761, final concentration 22 mg/ml)

0.065 g Glucose (Sigma G7021, final concentration 6.5 mg/ml)

900 ml double deionised H_2O

EBSS was oxygenated by bubbling with 95% O_2 and chilled on ice before use.

Serum free culture medium was prepared by mixing the following reagents together under sterile conditions and stored at 4 ˚C until use.

100 ml F12 (Sigma N4888)

100 ml Dulbecco's modified Eagles' medium (DMEM) (Sigma D5671)

1 mg Insulin (Sigma I6634, final concentration 5 μg/ml)

2 mg apo-transferrin (Sigma T1147, final concentration 10 μg/ml)

3 ml HEPES buffer (Sigma H0887)

0.24 g Na_2HCO_3 (Sigma S5761, final concentration 0.12 mg/ml)

3 ml antibiotics (100 mg Gentamycin (Sigma G1264) and 100 mg Kanamycin (Sigma K1377) diluted in 20 ml sterile double deionised water)

2 ml Putrescene (161.1 mg Putrescene (Sigma P5780) diluted in 100 ml ddH_2O)

20 μl Progesterone (6.29 mg Progesterone (Sigma P8783) diluted in 100 ml ethanol)

20 μl Na_2SeO_3 (5.2 mg Na_2SeO_3 (Sigma S5261) diluted in 100 ml sterile ddH_2O)

2 ml $_L$-glutamine (6.344 g $_L$-glutamine (Sigma G2128) diluted in 100 ml ddH_2O)

Medium was warmed and equilibrated in a 37 ˚C humidified incubator containing 5%

CO_2 for at least one hour before use.

2.10 IMMUNOFLUORESCENCE ON CULTURED EXPLANTS

Explants were bleached in methanol: 30% Hydrogen peroxide (5:1) for 1-2 hours at 4 ˚C with agitation prior to rehydration through descending methanol series to PBST1. Antigen retrieval was carried out by microwaving the explants for 2 minutes in sodium citrate (10 mM). They were then blocked in PBST1 with 5% goat serum (Sigma) (blocking solution) for 1 hour at 4 ˚C with rocking. Rabbit anti-Olig2 antibody (1:200 in blocking solution) was added to the explants and incubated overnight at 4 ˚C with agitation. Explants were washed in PBST1 for 30 minutes at room temperature prior to overnight washes at 4 ˚C with several changes of PBST1. A fluorescently conjugated goat anti-rabbit secondary antibody (goat anti-rabbit Alexa568, 1:200, Molecular Probes) was added to the explants at 4 ˚C overnight before washing in PBST1 for 30 minutes at room temperature and 4 ˚C overnight with rocking. Explants were post-fixed in 4% PFA for 1 hour at room temperature and cleared and kept in 60% glycerol.

2.11 PHOTO IMAGING

Slides for immunohistochemistry, *in situ* hybridization and TUNEL were examined and photographed with a Leica DMLB upright compound microscope with a DSC480 digital camera. Double immunofluorescence reacted slides and whole mount immunofluorescent explants were imaged with a Leica TCS NT confocal microscope. Whole mount *in situ* hybridization and TUNEL reacted embryos were either photographed on a Wild M5A dissecting microscope with a Nikon Coolpix 995 digital camera or scanned and reconstructed by optical projection tomography (OPT) microscope (Sharpe et al., 2002) at the MRC Human Genetic Unit in

Edinburgh.

2.12 PROTEIN EXTRACTION FROM MOUSE EMBRYOS

E12.5 mouse whole heads or telencephalic tissue was dissected in cold PBS and frozen on dry ice immediately. The telencephalon was dissected into dorsal and ventral, or rostral, middle and caudal part, respectively. Tissues were washed and homogenized in freshly made buffer H (20 mM Tris-HCl with the following protease inhibitors: 1 μg/ml Leupeptin, 1 μg/ml Aprotinin, 17 μg/ml PMSF) and then mixed with Laemmli SDS sample buffer (25 mM Tris-HCl, 2% SDS) prior to sonicating for three times, 30 seconds each. β-Mercaptoethanol was added to the mix at a final concentration of 5%, and then samples were boiled for 10 minutes, aliquoted and stored at -70 ˚C. Proteins were quantified with BSA (bicinchoninic acid) Protein Assay Reagent (PIERCE) according to the manufacturer's instructions. Each protein sample has been tested at least in two individual western blots, and at least two embryos from each genotype were analysed.

2.13 WESTERN BLOTTING

10 μg of protein sample was loaded to a precast gel (Invitrogen) and run for 1-1.5 hours at 150V with appropriate running buffer (Table 2.6). After transferring samples to a nitrocellulose membrane (Bio-Rad) for 2 hours at 150V at 4 ˚C, the membrane was blocked in PBS with 0.25% Tween-20 and 10% goat serum (blocking buffer), and then incubated with primary antibody (Table 2.6) for an hour at room temperature or overnight at 4 ˚C. After incubating with HRP-conjugated anti-mouse or anti-rabbit IgG secondary antibody (1:200, Dako cytomation) for 45-60 minutes at room temperature, signal was detected using ECL Plus detection (GE Healthcare) on an X-ray film (Kodak, BioMax, XAR film, Sigma) according to the instructions of

the manufacturer. Following the detection of primary antibody, the membrane was incubated for an hour with rabbit anti-β-actin antibody (1:500, Abcam) to confirm loading and allow normalization. Band intensity was scanned and measured using a densitometer and the Quantity One-4.0.3 software (Bio-Rad).

Antibody	Gel	Running Buffer (RB)	Transfer Buffer (TB)	Antibody Conditions
rabbit anti-Gli3	NuPAGE 3-8% Tris Acetate	NuPAGE Tris-Acetate RB	NuPAGE TB	1:100, Santa Cruz, 1 hour, RT
mouse anti-Pax6	NOVEX 12% Tris-Glycine	Tris Glycine RB	Tris Glycine TB	1:200, DSHB, O/N, 4 ˚C
mouse anti-Shh	NuPAGE Novex 10% Bis-Tris	NuPAGE MES SDS RB	NuPAGE TB	1:25, DSHB, O/N, 4 ˚C

Table 2.6 Antibodies and corresponding gels and buffers used for western blotting in this thesis. Gels and buffers were obtained from Invitrogen.
RT, room temperature; O/N, overnight.

2.14 DATA ANALYSIS AND GRAPH PLOTTING

Statistical analyses were done and graphs were generated by EXCEL (Microsoft) and Sigmastat (Systat Software Inc.). Statistical tests used in this thesis were Student's *t*-test (most cases) and One Way ANOVA (for comparison of Gli3 protein expression in rostral, middle and caudal parts). Each sample corresponded to average measurements from each embryo. When $P<0.05$, difference between samples was considered significant.

Chapter 3: Gli3 expression in the developing telencephalon

3.1 INTRODUCTION

As mentioned in the Introduction, Gli3 acts as an important regulator of the Shh signalling pathway. When Shh is present, full length Gli3 responds to Shh and functions as a transcriptional activator (Gli3-F). In the absence of Shh, Gli3 protein is cleaved to form a short cleaved form of Gli3 (Gli3-C), which acts as a transcriptional repressor (Ruiz i Altaba, 1999; Sasaki et al., 1999; Shin et al., 1999). Gli3 activity has been shown to be negatively regulated by Shh in spinal cord and limbs (Masuya et al., 1995; Marigo et al., 1996; Ruiz i Altaba, 1998; Wang et al., 2000). Clues to gene function can often be obtained by examining when and where a gene is expressed, thus Gli3 expression is studied here.

The expression of *Gli3* mRNA is first detected around E7, and is found throughout embryogenesis in derivatives of both the ectoderm and the mesoderm (Hui et al., 1994). The onset of the expression in the neural ectoderm begins at the primitive streak stage. *Gli3* is first expressed in rather broad domains; in general, the expression domain becomes more restricted at later stages of development. *Gli3* is normally expressed in the telencephalon, the diencephalon, the midbrain and the hindbrain during gestation and in the cerebellum during postnatal development of the wild type embryos (Schimmang et al., 1992; Hui and Joyner, 1993; Hui et al., 1994).

However, there is no detailed description of *Gli3* mRNA or protein expression in the developing telencephalon, or whether there is any Gli3 protein made in the $Gli3^{Xt/Xt}$ mice. Here, by using *in situ* hybridization, the expression pattern of *Gli3* mRNA is studied on coronal sections in E12.5 and E14.5 wild type embryos, and the distribution of the two isoforms of Gli3 protein in the dorso-ventral and rostro-caudal

axes of the developing telencephalon is examined by western blot.

The *Gli3* mRNA *in situ* hybridization experiment described in this chapter was completed in collaboration with Vassiliki Fotaki. Some of the results in this chapter have been published (Zaki et al., 2005; Fotaki et al., 2006) and these papers are bound into this thesis and will not be cited again in this chapter.

3.2 RESULTS

3.2.1 *Gli3* mRNA expression

The expression of *Gli3* mRNA in mouse forebrain was examined at E12.5 and E14.5. *In situ* hybridization showed that in the telencephalon of E12.5 wild type embryos, *Gli3* expression was found in the ventricular zone of the developing neocortex and cortical midline at both ages (Fig. 3.1A and B). No expression was detected in the choroid plexus (Fig. 3.1B), in agreement with previous studies (Grove et al., 1998). In the ventral telencephalon, there was a ^{high}lateral-to-^{low}medial gradient of expression of *Gli3* through the ventricular zone of the lateral (LGE) and medial ganglionic eminence (MGE) (Fig. 3.1B). *Gli3* expression was also found in the ventricular zone of diencephalon, in a high to low gradient from the epithalamus through dorsal to ventral thalamus (Fig. 3.1A), and in the hypothalamus at the level of the optic chiasm (Fig. 3.1B). At E14.5, *Gli3* is found in the ventricular zone of the neocortex and the ganglionic eminences (GE) (Fig. 3.1C), and the expression at E14.5 seems to be reduced compared to E12.5.

3.2.2 Gli3 protein expression

The structure of the two isoforms of Gli3 protein and the cleavage site are shown in

Figure 3.1D. To detect expression of Gli3 in wild type embryos and whether there is any Gli3 protein made in the *Gli3*$^{Xt/Xt}$ mutants, western blot and immunohistochemistry were performed on wild type and *Gli3*$^{Xt/Xt}$ mutants. At present, there are several commercial antibodies directed against Gli3 available (Table 3.1), and their epitopes are shown in Figure 3.1E. All of them were evaluated by western blot, but only the rabbit anti-Gli3 antibody (Santa Cruz, H-280) gave reliable results.

Name	Species	Epitope	Source
Gli3 antibody (ab6050)	Rabbit	amino acids 45-57	Abcam
GLI-3 (H-280)	Rabbit	amino acids 1-280	Santa Cruz Biotechnology
GLI-3 (N-19)	Goat	N-terminus	Santa Cruz Biotechnology
GLI-3 (C-20)	Goat	C-terminus	Santa Cruz Biotechnology

Table 3.1 Commercial anti-Gli3 antibodies tested in this thesis.

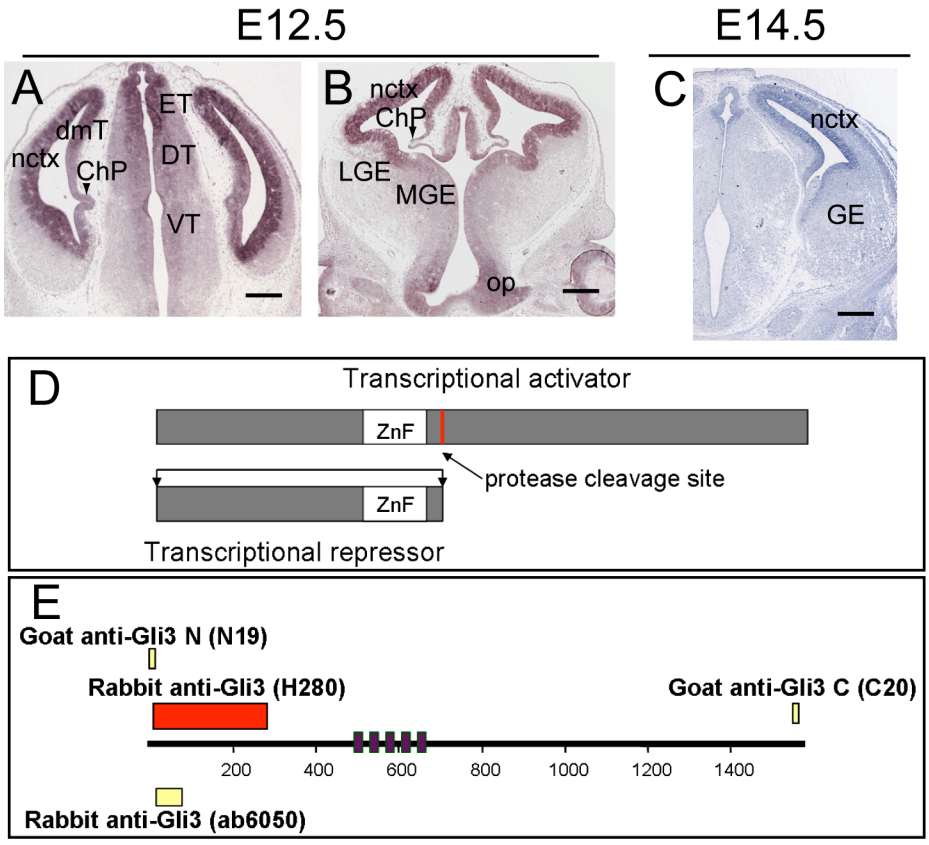

Figure 3.1 *In situ* hybridization on E12.5 (**A** and **B**) and E14.5 (**C**) wild type coronal sections show *Gli3* mRNA expression. At E12.5, *Gli3* is expressed in the epithalamus (ET), dorsal (DT) and ventral (VT) thalamus (**A**) and hypothalamus at the level of optic chiasm (op) (**B**) of the diencephalon. In the telencephalon, *Gli3* is highly expressed in the neocortex (nctx) and dorso-medial telencephalon (dmT), but not in the adjacent choroid plexus (ChP) (**A** and **B**). In the ventral telencephalon, *Gli3* expression has a ^{high}lateral-to-^{low}medial gradient (**B**). At E14.5, Gli3 expression is observed in the ventricular zone of the neocortex (nctx) and the ganglionic eminences (GE) (**C**). Scale bars, 250 μm. **D** shows schematically the protease cleavage site of the Gli3 protein and the two isoforms. The zinc finger domain (ZnF) is the DNA binding site. (**E**) Schematic diagram of the Gli3 protein. The purple boxes represent the five zinc fingers. The commercial anti-Gli3 antibodies used in this thesis with their corresponding epitopes (boxed area) are shown above and below the Gli3 protein.

Western blots showed bands at approximately 170 kDa and 80 kDa in E12.5 and E14.5 wild type extracts from dorsal and ventral telencephalon that were absent from *Gli3*$^{Xt/Xt}$ tissue (Fig. 3.2A) and corresponded to the previously described full-length (Gli3-F) and cleaved forms (Gli3-C) of Gli3 (Dai et al., 1999; Ruiz i Altaba, 1999). The antibody also detected non-specific bands of intermediate size and unknown identity (Fig. 3.2A). At E12.5 levels of Gli3 protein were approximately two-fold higher in the dorsal than in the ventral telencephalon (Fig. 3.2B), reflecting the pattern of *Gli3* mRNA expression (Fig. 3.1A and B). Overall, the highest concentration of Gli3 was of the cleaved form in the dorsal telencephalon (mean density is 5.62 ± 0.30 in the dorsal telencephalon, and 2.66 ± 0.85 in the ventral telencephalon, Student's *t* test, $p<0.05$, n=4, Fig. 3.2C). The ratio between the cleaved and full length isoforms was quantified in these tissues at E12.5. Dorsally, the cleaved form was present at 2.75 times (± 0.45, n=7) the concentration of the full length form, whereas ventrally the ratio was lower, at 1.33 (± 0.50, n=8) (Fig. 3.2D). These differences are statistically significant (Student's *t* test, $p<0.05$, n=7/8).

As *Gli3*$^{Xt/Xt}$ mutant embryos show morphological defects along the antero-posterior axis (see Chapter 5), the distribution of Gli3 proteins was also measured in rostral (rTel), middle (mTel) and caudal (cTel) wild type telencephalon (Fig. 3.2B) at E12.5. Although tissue from 8 different embryos was analyzed, it was not possible to detect any significant difference between the ratio of the two Gli3 isoforms and the total amount of Gli3 protein in rostral, middle and caudal telencephalon. Two individual western examples (Fig. 3.2B) are shown here. β-actin expression was used to confirm equal loading. Overall, sample 1 seems to have more full length Gli3 protein (Gli3-F) than sample 2 (Fig. 3.2B). In sample 1, rostral telencephalon (R1) seems to have less Gli3-F than the other two parts (M1 and C1) of the telencephalon, while in sample 2 the caudal telencephalon (C2) has the lowest amount of Gli3-F protein (Fig. 3.2B). The quantification results showed that overall there is slightly more Gli3

(Gli3-C+Gli3-F) in the middle telencephalon than in the rostral or caudal parts (n=4) (Fig. 3.2E), and the ratio between cleaved Gli3 isoform and the full length in rostral, middle and caudal telencephalon is 3.4 (± 1.3, n=5), 4.4 (± 1, n=6) and 5.6 (± 1.6, n=5) respectively (Fig. 3.2F). None of these differences is significant (One Way ANOVA, SigmaStat), which might be due to variations between embryonic dissections.

Once the rabbit anti-Gli3 antibody (Santa Cruz, H-280) had been validated by western blot, it was used for immunohistochemistry on wild type (Fig. 3.3A and B) and *Gli3*$^{Xt/Xt}$ mutants (Fig. 3.3A' and B') on coronal paraffin sections. At both E12.5 and E14.5, Gli3 seems to be expressed not only in the cerebral cortex and thalamus of the wild type embryos (Fig. 3.3A and B), but also in these regions of *Gli3*$^{Xt/Xt}$ mutants (Fig. 3.3A' and B'). The Gli3 immunostaining in the mutants might reflect the bands that appeared in the western blot with the mutant tissues (Fig. 3.2A). Because this antibody gave strong signal in the mutant tissue, it was not used further for protein expression studies. Although the protein expression in the wild type embryos resembles the ^{high}dorsal-to-^{low}ventral mRNA expression pattern (Fig. 3.1A and B).

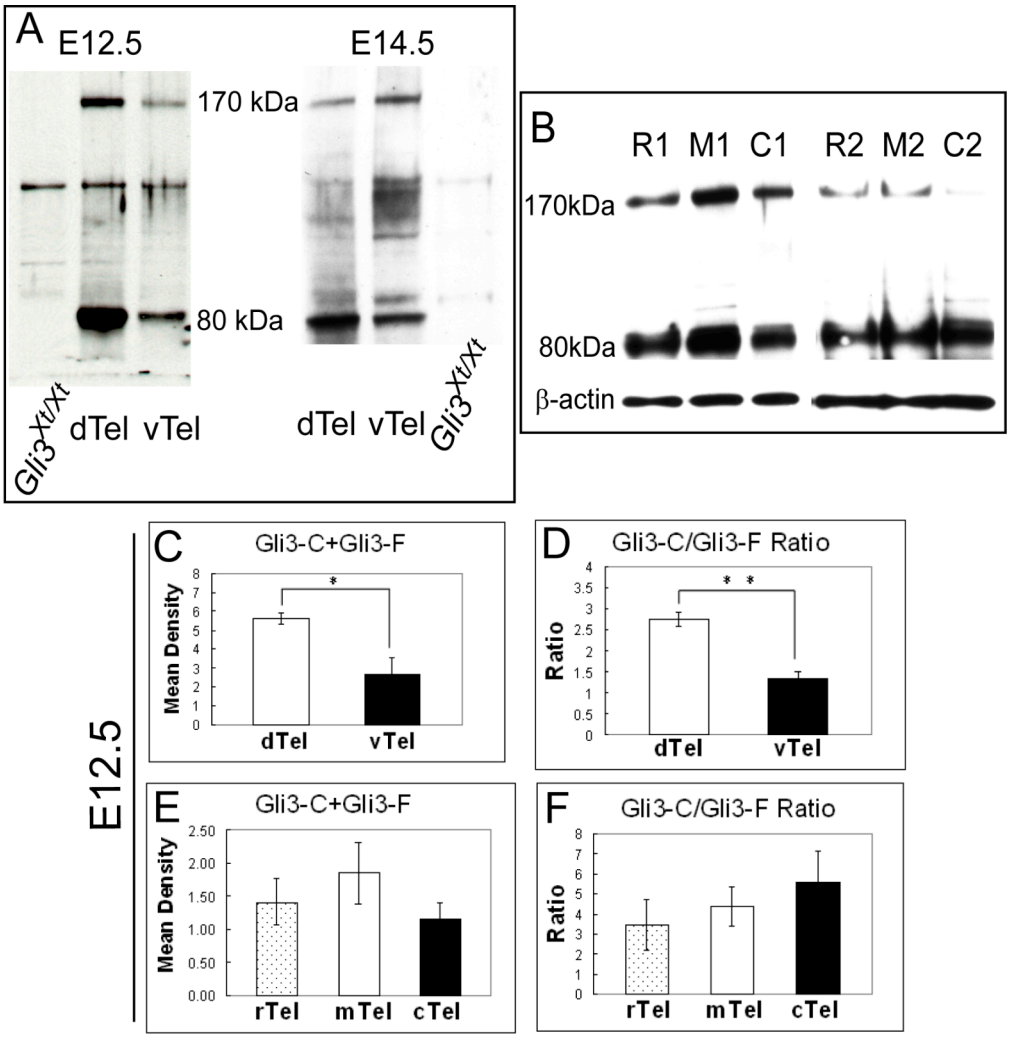

Figure 3.2 (**A**) Western blot of *Gli3*$^{Xt/Xt}$ mutant head and wild type dorsal (dTel) and ventral (vTel) telencephalic tissue with rabbit anti-Gli3 antibody (Santa Cruz, H-280) at E12.5 and E14.5. At both ages, bands at 170k Da and 80 kDa are observed in the wild type dorsal and ventral telencephalon, corresponding to the full length (Gli3-F) and cleaved (Gli3-C) isoform of Gli3 protein, respectively. These bands are absent in the *Gli3*$^{Xt/Xt}$ mutant tissue. At E12.5, the total amount (mean density) of Gli3 (Gli3-F+Gli3-C) (**C**) in the dorsal telencephalon is significantly increased than that of the ventral telencephalon. (**D**) The measure relative ratio between cleaved and full length Gli3 (Gli3-C/Gli3-F) shows there is about three times more cleaved Gli3 in the dorsal telencephalon than in the ventral telencephalon. Two individual western blots with different rostral (R), middle (M) and caudal (C) telencephalic (Tel) samples show Gli3 expression along the rostro-caudal axis. β-actin was used as loading control (**B**). The measurements of mean density of total amount of Gli3 protein (**E**) and the relative ratio between the two isoforms (**F**) did not show any significant among groups.

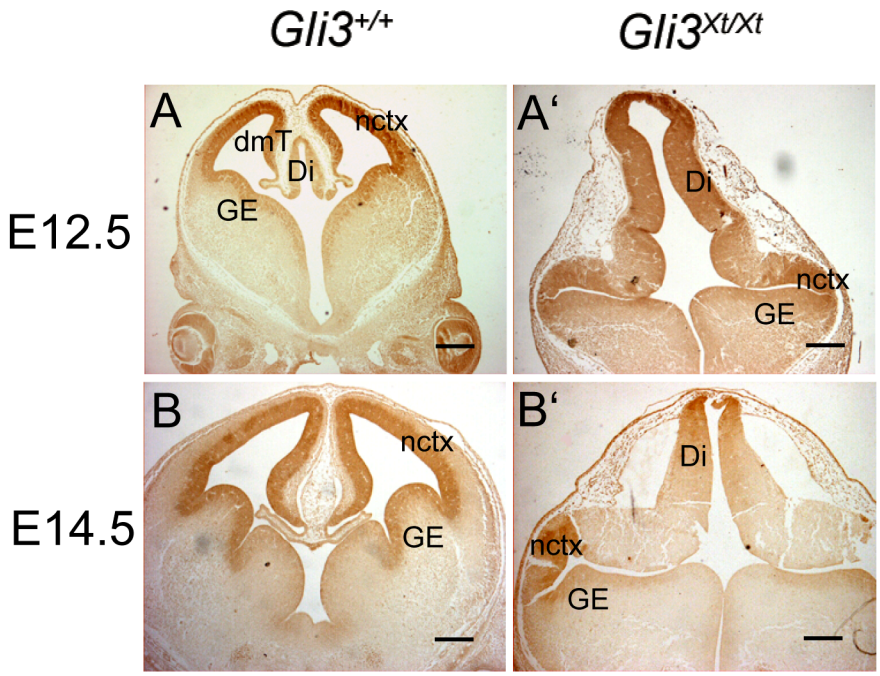

Figure 3.3 Gli3 immunohistochemistry with rabbit anti-Gli3 antibody (Santa Cruz, H280) on wild type (**A** and **B**) and *Gli3*$^{Xt/Xt}$ mutant (**A'** and **B'**) coronal sections at E12.5 and E14.5. Gli3 protein is observed in the diencephalon (Di), the neocortex (nctx) and ganglionic eminences (GE) of both wild type (**A** and **B**) and the mutant (**A'** and **B'**) embryos at both ages. Gli3 is also expressed in the wild type dorso-medial telencephalon (dmT) (**A** and **B**). Scale bars, 250 μm.

3.3 DISCUSSION

The morphogen sonic hedgehog (Shh), a member of the Hedgehog (Hh) family of secreted proteins, is expressed in the ventral neural tube including the ventral forebrain (Echelard et al., 1993; Riddle et al., 1993), and is involved in ventral cell fate specification in all regions of the neural tube (Ericson et al., 1995a; Ingham and McMahon, 2001). In the ventral neural tube and the posterior part of the limbs, production of full length Gli3 (transcriptional activator) responds to Shh. In the dorsal part of the neural tube or the anterior part of the limb bud where Shh is not present, Gli3 is cleaved to a transcriptional repressor (Ruiz i Altaba, 1998; Murone et al., 1999; Ruiz i Altaba, 1999; von Mering and Basler, 1999; Aza-Blanc et al., 2000), and the expression of Gli3 results in the repression of Shh target genes (Ruiz i Altaba, 1999; Persson et al., 2002).

Gli3 is highly expressed in the developing telencephalon, and this strong expression indicates a function of Gli3 in patterning the developing telencephalon. In addition, Gli3 is highly expressed in the ventricular zone, indicating a role in proliferation. The protein expression in the telencephalon, shown by western blot, reflects the mRNA expression of *Gli3*, which has a ^{high}dorsal-to-^{low}ventral pattern. Furthermore, the cleaved isoform of Gli3 is about three times more concentrated than the full length isoform in the dorsal telencephalon, while in the ventral telencephalon, the amounts of full length and cleaved isoforms of Gli3 are about the same. The ratios of the cleaved to the full length isoforms of Gli3 in the dorsal and ventral telencephalon are analogous to those described in the anterior and posterior limb bud respectively (Wang et al., 2000; Litingtung et al., 2002; Chen et al., 2004), and this ratio was suggested to be crucial for digit number and identity (Persson et al., 2002; Wang et al., 2007). The difference in the ratio of the two isoform of Gli3 in the dorsal and ventral telencephalon might also be important for dorso-ventral patterning of the

forebrain. The absence of Shh in the dorsal telencephalon may account for the high levels of the cleaved Gli3 isoform. As described in the *Drosophila* anterior wing bud (Methot and Basler, 1999) and vertebrate anterior limb bud (Wang et al., 2000), Gli3 in the dorsal telencephalon might act as a repressor of the Shh signalling pathway.

The anti-Gli3 antibody used also detected positive signals in the $Gli3^{Xt/Xt}$ mutant embryos by immunohistochemistry, which might correspond to one (or several) of the bands with unknown identity detected by western blot. This (these) band(s) could correspond either to some other antigens that crossreact with this rabbit anti-Gli3 antibody (e.g. Gli2). It is also possible that some Gli3 protein is made by the non-functional fusion transcripts in the $Gli3^{Xt/Xt}$ mutant embryos (Buscher et al., 1998), although there did not seem to appear any shifts in the size of the protein bands in $Gli3^{Xt/Xt}$ mutant tissues compared to wild types, making this possibility less likely.

Chapter 4: Analyses of *Gli3*$^{Xt/Xt}$ mutant forebrain after E12.5 suggest an earlier requirement for Gli3 during development

4.1 INTRODUCTION

Gli3$^{Xt/Xt}$ mouse mutants exhibit many forebrain malformations. Previous studies have shown that the mutant mice have a smaller dorsal telencephalon compared to the wild type embryos, and they do not have olfactory bulbs (Franz, 1994; Theil et al., 1999; Aoto et al., 2002). The expression of dorsal telencephalic markers, like *Emx1* and *Emx2*, are either lost or reduced from the dorsal telencephalon of the *Gli3*$^{Xt/Xt}$ mutants (Theil et al., 1999; Tole et al., 2000a). The dorso-medial telencephalic wall of the *Gli3*$^{Xt/Xt}$ mutant fails to invaginate, and the hippocampus and the choroid plexus of the lateral ventricles do not form (Hui and Joyner, 1993; Grove et al., 1998; Theil et al., 1999; Tole et al., 2000a). The expression of a number of *Wnt* and *Bmp* genes are specifically lost from the *Gli3*$^{Xt/Xt}$ dorso-medial telencephalon, including *Bmp2*, *4*, *6* and *7* and *Wnt 2b*, *3a* and *5a*, but their expression in the adjacent diencephalon remains (Grove et al., 1998; Theil et al., 1999; Tole et al., 2000a). Histological analyses have suggested lack of lamination of the *Gli3*$^{Xt/Xt}$ mutant neocortex (Franz, 1994; Theil et al., 1999). Recently, Theil (2005) showed that the organization of the ventricular zone, the apical/basal cell polarity of cortical progenitors and the differentiation of early born cortical neurons are affected in the *Gli3*$^{Xt/Xt}$ mutants from E11.5 (Theil, 2005).

Several studies have reported ectopic expression of ventral markers, such as *Mash1*, *Dlx2*, *Gsh2* and *Islet1*, in the *Gli3*$^{Xt/Xt}$ mutant dorsal telencephalon along the rostro-caudal axis at E12.5 (Tole et al., 2000a; Rallu et al., 2002b; Kuschel et al.,

2003). However, most of these analyses were carried out by whole mount *in situ* hybridization, and they did not clearly define the limits of each forebrain structure.

The size reduction of *Gli3*$^{Xt/Xt}$ telencephalon suggested that Gli3 might affect one of the following factors that ensure the telencephalon grows at the right rate to produce the correct numbers of cells at the right time and place:

1. Commitment of cells to their particular fates (specification)
2. Rate of cell proliferation
3. Rate of cell exiting the cell cycle to differentiate
4. Rate of cell migration in and out of the tissue
5. Rate of cell death

In this chapter, markers which are normally expressed in different regions within the forebrain were analysed in detail in E12.5 wild type and *Gli3*$^{Xt/Xt}$ mutant embryos. The expression of ventral markers such as Mash1, Dlx2, Gsh2 and Islet1 were found confined to ventral telencephalon and ventral thalamus in more caudal sections of the *Gli3*$^{Xt/Xt}$ mutant embryos, in contrast to previous publications. Their expression in the most rostral forebrain sections was found expanded in the mutants, in agreement with previous results. Similar results were observed at later stages of development, although the neocortex of the *Gli3*$^{Xt/Xt}$ mutants became highly disorganized. Rosette-like structures are found in the neocortical area of the *Gli3*$^{Xt/Xt}$ mutants from E13.5, and these rosettes comprised well organized neocortical progenitors.

The boundary between the telencephalon and the diencephalon was found to be compromised in the *Gli3*$^{Xt/Xt}$ mutants, and clusters of cells that have eminentia thalami identity were found at E12.5 in the neocortical area of the *Gli3*$^{Xt/Xt}$ mutants. These two types of cells were well segregated from each other at later developmental

stages examined (E13.5 to E16.5). Diencephalic cells were also observed in the most rostral sections of the *Gli3*$^{Xt/Xt}$ mutant telencephalon at E12.5. The mutant diencephalon was found join with the septum of the ventral telencephalon in more rostral areas than in the wild types.

Finally, a 73% reduction of the dorsal telencephalon, and about 20% reduction of the ventral telencephalon of the *Gli3*$^{Xt/Xt}$ mutant embryos was found at E12.5. However, no cell proliferation or cell death defects were detected in E12.5 *Gli3*$^{Xt/Xt}$ mutant telencephalon, suggesting that the telencephalic size reduction must have been initiated at earlier developmental stages.

Some of the immunohistochemical experiments and cell proliferation measurements described in this chapter were done in collaboration with Vassiliki Fotaki and Paulette Zaki, and many of the results in this chapter have already been published (Fotaki et al., 2006). This paper is bound into this thesis and will not be cited again in this chapter.

4.2 RESULTS

4.2.1 Identification of the limits of the dorsal telencephalon in *Gli3*$^{Xt/Xt}$ mutants

To study the dorso-ventral patterning of the *Gli3*$^{Xt/Xt}$ mutant forebrains, E12.5 wild type and mutant forebrain sections were immunoreacted with Pax6, which is highly expressed in the dorsal telencephalon and diencephalon (Walther and Gruss, 1991; Stoykova and Gruss, 1994; Mastick et al., 1997), and Mash1, which is expressed in the ventral telencephalon and diencephalon (Lo et al., 1991; Guillemot and Joyner, 1993; Porteus et al., 1994). Figure 4.1 shows wild type and mutant forebrain sections in caudal to rostral order. The expression of Pax6 and Mash1 is relatively normal in

caudal sections of *Gli3*$^{Xt/Xt}$ mutant embryos (Fig. 4.1A' and D') compared to wild types (Fig. 4.1A and D). In these caudal sections of wild type embryos, the telencephalic vesicles are clearly visible. However, only the most caudal tips of the telencephalic lobes are observed in the corresponding *Gli3*$^{Xt/Xt}$ mutant sections. This may be due to the diminished size of the *Gli3*$^{Xt/Xt}$ telencephalon compared to wild types and/or the alteration of the relative three dimensional positions of the telencephalon and the diencephalon. In middle sections along the rostro-caudal axis of the telencephalon, Pax6 is strongly expressed in the diencephalon, including the ventral thalamus and the eminentia thalami (Fig. 4.1B). In the telencephalon, Pax6 expression has a ^{high}lateral-to-^{low}medial gradient. This gradient of expression is lost in *Gli3*$^{Xt/Xt}$ mutants, probably because the dorso-medial telencephalon is lost in the mutants, and the highly Pax6 expressing diencephalon and neocortex are joined directly (Fig. 4.1B'). At this level, Mash1 expression is normally observed in the ventral thalamus and hypothalamus of the diencephalon and the ganglionic eminences (GE), but not in the neocortex (Fig. 4.1E). In comparable *Gli3*$^{Xt/Xt}$ sections, Mash1 immunoreactivity is also present in the GE (Fig. 4.1E') and absent from the Pax6 positive area dorsally to the GE (compare Fig. 4.1B' with E'). This suggests that the Mash1 negative region (area between the lines in Fig. 4.1E') is neocortical tissue, and the Mash1 staining in the adjacent region most likely corresponds to diencephalic tissue (ventral thalamus (VT) and/or eminentia thalami (EmT) in Fig. 4.1E'). The expression of Pax6 at most rostral sections of the wild type and mutant embryos is confined to the dorsal telencephalon (Fig. 4.1C and C'). The rostral expression of Mash1 is confined to the ventral area of wild type embryos (Fig. 4.1F), whereas in *Gli3*$^{Xt/Xt}$ mutants, Mash1 expression is found throughout the telencephalic vesicle (Fig. 4.1F'). Note that at very rostral level of the mutants, Mash1 and Pax6 are coexpressed in the dorsal part of the telencephalon (Fig. 4.1C' and F').

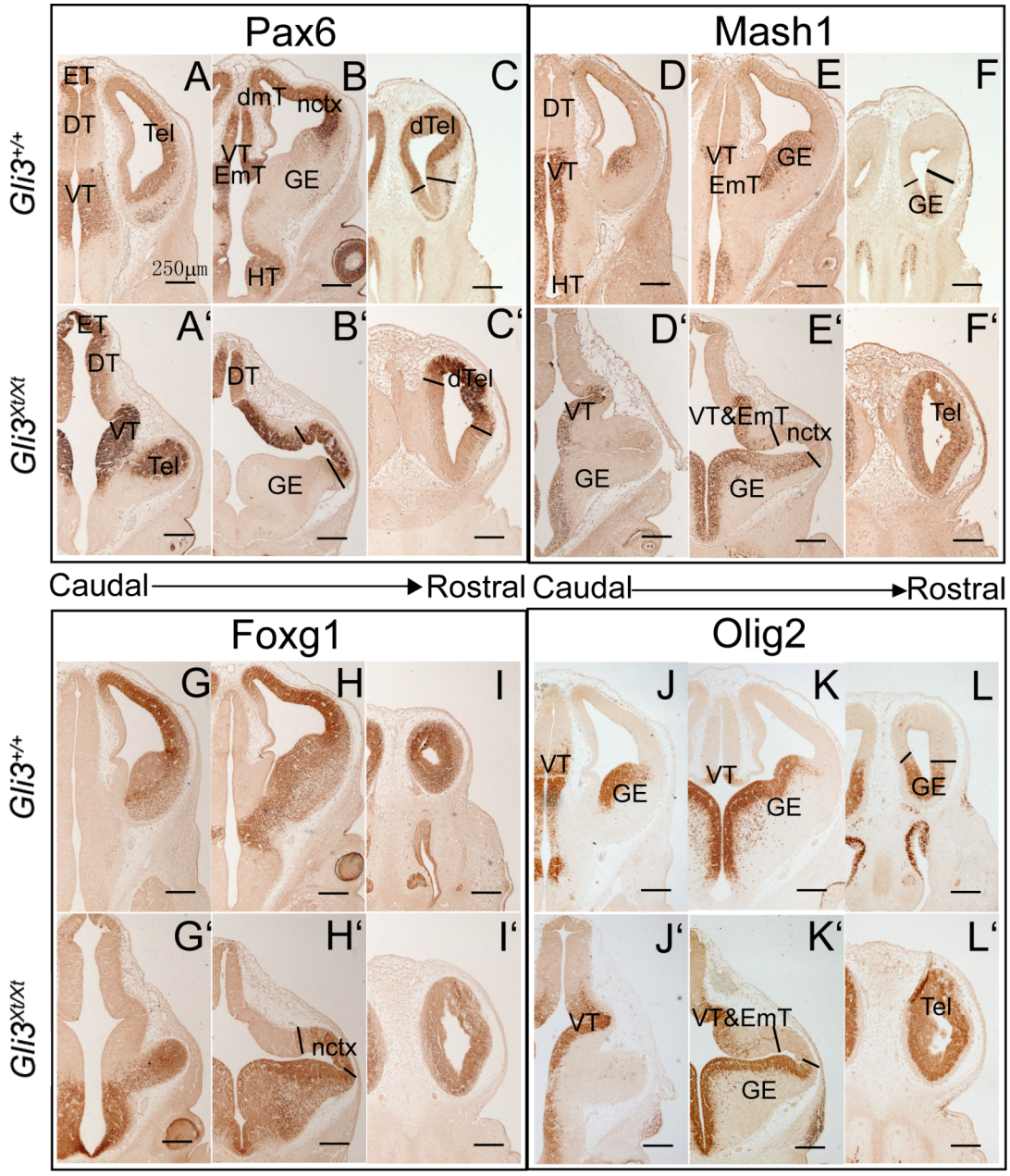
Pax6
Mash1
Foxg1
Olig2
Gli3+/+
Gli3Xt/Xt
A
B
C
D
E
F
G
H
I
J
K
L
A'
B'
C'
D'
E'
F'
G'
H'
I'
J'
K'
L'
ET
DT
Tel
VT
dmT
nctx
EmT
GE
dTel
HT
VT&EmT
250μm
Caudal
Rostral
Caudal
Rostral

Figure 4.1 Pax6, Mash1, Foxg1 and Olig2 immunoreactivity on E12.5 wild type (*Gli3*$^{+/+}$) (**A**-**L**) and *Gli3*$^{Xt/Xt}$ mutants (**A'**-**L'**) forebrain coronal sections. In the diencephalon, Pax6 is expressed in the epithalamus (ET), dorsal (DT) and ventral (VT) thalamus in both wild types (**A**) and mutants (**A'**) in more caudal sections. Moving to middle sections, Pax6 expression is observed in the eminentia thalami (EmT) in the wild type diencephalon (**B**). In the telencephalon (Tel), Pax6 is expressed highly in the neocortex (nctx) and lightly in the dorso-medial telencephalon (dmT) and is absent in the ventral telencephalon (ganglionic eminences, GE) (**B**). In the mutants, Pax6 is continuously highly expressed in the diencephalon and dorsal telencephalon (**B'**). Rostrally, Pax6 expression is restricted to the dorsal telencephalon (dTel) of both the wild types (**C**) and mutants (**C'**). Mash1 expression is observed in ventral thalamus, hypothalamus (HT) and GE in both wild types (**D**) and mutants (**D'**). The neocortex in mid-telencephalic sections is negative for Mash1 in both wild types (**E**) and mutants (area between lines in **E'**). Rostrally, Mash1 expression is restricted in the ventral telencephalon of the wild types (**F**), but is found throughout the telencephalic vesicles of the *Gli3*$^{Xt/Xt}$ mutants (**F'**). Foxg1 delineates the telencephalon of wild type (**G**-**I**) and *Gli3*$^{Xt/Xt}$ mutant (**G'**-**I'**) embryos. The area between the lines in **H'** corresponds to the mutant neocortex. Olig2 is expressed in the ventral thalamus and the GE in more caudal sections of both the wild type (**J** and **K**) and mutant (**J'** and **K'**) embryos. Rostrally, Olig2 expression is observed throughout the telencephalic lobes of the mutant embryos (**L'**) in contrast to the restricted expression ventrally in the wild types (**L**). Scale bars, 250 μm.

To confirm that the Mash1 positive tissue dorsally to the neocortex is diencephalic, but not telencephalic, in middle telencephalic sections of *Gli3*$^{Xt/Xt}$ embryos (Fig. 4.1E'), immunohistochemistry was performed using an antibody against Foxg1. Foxg1 is expressed in the dorsal and ventral telencephalon and is absent from the dorsal and ventral diencephalon (Tao and Lai, 1992; Hanashima et al., 2002). Foxg1 expression delineates the telencephalon and is observed in both wild type and *Gli3*$^{Xt/Xt}$ embryos throughout the rostro-caudal axis (Fig. 4.1G-I and G'-I'). In the middle part of the telencephalon (Fig. 4.1G'), Foxg1 is absent from the Mash1 positive tissue dorsally to the neocortex of the *Gli3*$^{Xt/Xt}$ mutants (VT & EmT in Fig. 4.1E'), confirming that this tissue is not telencephalic. These results clearly delineate the neocortical region and confirm that in middle sections along the rostro-caudal axis, Mash1 positive tissue dorsally to the Foxg1 positive neocortical region is diencephalic. In rostral wild type (Fig. 4.1I) and *Gli3*$^{Xt/Xt}$ mutant sections (Fig. 4.1I'), Foxg1 expression is observed throughout the telencephalic vesicles, suggesting that the Mash1 positive region in the *Gli3*$^{Xt/Xt}$ mutants is telencephalic tissue (compare Fig. 4.1F' with Fig. 4.1I').

To provide additional evidence for this, the expression of several ventral forebrain markers was examined in wild type and *Gli3*$^{Xt/Xt}$ mutant embryos. Olig2 is expressed in the precursors of both the lateral (LGE) and medial (MGE) ganglionic eminences of the wild types (Fig. 4.1J-L) (Lu et al., 2000; Zhou et al., 2000). The expression of Olig2 is generally broader than that of Mash1 in the wild type embryos (compare Fig. 4.1D, E and F with Fig. 4.1J, K and L) (Gokhan et al., 2005; Parras et al., 2007). In the *Gli3*$^{Xt/Xt}$ mutants, Olig2 positive area seems to be also broader than Mash1 expression (compare Fig. 4.1D', E' and F' with Fig. 4.1J', K' and L'). The expression of Olig2 is confined to the mutant ventral telencephalon and ventral thalamus in more caudal sections (Fig. 4.1J' and K'), but expanded to the dorsal area in rostral sections (Fig. 4.1L'), similar to what is observed with the Mash1

expression.

A number of ventral telencephalic markers that were previous described to be ectopically expressed were re-examined in *Gli3*$^{Xt/Xt}$ mutants. The expression pattern of Islet1 is normally observed in the postmitotic neurons of the GE and ventral thalamus of the wild type (Fig. 4.2A and B) (Wang and Liu, 2001). Its expression is not found in the neocortical area of the *Gli3*$^{Xt/Xt}$ mutants in middle telencephalic sections along the rostro-caudal axis (Fig. 4.2A'). In rostral sections of the mutant embryos (Fig. 4.2B'), dispersed Islet1 positive cells are detected in a more dorsal area, besides its normal expression in GE. This ectopic expression is never detected in the wild type dorsal telencephalon (Fig. 4.2B). The expansion of Islet1 in the mutant rostral sections is less prominent than those of the progenitor markers, such as Mash1 and Olig2 (compare Fig. 4.1F', L' with Fig. 4.2B'). Islet1 expression in the mutant in a ventral region that probably corresponds to the telencephalic septum seems to be expanded (arrowheads in Fig. 4.2B'). The expression of two other ventral markers, Dlx and Gsh2 was confined to the ventral telencephalon and the ventral thalamus and/or eminentia thalami region in *Gli3*$^{Xt/Xt}$ embryos (VT & EmT in Fig. 4.2C' and D') as in the wild types (Fig. 4.2C and D) in middle sections, in contrast to previous reports (Theil et al., 1999; Tole et al., 2000a; Rallu et al., 2002b). In addition, the expression pattern of *Shh* transcript in the zona limitans intrathalamica (ZLI) (Echelard et al., 1993; Marti et al., 1995a) defines the border between the dorsal and ventral thalamus (Figdor and Stern, 1993; Porteus et al., 1994; Kiecker and Lumsden, 2004). *Shh* mRNA expression is present in both wild type and *Gli3*$^{Xt/Xt}$ sections (Fig. 4.2E and E'), showing clearly that the Mash1, Olig2, Islet1, Dlx and Gsh2 expressing area below the ZLI corresponds to ventral thalamus in both wild types and mutants. Furthermore, the region that corresponds to the mutant neocortex (area of tissue between the lines in Fig. 4.1E', K', Fig. 4.2A', C' and D') does not express any of these markers. Altogether these results show that the

previously described ectopic expression of Mash1, Islet1, Dlx and Gsh2 at middle parts of the *Gli3*$^{Xt/Xt}$ dorsal telencephalon (Tole et al., 2000a; Rallu et al., 2002b; Kuschel et al., 2003) actually reflects expression in the diencephalon (ventral thalamus and/or eminentia thalami). However, in the rostral telencephalon of *Gli3*$^{Xt/Xt}$ mutant embryos, these ventral markers are expanded to a more dorsal area, in agreement with previous published results (Theil et al., 1999; Tole et al., 2000a; Rallu et al., 2002b).

To further examine the properties of the rostral expansion of the *Gli3*$^{Xt/Xt}$ ventral telencephalon, Nkx2.1 immunoreactivity was performed on E12.5 wild type and *Gli3*$^{Xt/Xt}$ mutant sections. Nkx2.1 is expressed in the precursor cells of the MGE (Shimamura et al., 1995; Sussel et al., 1999), but not the LGE, of the wild type embryos, and the expression can only be seen in more caudal sections (Fig. 4.2F and G). Nkx2.1 expression seems to be confined to the medial part of the ganglionic eminences of the mutant embryos in more caudal sections, although the distinct bulging shape of the MGE and LGE is lost (Fig. 4.2F'). Rostrally, no Nkx2.1 expression is observed in the mutant embryos (Fig. 4.2G'), similar to the wild types. This result suggests that the precursor cells from the MGE of the *Gli3*$^{Xt/Xt}$ mutant embryos do not contribute to the rostral expansion of the ventral telencephalon at E12.5.


Gli3+/+
Gli3Xt/Xt
Gli3+/+
Gli3Xt/Xt
Islet1
Shh
Gsh2
Nkx2.1
Dlx
A
A‘
B
B‘
C
C‘
D
D‘
E
E‘
F
F‘
G
G‘
DT
VT
EmT
GE
VT&EmT
nctx
ZLI
HT
MGE

Figure 4.2 Forebrain marker analyses in wild types (*Gli3*$^{+/+}$) (**A**-**G**) and *Gli3*$^{Xt/Xt}$ mutants (**A'**-**G'**) E12.5 coronal sections. Islet1 is expressed in the ventral thalamus (labelled VT in the wild types and VT & EmT in the mutants) and ventral telencephalon (GE) of both wild types (**A**) and mutants (**A'**). Rostrally, Islet1 expression is restricted to the postmitotic cells in the wild type ventral telencephalon (**B**), but in the mutants, it is found in a more dorsal area (arrows in **B'**). The expression of Islet1 in the mutant septum seems to be expanded (arrowheads in **B'**) compared to that of the wild types (arrowhead in **B**). Gsh2 and Dlx expression are found in the ventral thalamus (VT or VT & EmT) and ventral telencephalon (GE) of both the wild type (**C** and **D**) and mutants (**C'** and **D'**). Note that no ectopic expression of any of these markers is observed in the neocortical area of the mutants (area between lines in **C'** and **D'**). *Shh* mRNA expression is observed in the zona limitans intrathalamica (ZLI) which defines the border between the dorsal (DT) and ventral (VT) thalamus, and hypothalamus (HT) of the wild type (**E**) and mutant embryos (**E'**). Nkx2.1 expression is confined to the medial ganglionic eminence (MGE) of both wild type (**F**) and *Gli3*$^{Xt/Xt}$ mutant (**F'**) embryos in middle sections, and is absent in rostral sections of wild types (**G**) and mutants (**G'**). Scale bars, 250 μm.

4.2.2 The *Gli3*$^{Xt/Xt}$ neocortex contains clusters of cells with characteristics of the eminentia thalami

In the Foxg1 expressing neocortical area of the *Gli3*$^{Xt/Xt}$ mutant embryos, some negative patches of expression were observed (Fig. 4.1H' and Fig. 4.3A'), which were not detected in any sections of the wild type telencephalon (Fig. 4.1H and Fig. 4.3A). A similar patchy staining was observed with Lhx2 expression (Fig. 4.3B' and C'), which is normally found throughout the neocortex with a ^{high}medial-to-^{low}lateral gradient (Fig. 4.3B and C) (Monuki et al., 2001). This gradient of expression is lost in the *Gli3*$^{Xt/Xt}$ mutant dorsal telencephalon (Fig. 4.3C'), although Lhx2 expression in the dorsal thalamus seems to be intact (compare thalamic expression in Fig. 4.3C with C'). The Foxg1 and Lhx2 negative area is positive for Pax6 (Fig. 4.1B') in the *Gli3*$^{Xt/Xt}$ mutants. In wild types, Pax6 is expressed not only in the dorsal telencephalon and ventral thalamus, but also in the ventricular zone of the eminentia thalami (Fig. 4.1B) (Puelles et al., 2000), which forms part of the rostral boundary between the diencephalon and the telencephalon (Porteus et al., 1994; Puelles and Rubenstein, 2003). It is possible that these Foxg1 and Lhx2 negative patches of cells are comprised cells from the eminentia thalami, since they do not express markers of ventral thalamus, such as Mash1, Olig2, Islet1, Dlx and Gsh2 (Fig. 4.1E', K', 4.2A', C' and D'). To test whether these patches have an eminentia thalami identity, immunohistochemistry of several eminentia thalami markers was performed. Calretinin is expressed in the postmitotic somata and fibers of the eminentia thalami in wild type embryos (Fig. 4.3D and E) (Abbott and Jacobowitz, 1999). In *Gli3*$^{Xt/Xt}$ mutants, the eminentia thalami is intensely stained with calretinin (Fig. 4.3E'), and the mutant eminentia thalami is observed in a region dorsal to the neocortex (Fig. 4.3D' and E'). In addition, small calretinin positive cell clusters are observed in the

mutant neocortex (Fig. 4.3D' and E').

To provide additional evidence about the eminentia thalami nature of these clusters, the expression pattern of Lim2 (also known as Lhx5) was examined, which specifically labels the eminentia thalami and ventral thalamus in E12.5 wild types, with more intense expression in the postmitotic cells (Fig. 4.3F and G) (Sheng et al., 1997). The antibody used recognized both Lim1 (Lhx1) and Lim2 (Lhx5) proteins, but *Lim1* mRNA expression is very weak in these tissues at this age (Sheng et al., 1997). In the *Gli3*$^{Xt/Xt}$ mutant neocortex, Lim2 immunostaining showed a strong and patchy expression (Fig. 4.3F' and G'), similar to that observed with calretinin, and complementary to the Foxg1 negative patches (compare Fig. 4.3A', D' and F'). Note that the Lim2 positive clusters appearing in the *Gli3*$^{Xt/Xt}$ mutant neocortex were intensely stained, suggesting they might share some properties with the postmitotic cells of the eminentia thalami (Fig. 4.3G'). To further confirm the eminentia thalami identity of these clusters, double immunofluorescence for Foxg1 and Lim2 was performed on E12.5 wild type and *Gli3*$^{Xt/Xt}$ sagittal sections. In wild types, Lim2 immunostaining was confined in the eminentia thalami, whereas Foxg1 specifically labelled the dorsal and ventral telencephalon (Fig. 4.3H). In *Gli3*$^{Xt/Xt}$ mutants, clusters of Lim2 positive cells were found in the Foxg1 positive area, and Foxg1 and Lim2 expression did not co-localize (Fig. 4.3H').

Finally, Pax2, a well described marker of the hindbrain, optic chiasm and optic stalk (Nornes et al., 1990; Puschel et al., 1992), labels a distinct population of eminentia thalami cells, found in a region close to the choroid plexus in wild type sections (Fig. 4.3I). In the *Gli3*$^{Xt/Xt}$ mutants, dispersed Pax2 positive cells were detected (Fig. 4.3I'), similar to what was observed with the calretinin and Lim2 staining.

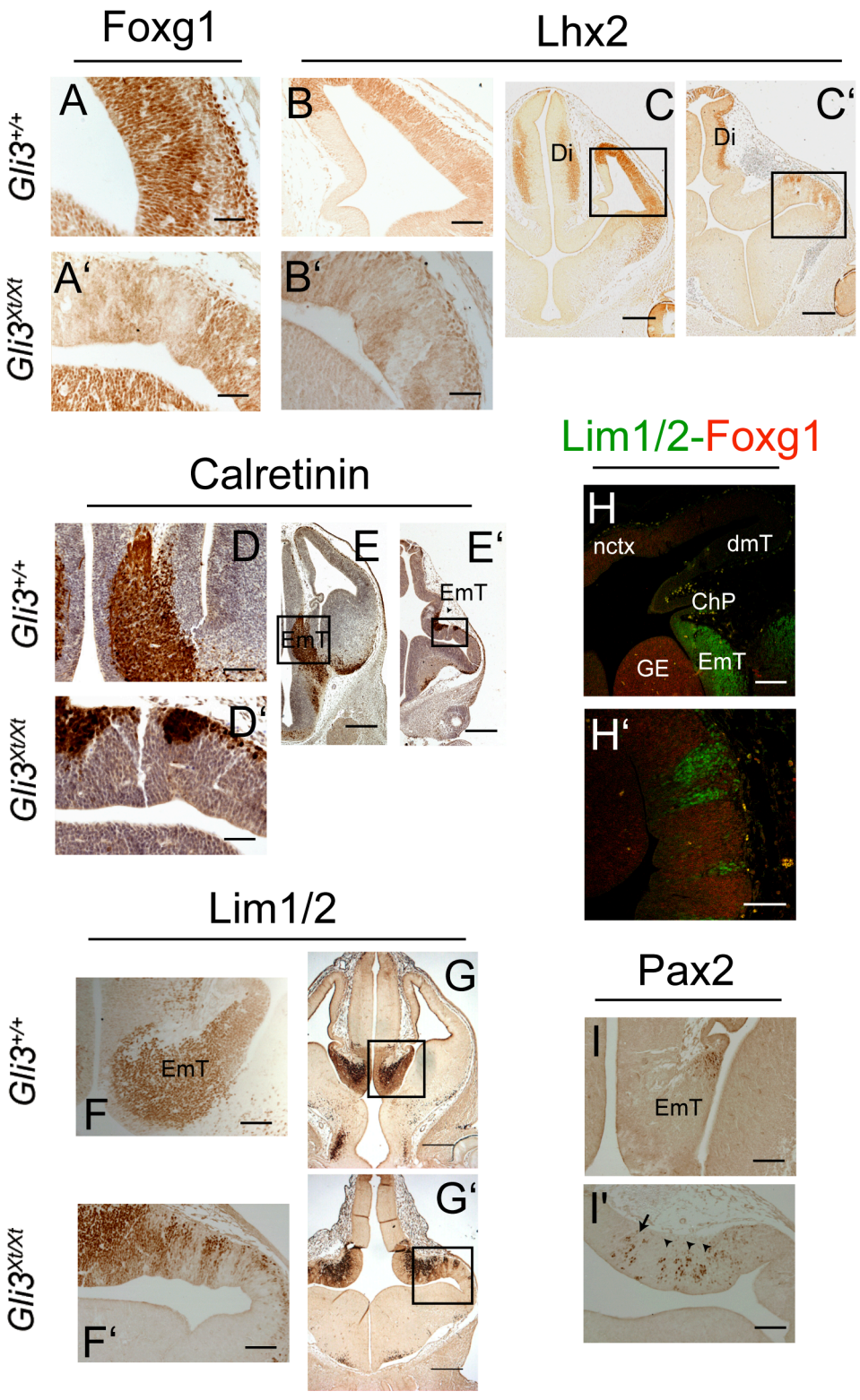
Foxg1
Lhx2
Gli3+/+
Gli3Xt/Xt
A
A‘
B
B‘
C
C‘
Di
Di
Calretinin
D
D‘
E
E‘
EmT
EmT
Lim1/2-Foxg1
H
H‘
nctx
dmT
ChP
GE
EmT
Lim1/2
F
F‘
EmT
G
G‘
Pax2
I
I'
EmT

Figure 4.3 Marker analyses of E12.5 wild type (*Gli3*$^{+/+}$) (**A**-**I**) and *Gli3*$^{Xt/Xt}$ mutant (**A'**-**I'**) dorsal telencephalon and eminentia thalami on coronal (**A**-**G**, **I** and **A'**-**G'**, **I'**) and sagittal sections (**H** and **H'**). Foxg1 shows a patchy expression in the *Gli3*$^{Xt/Xt}$ mutant neocortex (**A'**) which is never observed in the wild type dorsal telencephalon (**A**). Lhx2 is expressed in the wild type dorsal telencephalon with a ^{high}medial-to-^{low}lateral gradient (**B** and **C**). This gradient is lost in the mutant neocortex, revealing the presence of immunonegative patches (**B'** and **C'**). **B** and **B'** are high magnification images of boxed area in **C** and **C'**, respectively. Calretinin expression is detected in both wild type (**D** and **E**) and mutant (**D'** and arrowhead in **E'**) eminentia thalami (EmT). In the mutants, calretinin positive clusters are found within the neocortical area (Foxg1 positive) but they do not express Foxg1 (compare **A'** with **D'**). **D** and **D'** are high magnification images of boxed areas in **E** and **E'**, respectively, and they are counterstained with cresyl violet. Lim2 is expressed in both the wild type (**F** and **G**) and mutant (**F'** and **G'**) eminentia thalami, with more intensity in the postmitotic cells (**G** and **G'**). Lim2 positive clusters were also found in the neocortical area of the mutants (**F'** and **G'**). **F** and **F'** are high magnification images of boxed area in **G** and **G'**. Double immunofluorescence with Foxg1 (red) and Lim2 (green) labels telencephalon (nctx + dmT + GE) and eminentia thalami (EmT) respectively on sagittal sections of wild type embryos (**H**). In the mutants, the Foxg1 negative patches within the neocortical area are immunopositive for Lim2 (**H'**). Pax2 is found to be expressed in a small population of cells of the eminentia thalami near the choroid plexus (ChP) in the wild type embryos (**I**). In the mutants, Pax2 positive clusters are found not only in the area that is positive for Lim2 but negative for Foxg1 (arrow in **I'**), but also among the Foxg1 negative patches (arrowheads in **I'**). **A'**, **B'**, **D'** and **F'** are serial sections from the same specimen. Scale bars, **A**, **A'**, **B'** and **D'**, 50 μm; **B**, **F**, **F'**, **H'**, **I**, and **I'**, 100 μm; **D** and **H**, 150 μm; **C**, **C'**, **G** and **G'**, 250 μm; **E** and **E'**, 400 μm.

The above results strongly suggest that the cell clusters observed in the neocortical area of the *Gli3*$^{Xt/Xt}$ mutants are diencephalic. However, because calretinin and Lim2 also label the earliest born neurons in the marginal zone, the Cajal-Retzius cells, which are negative for Foxg1 (del Rio et al., 1995; Super et al., 1998; Hevner et al., 2001; Hevner et al., 2003; Yamazaki et al., 2004), it was possible that the calretinin and Lim2 positive clusters in the *Gli3*$^{Xt/Xt}$ neocortex comprised this cell type. To examine this possibility, the expression of reelin, which is also found in Cajal-Retzius cells (Alcantara et al., 1998), and calbindin, which is not normally observed in this cell population (Hevner et al., 2003; Jimenez et al., 2003) was performed on wild type and *Gli3*$^{Xt/Xt}$ mutant embryos. In the wild types, Reelin positive cells are found in the eminentia thalami and the Cajal-Retzius cells in the marginal zone (Fig. 4.4A and B). No reelin positive cell clusters were observed in the *Gli3*$^{Xt/Xt}$ mutants (Fig. 4.4A' and B'), and in fact, there were less reelin positive cells in the mutants compared to wild types (compare Fig. 4.4B with B'), in accordance with recently published data (Theil, 2005). Calbindin expression was detected intensely in the ventral telencephalon (Fig. 4.4C and C') (Davila et al., 2005) and lightly in the eminentia thalami neurites of the wild types and mutants (Fig. 4.4D and D'). In the mutants, it was also detected near the calretinin positive clusters in the neocortex (Fig. 4.4C' and D'). These results indicate that Cajal-Retzius cells are not the major component of the calretinin and Lim2 positive clusters.

In the calretinin and calbindin positive regions in the mutant neocortex, a few dispersed reelin positive cells (arrows in Fig. 4.4B') were found, suggesting that a few Cajal-Retzius cells (Fig. 4.4B) may contribute to these clusters. However, it is also possible that these reelin positive cells are actually derived from the eminentia thalami, because reelin labels a population of eminentia thalami cells (Fig. 4.4A) (Takiguchi-Hayashi et al., 2004).

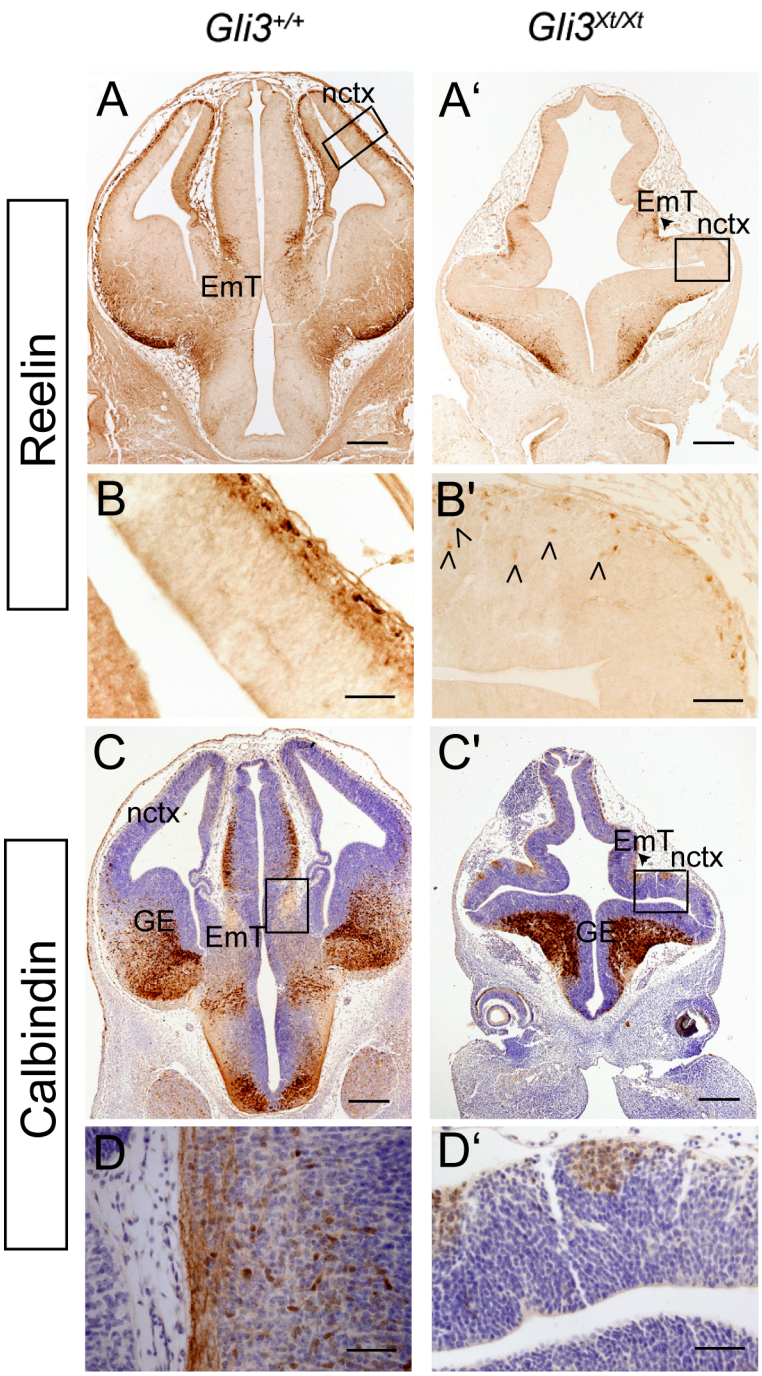
Gli3+/+
Gli3Xt/Xt
Reelin
Calbindin
A
nctx
EmT
A‘
EmT
nctx
B
B'
C
nctx
GE
EmT
C'
EmT
nctx
GE
D
D‘

Figure 4.4 Reelin and calbindin expression on E12.5 wild type (*Gli3*$^{+/+}$) (**A**-**D**) and *Gli3*$^{Xt/Xt}$ mutant (**A'**-**D'**) coronal sections. **B**, **B'**, **D**, and **D'** are high magnification images of boxed areas in **A**, **A'**, **C** and **C'** respectively. Reelin expression is found in the Cajal-Retzius cells which are located in the outer layer of the neocortex (nctx) of wild type embryos (**A** and **B**). In the mutants, there are fewer Reelin positive cells in the neocortical area, and these are not located in the outer layer (arrowheads in **B'**). Reelin also labels cells in the eminentia thalami (EmT) of both wild type (**A**) and mutant (**A'** and arrowheads in **B'**) embryos. Calbindin is expressed in the somata and fibers in the ventral telencephalon (GE) and fibers in eminentia thalami of both wild type (**C** and **D**) and mutant (arrowhead in **C'**) embryos. Small clusters of calbindin positive cells are present in the mutant neocortical area (**C'** and **D'**). **C**, **C'**, **D** and **D'** are counterstained with cresyl violet. Scale bars, **A**, **A'**, **C** and **C'**, 250 μm; **B**, **B'**, **D** and **D'**, 50 μm.

The expression of Lim2 and Pax2 were also examined in rostral telencephalic sections of the wild type and *Gli3*$^{Xt/Xt}$ mutant embryos. In the wild type embryos, Lim2 is continuously found in the diencephalon from the eminentia thalami to most rostral end of the diencephalon, lamina terminalis (Sheng et al., 1997) (Fig. 4.5A). This diencephalic expression is joined with its expression in the septum (Fig. 4.5A). In comparable *Gli3*$^{Xt/Xt}$ mutant sections, Lim2 expression is observed in both the lamina terminalis (arrow in Fig. 4.5A') and the septum (arrowhead in Fig. 4.5A'), but these two structures have not joined yet. Note there are clusters of Lim2 positive cells in the neocortical area of the *Gli3*$^{Xt/Xt}$ mutant embryos at this level (Fig. 4.5A'). The lamina terminalis and the septum finally join in more rostral sections of the mutant embryos (Fig. 4.5B'), and Lim2 expression seems to be increased compared to that in wild types (Fig. 4.5A and B). Pax2 expression is highly observed in the septum, and in a few dispersed cells in the lamina terminalis of the wild type embryos (Fig. 4.5C) (V. Fotaki, unpublished data). In the *Gli3*$^{Xt/Xt}$ mutant embryos, Pax2 expression is observed in the septum, and its expression seems to be expanded (arrowhead in Fig. 4.5C'). Pax2 expression is also found ectopically in the lamina terminalis (arrow in Fig. 4.5C). These results suggest that the mutant diencephalon joins abnormally with the ventral telencephalon in more rostral areas, and the mutant septum seems to be enlarged.

Altogether, these results clearly show that the neocortex of *Gli3*$^{Xt/Xt}$ embryos contains not only neocortical cells but also cells of eminentia thalami identity, and the rostral and ventral border between the telencephalon and diencephalon is compromised in the mutants.

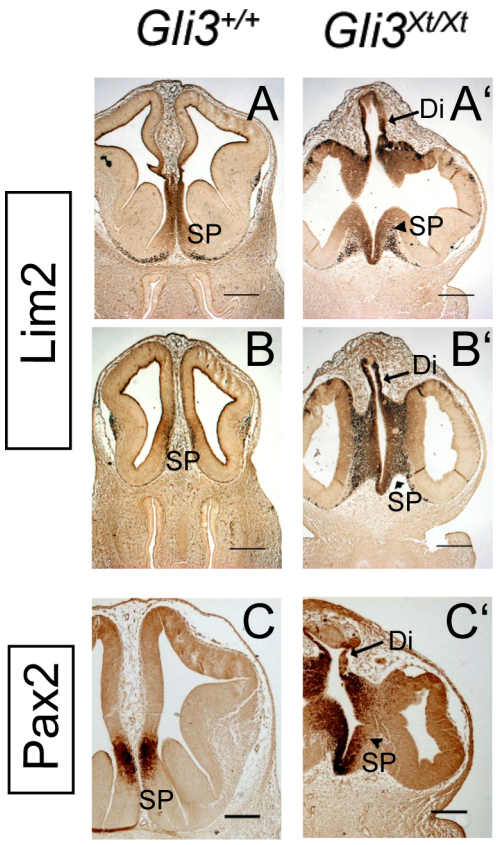

Figure 4.5 Lim2 and Pax2 immunoreactivity in E12.5 wild type (*Gli3*$^{+/+}$) (**A**-**C**) and *Gli3*$^{Xt/Xt}$ mutant (**A'**-**C'**) rostral telencephalic sections. Lim2 is expressed in wild type lamina terminalis at the rostral end of the diencephalon (Di), and the septum (SP) in the ventral telencephalon (**A** and **B**). In the *Gli3*$^{Xt/Xt}$ mutant embryos, expression of Lim2 in both lamina terminalis (arrow in **A'** and **B'**) and septum (arrowhead in **A'** and **B'**) is expanded. Pax2 expression in the *Gli3*$^{Xt/Xt}$ mutants is not only observed in the septum (arrowhead in **C'**) as in the wild types (**C**), but also ectopically in the lamina terminalis (arrow in **C'**). Note that Pax2 expression in the mutant septum also seems to be expanded. Scale bars, 250 μm.

4.2.3 The size of dorsal telencephalon of the *Gli3*$^{Xt/Xt}$ mutant is severely decreased

Having defined the telencephalic area of the *Gli3*$^{Xt/Xt}$ mutant, volumetric and areal measurements were carried out on E12.5 wild type and *Gli3*$^{Xt/Xt}$ mutant telencephalon to define the actual three and two dimensional sizes of the mutant dorsal and ventral telencephalon and to discover if there are any areal differences along the rostro-caudal axis (see Chapter 2.5 for details). Briefly, E12.5 embryos were cut in the coronal plane, and immunohistochemistry for different gene markers was carried out in serial sections. Foxg1 and Pax6 expression domains were used to identify the extent of the entire telencephalon and the dorsal telencephalic tissue, respectively, in wild type and *Gli3*$^{Xt/Xt}$ mutant embryos. The total volumes of Foxg1 and Pax6 expression domains in the telencephalon were measured in wild type and mutant embryos. The area of expression of these markers at defined rostral, middle and caudal sections was also compared. Caudal and rostral telencephalic sections were defined as the sections located at a distance of about 30 μm from the most caudal and most rostral tips of the telencephalic lobes, respectively, in both wild type and *Gli3*$^{Xt/Xt}$ mutant embryos. The sections half way between the caudal and rostral ends were defined as middle telencephalic sections for these measurements. From now on, these terms will be used to refer to the different telencephalic levels. Examples of representative caudal, middle and rostral OPT sections of wild type and mutant embryos are shown in Figure 2.1. The expression pattern of Foxg1 in the *Gli3*$^{Xt/Xt}$ mutants (Fig. 4.1G', H' and I') was largely unchanged, although the three dimensional shape was different compared to the wild type. The volume of Foxg1 expression domain in the *Gli3*$^{Xt/Xt}$ telencephalon (0.77 ± 0.06 mm^3) was significantly decreased (Student's *t* test, $p<0.001$, n=4 per genotype) to about 53.5% compared to that of wild types (1.42 ± 0.08 mm^3) (Fig. 4.6A). Pax6 expression in the telencephalon was used to measure the volume of the dorsal telencephalon. The

volume of Pax6 expression in the telencephalon of the *Gli3*$^{Xt/Xt}$ mutants (0.20 ± 0.02 mm^3) is significantly decreased (Student's *t* test, p<0.001, n=4 per genotype) to about 27% of that of wild types (0.74 ± 0.04 mm^3) at E12.5 (Fig. 4.6A), as expected from the fact that the Pax6 expression domain in the dorso-medial telencephalon is lost in the mutants (Fig. 4.1A', B' and C'). Areal measurements of Pax6 expression on defined caudal, middle and rostral sections showed that the reduction of the Pax6 positive domain in the dorsal telencephalon was universal along the rostro-caudal axis in *Gli3*$^{Xt/Xt}$ mutants (Fig. 4.6B) (Table 4.1), and the difference is significant (Student's *t* test, p<0.001, n=4 per genotype). The most severe reduction of Pax6 expression is observed in the rostral sections of *Gli3*$^{Xt/Xt}$ mutant telencephalon (Fig. 4.6B) (Table 4.1).

Area (mm^2)	**rTel**	**mTel**	**cTel**
***Gli3*$^{+/+}$**	0.51±0.008	0.49±0.01	0.60±0.02
***Gli3*$^{Xt/Xt}$**	0.32±0.01	0.22±0.008	0.28±0.007
P value	≤0.001	≤0.001	≤0.001
Percentage of decrease in the mutants	37.3%	55.1%	53.3%

Table 4.1 Areas of Pax6 expression in rostral (rTel), middle (mTel) and caudal (cTel) telencephalon of the E12.5 wild type (*Gli3*$^{+/+}$) and *Gli3*$^{Xt/Xt}$ mutant embryos.

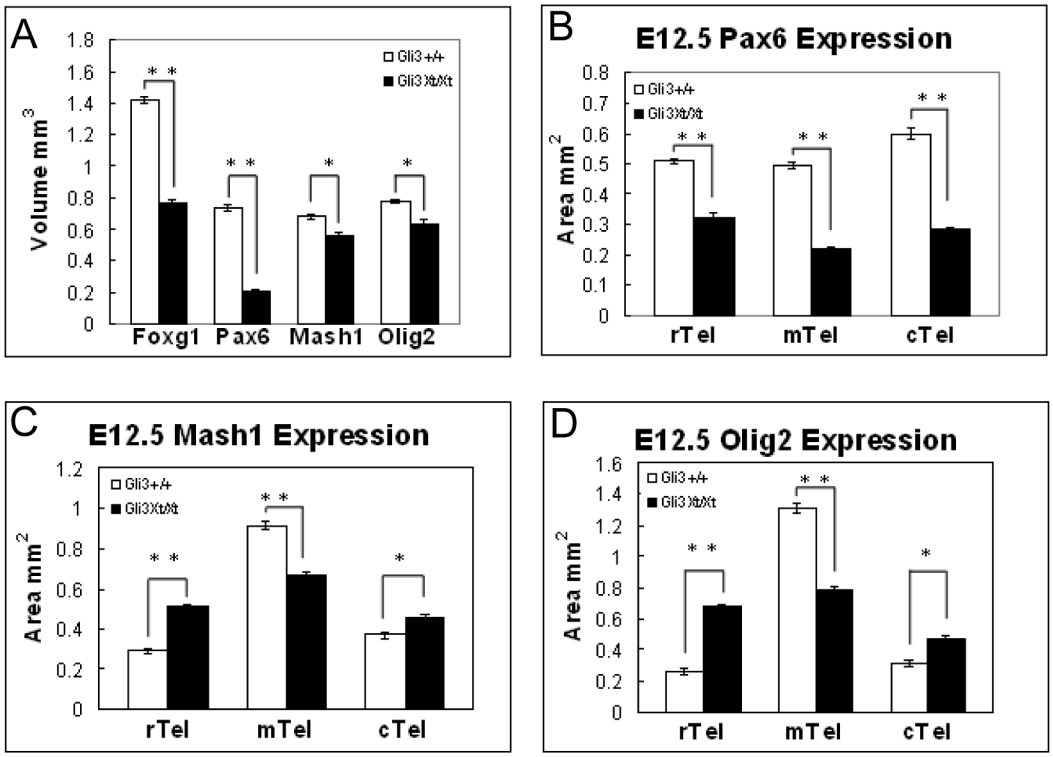

Figure 4.6 Volumetric (**A**) and areal (**B**, **C** and **D**) measurements of Foxg1, Pax6, Mash1 and Olig2 expression domain in the telencephalon of wild type (*Gli3*$^{+/+}$) and *Gli3*$^{Xt/Xt}$ mutant embryos. (**A**) The volume of Foxg1 expressing telencephalon in the mutants is decreased to about 53.5% of the wild type. The volume of Pax6 positive dorsal telencephalon is decreased in the mutants to 27% of the wild type embryos, and the reduction of the Pax6 positive area in the mutants is continuous throughout the rostro-caudal axis (**B**). The volumes of the expression domain of two ventrally expressing markers, Mash1 and Olig2, in the telencephalon are also significantly decreased in the mutants to about 80% to those of wild types. The reduction of Mash1 (**C**) and Olig2 (**D**) expression is only observed in middle parts of the *Gli3*$^{Xt/Xt}$ mutants. Their expression in rostral parts of the mutant telencephalon shows a most prominent expansion (**C** and **D**).

4.2.4 E12.5 *Gli3*$^{Xt/Xt}$ ventral telencephalon is smaller than that of the wild type embryos

Along with the measurements in the dorsal telencephalon, the overall volume of the E12.5 wild type and *Gli3*$^{Xt/Xt}$ ventral telencephalon was measured using the Mash1 and Olig2 expression domains. The areas of expression of these markers were also measured in defined rostral, middle and caudal sections. At E12.5, Mash1 expression was confined to the ventral telencephalon on caudal (Fig. 4.1D') and middle (Fig. 4.1E') *Gli3*$^{Xt/Xt}$ sections as in the wild types (Fig. 4.1D and E), as discussed before, whereas in very rostral sections of the *Gli3*$^{Xt/Xt}$ ventral telencephalon, Mash1 expression was observed throughout the telencephalic vesicles (Fig. 4.1F'), in contrast to the ventrally restricted positive cells in the wild type embryos (Fig. 4.1F). The total volume of Mash1 expression domain in the *Gli3*$^{Xt/Xt}$ mutants (0.56 ± 0.04 mm^3) showed a significant 17.7% reduction (Student's *t* test, $p<0.05$, n=4 per genotype) compared to that of wild types (0.68 ± 0.04 mm^3) (Fig. 4.6A). Interestingly, this reduction is observed only in the mid-telencephalic sections, whereas in the caudal and rostral parts of the telencephalon, Mash1 expression is expanded (Fig. 4.6C) (Table 4.2). All these differences between wild types and mutants are significant (Student's *t* test, $p<0.05$, n=4 per genotype). Olig2 expression was also measured in wild types and *Gli3*$^{Xt/Xt}$ mutant embryos. The expression of Olig2 is generally broader than that of Mash1 in wild type embryos (compare Fig. 4.1G, H and I with Fig. 4.1J, K and L). In the mutants, the Olig2 positive area seemed to be also broader than the Mash1 positive domain (compare Fig. 4.1D', E' and F' with Fig. 4.1J', K' and L'). The Olig2 expression domain in the *Gli3*$^{Xt/Xt}$ mutants (0.63 ± 0.06 mm^3) showed a significant 19.2% reduction (Student's *t* test, $p<0.05$, n=2 per genotype) compared to that of wild type embryos (0.78 ± 0.01 mm^3) (Fig. 4.6A), and this reduction was only observed in the middle sections of the mutant telencephalon (Fig. 4.6D) (Table 4.3), similar to what was observed with the

Mash1 expression domains. Note that both Mash1 and Olig2 expression showed a most prominent expansion at rostral telencephalic sections of the mutants (Table 4.2 and 4.3). These data suggest that the overall size of the *Gli3*$^{Xt/Xt}$ mutant ventral telencephalon is smaller than that of wild types at E12.5, but this reduction occurs only in the middle part of the ventral telencephalon.

Area (mm^2)	rTel	mTel	cTel
***Gli3*$^{+/+}$**	0.29±0.01	0.91±0.02	0.37±0.02
***Gli3*$^{Xt/Xt}$**	0.51±0.01	0.66±0.02	0.46±0.01
P value	≤0.001	0.001	0.036
Percentage of changes in the mutants	75.9%	27.5%	24.3%

Table 4.2 Areas of Mash1 expression in rostral (rTel), middle (mTel) and caudal (cTel) telencephalon of the E12.5 wild type (*Gli3*$^{+/+}$) and *Gli3*$^{Xt/Xt}$ mutant embryos.

Area (mm^2)	rTel	mTel	cTel
***Gli3*$^{+/+}$**	0.26±0.02	1.31±0.03	0.31±0.02
***Gli3*$^{Xt/Xt}$**	0.68±0.02	0.78±0.02	0.47±0.01
P value	≤0.001	≤0.001	0.02
Percentage of changes in the mutants	161.5%	40.5%	51.6%

Table 4.3 Areas of Olig2 expression in rostral (rTel), middle (mTel) and caudal (cTel) telencephalon of the E12.5 wild type (*Gli3*$^{+/+}$) and *Gli3*$^{Xt/Xt}$ mutant embryos.

4.2.5 The *Gli3*$^{Xt/Xt}$ mutant telencephalon becomes progressively disorganized after E12.5

To study the development of *Gli3*$^{Xt/Xt}$ mutant telencephalon after E12.5, wild type and *Gli3*$^{Xt/Xt}$ mutant embryos were analysed from E13.5 to E16.5 using several telencephalic markers. The mutant telencephalon was found progressively disorganized after E12.5. Pax6 and Mash1 expression was examined by

immunohistochemistry on caudal to rostral sections at E13.5 and E14.5. In more caudal sections at both ages, Pax6 immunoreactivity was confined to the dorsal telencephalon, the epithalamus, the dorsal and ventral thalamus and the eminentia thalami (Fig. 4.7A, E, A' and E'), and the expression of Mash1 was confined to the ventral telencephalon, the ventral thalamus and the hypothalamus (Fig. 4.7C, G, C' and G') in both wild type and *Gli3*$^{Xt/Xt}$ mutant embryos. Rostrally, Pax6 is expressed not only in the dorsal telencephalon of wild types, but also intensely in cells of the mantle layer of the GE (indicated by arrows in Fig. 4.7B and F). Pax6 expression in the dorsal telencephalon was still visible in the E13.5 *Gli3*$^{Xt/Xt}$ mutants (area between the lines in Fig. 4.7B'), but at a reduced level compared to wild types (Fig. 4.7B). There were also some strongly labelled Pax6 cells observed in the outer layer of the dorsal telencephalic lobes (arrows in Fig. 4.7B'), which are likely to be those detected in the wild type ventral telencephalon (compare cells indicated by arrows in Fig. 4.7B with B'). At E14.5, the normal expression of Pax6 in the *Gli3*$^{Xt/Xt}$ mutant dorsal telencephalon seemed to be lost completely. Instead, the strong Pax6 expressing ventral cells were detected in the outer layer of the mutant telencephalic lobes (Fig. 4.7F'). In these rostral sections, Mash1 expression was confined to the ventral territory of the wild type embryos (Fig. 4.7D and H), but in the *Gli3*$^{Xt/Xt}$ mutants (Fig. 4.7D' and H'), it was found throughout the telencephalic vesicles at both E13.5 and E14.5, similar to the results at E12.5. Note that Mash1 expression in the mutant septum is expanded at both ages (arrowheads in Fig. 4.7D' and H'), and the diencephalon joins with the ventral telencephalon in very rostral sections, which is never observed in wild types.

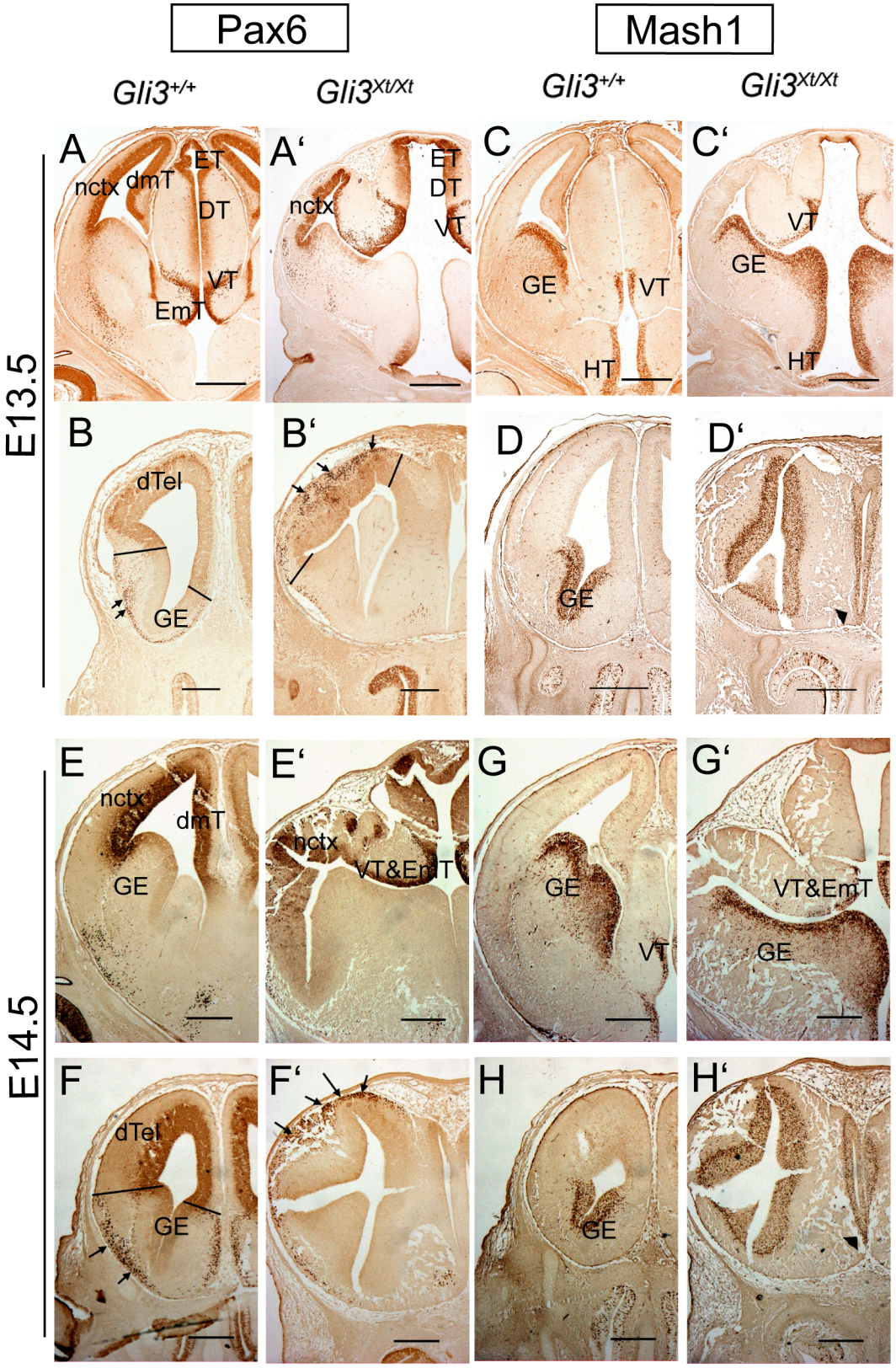
Pax6
Mash1
Gli3+/+
Gli3Xt/Xt
Gli3+/+
Gli3Xt/Xt
E13.5
E14.5
A
A‘
C
C‘
B
B‘
D
D‘
E
E‘
G
G‘
F
F‘
H
H‘
ET
DT
VT
EmT
nctx
dmT
dTel
GE
HT
VT&EmT

Figure 4.7 Expression of Pax6 and Mash1 in E13.5 and E14.5 wild type (*Gli3*$^{+/+}$) (**A**-**H**) and *Gli3*$^{Xt/Xt}$ mutant (**A'**-**H'**) coronal sections. In caudal sections at both E13.5 and E14.5, Pax6 expression is found in the epithalamus (ET), dorsal (DT) and ventral (VT) thalamus, the eminentia thalami (EmT), the neocortex (nctx) and the dorso-medial telencephalon (dmT) of the wild types (**A** and **E**). In the mutants (**A'** and **E'**), the expression pattern is similar except the dorso-medial telencephalon is not present. Mash1 expression at this level is confined to the ventral thalamus (VT), the hypothalamus (HT) and the ventral telencephalon (GE) of both wild type (**C** and **G**) and mutant (**C'** and **G'**) embryos. Rostrally, Pax6 expression in the E13.5 mutant embryos (**B'**) is still visible in the dorsal telencephalon (dTel) but at a reduced level compared to that of wild types (**B**). The intensely stained Pax6 positive cells in the ventral telencephalon of the wild type (arrows in **B**) are observed in a more dorsal area in mutant embryos (arrows in **B'**). These mis-located cells are also observed at E14.5, and the normal Pax6 expression in the dorsal telencephalon (**F**) seems to have disappeared completely in the mutants (**F'**). In rostral sections, Mash1 expression is found throughout the telencephalic vesicles of the mutants (**D'** and **H'**) in great contrast to the wild type expression pattern (**D** and **H**) at both ages. Mash1 expression in the mutant septum seems to be expanded at both ages (arrowheads in **D'** and **H'**). Scale bars, 250 μm.

At E13.5, Nkx2.1 expression was confined to the precursors of the MGE in mid-telencephalic sections, and was not observed in rostral sections of wild type and mutant embryos (Fig. 4.8A, A', B and B'), similar to what was observed at E12.5 (Fig. 4.2F, F', G and G'). In E13.5 wild types and *Gli3*$^{Xt/Xt}$ mutants, Olig2 expression was still restricted to progenitor cells of the ventral thalamus and GE in caudal sections (Fig. 4.8C and C'). Rostrally, expression of Olig2 was found throughout the telencephalic lobes of mutants (Fig. 4.8D'), in contrast to the ventrally restricted expression in wild types (Fig. 4.8D). At both E13.5 and E14.5, Islet1 expression in middle sections was confined to the postmitotic neurons of the GE in both wild type (Fig. 4.8E and G) and *Gli3*$^{Xt/Xt}$ mutant embryos (Fig. 4.8E' and G'). In rostral sections of the mutants at both ages, Islet1 expression was found in the outer layers of the whole telencephalic lobes (Fig. 4.8F' and H'), and the expansion at these ages was more severe than that observed at E12.5 (Fig. 4.2B'). At both ages, Islet1 expression in the postmitotic cells of the mutant septum seems to be also expanded (arrowheads in Fig. 4.8F'and H').

To study the development of the diencephalic clusters observed in the mutant neocortex, the eminentia thalami marker calretinin, and Lim2 expression, were examined at E14.5 wild type and *Gli3*$^{Xt/Xt}$ mutants. At this age, calretinin and Lim2 were highly expressed in the ventral thalamus, the eminentia thalami, and in the marginal zone of the neocortex in wild types (Fig. 4.9A and B). In *Gli3*$^{Xt/Xt}$ mutants, this expression was found intensely in the ventral thalamus and eminentia thalami region, and also in the Foxg1 positive area (Fig. 4.9C') in the form of clusters (arrows in Fig. 4.9A' and B'). Note that at this age, Foxg1 expression in the mutants allowed the detection of rosette-like structures (Fig. 4.9C'), which were never observed in wild types (Fig. 4.9C) (see Chapter 4.2.6). These results suggest that at later developmental stages, diencephalic cells are still present in the *Gli3*$^{Xt/Xt}$ mutant neocortex, and seem to be well segregated from telencephalic cells.

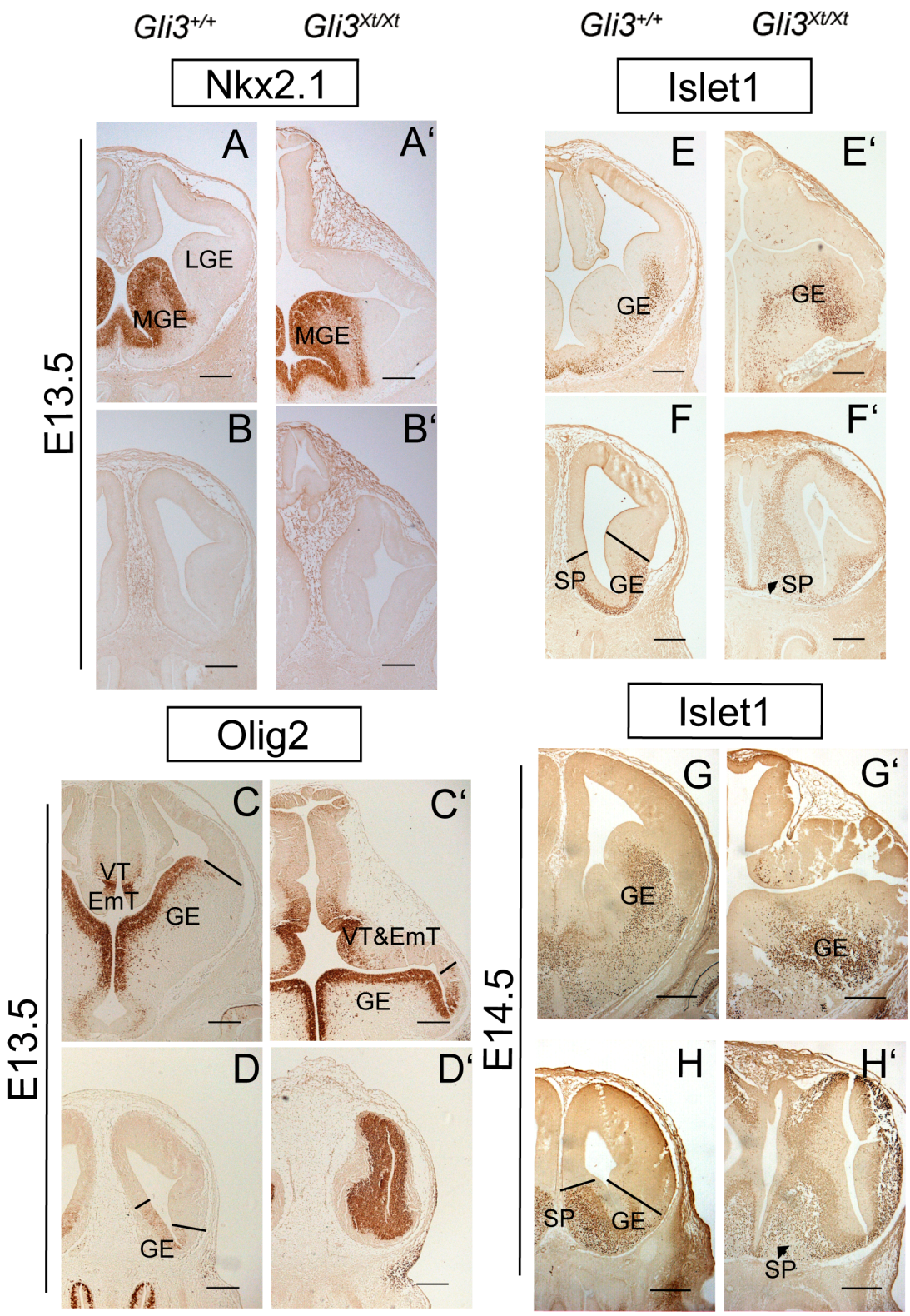
Gli3+/+
Gli3Xt/Xt
Nkx2.1
A
A‘
LGE
MGE
MGE
B
B‘
E13.5
Gli3+/+
Gli3Xt/Xt
Islet1
E
E‘
GE
GE
F
F‘
SP
GE
SP
Olig2
C
C‘
VT
EmT
GE
VT&EmT
GE
D
D‘
GE
E13.5
Islet1
G
G‘
GE
GE
H
H‘
SP
GE
SP
E14.5

Figure 4.8 Marker analyses in E13.5 and E14.5 wild type (*Gli3*$^{+/+}$) (**A**-**H**) and *Gli3*$^{Xt/Xt}$ mutant (**A'**-**H'**) coronal sections. At E13.5, Nkx2.1 is restricted to the medial ganglionic eminence (MGE) of both wild types (**A**) and mutants (**A'**) in middle sections. No Nkx2.1 expression is observed at rostral levels (**B** and **B'**). Olig2 and Islet1 expression is observed in the ventral thalamus (VT) and the ganglionic eminences (GE) of E13.5 and/or E14.5 wild type (**C**, **E** and **G**) and mutants (**C'**, **E'** and **G'**) in middle telencephalic sections. Rostrally, expression of these markers is observed throughout the telencephalic lobes of mutants (**D'**, **F'** and **H'**), in contrast to that of wild types (**D**, **F** and **H**). Note that at both ages, Islet1 expression in the mutant septum (SP) is expanded (arrowheads in **F'** and **H'**) compared to that of the wild types (**F** and **H**). EmT, eminentia thalami; LGE, lateral ganglionic eminence. Scale bars, 250 μm.

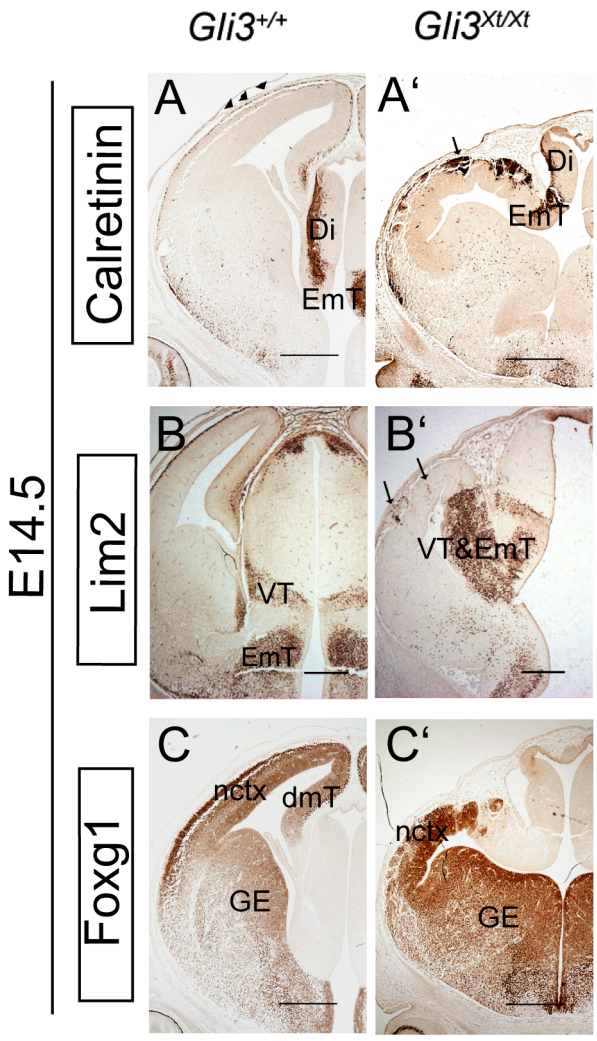

Figure 4.9 Calretinin, Lim2 and Foxg1 expression in E14.5 wild type (*Gli3*$^{+/+}$) (**A**-**C**) and *Gli3*$^{Xt/Xt}$ mutant (**A'**-**C'**) coronal sections. Calretinin is expressed in the postmitotic layer of the diencephalon (Di), the eminentia thalami (EmT), the Cajal-Retzius cells in the marginal zone of the wild types (indicated by arrowheads in **A**). Calretinin positive clusters (indicated by an arrow in **A'**) are observed in the Foxg1 positive area in the mutant neocortex (nctx, **C'**), but not in the dorsal (dmT + nctx) or ventral (GE) telencephalon of wild types (**C**). Lim2 is expressed in the ventral thalamus and the eminentia thalami in wild type (**B**) and mutant (**B'**) embryos. Lim2 positive clusters are also observed in mutant neocortex (arrows in **B'**). Scale bars, 250 μm.

4.2.6 Rosettes form in the residual *Gli3*$^{Xt/Xt}$ neocortex after E12.5

From E13.5, Foxg1 positive and calretinin negative rosette-like structures were detected in the *Gli3*$^{Xt/Xt}$ neocortical region close to the ventricular zone (Fig. 4.10A, B, C, D, E, F and G). Although the number and size of these structures were variable, they all consistently contained a central lumen. There was no obvious correlation between the frequency of their appearance and position within the neocortex. These rosettes were positive for Pax6 (Fig. 4.7E' and 4.10H) and negative for Mash1 (Fig. 4.7G'), indicating that they comprised neocortical tissue and did not have a ventral telencephalic or diencephalic character. They were immunopositive for markers of neural progenitors, such as Pax6 (Fig. 4.10H), BrdU (Fig. 4.10I), and nestin (Fig. 4.10J), and negative for the postmitotic neuronal marker β-III-tubulin (Tuj1) (Fig. 4.10K). The expression of Tbr2, which is normally detected in the cortical intermediate zone and early postmitotic neurons (Englund et al., 2005) was found in the outermost cells of the rosettes (Fig. 4.10L). At later stages, rosettes became more numerous and were also found close to the pial surface (Fig. 4.10B, C and F). At E16.5, the lumen in the centre of the rosettes was not as clearly distinguishable as in previous stages (Fig. 4.10F'). These findings indicate that the rosettes contain well organized proliferating neocortical cells.

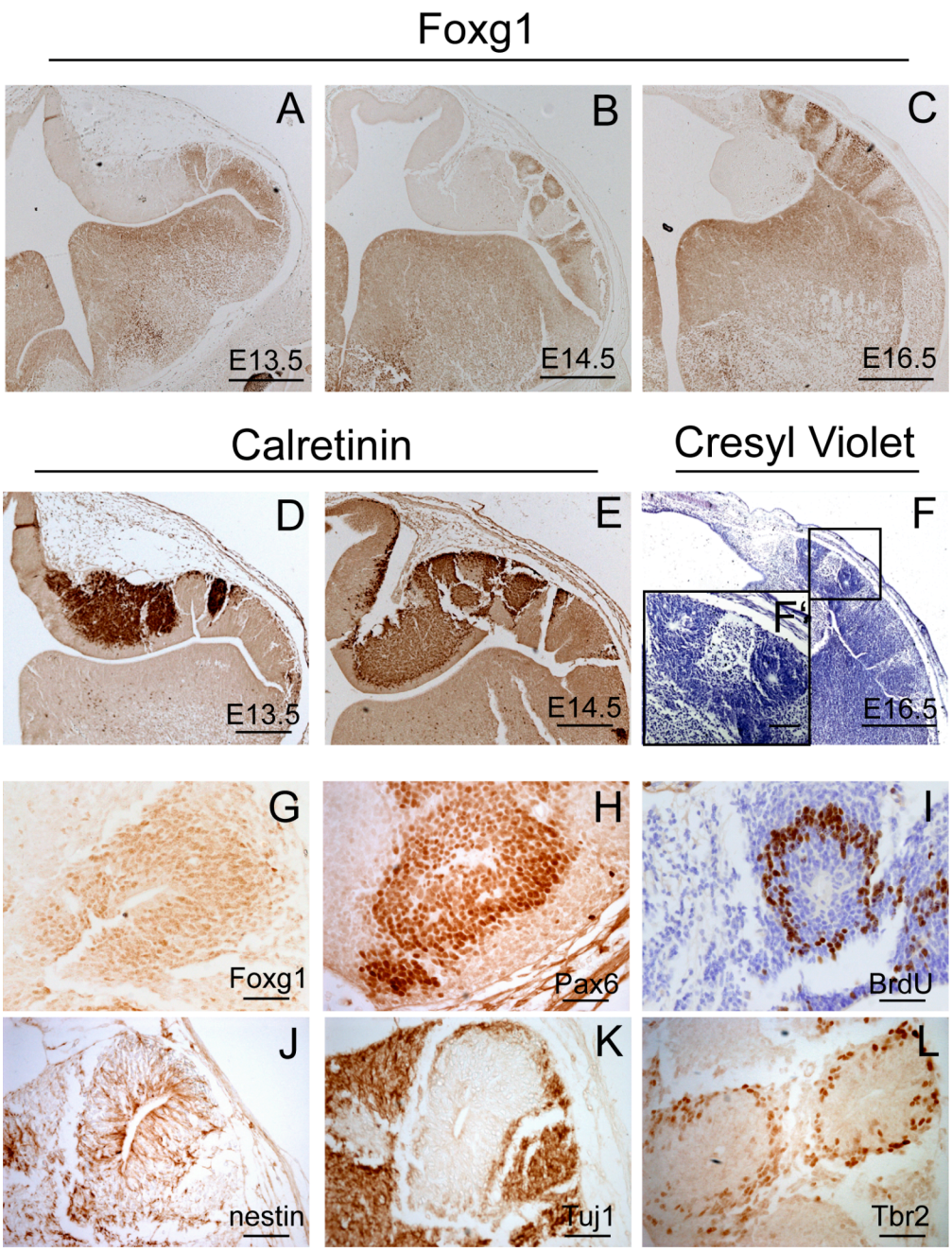

Figure 4.10 Marker analyses on *Gli3*$^{Xt/Xt}$ mutant coronal sections from E13.5 to E16.5. Foxg1 negative patches are observed at E13.5 (**A**), E14.5 (**B**) and E16.5 (**C**). These patches are positive for calretinin at E13.5 (**D**) and E14.5 (**E**), but not at E16.5. **A**, **D** and **B**, **E** are serial sections from the same specimens. Cresyl violet staining at E16.5, shows a greater number of rosettes with a lumen (**F**, **F'**). **F'** is a high magnification image of the boxed area in **F**. These rosettes are positive for Foxg1 (**G**), Pax6 (**H**), BrdU (**I**), and nestin (**J**) and negative for β-III-tubulin (Tuj1) (**K**), showing their neocortical progenitor properties. Tbr2 is expressed in the outermost cells of the rosettes (**L**). Scale bars, **A**-**F**, 500 μm; **G**-**L**, 50 μm.

4.2.7 Cell proliferation and cell death properties are unchanged in E12.5 *Gli3*$^{Xt/Xt}$ telencephalon

The volumetric measurements showed that the *Gli3*$^{Xt/Xt}$ dorsal telencephalon was severely decreased in size compared to that of wild type embryos at E12.5. The dorsal telencephalon of the mutants became progressively disorganized later in development. To determine whether there were any gross abnormalities in the proliferative characteristics of the *Gli3*$^{Xt/Xt}$ neocortex, a short pulse of BrdU was administered to label the proliferating cells within the ventricular zone in both wild types and mutants at E12.5 and E13.5. Immunohistochemistry using an antibody against BrdU showed no obvious differences between mutants and control embryos at both E12.5 and E13.5 (Fig. 4.11A, A', E and E'). Cell counts were done in sampling bins throughout the thickness of the neocortex of the wild type and mutant embryos. At both ages, the labelling indices (LI), which is the percentage of cells that are in S-phase during a 30-minute period, in the wild type and mutant dorsal telencephalon were very similar (Fig. 4.11H and I) (Table 4.4). The thickness of the postmitotic neuronal layer (PL) which is negative for BrdU was also similar between wild type and mutant embryos (Fig. 4.11B, B', H and I) (Table 4.4), in agreement with the staining observed using an antibody against β-III-tubulin (Tuj1), which selectively marks the postmitotic neuronal layer (Fig. 4.11C, C', D and D').

E12.5	BrdU Labelling Index (LI)	Postmitotic Layer (PL)
***Gli3*$^{+/+}$ (n=6)**	55.1%±3.1%	19.4%±4.5%
***Gli3*$^{Xt/Xt}$ (n=6)**	49.9%±3.9%	25.4%±3.2%
P value	0.31	0.31
E13.5	**BrdU Labelling Index (LI)**	**Postmitotic Layer (PL)**
***Gli3*$^{+/+}$ (n=2)**	43.0%±1.6%	33.5%±2.9%
***Gli3*$^{Xt/Xt}$ (n=2)**	35.4%±4.62%	31.2%±1.3%
P value	0.17	0.50

Table 4.4 BrdU labelling indices (LI) and postmitotic layer (PL) measurements at E12.5 and E13.5 wild type (*Gli3*$^{+/+}$) and *Gli3*$^{Xt/Xt}$ mutant embryos.

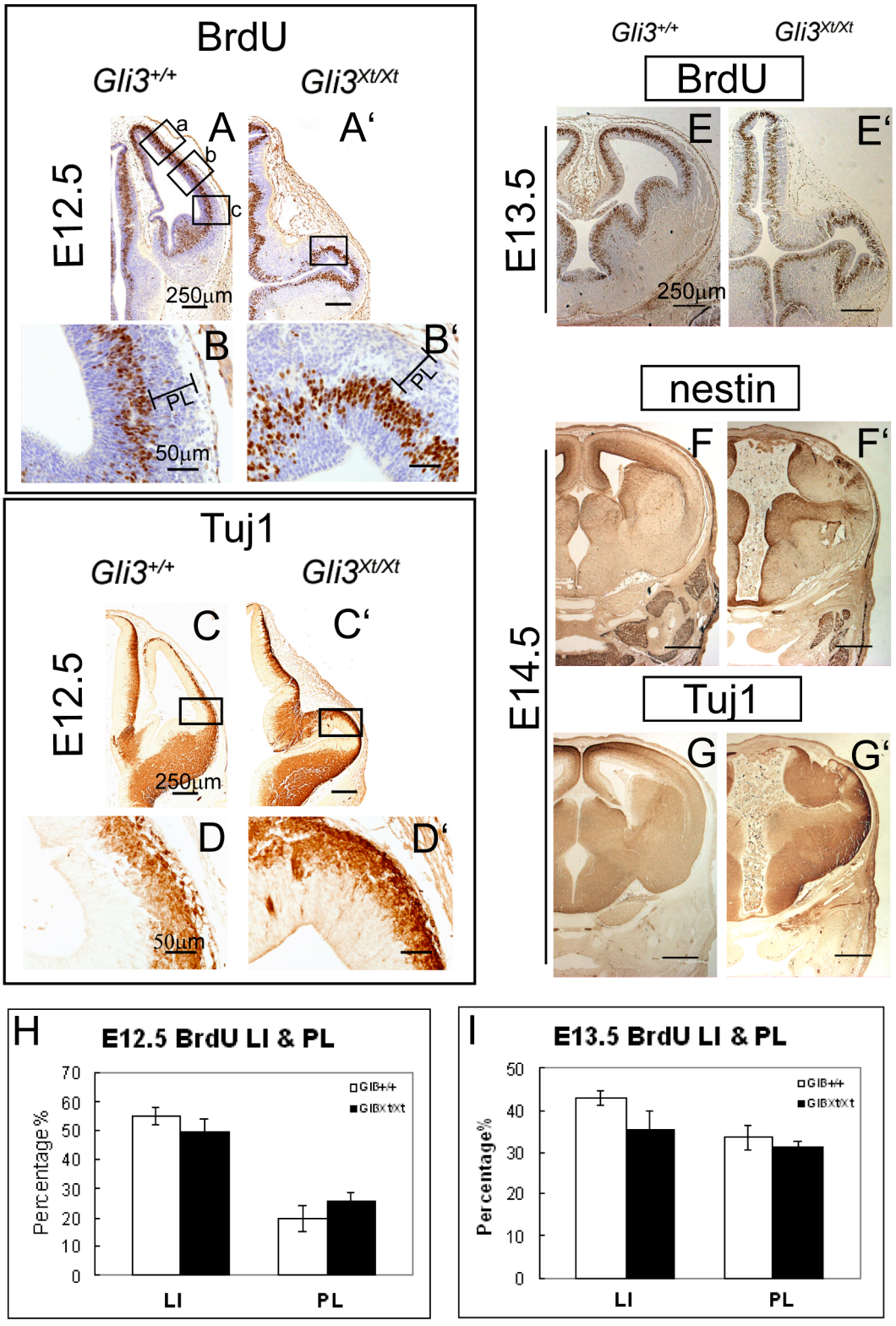
BrdU
Gli3+/+
Gli3Xt/Xt
E12.5
A
A'
a
b
c
250µm
B
B'
PL
50µm
Tuj1
C
C'
D
D'
E13.5
E
E'
nestin
F
F'
E14.5
Tuj1
G
G'
H
E12.5 BrdU LI & PL
Percentage%
GIB+/+
GIBXt/Xt
LI
PL
I
E13.5 BrdU LI & PL

Figure 4.11 BrdU and β-III-tubulin (Tuj1) expression in E12.5 wild type (*Gli3*$^{+/+}$) (**A**-**D**) and *Gli3*$^{Xt/Xt}$ mutant (**A'**–**D'**) coronal sections. **B**, **B'**, **D** and **D'** are high magnification images of the boxed areas in **A** (box c), **A'**, **C** and **C'** respectively. Box a, b and c in A corresponds to the sampling bins for BrdU counting. BrdU is expressed by cells that are in S-phase in both wild type (**A** and **B**) and *Gli3*$^{Xt/Xt}$ mutants (**A'** and **B'**). The labelling index (LI) of the BrdU positive cells shows no differences between wild type and mutant dorsal telencephalon (**H**). Tuj1 expression is observed in the postmitotic layer (PL) of wild type (**C** and **D**) and mutant (**C'** and **D'**) telencephalon. Note the thickness of this layer is similar between wild types and mutants (compare **B** with **B'**, **D** with **D'**, **H**). BrdU expression in E13.5 wild type (**E**) and mutant (**E'**) coronal sections show similar results (**I**) as in E12.5. Nestin and Tuj1 expression on E14.5 coronal sections show complementary staining in both wild type (**F** and **G**) and mutant (**F'** and **G'**) embryos. Scale bars, **A**, **C**, **A'**, **C'**, **E**-**G** and **E'**-**G'**, 250 μm; **B**, **D**, **B'** and **D'**, 50 μm.

Nestin and Tuj1 immunohistochemistry was studied in E14.5 wild type and *Gli3*$^{Xt/Xt}$ mutant embryos. Nestin is expressed in the proliferating cells and fibres (Dahlstrand et al., 1995), and Tuj1 is expressed by the postmitotic neurons. Their expression at E14.5 seems to be complementary to each other in both wild type and mutant embryos (Fig. 4.11F, F', G and G'). These results demonstrate that no obvious change is detected in cell proliferation and differentiation in the *Gli3*$^{Xt/Xt}$ mutants between E12.5 and E14.5, suggesting that the size reduction of *Gli3*$^{Xt/Xt}$ telencephalon might be the result of a cell proliferation and/or differentiation defect occurring at earlier developmental stages.

Cell death properties were studied in the E12.5 wild type and *Gli3*$^{Xt/Xt}$ mutant telencephalon, by using terminal deoxynucleotidyl transferase (TdT)-mediated dUTP-biotin nick end labelling (TUNEL) method on sections. In wild type embryos, many dying cells were detected in the dorso-midline area (Fig. 4.12A), which were never observed in the *Gli3*$^{Xt/Xt}$ mutants (Fig. 4.12A'), possibly due to the loss of cortical hem and the surrounding dorsal telencephalic tissue. Only a few TUNEL positive cells were observed in both the wild type and the *Gli3*$^{Xt/Xt}$ mutant dorsal (Fig. 4.12B and B') and ventral (Fig. 4.12C and C') telencephalon. The number of TUNEL positive cells per 1000 cells calculated showed no difference between the wild type and mutant telencephalon (Fig. 4.12D). These suggest that size reduction of *Gli3*$^{Xt/Xt}$ telencephalon might be the result of cell death defect occurring at earlier developmental stages.

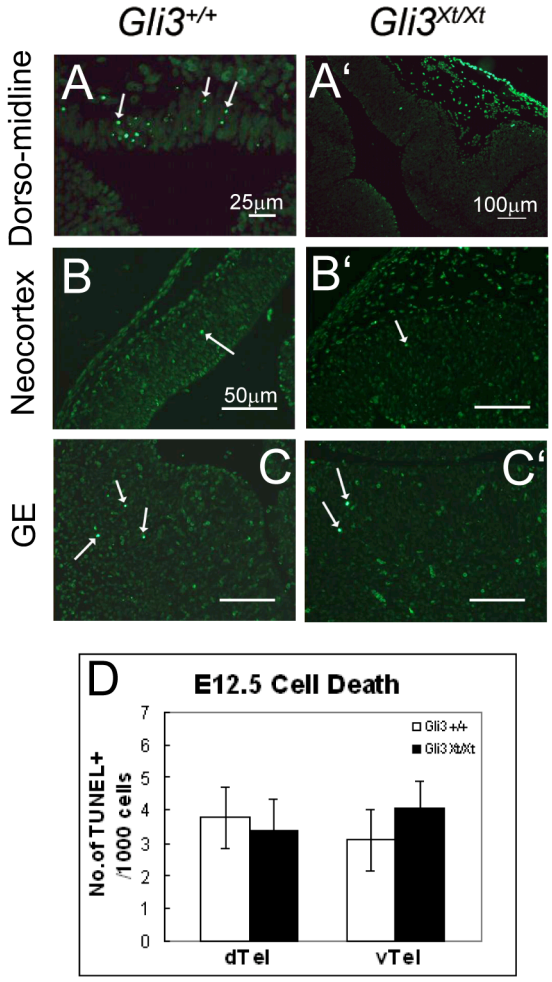

Figure 4.12 TUNEL on E12.5 wild type (*Gli3*$^{+/+}$) (**A**-**C**) and *Gli3*$^{Xt/Xt}$ mutants (**A'**-**C'**) coronal sections. Many TUNEL positive cells are present in the wild type dorso-midline area (**A**), but not in the *Gli3*$^{Xt/Xt}$ mutants (**A'**). Very few TUNEL positive cells are observed in the dorsal (neocortex, **B** and **B'**) and ventral (GE, **C** and **C'**) wild type (**B** and **C**) and mutant (**B'** and **C'**) telencephalon. No significant differences in the number of TUNEL positive cells per 1000 cells within the telencephalon are detected between wild type and mutant embryos (**D**). Scale bars, **A**, 25 μm; **B**, **C**, **B'** and **C'**, 50 μm; **A'**, 100 μm.

4.3 DISCUSSION

4.3.1 No ectopic expression of ventral telencephalic markers in middle sections of the *Gli3*$^{Xt/Xt}$ mutant dorsal telencephalon

A reduction in the size of the dorsal telencephalon and lack of the dorso-midline invagination have been reported in *Gli3*$^{Xt/Xt}$ mutant embryos (Grove et al., 1998; Theil et al., 1999; Tole et al., 2000a). However, these studies neither delineated the telencephalon of the *Gli3*$^{Xt/Xt}$ mutants, nor measured its actual size. In this study, the *Gli3*$^{Xt/Xt}$ neocortex was precisely defined, using Foxg1 as a marker of the whole telencephalon (Tao and Lai, 1992; Hanashima et al., 2002). The dorsal telencephalon was defined using the expression domain of Pax6 (Walther and Gruss, 1991; Stoykova and Gruss, 1994; Mastick et al., 1997), and the ventral telencephalon using Mash1 (Lo et al., 1991; Guillemot and Joyner, 1993) and Olig2 (Lu et al., 2000; Zhou et al., 2000). The analysis presented in this chapter has shown that between E12.5 and E14.5 the Mash1, Olig2, Islet1, Dlx2 and Gsh2 positive areas, dorsally to the neocortex of the *Gli3*$^{Xt/Xt}$ mutant embryos, in middle sections along the rostro-caudal axis of the telencephalon, corresponds to the ventral thalamus and eminentia thalami, in contrast to previous publications that had interpreted this staining as ventral telencephalon (Tole et al., 2000a; Rallu et al., 2002b; Kuschel et al., 2003). This difference may be due to the fact that previous studies did not define the limits of the telencephalon and did not take into account the possibility that many ventral telencephalic markers are also expressed in the ventral thalamus. However, the Mash1, Olig2 and Islet1 expression in the very rostral telencephalon of the *Gli3*$^{Xt/Xt}$ mutants is expanded into the dorsal telencephalon, agreeing with previous results (Tole et al., 2000a; Kuschel et al., 2003). The areal measurements of ventral markers further support the conclusion that the rostral telencephalon of the mutants is

enlarged at E12.5. This expansion is also observed at E13.5 and E14.5.

Another finding in very rostral sections of the *Gli3*$^{Xt/Xt}$ mutants is that at least some of the cells are expressed both dorsal telencephlic marker Pax6 and ventral telencephalic marker, such as Mash1 and Olig2. It will be interesting to know the fates of these cells and the reason they express both dorsal and ventral markers.

4.3.2 Neocortical cells form rosettes surrounded by eminentia thalami cells in *Gli3*$^{Xt/Xt}$ mutants

The *Gli3*$^{Xt/Xt}$ mutant telencephalon becomes highly disorganized at later developmental stages. Previous work has described the formation of some 'finger-like' structures in the neocortical area of the *Gli3*$^{Xt/Xt}$ mutants (Theil et al., 1999), but further studies of the properties of these cells were lacking. Rosette-like structures start to form at around E13 in the mutant neocortex, and comprise a central lumen surrounded by neural progenitor cells. The distribution of BrdU positive S-phase cells largely resembles that of the wild type ventricular zone. Tbr2 expression in the outermost layers of the rosettes further suggests that the wall of the rosettes is very similar to the ventricular zone of the wild type neocortex. As development proceeds, these rosettes become more numerous, and are located in the area near the pial surface, and are well segregated from the surrounding tissue. In fact, these rosettes are surounded by diencephalic cells, suggesting that the formation of those rosettes might be the results that the telencephalic and diencephalic cells do not mix together. Studies of other mutations with brain heterotopias suggested that the formation of rosette-like structures might have been the result of changes in cell polarity or cell migration properties (Costa et al., 2001; Li et al., 2003; Klezovitch et al., 2004). A recent study showed apical-basal cell polarity defects in the *Gli3*$^{Xt/Xt}$

neocortical area (Theil, 2005), which might be one cause for the formation of the rosettes. The fact that these rosettes are located near the ventricular zone at E13.5 but are found near the pial surface at E16.5, suggests that the migration properties of these cells might be changed.

Patches of Foxg1 negative cells are present in the *Gli3*$^{Xt/Xt}$ dorsal telencephalon at E12.5, and these clusters are expressing markers of the neighbouring eminentia thalami such as calretinin, Lim2 and Tbr1 (Sheng et al., 1997; Abbott and Jacobowitz, 1999; Puelles et al., 2000). Additionally, Pax2, which was described here for the first time as a marker for an eminentia thalami population found close to the choroid plexus of the wild types, was also found in the *Gli3*$^{Xt/Xt}$ neocortical area. These results suggest that the boundary between the telencephalon and the diencephalon is compromised when Gli3 is lost. What might happen in the mutants is that loss of the cortical hem region and failure of the dorso-medial telencephalic wall to invaginate may result in an abnormal joining of the residual telencephalon with the diencephalon. The dorso-medial telencephalon in the wild types serves as a physical and (or) a possible signalling boundary to prevent the mixing of the cells from each territory (Grove et al., 1998; Grove and Tole, 1999). The loss of this restriction in the *Gli3*$^{Xt/Xt}$ mutants may result in the mixing of cell types in that region.

There are other factors that might also contribute to the abnormalities described above. For example, the ZLI, the boundary between the dorsal and ventral thalamus (Figdor and Stern, 1993; Porteus et al., 1994; Kiecker and Lumsden, 2004), is characterized by *Shh* expression (Hashimoto-Torii et al., 2003; Kiecker and Lumsden, 2004) and considered as an organizer of the diencephalon (Echevarria et al., 2003; Vieira et al., 2005). The expression of *Shh* seems to be confined to its normal place in the *Gli3*$^{Xt/Xt}$ mutants. However, the orientation is different from that of wild type

embryos. This change in orientation might affect Shh signalling diffusion or transduction in the mutant embryos, because the relative distance between the ZLI and the neocortex is altered, which might influence the formation of the telencephalic-diencephalic boundary, or even the patterning of the telencephalon, as studies have shown that in zebrafish Shh could act directly over a distance up to 200 μm (Lewis et al., 2001).

4.3.3 The volume of *Gli3*$^{Xt/Xt}$ telencephalon is severely reduced at E12.5

The Foxg1 positive telencephalon of the *Gli3*$^{Xt/Xt}$ mutant is only about 53.5% the volume of wild types. The dorsal telencephalon of the *Gli3*$^{Xt/Xt}$ mutants is decreased severely to about 27% of the wild type dorsal telencephalon. In addition to this reduction, clusters of eminentia thalami cells are present in the neocortical area of the mutants. A 20% reduction of the ventral telencephalon of *Gli3*$^{Xt/Xt}$ mutant embryos has also been shown here. Interestingly, this reduction is only observed in middle telencephalic sections, whereas the rostro-ventral and caudo-ventral telencephalon is significantly enlarged in the mutants. The study of markers that are normally expressed in the septum of the ventral telencephalon, such as Islet1, Pax2 and Lim2 (Sheng et al., 1997; Wang and Liu, 2001) in very rostral telencephalic sections, reveals that the mutant septum is enlarged and probably undergoes a shape change (Chapter 5.2.8). These results also indicate that the most rostral boundary between the telencephalon and diencephalon is formed abnormally in *Gli3*$^{Xt/Xt}$ mutants.

The volumes of *Gli3*$^{Xt/Xt}$ mutant telencephalon are hard to measure in later developmental stages because the mutant telencephalon becomes highly disorganized and rosettes appear. The fact that no defects in cell proliferation, cell differentiation or cell death properties were detected suggests that the phenotypes observed at E12.5

must be a consequence of an earlier defect of the *Gli3*$^{Xt/Xt}$ mutants. Interestingly, analysis with a short pulse of BrdU at E12.5 revealed that the residual neocortex of the *Gli3*$^{Xt/Xt}$ embryos shares properties with the lateral neocortex of the wild type (Fig. 4.11), indicating a more extensive area of the dorsal telencephalon in *Gli3*$^{Xt/Xt}$ mutants may be lost, rather than just the cortical hem region, as previously reported (Grove et al., 1998).

Chapter 5: Analyses of *Gli3*$^{Xt/Xt}$ mutant forebrain at E10.5 suggest that Gli3 is involved in forebrain regionalization during early embryogenesis

5.1 INTRODUCTION

Gli3 starts to be expressed as early as E7 during mouse development (Hui et al., 1994) in the derivatives of the ectoderm and the mesoderm, suggesting Gli3 might be involved in early forebrain patterning events. Forebrain analyses at E12.5 and at later stages of the *Gli3*$^{Xt/Xt}$ mutant embryos (Chapter 4) have shown that they have a smaller telencephalon compared to that of the wild types. Cell proliferation and cell death studies at E12.5 showed no differences between the mutant and control embryos. These results indicate that the defects of the *Gli3*$^{Xt/Xt}$ mutants must have happened in early developmental stages. Here in this Chapter, *Gli3*$^{Xt/Xt}$ mutants were analysed at E10.5, when neurogenesis starts.

So far, marker analysis has been carried out in the *Gli3*$^{Xt/Xt}$ mutant telencephalon by several groups. However, there are some contradictions in their results. For example, the expression of the ventral marker *Nkx2.1* was shown to be expanded to a more dorsal area of the *Gli3*$^{Xt/Xt}$ mutants by whole mount *in situ* hybridization at E11.5 (Aoto et al., 2002). Interestingly, *Nkx2.1* expression has been shown to be confined to the medial ganglionic eminences (MGE) of the *Gli3*$^{Xt/Xt}$ mutants at E10.5 and E12.5 by other groups (Tole et al., 2000a; Kuschel et al., 2003). This contradiction among different studies might be because most of these experiments were done by whole mount *in situ* hybridization, which does not allow visualizing with precision the expression domains of a given marker. In addition, these studies neither measured the relative sizes of the telencephalic structures, nor explored the

differences between ages. The study of the expression pattern by immunohistochemistry of several forebrain ventral markers, such as Nkx2.1, Olig2, Dlx2, Islet1 and Gsh2 is presented in this chapter and they all showed an expansion at E10.5 in *Gli3*$^{Xt/Xt}$ mutants.

The cortical hem and the adjacent hippocampus and the choroid plexus were reported to be lost in the *Gli3*$^{Xt/Xt}$ mutant (Grove et al., 1998). The results obtained from the analyses of E12.5 *Gli3*$^{Xt/Xt}$ mutant embryos suggest that part of the dorsal telencephalon is also lost. To study the possibility of a more extensive loss of the mutant telencephalon, *Wnt8b* expression was examined by whole mount *in situ* hybridization, revealing the expression of *Wnt8b* in *Gli3*$^{Xt/Xt}$ mutant telencephalon was completely lost, while the expression in the diencephalon was preserved at E9.5 and E10.5. These results suggest the dorso-medial telencephalon might never have been specified in the mutants.

Shh has been shown to induce ventral fate along the antero-posterior axis along the neural tube (Ericson et al., 1995a; Marti et al., 1995b; Roelink et al., 1995; Chiang et al., 1996; Dale et al., 1997; Shimamura et al., 1997; Kohtz et al., 1998; Kohtz et al., 2001). In the anterior limb and the dorsal spinal cord, Gli3 is shown to repress *Shh* expression (Buscher et al., 1997; Masuya et al., 1997; Ruiz i Altaba, 1998). It is possible that an ectopic *Shh* expression results in the malformations of *Gli3*$^{Xt/Xt}$ mutant telencephalon. This possibility has been tested by several groups by whole mount *in situ* hybridization from E8.5 to E11.5 (Theil et al., 1999; Tole et al., 2000a; Aoto et al., 2002), showing no obvious difference in the expression pattern of *Shh* between *Gli3*$^{Xt/Xt}$ mutants and control embryos. The expression of *Shh* downstream targets, including *Ptch1* and *Gli1*, has also been examined by whole mount *in situ* hybridization (Theil et al., 1999; Tole et al., 2000a; Aoto et al., 2002). Their expression in the *Gli3*$^{Xt/Xt}$ mutants has been reported to be identical with those of the

wild types. In this chapter, *Shh* mRNA expression was studied by whole mount *in situ* hybridization at E10.5, and those embryos were sectioned afterwards to further explore any differences between wild type and mutant embryos. The Shh protein expression pattern in $Gli3^{Xt/Xt}$ mutants was also studied here at E9.5 and E10.5. However, no significant difference was detected between the wild type and mutants in Shh mRNA and protein expression pattern. Expression of Shh early transcriptional target cyclin D1 (Kenney and Rowitch, 2000; Ishibashi and McMahon, 2002) was analysed in this chapter, showing no obvious difference in the mutants compared to wild types. These results indicate that Shh signalling might not be responsible for the expansion of ventral markers in $Gli3^{Xt/Xt}$ mutant ventral telencephalon.

Aoto and colleagues (2002) have proposed that the $Gli3^{Xt/Xt}$ mutant dorsal telencephalon is reduced in size, while the ventral thalamus is significantly expanded, basing this on the expression pattern of *Pax6* and *Engrailed2* (*En2*) by whole mount *in situ* hybridization. However, no measurements were done in the ventral telencephalon. In this chapter, detailed measurements of the volume of the whole telencephalon, and of the dorsal and ventral telencephalon were carried out at E10.5. The overall size of the $Gli3^{Xt/Xt}$ mutant telencephalon was found to be reduced. Compared to the wild type embryos, the volume of $Gli3^{Xt/Xt}$ mutant dorsal telencephalon displayed a 62.2% reduction, and the volume of the mutant ventral telencephalon showed a 65% increase.

Cell proliferation was previously studied in E10.5 $Gli3^{Xt/Xt}$ mutant telencephalon with a short pulse of BrdU incorporation. The distribution of BrdU in the mutants was comparable with that of their wild type littermates (Theil et al., 1999). In this study, cell cycle kinetic parameters were analysed by the IddU/BrdU method, a more precise and sophisticated experimental approach, which allows the measuring of not only the labelling index but also the duration of the cell cycle and S-phase (Shibui et

al., 1989; Martynoga et al., 2005). At E10.5, no significant differences were found in the length of the cell cycle and S-phase between the *Gli3*$^{Xt/Xt}$ mutants and control embryos. However, a significant increase of the labelling index was observed in the mutant dorsal telencephalon.

Cell death has been reported to be reduced from the *Gli3*$^{Xt/Xt}$ dorsal telencephalon (Aoto et al., 2002), and no study has evaluated the cell death properties in the mutant ventral telencephalon. Cell death was examined by both on-section and whole-mount TUNEL, presenting a loss of TUNEL positive cells in the dorsal midline, as described before (Aoto et al., 2002), but an increase in the ventral midline area of the *Gli3*$^{Xt/Xt}$ mutants. This increase is universal along the rostro-caudal axis. In addition, in the ventral midline of the mutants, more β-III-tubulin positive cells were observed in all sections examined along the rostro-caudal axis, suggesting more cells exiting the cell cycle in the ventral area of the *Gli3*$^{Xt/Xt}$ mutants.

The results obtained from the cell cycle, cell death and differentiation analyses can not explain the size reduction of the *Gli3*$^{Xt/Xt}$ mutant dorsal telencephalon at E10.5 compared to wild types, suggesting that Gli3 might regulate an early specification event. The increase of cell death and differentiation in the *Gli3*$^{Xt/Xt}$ mutant ventral telencephalon at E10.5 might be responsible for the overall size reduction of the mutant ventral telencephalon at E12.5. However, because the changes in cell death and differentiation were observed along the rostro-caudal axis of the mutant ventral telencephalon, they can not explain why only the middle part of the E12.5 ventral telencephalon is reduced, whereas the rostral and caudal parts are expanded. These results leading to hypothesize that in addition to the size changes, the shape of the *Gli3*$^{Xt/Xt}$ mutant forebrain has also changed. In testing this hypothesis, embryos were scanned with an optical projection tomography (OPT) microscopy to get serial images of the entire forebrain. These revealed that the diencephalon and ventral

telencephalon (septum) of the *Gli3*$^{Xt/Xt}$ mutants are joined in a more rostral area than in the wild types. This was confirmed by the expression of diencephalic and (or) septal markers. These results suggest that the shape of the *Gli3*$^{Xt/Xt}$ mutant forebrain is changed between E10.5 and E12.5, and this might account for the differences in the size of the *Gli3*$^{Xt/Xt}$ ventral telencephalon along the rostro-caudal axis.

The *Wnt8b* whole mount *in situ* hybridization experiment described in this chapter was completed in collaboration with Vassiliki Fotaki.

5.2 RESULTS

5.2.1 Volumetric measurements at E10.5 show a reduction of *Gli3*$^{Xt/Xt}$ dorsal telencephalon

E10.5 embryos were analysed in a frontal plane: wild type (A-D) and *Gli3*$^{Xt/Xt}$ mutant (A'-D') examples are shown in Figure 5.1. These embryos were scanned and reconstructed by OPT. In rostral sections (Fig. 5.1D and D'), there is the dorsal and ventral telencephalon; in sections half way between the rostro-caudal tips of the telencephalon (defined as middle sections along the rostro-caudal axis) (Fig. 5.1C and C'), diencephalic tissue can be seen dorsal to the telencephalon in the mutants, but not in wild types; caudally (Fig. 5.1B and B'), the diencephalon becomes very obvious dorsally, and the dorsal and ventral telencephalon are still visible in both wild types and *Gli3*$^{Xt/Xt}$ mutants. Note that the diencephalon of the mutant embryos is more obvious than that of the wild types (compare Fig. 5.1B with B', C with C'), suggesting the diencephalon of the mutants might be enlarged, and this could lead to a shape change of the *Gli3*$^{Xt/Xt}$ mutant forebrain.

Foxg1 expression was examined throughout the rostro-caudal axis of the E10.5 wild type and *Gli3*$^{Xt/Xt}$ mutant telencephalon. As shown in Figure 5.2A, A', B, B', C and C', Foxg1 expression delineates the telencephalon in each level of sections of wild type (Fig. 5.2A, B and C) and *Gli3*$^{Xt/Xt}$ embryos (Fig. 5.2A', B' and C'). The Foxg1 negative diencephalic region in the *Gli3*$^{Xt/Xt}$ mutant forebrain sections seems to be more prominent than that of the wild type embryos (compare Fig. 5.2A with A', B with B'). Volumetric measurements of the whole telencephalon were carried out in wild types and mutants by measuring the Foxg1 expression domain (see Materials and Methods (Chapter 2.5) for detail). A significant 38.6% reduction (Student's *t* test, $p<0.001$, n=4 per genotype) of the volume of the *Gli3*$^{Xt/Xt}$ telencephalon (Fig. 5.2G) was recorded at E10.5 (Table 5.1).

Volume (mm^3)	*Gli3*$^{+/+}$	*Gli3*$^{Xt/Xt}$	P value
Tel (Foxg1)	0.048±0.0005	0.029±0.001	<0.001
dTel (Pax6)	0.038±0.002	0.014±0.001	<0.001
vTel (Olig2)	0.014±0.001	0.023±0.0008	<0.001

Table 5.1 Volume of wild type (*Gli3*$^{+/+}$) and *Gli3*$^{Xt/Xt}$ mutant telencephalon (Tel), dorsal (dTel) and ventral (vTel) telencephalon, calculated using specific gene marker expression domains.

The size of the dorsal telencephalon was measured using Pax6 expression domain in the telencephalon (green) of wild type (Fig. 5.2D-F) and *Gli3*$^{Xt/Xt}$ (Fig. 5.2D'-F') embryos. Pax6 is expressed in the dorsal telencephalon and diencephalon (Walther and Gruss, 1991; Stoykova and Gruss, 1994; Mastick et al., 1997). The Pax6 immunopositive area in caudal and middle sections in the *Gli3*$^{Xt/Xt}$ telencephalon (Fig. 5.2D' and E') seems to be reduced compared to the wild types (Fig. 5.2D and E). Rostrally, Pax6 is expressed throughout the telencephalic lobes in wild types (Fig. 5.2F), while in the *Gli3*$^{Xt/Xt}$ mutants (Fig. 5.2F'), Pax6 expression is maintained, although the positive area seems to be reduced dorsally. The measurements showed

that the volume of the Pax6 expressing tissue was significantly reduced (Student's *t* test, $p<0.001$, n=4 per genotype) in the *Gli3*$^{Xt/Xt}$ mutants to about 37.8% of that of wild type embryos (Fig. 5.2G) (Table 5.1), and this reduction was the same no matter which level of section was examined (Fig. 5.2H) (Table 5.2). These results show that at E10.5, the telencephalon and the dorsal telencephalon of *Gli3*$^{Xt/Xt}$ mutants is already smaller than that of wild type littermates.

Area (mm^2)	rTel	mTel	cTel
***Gli3*$^{+/+}$**	0.104±0.005	0.068±0.001	0.053±0.004
***Gli3*$^{Xt/Xt}$**	0.038±0.002	0.030±0.001	0.025±0.002
P value	<0.001	<0.001	0.014
Percentage of changes in the mutants	63.50%	55.90%	52.80%

Table 5.2 Areas of Pax6 expression in rostral (rTel), middle (mTel) and caudal (cTel) telencephalic sections of the E10.5 wild type (*Gli3*$^{+/+}$) and *Gli3*$^{Xt/Xt}$ mutant embryos.

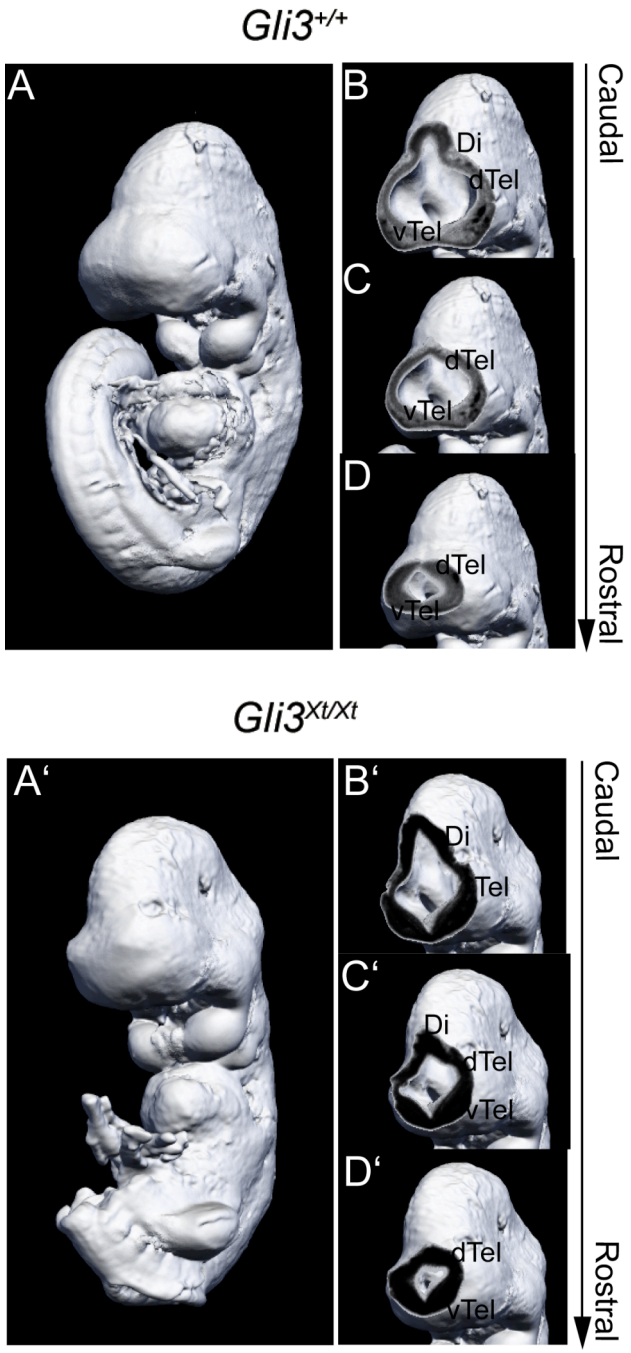

Figure 5.1 OPT images of wild type (*Gli3*$^{+/+}$) (**A**) and *Gli3*$^{Xt/Xt}$ mutant (**A'**) embryos at E10.5. E10.5 embryos are analysed on frontal sections along the rostro-caudal axis. The diencephalon (Di) is observed dorsally to the telencephalon in caudal (**B** and **B'**) sections of both wild type and mutant embryos, and in middle sections of the mutants (**C'**), but not in wild types (**C**). Dorsal (dTel) and ventral telencephalon (vTel) are observed on all sections of both genotypes (**B**-**D** and **B'**-**D'**). The tail of the *Gli3*$^{Xt/Xt}$ mutant presented here has been cut off (**A'**).

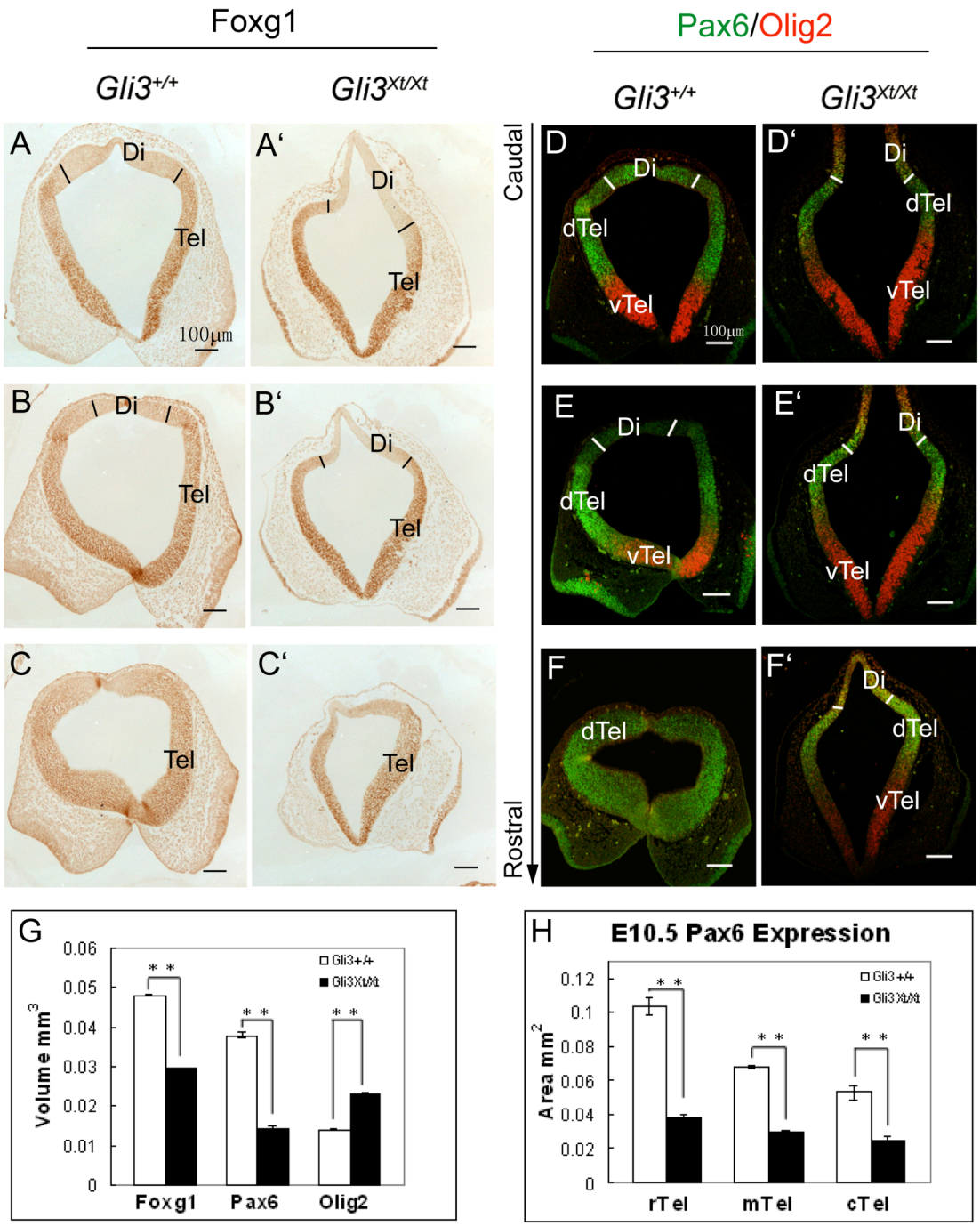
Foxg1
Pax6/Olig2
Gli3+/+
Gli3Xt/Xt
Gli3+/+
Gli3Xt/Xt
A
Di
Tel
100μm
A'
Di
Tel
B
Di
Tel
B'
Di
Tel
C
Tel
C'
Tel
Caudal
Rostral
D
Di
dTel
vTel
100μm
D'
Di
dTel
vTel
E
Di
dTel
vTel
E'
Di
dTel
vTel
F
dTel
F'
Di
dTel
vTel
G
Volume mm3
0.06
0.05
0.04
0.03
0.02
0.01
0
Gli3+/+
Gli3Xt/Xt
Foxg1
Pax6
Olig2
H
E10.5 Pax6 Expression
Area mm2
0.12
0.1
0.08
0.06
0.04
0.02
0
Gli3+/+
Gli3Xt/Xt
rTel
mTel
cTel

Figure 5.2 Marker analyses on frontal sections of wild type (**A**-**F**) and *Gli3*$^{Xt/Xt}$ mutant (**A'**-**F'**) forebrain from caudal to rostral. Foxg1 is expressed in the telencephalon (Tel) of the wild type (**A**-**C**) and mutant (**A'**-**C'**) embryos with a ^{high}ventral to ^{low}dorsal gradient, and not in the diencephalon (Di). Pax6 (green) and Olig2 (red) double immunofluorescence labelled the dorsal (dTel) and ventral (vTel) telencephalon respectively in both wild type (**D**, **E** and **F**) and mutant (**D'**, **E'** and **F'**) sections. Notice that on very rostral sections of the wild types, only Pax6 expression is observed. In the comparable section of mutant embryos, Olig2 expression can still be seen clearly (**F'**). Scale bars, 100 μm. (**G**) Volume measurements of Foxg1, Pax6 and Olig2 expression in wild type and mutant telencephalon. (**H**) Pax6 expression measurements in *Gli3*$^{Xt/Xt}$ mutant telencephalon show significant reduction (Student's *t* test, $p<0.001$, $n=4$ per genotype) in rostral, middle and caudal parts compared to those of wild type embryos.

5.2.2 Cell cycle parameters are not changed in *Gli3*$^{Xt/Xt}$ telencephalon at E10.5

To examine whether misregulation of cell cycle progression of telencephalic progenitors contributes to the reduced telencephalon of *Gli3*$^{Xt/Xt}$ mutant embryos, cell cycle kinetic parameters were analysed by the IddU/BrdU double labelling method at E10.5 in vivo (Shibui et al., 1989; Martynoga et al., 2005). IddU and BrdU are thymidine analogues, and they become incorporated into the DNA synthesized during the S-phase of the cell cycle (Gratzner, 1982). This method allows a calculation of the percentage of cells that are in S-phase during a certain time period (LI), the length of S-phase (T_S) and the length of the cell cycle (T_C) (Chapter 2.6) (Martynoga et al., 2005). The distribution of IddU and BrdU was very similar between wild type and mutant sections (Fig. 5.3A and A'). Cell counts were done in sampling bins throughout the dorsal (Fig. 5.3B and B') and ventral (Fig. 5.3C and C') telencephalon. There was no significant difference (Student's *t* test, n=5 per genotype) in either T_C or T_S between the wild type and *Gli3*$^{Xt/Xt}$ mutant dorsal or ventral telencephalon (Fig. 5.3D) (Table 5.3). Interestingly, although the average T_S of the wild type and mutant dorsal telencephalon were quite similar (Fig. 5.3D) (Table 5.3), the labelling index (LI), which is the percentage of all the proliferating cells that are in S-phase, was significantly increased (Student's *t* test, $p<0.005$, n=5 per genotype) in the *Gli3*$^{Xt/Xt}$ dorsal telencephalon compared to wild types (Fig. 5.3E) (Table 5.3), suggesting a larger progenitor pool in the *Gli3*$^{Xt/Xt}$ dorsal telencephalon. In the ventral telencephalon, no significant difference was detected in LI between the two groups (Fig. 5.3E) (Table 5.3). These results suggest that the proliferation rate of the *Gli3*$^{Xt/Xt}$ mutant is unlikely to contribute to the reduced size of the telencephalon, and the cell cycle parameters are not severely affected by the loss of Gli3 at this age.

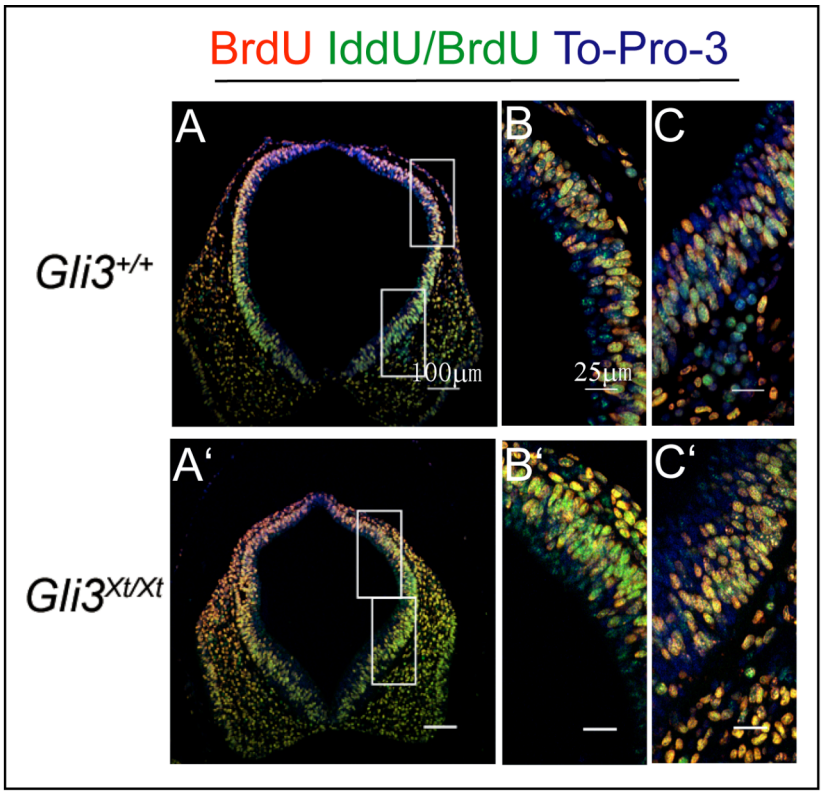
BrdU IddU/BrdU To-Pro-3
A
B
C
Gli3+/+
100µm
25µm
A‘
B‘
C‘
Gli3Xt/Xt

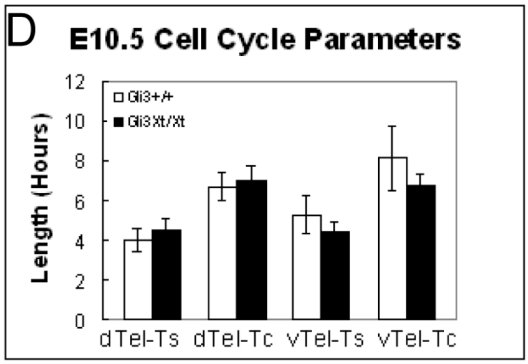
D
E10.5 Cell Cycle Parameters
Length (Hours)
12
10
8
6
4
2
0
Gli3+/+
Gli3Xt/Xt
dTel-Ts
dTel-Tc
vTel-Ts
vTel-Tc

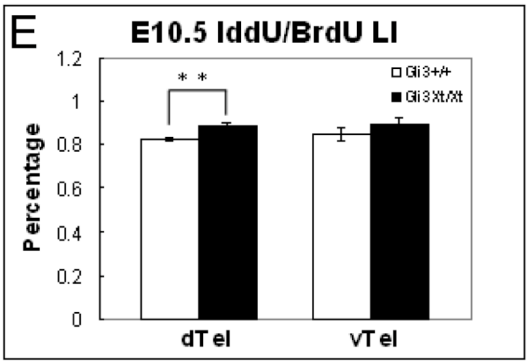
E
E10.5 IddU/BrdU LI
Percentage
1.2
1
0.8
0.6
0.4
0.2
0
* *
Gli3+/+
Gli3Xt/Xt
dTel
vTel

Figure 5.3 IddU and BrdU double immunofluorescence on wild type (**A**-**C**) and *Gli3*$^{Xt/Xt}$ mutant (**A'**-**C'**) frontal sections. Cells labelled with only IddU are green, and cells immunoreacted with BrdU are yellow (both red and green). To-Pro-3 is used to stain the nuclei (blue). The expression of IddU and BrdU is similar between wild types (**A**-**C**) and *Gli3*$^{Xt/Xt}$ mutants (**A'**-**C'**). **B**, **C** and **B'**, **C'** are higher magnification images of the boxed area in **A** and **A'** respectively, showing dorsal (**B** and **B'**) and ventral (**C** and **C'**) expression of IddU and BrdU. Scale bars, **A** and **A'**, 100 μm; **B**, **B'**, **C** and **C'**, 25 μm. Cell cycle kinetic parameters including length of S-phase (T_S) and cell cycle (T_C) were calculated in wild type and *Gli3*$^{Xt/Xt}$ mutant dorsal (dTel) and ventral (vTel) telencephalon respectively. No significant differences were detected between any of them (n=5). The labelling index (LI) of IddU and BrdU during 2 hours period was measured in wild type and mutant dorsal and ventral telencephalon (**E**). A significant (Student's t test, $p<0.001$, n=5 per genotype) increase of IddU and BrdU positive cells was observed in the mutant dorsal telencephalon but not ventrally.

dTel	T_S (hours)	T_C (hours)	LI
***Gli3*$^{+/+}$**	4.01±0.60	6.67±0.71	82.7±1%
***Gli3*$^{Xt/Xt}$**	4.47±0.63	6.95±0.83	88.8±0.9%
P value	0.62	0.81	0.0019

vTel	T_S (hours)	T_C (hours)	LI
***Gli3*$^{+/+}$**	5.31±0.98	8.17±1.62	84.5±2.8%
***Gli3*$^{Xt/Xt}$**	4.44±0.47	6.70±0.61	89.6±3%
P value	0.45	0.43	0.26

Table 5.3 Measurements of cell cycle parameters in dorsal (dTel) and ventral (vTel) telencephalon of wild type (*Gli3*$^{+/+}$) and *Gli3*$^{Xt/Xt}$ mutant embryos at E10.5, including length of S-phase (T_S), cell cycle (T_C) and labelling indices (LI).

5.2.3 More Tuj1 positive cells are found in E10.5 *Gli3*$^{Xt/Xt}$ ventral telencephalon

In addition to cell proliferation rate, the rate of cells exiting from the cell cycle to differentiate also needs to be tightly controlled to get the correct numbers of neurons produced. The expression of β-III-tubulin (Tuj1), an early marker of differentiating neurons (Lee et al., 1990; Menezes and Luskin, 1994), was examined in sets of caudal to rostral sections of wild type (Fig. 5.4A-F) and *Gli3*$^{Xt/Xt}$ mutant (Fig. 5.4A'-F') telencephalon at E10.5. Tuj1 expression was observed in both wild type and mutant ventral telencephalon but not in the dorsal telencephalon (Fig. 5.4A-C and A'-C'), suggesting early cell differentiation does not contribute to the small dorsal telencephalon of the *Gli3*$^{Xt/Xt}$ mutant embryos. In the mutant ventral telencephalon, there are significantly more Tuj1 labelled cells in all levels of sections examined compared to wild types (compare Fig. 5.4D with D', E with E' and F with F'). Counts were made in 15 μm wide bins throughout the ventricular zone. Both the percentage of Tuj1 positive cells to total numbers of cells (counterstained with cresyl violet) (Fig. 5.4G) and the density (Fig. 5.4H) of Tuj1 positive cells per mm^2 were increased significantly (Student's *t* test, $p<0.005$, n=4 per genotype) in the mutant ventral telencephalon compared to those of the wild types. This result indicates that

there may be more cells leaving the cell cycle to differentiate in the *Gli3*$^{Xt/Xt}$ ventral telencephalon at E10.5.

Tuj1+	Percentage	Density (no. cells/mm^2)
Gli3$^{+/+}$	9.25±1.2%	2271±426
Gli3$^{Xt/Xt}$	20.4±1.9%	4043±301
P value	0.00014	0.003

Table 5.4 Measurements of percentage and density of Tuj1 positive cells in ventral telencephalon of wild type (*Gli3*$^{+/+}$) and *Gli3*$^{Xt/Xt}$ mutant embryos at E10.5.

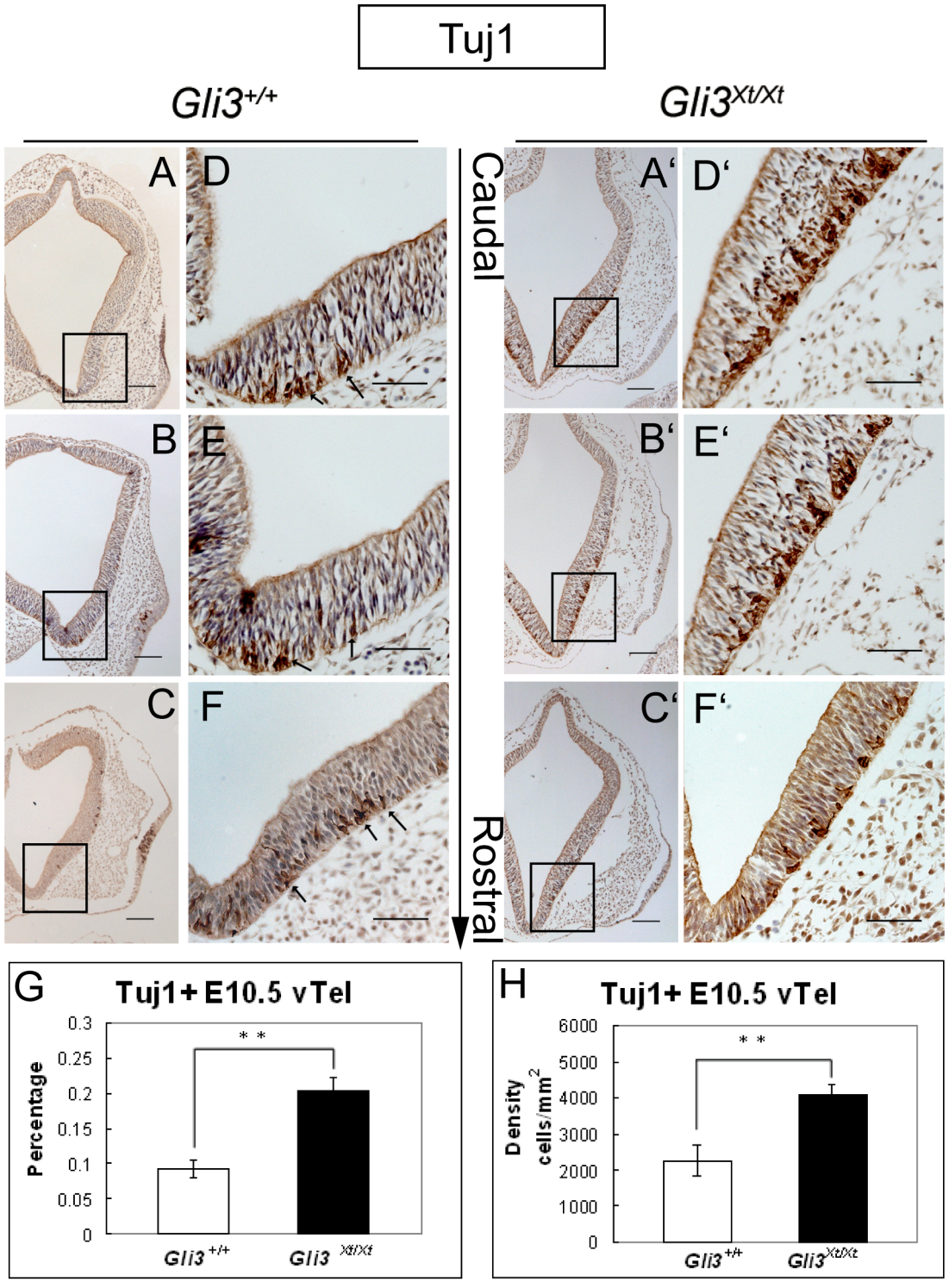
Tuj1
Gli3+/+
Gli3Xt/Xt
A
D
B
E
C
F
A‘
D‘
B‘
E‘
C‘
F‘
Caudal
Rostral
G
Tuj1+ E10.5 vTel
Percentage
0.3
0.25
0.2
0.15
0.1
0.05
0
* *
Gli3 +/+
Gli3 Xt/Xt
H
Tuj1+ E10.5 vTel
Density cells/mm2
6000
5000
4000
3000
2000
1000
0
* *
Gli3+/+
Gli3Xt/Xt

Figure 5.4 β-III-tubulin (Tuj1) immunohistochemistry on wild type (**A**-**F**) and *Gli3*$^{Xt/Xt}$ mutant (**A'**-**F'**) frontal sections in caudal to rostral order. Sections were counterstained with cresyl violet. **D**, **D'**, **E**, **E'**, **F** and **F'** are higher magnification images of boxed areas in **A**, **A'**, **B**, **B'**, **C** and **C'**, respectively. Almost no Tuj1 positive cells are found in the wild type (**A**, **B** and **C**) and *Gli3*$^{Xt/Xt}$ mutant (**A'**, **B'** and **C'**) dorsal telencephalon. More Tuj1 positive cells are found in the *Gli3*$^{Xt/Xt}$ mutant ventral telencephalon at all levels (**D'**, **E'** and **F'**) compared to those of the wild types (**D**, **E** and **F**). Scale bars, **A**, **A'**, **B**, **B'**, **C**, and **C'**, 250 μm; **D**, **D'**, **E**, **E'**, **F** and **F'**, 100 μm. Both the percentage (**G**) and the density (**H**) of Tuj1 positive cells are significantly increased in the mutant ventral telencephalon (Student's *t* test, $P<0.005$, n=4 er genotype).

5.2.4 Apoptotic cells are lost in *Gli3*$^{Xt/Xt}$ dorsal telencephalon while more apoptotic cells are located in *Gli3*$^{Xt/Xt}$ ventral telencephalon at E10.5

Programmed cell death is an important mechanism that determines the size and shape of the vertebrate nervous system (Oppenheim, 1991). Much of the programmed cell death happens via apoptosis, a well characterized genetic program that exhibits specific morphological features such as membrane blebbling, nuclear segmentation, chromatin condensation, DNA fragmentation, and the appearance of apoptotic bodies (Kerr et al., 1972; Vaux and Korsmeyer, 1999). To study cell death in *Gli3*$^{Xt/Xt}$ mutant telencephalon, E10.5 wild type and *Gli3*$^{Xt/Xt}$ mutant embryos were embedded in plastic and sectioned at 4 μm. By histological stain, clusters of pyknotic cells were observed in the dorsal midline of wild type embryos (Fig. 5.5A), whereas no such were detected in the same area of the mutants (Fig. 5.5A'). By contrast, many clusters of pyknotic cells were observed in the ventral midline of *Gli3*$^{Xt/Xt}$ mutant embryos (indicated by arrows in Fig. 5.5B'). Pyknotic clusters were also detected in the ventral midline of the wild types (indicated by arrows in Fig. 5.5B), but in fewer numbers compared to those in the mutants. To detect the DNA fragmentation, both whole-mount (Fig. 5.5C, D, C' and D') and on-section (Fig. 5.5E, F, E' and F') terminal deoxynucleotidyl transferase (TDT)-mediated dUTP-biotin nick end labelling (TUNEL) were performed in the wild type and *Gli3*$^{Xt/Xt}$ mutant telencephalon. Some whole-mount TUNEL labelled embryos were visualized and reconstructed by optical projection tomography (OPT) (Sharpe et al., 2002), showing that apoptotic cells are located in the telencephalic neuroepithelium (green cells in sagittal sections in Fig. 5.5D and D'; and supplementary movies). At E10.5, TUNEL positive cells are mainly restricted to the dorsal midline area in wild types (arrowheads in Fig. 5.5C, D, E and F), from the diencephalic-telencephalic junction to the anterior dorsal telencephalic roof (Furuta et al., 1997; Aoto et al., 2002). In the *Gli3*$^{Xt/Xt}$ mutants, almost no TUNEL labelled cells were observed in the dorsal

midline area (arrowheads in Fig. 5C', D', E' and F'), in agreement with previous publications (Aoto et al., 2002). This reduction of dying cell in the dorsal midline area of the mutants can not explain the size reduction of the mutant dorsal telencephalon. In fact, this result suggests that the dorsal midline tissue in the *Gli3*$^{Xt/Xt}$ mutants may be completely lost. There is a small population of apoptotic cells located in the ventral midline area of wild type embryos (arrows in Fig. 5.5D, E and F). In the ventral midline of *Gli3*$^{Xt/Xt}$ mutant embryos, more apoptotic cells are observed (arrows in Fig. 5.5D', E' and F' and supplementary movies) compared to wild types, indicating that more cells are dying in the ventral telencephalon. Furthermore, the increase in TUNEL positive cells is universal along the rostro-caudal axis of the mutant ventral telencephalon (compare Fig. 5E with E', F with F'). This increase of apoptotic cells might be one of the causes leading to the decrease in the overall volume of the mutant ventral telencephalon at later developmental stages, as shown at E12.5 (Chapter 4.2.4).

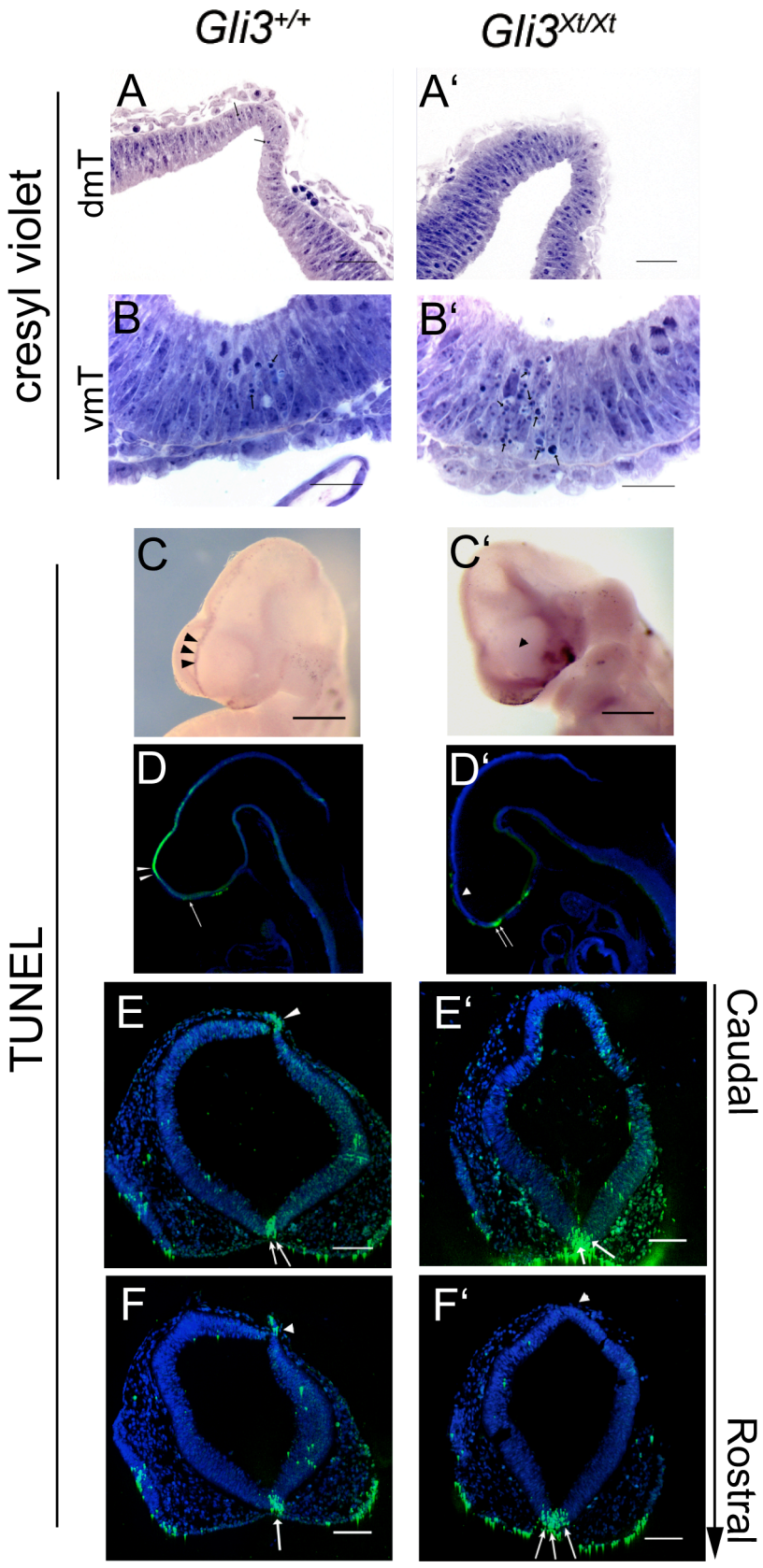
Gli3+/+
Gli3Xt/Xt
cresyl violet
dmT
vmT
A
A‘
B
B‘
TUNEL
C
C‘
D
D‘
E
E‘
F
F‘
Caudal
Rostral

Figure 5.5 Clusters of pyknotic cells are observed in the dorsal and ventral midline of wild types (arrows in **A** and **B**). In the *Gli3*$^{Xt/Xt}$ mutant embryos, few pyknotic cells are found in the dorsal midline (**A'**), and more are observed in the ventral midline (arrows in **B'**) by cresyl violet staining on plastic sections. DNA fragmentation revealed by whole mount (**C**, **C'**, **D** and **D'**) and on section (**E**, **E'**, **F** and **F'**) TUNEL in *Gli3*$^{+/+}$ (**C**, **D**, **E** and **F**) and *Gli3*$^{Xt/Xt}$ mutant (**C'**, **D'**, **E'** and **F'**) embryos. Some of the whole mount TUNEL labelled embryos (**C** and **C'**) were scanned with optical projection tomography (OPT) allowing for digital reconstruction, and examples of sagittal sections are shown in **D** and **D'**. The TUNEL positive cells that are normally observed in the dorsal midline of the wild type (arrowheads in **C**, **D**, **E** and **F**) are lost in the *Gli3*$^{Xt/Xt}$ mutants (arrowheads in **C'**, **D'**, **E'** and **F'**). In the *Gli3*$^{Xt/Xt}$ mutants, more apoptotic cells are discovered in the ventral midline area (arrows in **D'**, **E'** and **F'**) compared to the wild type embryos (arrows in **D**, **E** and **F**). Scale bars, **A** and **A'**, 50 μm; **B** and **B'**, 25 μm; **C**, **C'**, **E**, **E'**, **F** and **F'**, 100 μm.

5.2.5 *Wnt8b* expression is lost in the *Gli3*$^{Xt/Xt}$ telencephalon

The volumetric measurements at E10.5 have shown that the dorsal telencephalon of *Gli3*$^{Xt/Xt}$ mutants is severely reduced at this age. However the rate of cell proliferation, cell cycle exit or cell death does not seem to contribute to the phenotype, suggesting an earlier defect in dorsal telencephalic patterning of this mutant. To examine whether the dorso-medial telencephalon is ever specified, *Wnt8b* expression was examined in E10.5 and E9.5 *Gli3*$^{Xt/Xt}$ mutant embryos. E10.5 embryos labelled with *Wnt8b* were scanned and reconstructed with OPT. In the forebrain, *Wnt8b* is expressed in the dorso-medial telencephalon, including the cortical hem, the hypothalamus, and the eminentia thalami (Lako et al., 1998; Richardson et al., 1999). *Wnt8b* expression was found in the telencephalon (arrows in Fig. 5.6A, B, C and D) and the diencephalon (arrowheads in Fig. 5.6A, B, C and D) of both E10.5 (Fig. 5.6A, B and C) and E9.5 (Fig. 5.6D) wild type embryos. Figure 5.6C and C' are E10.5 wild type and mutant sagittal views of OPT reconstructed images. The bright green corresponds to *Wnt8b* expression. In the *Gli3*$^{Xt/Xt}$ mutants (Fig. 5.6A', B' and D'), the normal expression in the telencephalon (arrows in Fig. 5.6A, B and D; and bright green in dorso-medial telencephalon in Fig. 5.6C) is lost, but the diencephalic staining remains (arrowheads in Fig. 5.6A', B' and D'; bright green in EmT and hypothalamus indicated by arrowheads in Fig. 5.6C') at both ages. *Wnt8b* expression (Lako et al., 1998; Richardson et al., 1999) is observed in a broader domain (the dorso-medial telencephalic wall, including the future hippocampus) than *Wnt3a*, which was described as a marker of the cortical hem area in wild type embryos (Grove et al., 1998). The loss of *Wnt8b* expression in the *Gli3*$^{Xt/Xt}$ mutant telencephalon suggests a more extensive loss than just the previously reported loss of the cortical hem area in the *Gli3*$^{Xt/Xt}$ mutants (Grove et al., 1998). Furthermore, this loss of *Wnt8b* telencephalic expression indicates that the dorso-medial telencephalon might never have been specified in the mutants. The above results show that Gli3 is

required for the specification the dorsal telencephalon at very early stages during development.

5.2.6 Ventral markers are expanded in E10.5 *Gli3*$^{Xt/Xt}$ embryos

Along with the analysis in the E10.5 dorsal telencephalon, *Gli3*$^{Xt/Xt}$ ventral telencephalon was also examined at E10.5, using several markers that are normally expressed in the ventral telencephalon, including Olig2, Islet1, Dlx, Gsh2 and Nkx2.1. Mash1 protein expression was also examined, but at this age, positive cells are seen not only in the ventral telencephalon, but also are found scattered in more dorsal regions of the wild type embryos, which is less informative (data not shown).

Olig2 expression was examined in defined rostral, middle and caudal wild type and *Gli3*$^{Xt/Xt}$ mutant forebrain sections as shown in Figure 5.2D-F and D'-F' (red). In caudal and middle sections, the expression pattern of Olig2 appears relatively normal in the *Gli3*$^{Xt/Xt}$ telencephalon (Fig. 5.2D' and E'), except that the Olig2 expression seems to be expanded into more dorsal areas compared to wild types (Fig. 5.2D and E). Moving rostrally, Olig2 expression is no longer visible in the wild type (Fig. 5.2F). In the *Gli3*$^{Xt/Xt}$ mutants (Fig. 5.2F'), Olig2 expression is clearly visible ventrally, and the diencephalic expression can be still seen dorsally. The measurements of the Olig2 expressing domain in the telencephalon of both wild types and *Gli3*$^{Xt/Xt}$ mutants at E10.5 showed that the volume of the Olig2 expression domain in the *Gli3*$^{Xt/Xt}$ telencephalon was increased remarkably (Student's *t* test, $p<0.001$, n=4 per genotype) to about 165% of that of the wild types (Fig. 5.2G) (Table 5.1), and this significant increase (Student's *t* test, $p<0.05$, n=4 per genotype) was universal along the rostro-caudal axis (Fig. 5.7G) (Table 5.5). Furthermore, the most prominent expansion is observed in the rostro-ventral *Gli3*$^{Xt/Xt}$ telencephalon, and is about three times the size of the wild type.

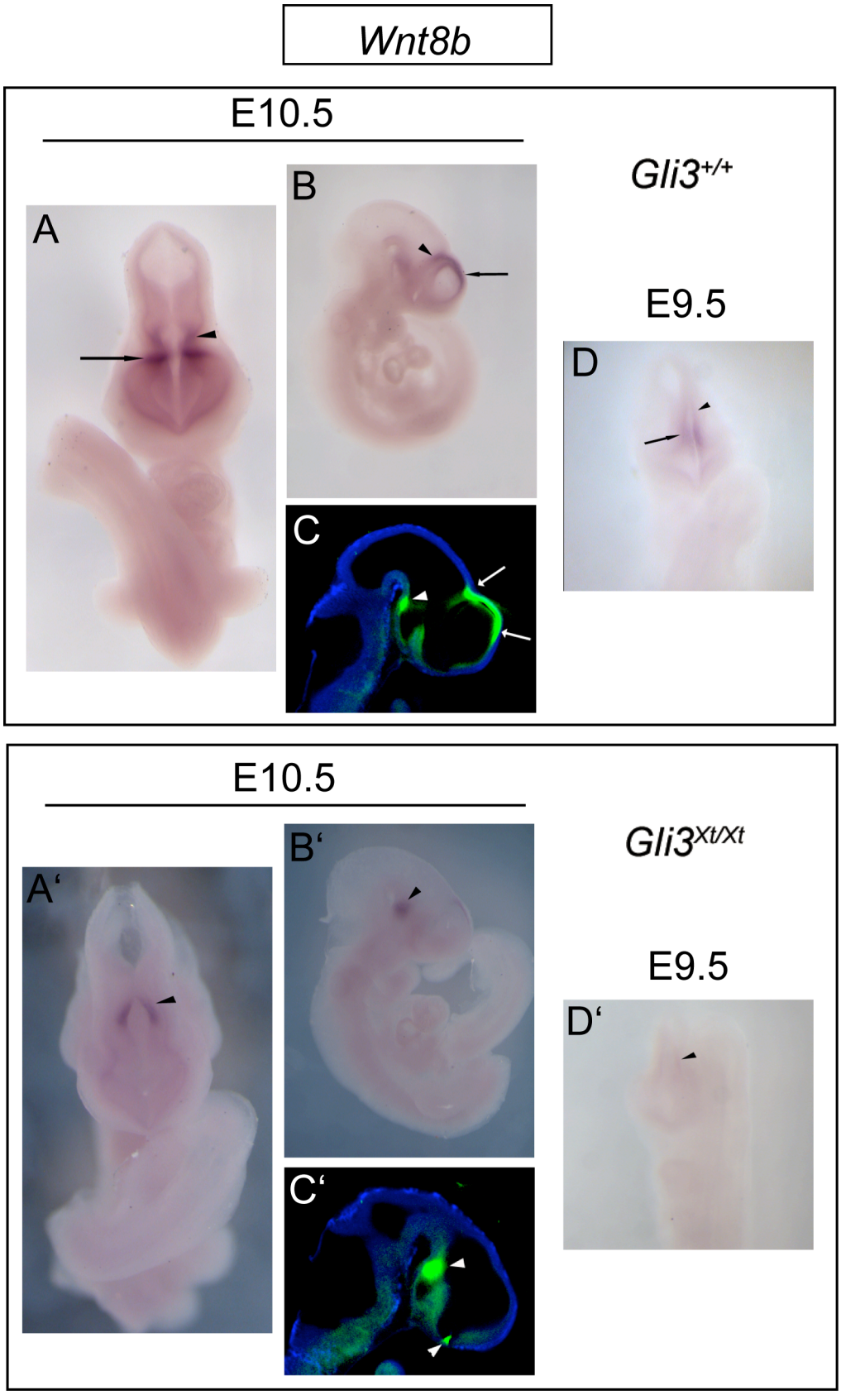
Wnt8b
E10.5
A
B
C
Gli3+/+
E9.5
D
E10.5
A‘
B‘
C‘
Gli3Xt/Xt
E9.5
D‘

Figure 5.6 Whole mount *in situ* hybridization of *Wnt8b* expression in E10.5 (**A**-**C** and **A'**-**C'**) and E9.5 (**D** and **D'**) wild type (**A**-**D**) and *Gli3*$^{Xt/Xt}$ mutant (**A'**-**D'**) embryos. **A**, **A'**, **D** and **D'** are frontal views and **B** and **B'** are side views. After labelling with *Wnt8b*, some E10.5 embryos were scanned and reconstructed by OPT microscopy, **C** and **C'** are mid-sagittal examples. *Wnt8b* is expressed in the dorso-medial telencephalon (arrow in **A**-**D**) and adjacent diencephalon (arrowheads in **A**-**D**) of the wild type embryos at both ages. The telencephalic expression is lost from the *Gli3*$^{Xt/Xt}$ mutant embryos, but the diencephalic expression (in eminentia thalami and hypothalamus) remains (arrowheads in **A'**-**D'**). The very light staining in the ventral telencephalon is background.

Area (mm^2)	rTel	mTel	cTel
***Gli3*$^{+/+}$**	0.01±0.002	0.033±0.001	0.018±0.002
***Gli3*$^{Xt/Xt}$**	0.03±0.002	0.042±0.001	0.028±0.003
P value	<0.001	<0.001	0.021
Percentage of changes in the mutants	200.00%	27.30%	55.60%

Table 5.5 Areas of Olig2 expression in rostral (rTel), middle (mTel) and caudal (cTel) telencephalic sections of the E10.5 wild type (*Gli3*$^{+/+}$) and *Gli3*$^{Xt/Xt}$ mutant embryos.

To test whether this expansion was Olig2 specific, expression of several other genes that usually mark different regions or specific cells type of the ventral telencephalon was examined. Nkx2.1 expression only starts to become obvious in more caudal sections of the wild type ventral telencephalon (Fig. 5.7A), that will become the future medial ganglionic eminence (MGE) (Shimamura et al., 1995; Sussel et al., 1999). Very little Nkx2.1 expression can be found rostrally in wild type sections (Fig. 5.7B). In the *Gli3*$^{Xt/Xt}$ mutant embryos, Nkx2.1 expression can be found not only in more caudal sections (Fig. 5.7A'), but also in very rostral sections (Fig. 5.7B'), and the expression seems to be expanded dorsally compared to that in wild types (compare Fig. 5.7A with A', B with B'). Gsh2 is expressed in the ventricular zone of the wild type ventral telencephalon, and the highest expression is found in the future lateral ganglionic eminence (LGE) (the area below the line in Fig. 5.7C), as described before (Corbin et al., 2000; Toresson et al., 2000). In the *Gli3*$^{Xt/Xt}$ mutants, Gsh2 expression seems to be expanded to a more dorsal domain (the area below the line in Fig. 5.7C'). Islet1 is expressed in the postmitotic neurons of the ventral telencephalon in wild types (Wang and Liu, 2001), and the expression can only be found in more caudal sections at E10.5 (Fig. 5.7D and E). In the *Gli3*$^{Xt/Xt}$ mutants, Islet1 expression can be clearly seen on more rostral sections compared to wild types, and, in addition, it seems to be expanded (Fig. 5.7D' and E'). Dlx2 is primarily expressed in wild type postmitotic ventral forebrain cells (Fig. 5.7F) (Eisenstat et al., 1999; Puelles et al., 2000). In the *Gli3*$^{Xt/Xt}$ mutants, Dlx2 positive cells seem to be more numerous and the expression domain seems to be broader compared to wild types (Fig. 5.7F').

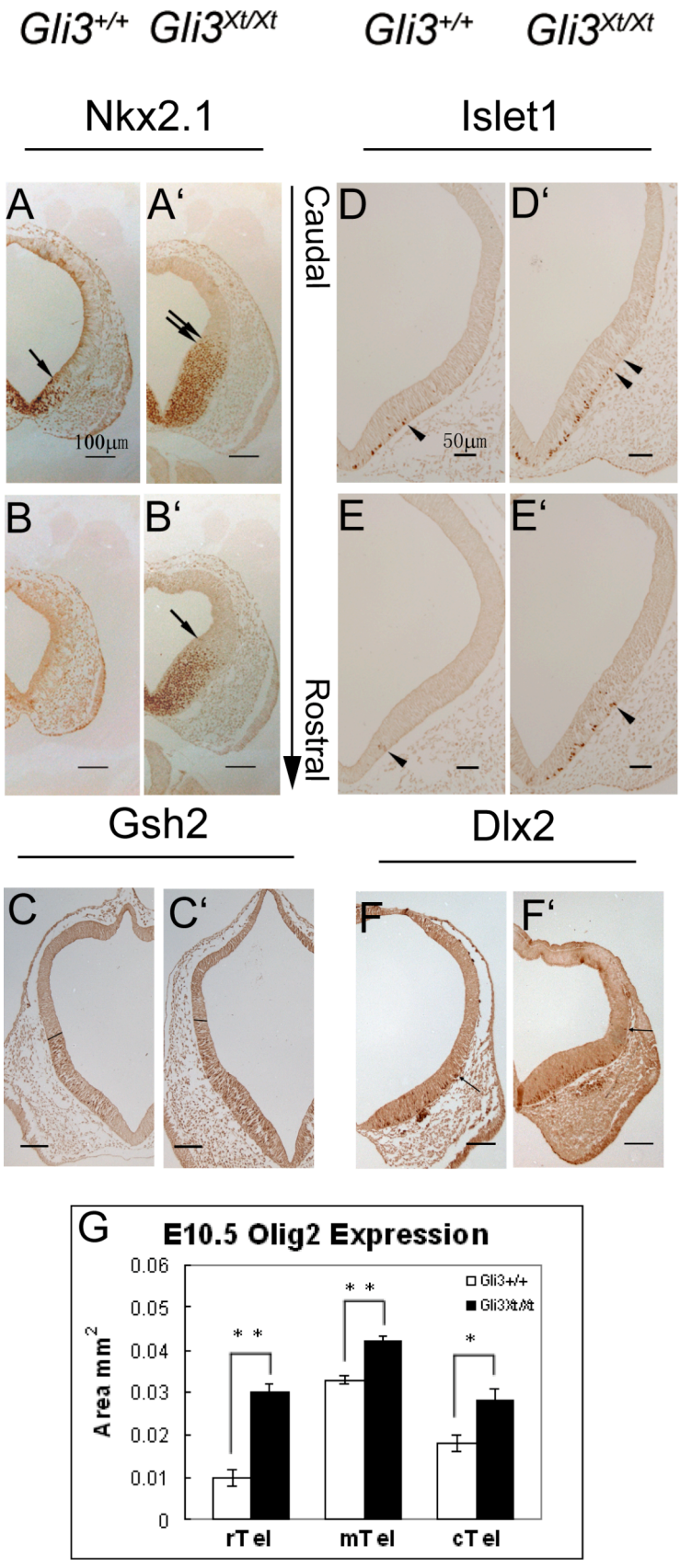
Gli3+/+ Gli3Xt/Xt
Gli3+/+ Gli3Xt/Xt
Nkx2.1
Islet1
A
A‘
D
D‘
Caudal
100μm
50μm
B
B‘
E
E‘
Rostral
Gsh2
Dlx2
C
C‘
F
F‘
G
E10.5 Olig2 Expression
Area mm2
0.06
0.05
0.04
0.03
0.02
0.01
0
Gli3+/+
Gli3Xt/Xt
* *
* *
*
rTel
mTel
cTel

Figure 5.7 Marker analyses in wild type (**A**-**F**) and *Gli3*$^{Xt/Xt}$ mutant (**A'**-**F'**) ventral telencephalon. Nkx2.1 and Islet1 expression is observed in caudal sections of wild type embryos (**A**, **B**, **D** and **E**), but is also obvious in rostral *Gli3*$^{Xt/Xt}$ sections (compare **B** with **B'**, **E** with **E'**). On all sections examined, Nkx2.1 (arrows in **A**, **A'**, **B**, **B'**), Gsh2 (line in **C** and **C'**), Islet1 (arrowheads in **D**, **D'**, **E** and **E'**) and Dlx2 (arrow in **F** and **F'**) expression in the mutant embryos is expanded dorsally. Scale bars, **A**-**C**, **A'**-**C'**, **F** and **F'**, 100 μm, **D**, **D'**, **E** and **E'**, 50 μm. Measurements of Olig2 expression in *Gli3*$^{Xt/Xt}$ mutant rostral, middle and caudal sections (**G**) show significant (Student's *t* test, $p<0.05$, $n=4$ per genotype) expansion compared to those of wild types. The most prominent increase is observed in the rostral part of the mutants.

5.2.7 Shh is not ectopically expressed in the *Gli3*$^{Xt/Xt}$ telencephalon

Sonic hedgehog (Shh) has been shown to be vital for ventral telencephalic development. Especially during the period between E9 and E12, it is crucial for the induction of ventral cell fate (Ericson et al., 1995a; Machold et al., 2003; Fuccillo et al., 2004). Studies have shown that Gli3 acts as a major mediator of the Shh signalling pathway in limbs and spinal cord (Buscher et al., 1997; Ruiz i Altaba, 1998). These lead to the hypothesis that the *Gli3*$^{Xt/Xt}$ mutant phenotype might be caused by ectopic Shh expression in the dorsal telencephalon. Previous studies using whole mount *in situ* hybridization have shown that *Shh* transcript expression is confined to the *Gli3*$^{Xt/Xt}$ ventral telencephalon from E8.5 to E11.5 (Theil et al., 1999; Tole et al., 2000a; Aoto et al., 2002). This result was confirmed and expanded here: the expression of *Shh* in the mutant embryos is confined to the ventral telencephalon and caudal diencephalon, which corresponds to the ZLI, as in wild types at E10.5. After whole mount *in situ* hybridization, embryos were cut in a frontal plane to study the expression of *Shh* in detail. The expression pattern in the ventral telencephalon (Fig. 5.8A and A') and ZLI (Fig. 5.8B and B') is quite similar between the wild type and mutant embryos. In addition, Shh protein expression was studied by immunofluorescence on wild type and *Gli3*$^{Xt/Xt}$ mutant sagittal sections at E9.5 (Fig. 5.8C and C') and E10.5 (Fig. 5.8D and D'). Instead of being ectopically expressed in more dorsal areas as one might have expected, Shh expression seemed to be slightly reduced in the *Gli3*$^{Xt/Xt}$ mutant telencephalon at both ages (Fig. 5.8C, C', D and D'). In the E10.5 *Gli3*$^{Xt/Xt}$ mutant embryos, Shh expression seemed to occupy a smaller area than in wild types (compare area marked with white arrowheads in Fig. 5.8D with D'). At E9.5, Shh expression seems not only to be more restricted, but also to be more reduced in the mutant telencephalon (compare the brightness of fluorescence at the area indicated by arrowhead in Fig. 5.8C and C'). The expression pattern of Shh in the adjacent diencephalon also seemed to have changed in the mutants (Fig. 5.8C'

and D'). The diencephalic expression in E9.5 mutant embryos seemed to be a lot brighter than in wild types (compare Fig. 5.8C with C'). This might indicate that there is more Shh expressed in the mutant diencephalon compared to the wild type. However, immunofluorescence is not a quantitive method, and the brightness of signal might not actually reflect absolute amounts of protein.

The expression of several down stream targets of the Shh pathway has been studied previously, including Nkx2.1, Gli1 and Ptc1, and their expression pattern have not changed in the *Gli3*$^{Xt/Xt}$ mutants (Theil et al., 1999; Tole et al., 2000a; Aoto et al., 2002). Expression of another Shh target, cyclin D1, was studied in this chapter at E10.5. Cyclin D1 was shown to be one of the early transcriptional targets of Shh signalling in the diencephalon and the mesencephalon (Ishibashi and McMahon, 2002) and the cerebellum (Kenney and Rowitch, 2000). The expression pattern of cyclin D1 was similar between wild type and *Gli3*$^{Xt/Xt}$ mutant embryos (Fig. 5.8E and E'). These data suggest that the Shh signalling pathway does not seem to account for the expansion of *Gli3*$^{Xt/Xt}$ ventral telencephalon at E10.5. However, because both *Gli3* and *Shh* start to be expressed very early in development (at around E7), it is possible that Shh within or outside the telencephalon influences the patterning of *Gli3*$^{Xt/Xt}$ ventral telencephalon during these very early stages.

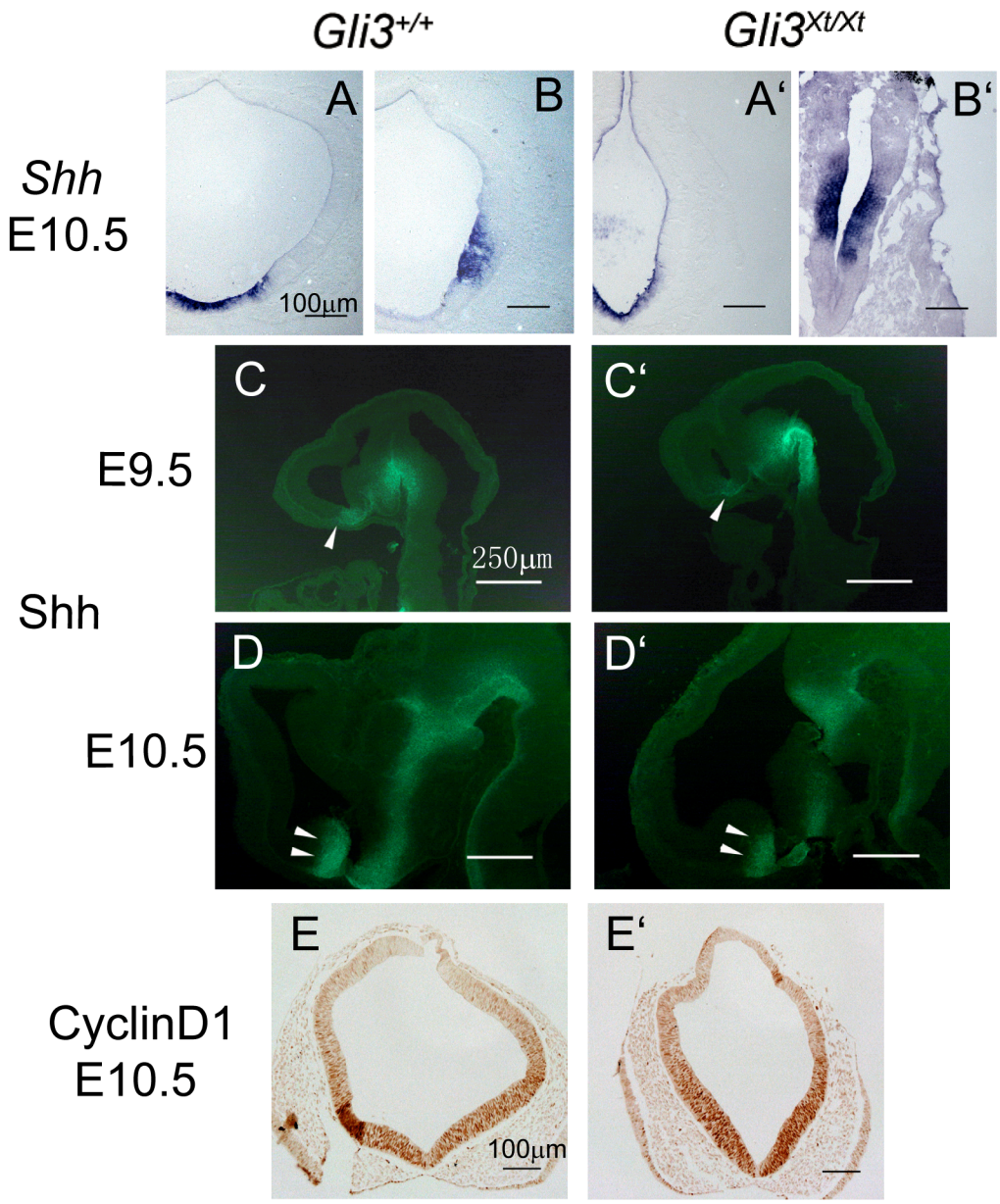

Figure 5.8 Expression of Shh mRNA (**A**, **B**, **A'** and **B'**) and protein (**C**, **D**, **C'** and **D'**) on wild type (**A**-**D**) and *Gli3*$^{Xt/Xt}$ mutant (**A'**-**D'**) embryos. After whole mount *in situ* hybridization at E10.5, embryos were sectioned on a frontal plane. *Shh* expression is observed in the ventral telencephalon (**A** and **A'**) and the diencephalon (ZLI) (**B** and **B'**) of wild type and mutant embryos. Fluorescent Shh expression was carried out on E9.5 (**C** and **C'**) and E10.5 (**D** and **D'**) wild type and mutant embryos. Shh expression in the mutant ventral telencephalon is slightly lower than that of the wild type (area indicated by arrowheads in **C**, **C'**, **D** and **D'**) at both ages. Cyclin D1 expression in the wild type (**E**) and mutant (**E'**) frontal sections is similar. Scale bars, **A**, **A'**, **B**, **B'**, **E** and **E'**, 100 μm; **C**, **C'**, **D** and **D'**, 250 μm.

5.2.8 The shape of the forebrain has changed in the *Gli3*$^{Xt/Xt}$ mutant embryos

The overall volume of the *Gli3*$^{Xt/Xt}$ E10.5 ventral telencephalon is bigger, but it becomes smaller at E12.5, compared to that of wild types. The increase in the numbers of dying cells and early differentiated cells in the *Gli3*$^{Xt/Xt}$ ventral telencephalon at E10.5 might result in an overall volume reduction of the *Gli3*$^{Xt/Xt}$ ventral telencephalon at E12.5. However, the increase in cell death and early differentiation do not exhibit any differences along the rostro-caudal axis, and can not explain the regional size differences of the mutant ventral telencephalon at E12.5. This lead to the hypothesis that a shape change might occur in the *Gli3*$^{Xt/Xt}$ mutant telencephalon, in parallel with the size change described above.

Pax2 and Lim2 expression in rostral telencephalic sections at E12.5 showed that the diencephalon and the septum of the mutants are joined in a more rostral area than in the wild types, and their expression in the mutant septum seems to be expanded (Chapter 4.2.2). At E10.5, Pax2 expression analysis on sagittal sections of *Gli3*$^{Xt/Xt}$ mutant embryos has shown that dispersed diencephalic cells are present in the dorsal telencephalic area, indicating the boundary between the telencephalon and the diencephalon is compromised (Fotaki et al., 2006). Pax2 expression was also examined in frontal sections at E10.5. In wild type frontal sections, Pax2 expression can only be found in the most rostral area of the telencephalon (Fig. 5.9A, B and C), and most of the Pax2 positive cells were found in the ventral area (arrowhead in Fig. 5.9C). In *Gli3*$^{Xt/Xt}$ mutant embryos, Pax2 expression was observed in all forebrain sections examined (Fig. 5.9A', B' and C'). In caudal sections, Pax2 was ectopically expressed in the dorsal area (arrows in Fig. 5.9A' and B'), which might correspond to the expression in the diencephalon, as described before (Fotaki et al., 2006). The Pax2 expression in the ventral telencephalon of the mutants starts to be obvious on more caudal sections compared to wild types, and its expression seems to be

expanded (Fig. 5.9B' and C'). Note that in very rostral sections, the expression of Pax2 occupies the whole telencephalic lobe of the *Gli3*$^{Xt/Xt}$ mutant embryos (Fig. 5.9C').

To further examine the possibility that the three dimensional shape of the *Gli3*$^{Xt/Xt}$ mutant forebrain is different from that of the wild type, E10.5 and E12.5 embryos were scanned and reconstructed by OPT microscopy (Fig. 5.1 and 5.10). In E10.5 sagittal sections, the cortical hem and the adjacent tissue, including the future hippocampus and choroid plexus, are lost in the *Gli3*$^{Xt/Xt}$ mutants (Grove et al., 1998; Tole et al., 2000a). The boundary between the telencephalon and the diencephalon (between red lines in Fig. 5.9A) is compromised in the mutants (Fotaki et al., 2006). These result in an abnormal joining of the diencephalon with the caudal part of the telencephalon (Fig. 5.10A') (Fotaki et al., 2006). The diencephalon is extended to a more rostral region in the mutants (approximately up to the red line in Fig. 5.10A'), in agreement with the results obtained from the OPT frontal images (Fig. 5.1B-D and B'-D'). The ventral telencephalon of the *Gli3*$^{Xt/Xt}$ mutants is expanded (up to the blue lines in Fig. 5.10A and A'), in agreement with the results of the volume measurements (Chapter 5.2.6).

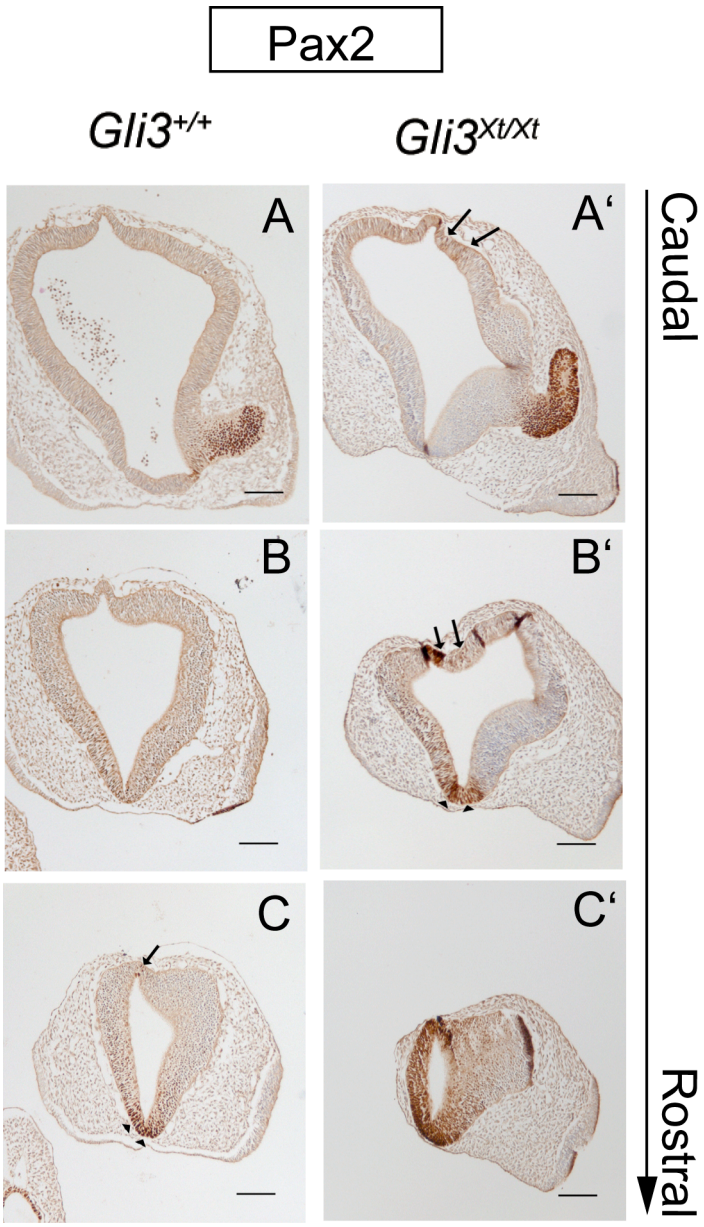

Figure 5.9 Pax2 immunoreactivity in caudal to rostral sets of frontal sections of wild type (**A**-**C**) and *Gli3*$^{Xt/Xt}$ mutant (**A’**-**C’**) embryos. Sections were counterstained with cresyl violet. Pax2 expression is observed in the optic stalk (**A** and **A’**) on both wild type and mutant caudal sections, and also in the dorsal most region of the mutant embryos (arrows in **A’**). In middle sections, only very few Pax2 positive cells are observed in wild type sections (**B**), but a lot more are found in both the dorsal and ventral midline of the mutant embryos (arrows and arrowheads respectively in **B’**). Dorsal and ventral midline expression of Pax2 is observed in rostral wild type sections (arrows and arrowheads respectively in **C**), whereas in the mutants, Pax2 is expressed throughout the vesicle (**C’**). Scale bars, 100 μm.

As development proceeds, both the wild type and *Gli3*$^{Xt/Xt}$ mutant telencephalon grow extensively. Sets of lateral-to-medial sagittal sections of E12.5 wild type and *Gli3*$^{Xt/Xt}$ mutant forebrains are shown in Figure 5.10B-D and B'-D'. Based on the gene marker analysis presented in Chapter 4 and 5, forebrain structures are marked by coloured lines in wild type and *Gli3*$^{Xt/Xt}$ mutant embryos. Dorsal telencephalon is the area between the red and blue lines, and ventral telencephalon corresponds to the area between the blue and green lines. At E12.5, the volume of the mutant dorsal telencephalon is significantly reduced compared to that of wild types (compare areas between red and blue lines in Fig. 5.10B with B', C with C', D with D'). In mid-sagittal sections of wild types, the dorsal telencephalon is no longer visible, and the ventral telencephalon is joined with the diencephalon via a structure known as lamina terminalis (arrow in Fig. 5.10D). In the *Gli3*$^{Xt/Xt}$ mutants, because the dorso-medial wall does not invaginate, the telencephalic lobe is still clearly seen (Fig. 5.10D'). The septum of the mutant (arrowhead in Fig. 5.10D') seems to be elongated, and joined with the diencephalon in a more anterior position compared to the wild type (compared Fig. 5.10D and D'). In more lateral sections of the wild type, the diencephalon is located posterior to the area between the red and green lines, which corresponds to the dorso-medial telencephalon and the eminentia thalami (Fig. 5.10B and C). In comparable mutant sections, the area between the red and green line is the diencephalon (Fig. 5.10B' and C'). In addition, clusters of diencephalic cells are present in the mutant dorsal telencephalon. The ventral telencephalon of mutant embryos is smaller compared to that of wild types (compare area between the blue and green lines in Fig. 5.10B with B', C with C') in these lateral sections. Note that in all the sections along the medial to lateral axis, the mutant diencephalon seems to be extended to a more rostral level (up to the red line from the left in Fig. 5.10B' and C' and blue line in D') compared to the wild type (Fig. 5.10B, C and D).

Coronal sections at rostral levels of E12.5 wild types reveals that the rostral end of

the diencephalon (the lamina terminalis) is joined with the septum (red arrow in Fig. 5.10E), and this joining is no longer visible on more rostral sections of the wild type telencephalon (Fig. 5.10F, G, H and I). This joining is observed in more rostral sections in the *Gli3*$^{Xt/Xt}$ mutants (red arrow in Fig. 5.10H' and I') than in the wild types, which indicates that the diencephalon (red arrows in Fig. 5.10E', F' and G') and the septum (red arrowheads in Fig. 5.10F' and G') of the mutants are enlarged as these structures can be seen in more sections of the mutants. These results agree with the Pax2 and Lim2 expression pattern at E12.5 (Chapter 4.2.2). These OPT imaging results and marker analysis have shown that the *Gli3*$^{Xt/Xt}$ mutant septum is enlarged, and the diencephalon is shifted in more rostral sections than the wild type embryos, supporting the hypothesis that the shape of the *Gli3*$^{Xt/Xt}$ mutant forebrain is changed and that this may account for the size difference of the *Gli3*$^{Xt/Xt}$ ventral telencephalon along the rostro-caudal axis.

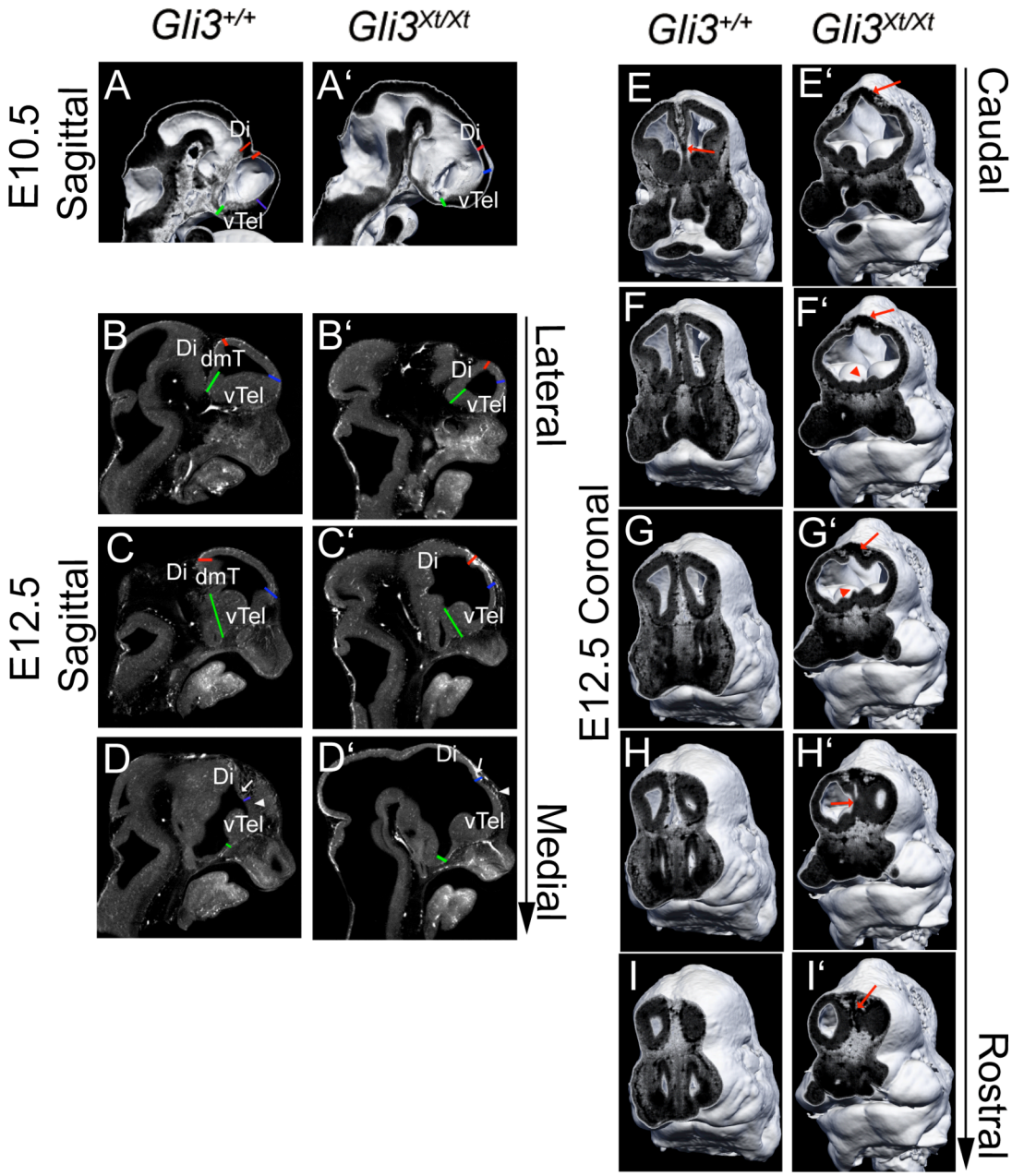
Gli3+/+
Gli3Xt/Xt
Gli3+/+
Gli3Xt/Xt
E10.5 Sagittal
E12.5 Sagittal
E12.5 Coronal
A
A'
B
B'
C
C'
D
D'
E
E'
F
F'
G
G'
H
H'
I
I'
Di
dmT
vTel
Lateral
Medial
Caudal
Rostral

Figure 5.10 Reconstructed OPT images of E10.5 and E12.5 wild type (**A**-**I**) and *Gli3*$^{Xt/Xt}$ mutant (**A'**-**I'**) embryos by OPT. **A** and **A'** is E10.5 wild type and mutant mid-sagittal sections, **B**-**D** and **B'**-**D'** are E12.5 sagittal sections from lateral to medial of wild type and *Gli3*$^{Xt/Xt}$ mutant embryos, and rostral is to the right side. The normal invagination of the dorso-medial telencephalon (dmT) (the area marked by red lines in **A**, and green and red line in **B** and **C**) is not observed in the mutant. The area between the red and green line in mutants is the diencephalon (Di) (**A'**, **B'** and **C'**). The blue line in **A**, **A'**, **B**, **B'**, **C** and **C'** indicates the relative boundary between the dorsal and ventral telencephalon (vTel), and marks the boundary between diencephalon and ventral telencephalon in **D** and **D'**. Sets of caudal to rostral coronal sections of wild type and *Gli3*$^{Xt/Xt}$ mutants are shown in **E**-**I** and **E'**-**I'**, respectively. The joining of the rostral end of the diencephalon and the septum is observed in **E** (arrow), but not in more rostral sections (**F**-**I**) of the wild type embryos. In the mutant, the joining of the rostral diencephalon (red arrow in **E'**, **F'** and **G'**) and the septum (red arrowhead in **E'**, **F'** and **G'**) is observed in most rostral sections (indicated by arrow in **H'** and **I'**) compared to of the wild types (**E-I**).

5.3 DISCUSSION

5.3.1 The loss of Gli3 results in a smaller dorsal telencephalon at E10.5

The volumetric measurements of E12.5 *Gli3*$^{Xt/Xt}$ mutant embryos have shown a smaller dorsal telencephalon compared to that of wild types. The fact that no cell proliferation or cell death changes could explain this reduction suggested an early cause for the dorsal telencephalic defect (see chapter 4). In this chapter, the volume of the dorsal telencephalon was measured at E10.5, when neurogenesis starts (Caviness, 1982; Caviness et al., 1995; Takahashi et al., 1995b). The *Gli3*$^{Xt/Xt}$ mutant dorsal telencephalon already showed a 61.2% reduction compared to that of wild types, even though the measurements at E10.5 also include the dispersed diencephalic cells found in the dorsal telencephalon (Fotaki et al., 2006). In the mutant telencephalon at E10.5, several dorsally expressed genes were shown to be lost specifically from the *Gli3*$^{Xt/Xt}$ mutant embryos, such as the dorsal telencephalic markers *Emx1* and *Emx2* (Theil et al., 1999; Tole et al., 2000a; Kuschel et al., 2003). The cortical hem and the expression of several *Wnt* and *Bmp* genes, including *Wnt2b*, *3a*, *5a*, *Bmp2*, *4*, *6* and *7*, are reported to be lost in the *Gli3*$^{Xt/Xt}$ mutant (Grove et al., 1998; Tole et al., 2000a). In this chapter, the expression of *Wnt8b* was shown to be lost specifically from the telencephalon. *Wnt8b* is expressed in the dorso-medial telencephalon (Lako et al., 1998; Richardson et al., 1999), in a broader area than *Wnt3a* expression (Grove et al., 1998). The loss of *Wnt8b* expression in the *Gli3*$^{Xt/Xt}$ mutant telencephalon suggests a more extensive dorsal telencephalic loss than just the cortical hem area.

Cell cycle kinetic parameters, including the duration of S-phase (T_S) and cell cycle (T_C), have been measured at this age by IddU/BrdU double labelling methods (Shibui et al., 1989; Martynoga et al., 2005) to test the possibility that a reduced proliferation

rate might contribute to the small telencephalon of mutant embryos. This method is more powerful than a short pulse of BrdU labelling, which gives only the numbers of cells which are in S-phase during a certain time period (the labelling index) (Shibui et al., 1989; Martynoga et al., 2005). These experiments revealed no differences in the length of S-phase or cell cycle between the wild type and mutant dorsal or ventral telencephalon, suggesting that the defects observed in the *Gli3*$^{Xt/Xt}$ mutant telencephalon at later developmental stages are not the result of changes in cell cycle parameters at E10.5.

Programmed cell death occurs during normal development of the central nervous system (Oppenheim, 1991). An increased cell death would result in decreased size of the *Gli3*$^{Xt/Xt}$ mutant dorsal telencephalon. Apoptotic cells were revealed by TUNEL staining in the wild type dorsal midline. However, in the *Gli3*$^{Xt/Xt}$ mutants instead of increased, TUNEL positive cells were found to be lost, specifically from the dorso-medial telencephalon, as previously reported (Aoto et al., 2002). This loss of dying cells from the mutant embryos can not explain the size reduction of the dorsal telencephalon. Rather, this result indicates that the cells which are normally undergoing apoptosis in the dorso-medial telencephalon are lost from the *Gli3*$^{Xt/Xt}$ mutant embryos.

Another possible reason for a small dorsal telencephalon is more dorsal progenitors of the *Gli3*$^{Xt/Xt}$ mutants leaving the cell cycle. β-III-tubulin (Tuj1) labels newly differentiated neurons outside the ventricular zone (Lee et al., 1990; Menezes and Luskin, 1994). At E10.5, no Tuj1 positive cells were observed in the dorsal telencephalon of both wild type and *Gli3*$^{Xt/Xt}$ mutant embryos.

These analyses suggest that the size reduction of *Gli3*$^{Xt/Xt}$ mutant dorsal telencephalon might not be the result of defects in cell proliferation, cell

differentiation or cell death at E10.5, and lead to the hypothesis that Gli3 is involved in early forebrain specification. In fact, the loss of *Wnt8b* expression in the *Gli3*$^{Xt/Xt}$ mutant telencephalon indicates that the dorso-medial telencephalon might have never been specified in the mutants. However, there is also the possibility that one or any combination of the following factors happened in the *Gli3*$^{Xt/Xt}$ mutant embryos earlier than E10.5:

Decreased cell proliferation
Increased cell death
More cells exiting the cell cycle (less cells re-entering the cell cycle)
More cells migrating out of the dorsal telencephalon

One thing revealed by the IddU/BrdU double labelling experiments at E10.5 was a significant increase of IddU and BrdU labelling indices in the *Gli3*$^{Xt/Xt}$ mutant dorsal telencephalon during the two hours pulse compared to those of wild types. This result shows that more cells were in S-phase during that two-hour period, and probably means that the mutant dorsal telencephalon has a larger population of progenitor cells during that time period. This enlargement of the precursor pool would be expected to result in an increased size of the dorsal telencephalon at later developmental stages. However, the dorsal telencephalon of E12.5 *Gli3*$^{Xt/Xt}$ mutant is still significantly reduced in size compared to the wild type and the BrdU labelling index of E12.5 mutant dorsal telencephalon is relatively normal. It is possible that one or any combination of the factors above, happening between the E10.5 to E12.5 period, might account for the dorsal telencephalic reduction. In addition, IddU and BrdU also label a second proliferative population (Takahashi et al., 1995a; Sheth and Bhide, 1997). The increased labelling index observed in the *Gli3*$^{Xt/Xt}$ mutant dorsal telencephalon might reflect an increase in this population.

5.3.2 The loss of Gli3 results in an enlarged ventral telencephalon at E10.5

The ventral telencephalon of the *Gli3*$^{Xt/Xt}$ mutant embryos is significantly enlarged to about 165% of that of wild types. This expansion is observed along the rostro-caudal axis, and the rostral part shows the most remarkable increase. This enlargement of ventral tissue in the *Gli3*$^{Xt/Xt}$ mutants does not seem to be due to an ectopic expression of Shh or the upregulation of Shh signalling in the telencephalon at E10.5. Shh transcript and protein seem to be confined to their normal expression domains within the forebrain (Theil et al., 1999; Tole et al., 2000a). The expression of several down stream targets of the Shh pathway has been studied previously, including Gli1 and Ptc1, which are also confined to their normal expression domain (Theil et al., 1999; Tole et al., 2000a). However, there is still the possibility that Shh sources, within or outside the telencephalon, induce ventral cell fate in the *Gli3*$^{Xt/Xt}$ mutants at early developmental stages, since both *Shh* and *Gli3* start to be expressed in the forebrain at around E7.5 (Echelard et al., 1993). Furthermore, Shh expression in the adjacent diencephalon might also influence telencephalic development at early stages. At E9.5, stronger Shh expression was observed in the mutant diencephalon compared to that of wild types. The loss of the dorso-medial telencephalon in the *Gli3*$^{Xt/Xt}$ mutants brings the diencephalon nearer to the telencephalon. This increases the possibility that the Shh source in diencephalon may induce ventral cell fates in *Gli3*$^{Xt/Xt}$ mutant embryos. In addition, Shh sources outside the telencephalon, such as the notochord, prechordal plate and floor plate, might be also involved in forebrain patterning during early embryogenesis, since evidence has shown that Shh can function in a distance up to 200 μm (Lewis et al., 2001).

5.3.3 Gli3 loss changes the shape of forebrain during early embryogenesis

One interesting result from the volumetric measurements reveals that the E10.5

mutant ventral telencephalon is significantly bigger compared to that of wild types, but at E12.5, although both the wild type and mutant ventral telencephalon grows extensively, the ventral telencephalon of the *Gli3*$^{Xt/Xt}$ mutants becomes smaller than that of wild types. This does not seem to be the result of changes in cell cycle parameters, but it is more likely explained by more cells leaving the cell cycle and by an increase in cell death observed in the ventral area of the *Gli3*$^{Xt/Xt}$ mutants. Furthermore, only the middle part of the ventral telencephalon is reduced at E12.5, suggesting that a shape change might have occurred in the *Gli3*$^{Xt/Xt}$ ventral telencephalon.

Both morphological and marker analyses of the *Gli3*$^{Xt/Xt}$ mutants have shown that at E10.5, the three dimensional shape of the mutant forebrain is different from that of wild types. The diencephalon is normally located caudally to the telencephalon but can be observed in more rostral telencephalic sections in the *Gli3*$^{Xt/Xt}$ mutant, as shown by the OPT images. Furthermore, the expression of Olig2 and Pax2 is found dorsally to the dorsal telencephalon in rostral telencephalic sections. The ventral telencephalon of *Gli3*$^{Xt/Xt}$ mutants also seems to have changed its shape. The expansion of ventral markers like Olig2, Nkx2.1 and Islet1 are more prominent rostrally. This leads to the possibility that the most rostro-ventral structure of the telencephalon, the septum, might be enlarged. The E12.5 OPT images revealed that in the mutants, the rostral end of the diencephalon, the lamina terminalis, joins with the septum in more rostral areas than in the wild types, suggesting that the diencephalon of the *Gli3*$^{Xt/Xt}$ mutants might be shifted rostrally and probably enlarged, as suggested by Aoto et al (2002). In the *Gli3*$^{Xt/Xt}$ mutant forebrain, the dorso-medial telencephalon fails to be specified, the diencephalon expands rostrally and the ventral telencephalon expands dorsally, towards the dorsal telencephalon. As a result, the relative positions of the *Gli3*$^{Xt/Xt}$ mutant forebrain structures are different from those observed in wild types.

Many previous marker analyses on the *Gli3*$^{Xt/Xt}$ mutants might not have taken this shape change into account. Most of them were carried out by whole mount *in situ* hybridization, and interpretation of their results was sometimes contradictory. For example, the expression of *Nkx2.1* was reported to be confined to ventral telencephalon at E10.5 by Theil et al. (1999) and at E12.5 by Tole et al. (2000a), but was shown to be expanded by Aoto et al. (2002) in E11.5 *Gli3*$^{Xt/Xt}$ mutant embryos. In this thesis, Nkx2.1 expression was examined systematically on sets of rostral to caudal sections throughout the wild type and mutant telencephalon. At E10.5, the expression of Nkx2.1 was indeed found expanded into more dorsal areas compared to the wild type, while at E12.5 Nkx2.1 was restricted to the MGE in middle sections as in wild types.

In total, the results shown in this chapter suggest that Gli3 regulates the specification of the dorso-medial telencephalon, and the regionalization along not only the dorso-ventral but also the rostro-caudal axis of the forebrain.

Chapter 6: Fibroblast growth factor 8 (Fgf8) is a potential candidate for inducing ectopic ventral telencephalic fate when Gli3 is absent

6.1 INTRODUCTION

As mentioned before, signalling centres that are located within and outside the telencephalon are important for forebrain patterning. The anterior source of fibroblast growth factors (Fgfs) impart positions along the antero-posterior (rostro-caudal) axis (Fukuchi-Shimogori and Grove, 2001, 2003; Garel et al., 2003). One of the family members, Fgf8, is expressed in the anterior neural ridge (ANR) (Crossley and Martin, 1995; Shimamura and Rubenstein, 1997) and has been demonstrated to regulate telencephalic patterning, cell proliferation and survival (Lee et al., 1997; Martinez et al., 1999; Storm et al., 2003; Storm et al., 2006). *Fgf8* null mutants die during gastrulation, whereas *Fgf8* hypomorphic and telencephalic conditional *Fgf8* knock-out mutants survive until birth. These mutants show an increase in dorsal telencephalic gene markers, such as *Pax6*, *Emx2* and *Tbr1*, and loss of ventral gene markers, such as *Nkx2.1*, *Dlx2* and *Dlx5* (Meyers et al., 1998; Sun et al., 1999; Garel et al., 2003; Storm et al., 2003; Storm et al., 2006). A recent study on mutants of Fgf receptors has shown that Fgfs act downstream of Shh and Gli3 to generate ventral cell fate (Gutin et al., 2006). In addition, ectopic application of Fgf8 can induce the expression of ventral markers and repress that of dorsal markers in dorsal telencephalic explants (Crossley et al., 2001; Kuschel et al., 2003).

Results from Chapters 4 and 5 suggest a rostral expansion of ventral telencephalic markers in the $Gli3^{Xt/Xt}$ telencephalon, and this expansion correlates to an expanded expression of *Fgf8* and its downstream gene *Sprouty2* in the ANR, as shown by

previously published results (Theil et al., 1999; Aoto et al., 2002; Kuschel et al., 2003). The possibility that ectopic *Fgf8* expression results in the expansion of ventral cell fate in the *Gli3*$^{Xt/Xt}$ mutant embryos was tested in this thesis with an explant culture system.

In vitro cultures with an antibody that blocks Fgf8b bioactivity (anti-Fgf8b antibody, R&D system) were carried out on wild type and *Gli3*$^{Xt/Xt}$ mutant forebrain explants at E9.5, one day before the expanded expression of ventral markers is observed in the *Gli3*$^{Xt/Xt}$ mutant rostral telencephalon. This antibody has been shown to block 100% of mouse Fgf8b activity on NR6R-3T3 fibroblasts after 1 hour incubation at 37 ℃ (according to manufacturer's information). Alternative splicing of the *Fgf8* gene gives rise to eight different protein isoforms (a-h) in mice and they differ in their N-terminus (Crossley and Martin, 1995; MacArthur et al., 1995a). The biological function of these isoforms is still unknown, but Fgf8b has been shown to have the strongest affinity for the three receptors, Fgfr1, Fgfr2 and Fgfr3 (MacArthur et al., 1995a; MacArthur et al., 1995b; Blunt et al., 1997). Deletion of Fgfr1 and Fgfr2 or Fgfr1 and Fgfr3 results in telencephalic abnormalities, including loss of ventral characters from early stages, and in cells along the dorso-ventral axis adopting a dorsal fate (Gutin et al., 2006). This suggests Fgf8b might be one potential isoform that is involved in forebrain patterning. E9.5 wild type and mutant forebrains were cut into halves, sagittally. One half was cultured in defined medium with the presence of the anti-Fgf8b antibody, and the other half was used as control. After 16 hours incubation, explants were fixed and immunoreacted with markers that were found expanded in the *Gli3*$^{Xt/Xt}$ ventral telencephalon at E10.5. The prediction of this experiment was that in the anti-Fgf8b treated wild type explants the expression of ventral markers would be reduced, but only slightly, compared to the non-treated half. If Fgf8 is directly responsible for the expansion of ventral telencephalic markers in the *Gli3*$^{Xt/Xt}$ mutant rostral telencephalon, we might have expected that in the

anti-Fgf8b treated explants of the *Gli3*$^{Xt/Xt}$ mutant embryos, the expression of ventral markers would be reduced more than in wild type explants. So far, only changes in Olig2 expression have been examined. Whether Fgf8 is responsible for the rostral expansion of ventral telencephalic markers in the *Gli3*$^{Xt/Xt}$ mutants has not been concluded yet.

6.2 RESULTS

Olig2 immunofluorescence was performed on cultured E9.5 *Gli3*$^{Xt/Xt}$ mutant and control telencephalon. At this stage, Olig2 is expressed in the ventral telencephalon and diencephalon (Lu et al., 2000). Preliminary results showed that Olig2 expression in the wild type ventral telencephalon of the anti-Fgf8b treated half seemed to be reduced slightly compared to the control half (compare the area pointed to by arrowheads in Fig. 6.1A and B). In the mutant explants, the difference between the anti-Fgf8b treated half (Fig. 6.1B') and the control (Fig. 6.1A') is still obscure. Olig2 expression is so robust in both the mutant control and anti-Fgf8b treated explants that any difference between them is hard to see. A detailed morphometric measurement might help detect any existing differences. For example, tracing the domain of Olig2 expression on each confocal stack image and averaging the Olig2 positive area would give a more precise result. This result does not exclude the possibility that Fgf8 may induce ventral cell fate in the *Gli3*$^{Xt/Xt}$ mutants, since only Olig2 expression has been tested with this explant culture experiment and further analysis, including the study of more ventral markers, such as Nkx2.1, Islet1, Dlx and Gsh2, should be undertaken.

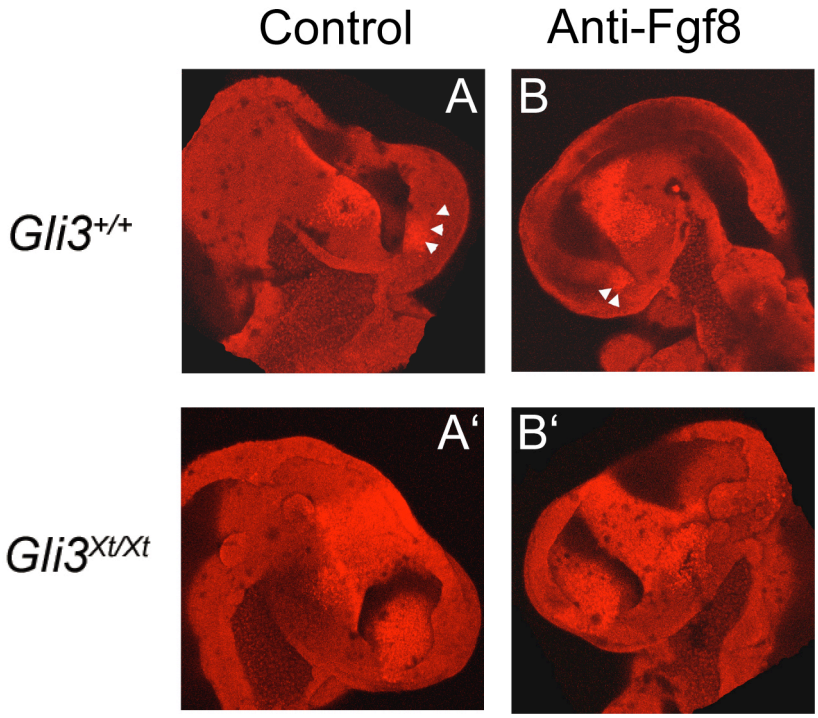

Figure 6.1 Olig2 immunoreactivity on wild type (**A** and **B**) and *Gli3*$^{Xt/Xt}$ mutant (**A'** and **B'**) explant cultures. **A** and **A'** were incubated with culture medium, and **B** and **B'** were incubated with anti-Fgf8b antibody added to the culture medium for 16 hours before being immunoreacted with Olig2. Olig2 expression in the ventral telencephalon seems to be reduced in the wild type explant with anti-Fgf8b (compare arrowheads pointed area in **A** with **B**). There seems to be no difference in Olig2 expression between *Gli3*$^{Xt/Xt}$ anti-Fgf8b treated explants and controls (compare **A'** with **B'**).

6.3 DISCUSSION

Fgf8 has been proposed to induce ventral cell fate in the telencephalon along the anterior-posterior axis. Fgf8-soaked beads can induce ventral cell fate and repress dorsal fate in dorsal telencephalic explant cultures, even if Shh signalling is inhibited with cyclopamine (Kuschel et al., 2003). A recent study has shown that Fgf8 signalling can generate telencephalic ventral fate independently of Shh (Gutin et al., 2006). Furthermore, the expression of *Fgf8* and its down stream target *Sprouty2* is remarkably expanded in the rostral telencephalon of the $Gli3^{Xt/Xt}$ mutants (Theil et al., 1999; Aoto et al., 2002; Kuschel et al., 2003). These results raise the possibility that Fgf8 is responsible for the expansion of ventral gene expression in the $Gli3^{Xt/Xt}$ mutant embryos. This hypothesis was tested in this chapter by an explant culture system. The structure of the Fgf8 gene is more complicated than that of other members of the Fgf family. It has been shown that there are eight protein isoforms in mice (a-h), and they differ in NH_2 terminus (Crossley and Martin, 1995; MacArthur et al., 1995a). Among them, Fgf8a and Fgf8b are expressed in the isthmus and play distinct roles in early patterning of the midbrain and anterior hindbrain of many species (Liu and Joyner, 2001; Sato and Nakamura, 2004; Olsen et al., 2006). Ectopic expression of Fgf8a in mice results in an extended midbrain (Lee et al., 1997), whereas ectopic expression of Fgf8b transforms midbrain to cerebellum (Liu et al., 1999), and Fgf8b has stronger transforming activity than Fgf8a (MacArthur et al., 1995b). Morphological changes induced by low levels of Fgf8b ectopic expression are similar to those induced by high levels of Fgf8a expression (Sato et al., 2001). These findings lead to the possibility that the differences in Fgf8a and Fgf8b bioactivity are due to the differences in the intensity of the signal generated by these isoforms (Sato et al., 2001; Sato and Nakamura, 2004). Furthermore, Fgf8b has the highest affinity with the three receptors (MacArthur et al., 1995a; MacArthur et al., 1995b; Blunt et al., 1997), and is likely the main molecule for activation of the

Ras-ERK (Ras-extracellular signal-regulated kinase) pathway, which is involved in Fgf8 signal transduction in the isthmus (Sato and Nakamura, 2004). In this study, an anti-Fgf8b antibody was used and the preliminary results have shown that anti-Fgf8b reduces Olig2 expression in the wild type telencephalon, which suggests that Fgf8b, at least partially, induces Olig2 expression in wild type embryos. Whether this is the case in the mutants is still unknown. This explant culture experiment in this thesis was not optimal for various reasons. First, only Olig2 expression was tested so far. Second, since *Fgf8* starts to be expressed in the embryonic ectoderm as early as E6 (Crossley and Martin, 1995) and is observed in rostral telencephalon at around E8 (Crossley and Martin, 1995; Aoto et al., 2002), blocking Fgf8 activity in the brain from E9.5 might be already too late for repressing ventral telencephalic fate. Third, Fgf8 is also highly expressed in the isthmus (Aoto et al., 2002), and this source might also influence the development of telencephalon. Last, the anti-Fgf8b antibody used in this study has been shown to neutralize the bioactivity of Fgf8b and Fgf8c on NR6R-3T3 fibroblasts but not that of Fgf8a. Although a previous study has shown that Fgf8b, but not Fgf8a, induces *Pax2* expression in the isthmus (Sato et al., 2001), it is possible that Fgf8a is also involved in forebrain patterning. In that case, the anti-Fgf8b is not sufficient to block completely Fgf8 activity in the telencephalon. In fact, other members of the Fgf family, like Fgf17 and Fgf18, are also expressed in the anterior pole of the cortical primordium (Bachler and Neubuser, 2001), suggesting they might work together to impart antero-posterior patterning.

It is also possible that the expansion of $Gli3^{Xt/Xt}$ mutant ventral telencephalon is the result of losing Wnts and Bmps expression from the dorso-medial telencephalon. There is evidence that Fgf8 and Wnts and Bmps are antagonists in patterning the forebrain (Shimogori et al., 2004). These possibilities will be discussed in the Discussion (Chapter 8).

6.4 FUTURE STUDIES

The conditions used in this culture experiment were not very well established and several changes should be made in future studies in order to improve the experimental protocol.

1) The concentration of anti-Fgf8b antibody used in this thesis was the one suggested by the manufacturer. The neutralizing ability of this antibody was commercially tested using this concentration in cell lines only (R&D system). The ability of this antibody to neutralize Fgf8b activity in tissue cultures has not been tested yet. In this aspect, a titer experiment with different doses of anti-Fgf8b antibody might be crucial to final the optimal antibody concentration for complete blockage of Fgf8b activity, using wild type ventral telencephalic tissue.

2) The effect of anti-Fgf8b antibody was only tested in a 16-hour culture in this thesis. A pilot experiment with different culture duration could be done to determine the optimal growth conditions. There is evidence that as culture time period increases, embryos show gradual morphological changes after Fgf8b bead implantation (Crossley et al., 2001).

3) In these experiments, E9.5 embryos were cultured flat on 6-well dishes, which might result in a poor penetration of the antibody. A more sophisticated rotating system would be helpful in this aspect (Moore-Scott et al., 2003).

4) In vitro culture normally used media with a high concentration of serum (Cockroft, 1991; Van Maele-Fabry et al., 1991). The medium used in this study contains 10% fetal bovine serum. This might influence the growth of the

explant, and the blockage of Fgf8, since Fgf8 is a member of the fibroblast growth factors. A recently developed serum-free culture technique for midgestation mouse embryos might be better for allowing growth factor studies to be performed without the potentially confounding effects of unknown factors variably present in the serum (Moore-Scott et al., 2003).

Chapter 7: Protein expression studies of Gli3 and the molecules that might interact with Gli3 in forebrain patterning by western blotting

7.1 INTRODUCTION

Sonic hedgehog (Shh) has been suggested to be important for dorso-ventral (DV) patterning in the CNS. The telencephalon of the *Shh*$^{-/-}$ mutants is severely hypoplastic and ventral structures are absent from very early stages along the neural tube (Chiang et al., 1996; Ishibashi and McMahon, 2002; Ishibashi et al., 2005). The expression of ventral telencephalic markers, such as Nkx2.1, Gsh1, Olig2 and Lhx6, is absent due to the loss of the most of the ventral telencephalon (Corbin et al., 2000; Lu et al., 2000; Corbin et al., 2003). On the contrary, dorsal telencephalic markers, including Emx1 and Pax6, are expressed throughout most of the remaining telencephalic tissue in the *Shh*$^{-/-}$ mutants (Chiang et al., 1996; Ohkubo et al., 2002). These results suggest that the telencephalon of the *Shh*$^{-/-}$ mutants is 'dorsalized'. *Foxg1*$^{-/-}$ mutant embryos exhibit similar phenotypes as the *Shh*$^{-/-}$ mutants: the ventral structures are not detectable even at very early developmental stages (Xuan et al., 1995; Martynoga et al., 2005). *Shh* expression is reported to be absent from the *Foxg1*$^{-/-}$ telencephalon at E10.5 by Huh et al. (1999), and they suggested that *Shh* might be responsible for the defects in ventral telencephalic development in *Foxg1*$^{-/-}$ embryos (Huh et al., 1999). Shh is shown to inhibit Gli3 being cleaved and the balance between full-length and cleaved isoforms of Gli3 is important for neural tube patterning (Persson et al., 2002; Meyer and Roelink, 2003; Lei et al., 2004; Stamataki et al., 2005). In the ventral spinal cord, increasing the level of full length Gli3 results in increased expression of ventral marker genes at the expense of dorsal genes (Lei et al., 2004; Stamataki et al., 2005), while overexpression of the cleaved

isoform of Gli3 represses ventral identities and induces dorsal marker genes' expression (Persson et al., 2002; Meyer and Roelink, 2003). Similarly in the telencephalon, it is possible that an increased level of cleaved Gli3 protein causes the dorsalization of the *Shh*$^{-/-}$ and *Foxg1*$^{-/-}$ mutant telencephalon.

Fuccillo et al. (2006) have shown that several defects observed in the *Shh*$^{-/-}$ mutants are rescued by removing *Pax6*. For example, in the *Shh*$^{-/-}$ single mutants, Dlx2 expression is lost, and the pallial-subpallial boundary (PSB) is compromised (Chiang et al., 1996; Rallu et al., 2002b). By removing *Pax6* from the *Shh*$^{-/-}$ mutants, expression of *Dlx2* in the dorso-lateral ganglionic eminence (dLGE) is rescued and the PSB is partially restored (Fuccillo et al., 2006). Based on the fact that more pronounced rescue of the ventral telencephalon was observed in the *Shh*$^{-/-}$;*Gli3*$^{-/-}$ compound mutants than that in *Shh*$^{-/-}$;*Pax6*$^{-/-}$ double mutants (Rallu et al., 2002b; Fuccillo et al., 2006) and *Gli3* expression was shown to be unaffected in either *Pax6*$^{-/-}$, or *Shh*$^{-/-}$;*Pax6*$^{-/-}$ compound mutants by *in situ* hybridization, Fuccillo and colleagues suggested that Pax6 might be required for Gli3 repressor function in DV patterning (Fuccillo et al., 2006). In addition, Pax6 is suggested to be important for many aspects of cortical development, such as proliferation, differentiation, cell-cell adhesion (Caric et al., 1997; Warren et al., 1999), and crucial for DV patterning (Stoykova et al., 2000; Toresson et al., 2000; Yun et al., 2001). Pax6 is expressed in the dorsal telencephalon, and the strongest expression is observed in the lateral neocortex. Interestingly, the results from analysing the forebrain of *Gli3*$^{Xt/Xt}$ mutants in Chapter 4 and 5 suggest that although the dorsal telencephalon is severely affected by the loss of Gli3, part of the dorsal telencephalon is still present in the *Gli3*$^{Xt/Xt}$ mutants, which most likely corresponds to the lateral cortex of wild types. Since the DV patterning and cell adhesion properties are affected in the *Gli3*$^{Xt/Xt}$ mutants, it is possible that this might be the result of changes in the amount of Pax6 protein in the *Gli3*$^{Xt/Xt}$ mutant telencephalon. Conversely, it is also possible that some of the defects

of the *Pax6*$^{Sey/Sey}$ mutants that are also observed in the *Gli3*$^{Xt/Xt}$ mutants, such as D/V patterning and cell adhesion defects, might be caused by changes in Gli3 protein levels.

In this chapter, western blot studies were used to analyze Gli3 expression in *Shh*$^{-/-}$ and *Foxg1*$^{-/-}$ mutants to test whether any changes in the amounts of the two isoforms were present in the telencephalon of these mutants. The results show that more cleaved Gli3 protein is produced when *Shh* is lost in the telencephalon (in both *Shh*$^{-/-}$ and *Foxg1*$^{-/-}$ mutants). Gli3 expression in *Pax6*$^{Sey/Sey}$ mutant telencephalon revealed that less cleaved Gli3 isoform is generated when *Pax6* is lost. Pax6 protein expression was analyzed in the *Gli3*$^{Xt/Xt}$ mutant telencephalon showing no significant differences in the amounts of Pax6 protein between *Gli3*$^{Xt/Xt}$ mutants and wild types. Shh protein expression was also studied in the *Gli3*$^{Xt/Xt}$ mutant telencephalon, but the results are not yet conclusive. These results shed lights on the possible functions of Gli3 in DV patterning and the interactions between Gli3 and these molecules (Shh, Foxg1 and Pax6).

7.2 RESULTS

7.2.1 More cleaved Gli3 is generated in *Shh*$^{-/-}$ and *Foxg1*$^{-/-}$ mutant telencephalon

As suggested in Chapter 3, Gli3 might act as a repressor of the Shh signalling pathway in the dorsal telencephalon. To test whether Gli3 expression is affected by the loss of Shh, Gli3 expression was examined in *Shh*$^{-/-}$ mutant telencephalon by western blot analysis. Both the full length (Gli3-F) and the cleaved (Gli3-C) isoforms of Gli3 were present in *Shh*$^{-/-}$ mutant telencephalic tissue (Fig. 7.1A). β-actin expression in these tissues was used to control the loadings and allow normalization of protein amounts. The relative ratio between the two isoforms (Gli3-C/Gli3-F) was

found increased in the *Shh*$^{-/-}$ mutants (8.66 ± 1.27) to about 5.97 times of that of the wild type telencephalon (1.45 ± 0.196) (Fig. 7.1C). The difference between the wild types and *Shh*$^{-/-}$ mutants is statistically significant (Student's *t* test, $p<0.05$, n=4 per genotype). In addition, the total amount of Gli3 (Gli3-C+Gli3-F) in the *Shh*$^{-/-}$ mutants (mean optical density (O.D): 4.00 ± 0.50) is significantly increased (Student's *t* test, $p<0.01$, n=4 per genotype) to about 2.23 times more than that in the wild type littermates (mean O.D: 1.79 ± 0.26) (Fig. 7.1B), suggesting there is more Gli3 produced in the telencephalon when Shh is lost. The increase of total amount of Gli3 (Gli3-C+Gli3-F) together with the ratio (Gli3-C/Gli3-F) change in *Shh*$^{-/-}$ mutants suggest that the increase of Gli3 observed in the *Shh*$^{-/-}$ mutant telencephalon is mainly due to an increase of the cleaved isoform (Gli3-C). These results demonstrate that more cleaved Gli3 protein is generated when Shh is absent, mimicking Gli3 expression in the wild type dorsal telencephalon, where Shh is not expressed (Chapter 3) (Echelard et al., 1993). And these results also suggest that the dorsalization of the *Shh*$^{-/-}$ telencephalon might be due to increased levels of Gli3 cleaved isoform.

Ventral telencephalic fate is not specified and *Shh* expression is completely lost in the telencephalon of *Foxg1*$^{-/-}$ mutant embryos (Xuan et al., 1995; Huh et al., 1999; Martynoga et al., 2005). This phenotype is highly reminiscent of that of *Shh*$^{-/-}$ mutants. Both isoforms of Gli3 are expressed in the *Foxg1*$^{-/-}$ mutant telencephalic tissue (Fig. 7.1D), and the ratio between them (11.40 ± 2.39) is increased significantly (Student's *t* test, $p<0.05$, n=4) to about 7.86 times that of the wild types (Fig. 7.1E). Note the ratio between the Gli3 isoforms is comparable between the *Shh*$^{-/-}$ and *Foxg1*$^{-/-}$ mutant telencephalon. It is possible that the change in ratio of Gli3 protein is due to the loss of Shh in the ventral telencephalon. However, this does not exclude the possibility that Foxg1 is required to maintain the balance between two Gli3 isoforms in the telencephalon.

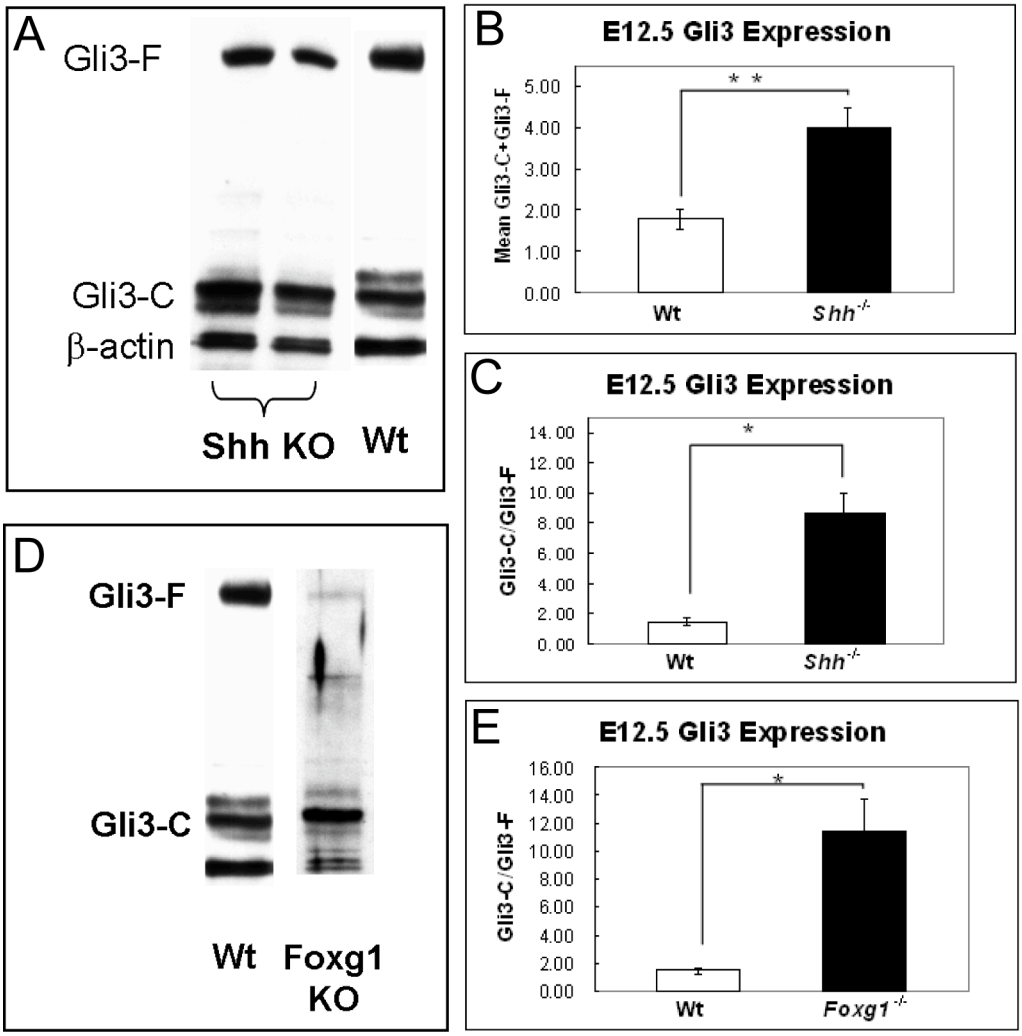

Figure 7.1 Western blot analysis shows expression of Gli3 in wild type (wt) and *Shh*$^{-/-}$ mutant (Shh KO) embryos (**A**). Both full length (Gli3-F) and short (Gli3-C) Gli3 protein are expressed in wild type and *Shh*$^{-/-}$ tissue. β-actin is used as loading control. The total amount (Gli3-C+Gli3-F) (**B**) and the ratio (Gli3-C/Gli3-F) (**C**) of Gli3 proteins are significantly increased in the *Shh*$^{-/-}$ mutant telencephalic samples. The expression of Gli3 in wild type and *Foxg1*$^{-/-}$ mutant (Foxg1 KO) embryos is shown in **D**. Both Gli3-C and Gli3-F are present and the ratio of them is significantly increased in the *Foxg1*$^{-/-}$ mutant telencephalon (**E**).

7.2.2 Less Gli3 is cleaved in the *Pax6*$^{-/-}$ mutant telencephalon

To test the possibility that Pax6 might be required for the generation of Gli3 in the telencephalon, western blot with an antibody against Gli3 was performed on *Pax6*$^{Sey/Sey}$ mutants. Both full length and cleaved isoforms of Gli3 were present in *Pax6*$^{Sey/Sey}$ mutant telencephalic tissue, and the total amount of Gli3 (Gli3-C+Gli3-F) was comparable with that of wild type littermates (Fig. 7.2A and B). Interestingly, the ratio of cleaved Gli3 to full length isoform in *Pax6*$^{Sey/Sey}$ mutants (0.69 ± 0.11) was significantly decreased (Student's *t* test, $p<0.05$, wild types=3 and *Pax6*$^{Sey/Sey}$ mutants=2) to about half that of wild types (1.45 ± 0.196) (Fig. 7.2C). This change in ratio is due to both an increase of full length Gli3 (26.7%) and a reduction of cleaved Gli3 (29.7%) in the mutant telencephalon and both changes are statistically significant (Student's *t* test, $p<0.05$, wild types=3, *Pax6*$^{Sey/Sey}$ mutants=2) (Fig. 7.2B), suggesting that less cleaved Gli3 protein is generated when Pax6 is lost. This result provides evidence for the hypothesis that Pax6 is required for the cleavage of Gli3.

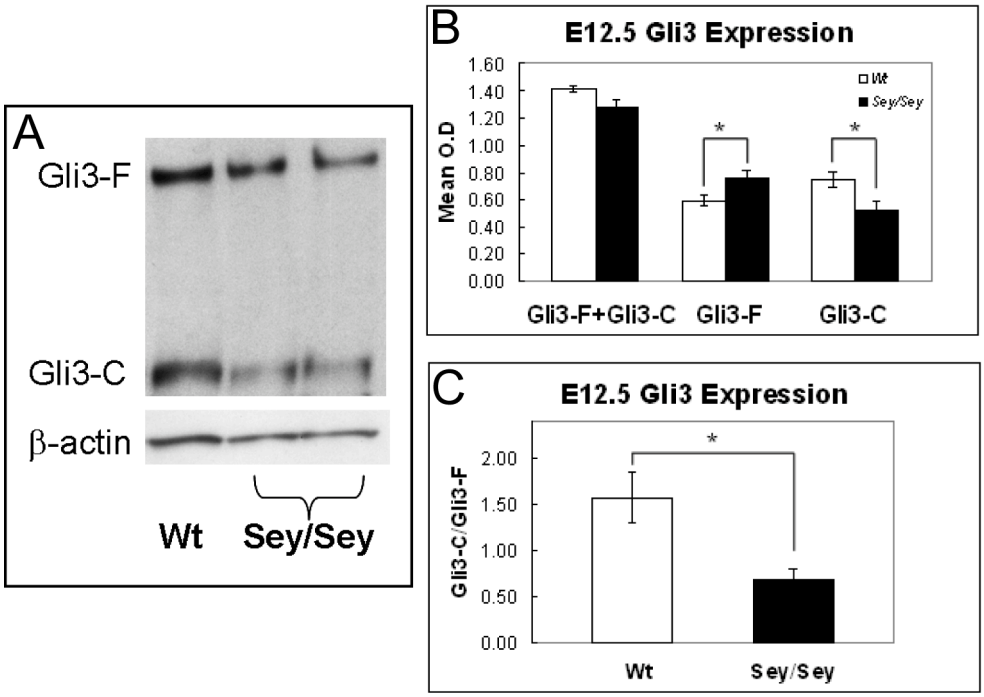

Figure 7.2 Western blot analyses with an antibody against Gli3 on wild type (wt) and *Pax6*$^{Sey/Sey}$ mutant (*Sey/Sey*) telencephalic extracts (**A**). Both isoforms of Gli3 protein (Gli3-C and Gli3-F) are observed in wild type and *Pax6*$^{Sey/Sey}$ mutant extracts, and β-actin is used as a loading control. The total amount of Gli3 (Gli3-C+Gli3-F) is comparable between wild type and *Pax6*$^{Sey/Sey}$ mutants. However, in the *Pax6*$^{Sey/Sey}$ mutant telencephalon, the amount of Gli3-F is increased significantly and Gli3-C is significantly reduced (**B**). As a result, the ratio of Gli3-C/Gli-F is significantly decreased in the *Pax6*$^{Sey/Sey}$ mutants compared to that of wild types (**C**).

7.2.3 Pax6 expression is unaltered in the *Gli3*$^{Xt/Xt}$ mutant telencephalon

To test whether Pax6 protein expression levels are changed in the *Gli3*$^{Xt/Xt}$ mutants, western blots with an antibody against Pax6 were carried out in *Gli3*$^{Xt/Xt}$ mutant telencephalic tissues. The amount of Pax6 protein in wild type (mean O.D: 3.20 ± 0.64) was similar to that found in *Gli3*$^{Xt/Xt}$ mutant telencephalon (mean O.D: 3.44 ± 0.68). Pax6 expression was further analysed on dorsal and ventral telencephalic tissues of wild type and *Gli3*$^{Xt/Xt}$ mutant embryos. In both samples, Pax6 was expressed highly in the dorsal telencephalon (mean O.D is 2.58 ± 0.56 in wild types and 2.90 ± 0.47 in mutants), and lightly in the ventral telencephalon (mean O.D is 0.62 ± 0.08 in wild types and 0.64 ± 0.21 in mutants) (Fig. 7.3B), corresponding to its expression pattern observed by immunohistochemistry (Fig. 4.1A-C and A'-C'). The differences of Pax6 expression between the dorsal and ventral telencephalon were significant (Student's *t* test, $p<0.05$, n=3 per genotype) in both wild type and *Gli3*$^{Xt/Xt}$ mutant embryos (Fig. 7.3C). These results show that Pax6 expression is not changed in the *Gli3*$^{Xt/Xt}$ mutant embryos and Gli3 loss does not affect the expression levels of Pax6 protein.

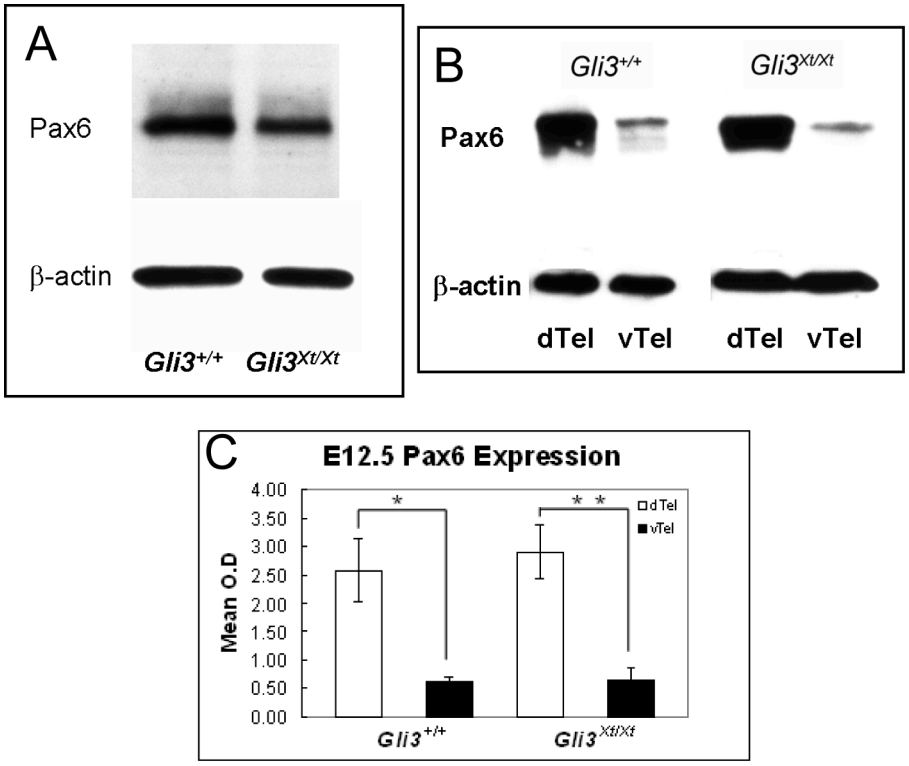

Figure 7.3 Western blots with anti-Pax6 antibody on wild type (*Gli3*$^{+/+}$) and *Gli3*$^{Xt/Xt}$ mutant telencephalic (**A**) as well as dorsal (dTel) and ventral (vTel) telencephalic extracts (**B**). β-actin expression in these tissues is used as loading control. Pax6 expression is unaltered in the *Gli3*$^{Xt/Xt}$ mutant embryos compared to wild types. The ^{high}dorsal-to-^{low}ventral expression pattern of Pax6 is observed in both wild type and mutant telencephalon (**C**).

7.2.4 The amount of Shh protein is not likely to be increased in *Gli3*$^{Xt/Xt}$ mutant telencephalon

As shown in Chapter 5, the Shh expression pattern is comparable in E10.5 and E9.5 wild type and *Gli3*$^{Xt/Xt}$ mutant embryos (Fig. 5.8). To explore whether there is any change in the amount of Shh protein produced in the *Gli3*$^{Xt/Xt}$ mutant telencephalon, western blots were performed with a Shh antibody. Mouse Shh is a glycoprotein that is proteolytically cleaved into two smaller isoforms (Bumcrot et al., 1995), a 19 kDa N-terminal peptide that mediates all Shh signalling activities (Hammerschmidt et al., 1997), and a 28 kDa C-terminal product that is responsible for the protein cleavage (Porter et al., 1995). The antibody used in this study is generated against the biologically active amino-terminal fragment of Shh (Ericson et al., 1996), and in theory, it should recognize both the full length and N-terminal Shh protein in wild type telencephalic and ventral telencephalic tissues, but not in wild type dorsal telencephalic extracts or *Shh*$^{-/-}$ mutant extracts. This antibody showed many bands, not only in wild type and *Gli3*$^{Xt/Xt}$ mutant embryos, but also in *Shh*$^{-/-}$ mutant telencephalic tissues, although at a lower level (lane a, b and c in Fig. 7.4, respectively). In wild type samples, four bands around 50 kDa were observed, which might correspond to the full length Shh protein (1, 2, 3 and 4 in lane a in Fig. 7.4). These bands disappeared in the *Shh*$^{-/-}$ mutant tissue (lane c in Fig. 7.4), but 1 and 2 appeared in the wild type dorsal telencephalon (lane d in Fig. 7.4), suggesting they might be non-specific bands. The other two bands around 50 kDa (band 3 and 4 in Fig. 7.4) might correspond to the lipid modified and unmodified full length Shh protein. They disappeared in wild type dorsal telencephalic tissue (lane d in Fig. 7.4), but were present in wild type and *Gli3*$^{Xt/Xt}$ ventral telencephalic extracts (lane e and g in Fig. 7.4) as well as in the *Gli3*$^{Xt/Xt}$ dorsal telencephalic extract (lane f in Fig. 7.4). There are several bands detected around 20 kDa, in which two are the most prominent and might correspond to the lipid modified and unmodified N-terminal

Shh protein (band 5 and 6 in Fig. 7.4). However, these bands also appeared in the wild type dorsal telencephalic tissue (lane d in Fig. 7.4). Nevertheless, these two bands seemed to be expressed at a lower level in the *Gli3*$^{Xt/Xt}$ mutant telencephalic extracts (lane b in Fig. 7.4), as well as in dorsal and ventral telencephalic extracts (lane f and g in Fig. 7.4, respectively) compared to those of wild types (lane a, d and e in Fig. 7.4). Whether there is any change in the amount of Shh protein in the *Gli3*$^{Xt/Xt}$ mutant telencephalon is still obscure, since this antibody does not seem to be good in distinguishing Shh bands by western blots.

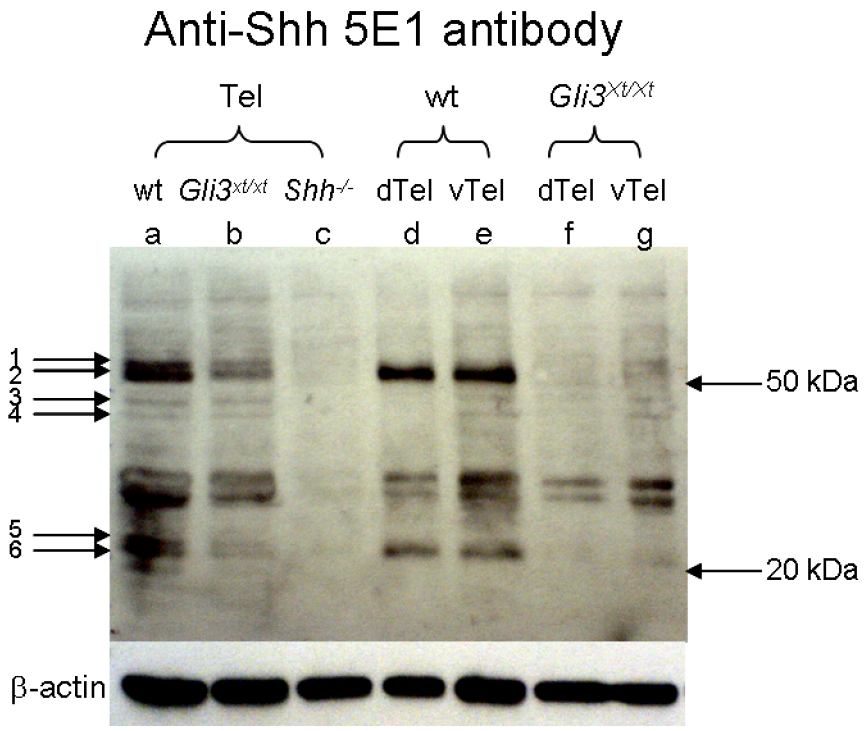

Figure 7.4 Western blot with anti-Shh antibody on wild type (lane a, d and e), *Gli3*$^{Xt/Xt}$ mutant (lane b, f and g), and *Shh*$^{-/-}$ mutant tissue (lane c). Lanes a, b and c are extracts from wild type, *Gli3*$^{Xt/Xt}$ mutant and *Shh*$^{-/-}$ mutant telencephalon (Tel), respectively. Lanes d and e are extracts from wild type dorsal (dTel) and ventral (vTel) telencephalon, respectively, and f and g are tissue from *Gli3*$^{Xt/Xt}$ mutant dorsal and ventral telencephalon, respectively. At least four bands (1, 2, 3 and 4) are observed at around 50 kDa in wild type tissue, which might correspond to the full length Shh protein. 5 and 6 are about 20 kDa, and they might correspond to the N-terminal Shh protein. β-actin expression is used as loading control.

7.3 DISCUSSION

The Gli3 expression study in Chapter 3 reveals that in the wild type dorsal telencephalon where Shh is not expressed, more cleaved Gli3 protein is produced. This result suggests that Gli3 in the dorsal telencephalon may act as a repressor of the Shh signalling pathway. In this chapter, the ratios between the two isoforms of Gli3 protein were examined in *Shh*$^{-/-}$ and *Foxg1*$^{-/-}$ mutant embryos, which lack ventral telencephalon and *Shh* expression (Xuan et al., 1995; Chiang et al., 1996; Huh et al., 1999; Ishibashi and McMahon, 2002; Ishibashi et al., 2005; Martynoga et al., 2005). The ratios of the Gli3 isoforms were found significantly increased in these mutants, agreeing with the notion that Shh prevents the cleavage of Gli3. In the absence of both Shh and Foxg1, Gli3 produces higher amounts of the cleaved isoform. This might be the primary cause of the dorsolization defects in both of these mutants. In addition, the total amount of Gli3 is significantly increased in the *Shh*$^{-/-}$ mutants, especially the cleaved isoform, indicating that Shh is required to repress Gli3 in the ventral telencephalon.

The ratio of Gli3 proteins in the Pax6 mutants is changed, although the total amount of Gli3 remains the same as in wild types. These results show that the predominant isoform of Gli3 is the full length protein when Pax6 is lost, in agreement with the hypothesis that Pax6 might be responsible for the cleavage of Gli3 (Fuccillo et al., 2006). However, this can not exclude the possibility that the change in the ratio of the Gli3 isoforms may simply be because the telencephalon of the *Pax6*$^{Sey/Sey}$ mutants is partially ventralized (Stoykova et al., 1996; Stoykova et al., 2000; Yun et al., 2001), and the expanded expression of *Shh* (Stoykova et al., 2000) inhibits the generation of more short Gli3 isoforms.

In the wild type, Pax6 is expressed in the dorsal telencephalon, and its highest

expression is observed in the lateral neocortex dorsally to the pallial-subpallial boundary (PSB) (Walther and Gruss, 1991; Stoykova et al., 2000). This region is ventralized, and the PSB is compromised when Pax6 is lost (Stoykova et al., 2000; Yun et al., 2001). Interestingly, this region is present in the *Gli3*$^{Xt/Xt}$ mutant embryos, whereas a large part of the rest of the dorsal telencephalon is lost (Grove et al., 1998; Theil et al., 1999; Tole et al., 2000a). This raises the possibility that Pax6 is crucial for the formation of the lateral cortex in *Gli3*$^{Xt/Xt}$ mutant embryos. Pax6 expression in the *Gli3*$^{Xt/Xt}$ mutants does not seem to have changed, which is in agreement with the results obtained from the immunohistochemistry.

The expression of Shh by western blots does not seem to show any changes in the *Gli3*$^{Xt/Xt}$ mutant telencephalon, in agreement with the results revealed from the immunohistochemistry and *in situ* hybridization experiments (Chapter 5.2.7). Quite a few bands are observed with the Shh antibody, not only in the wild type embryos, but also in the *Shh*$^{-/-}$ mutants. It is possible that this antibody recognizes the other members of the hedgehog family, namely, Indian hedgehog (Ihh) or Desert hedgehog (Dhh), although so far, there is no evidence for their expression in the developing telencephalon. These western blots also can not exclude the possibility that Shh is expressed at a low level in the *Gli3*$^{Xt/Xt}$ mutant dorsal telencephalon. This has never been observed by immunohistochemistry or *in situ* hybridization, and it might be possible since western blotting is a very sensitive approach. Shh expression was also studied using another anti-Shh antibody (Ab19897, Abcam), which also detected several bands in the *Shh*$^{-/-}$ mutant telencephalic tissue. A more specific anti-Shh antibody is crucial in this aspect.

Chapter 8: Discussion

Potential signalling centres have been identified and studied in the mouse forebrain, and there is evidence that they regulate the patterning process of the telencephalon along both the AP and DV axes (Shimamura and Rubenstein, 1997; Ye et al., 1998; Rubenstein et al., 1999; Lee et al., 2000; Fukuchi-Shimogori and Grove, 2001; Ragsdale and Grove, 2001; Hebert et al., 2002; O'Leary and Nakagawa, 2002; Ohkubo et al., 2002; Fukuchi-Shimogori and Grove, 2003; Garel et al., 2003; Grove and Fukuchi-Shimogori, 2003; Ligon et al., 2003). The candidate signalling molecules secreted from these signalling centres include Fibroblast growth factors (Fgf) (Fukuchi-Shimogori and Grove, 2001, 2003; Garel et al., 2003), Wingless-Int (Wnt) (Galceran et al., 2000; Lee et al., 2000), Bone morphogenetic proteins (Bmp) (Hebert and McConnell, 2000; Panchision et al., 2001), Sonic hedgehog (Shh) (Ericson et al., 1995b; Dale et al., 1997; Kohtz et al., 1998; Rubenstein and Beachy, 1998; Gunhaga et al., 2000; Machold et al., 2003; Fuccillo et al., 2006) and Retinoic acid (RA) (LaMantia, 1999; Toresson et al., 1999; Schneider et al., 2001; Smith et al., 2001; Marklund et al., 2004). In the developing telencephalon, these signalling molecules impart position and regulate regional growth by interacting with transcription factors. Studies have also demonstrated that these signalling centres interact with each other in the developing telencephalon. In this thesis, several approaches have been undertaken to elucidate the function of the transcription factor Gli3 in forebrain development. Severe telencephalic defects are observed in mice lacking functional Gli3, indicating a role in patterning the telencephalon.

8.1 Shh and Gli pathway in the developing forebrain

The Shh and Gli pathway is important for many aspects of the development of the CNS (Dahmane et al., 2001; Ruiz i Altaba et al., 2002a; Ruiz i Altaba et al., 2002b;

Ruiz i Altaba et al., 2003). In this thesis, the interaction between Shh and Gli3 has been analyzed by several approaches. Loss of Gli3 results in an expansion of ventral markers' expression in the telencephalon as early as E10.5 (Chapter 5.2.6). Shh is shown to be responsible for the generation of several of them, for example, Nkx2.1 and Olig2 (Goodrich et al., 1997; Kohtz et al., 1998; Lu et al., 2000; Zhou et al., 2000; Tekki-Kessaris et al., 2001; Rallu et al., 2002b; Gulacsi and Anderson, 2006). The expansion of the expression of ventral markers might be the result of ectopic activation of the Shh signalling pathway in the ventral telencephalon. This possibility has been tested here by *in situ* hybridization and immunohistochemistry (Chapter 5.2.7), and western blot analysis (Chapter 7.2.4). These results show no evidence for Shh and its downstream targets being ectopically expressed in $Gli3^{Xt/Xt}$ mutant ventral telencephalon, in agreement with previous works (Theil et al., 1999; Tole et al., 2000a; Aoto et al., 2002). However, the loss of tissue from the mutant dorsal telencephalon results in an abnormal joining of the telencephalon with the diencephalon, and a shape change of these structures. These changes might lead to changes in the position of these signalling centres and probably their diffusion in the extracellular matrix. The position of the Shh source in the diencephalon, particularly in the ZLI, is changed in the $Gli3^{Xt/Xt}$ mutants. In addition, there is evidence that the mutant diencephalon is bigger compared to that of the wild types (Aoto et al., 2002) (this study). It is possible that Shh signalling from the diencephalon influences gene expression in the $Gli3^{Xt/Xt}$ mutant telencephalon. Other sources of Shh outside the forebrain might also be involved in telencephalic patterning during early embryogenesis, for example, Shh in the notochord, the floor plate and the prechordal plate (Echelard et al., 1993; Krauss et al., 1993; Roelink et al., 1994; Ericson et al., 1995a; Marti et al., 1995b; Roelink et al., 1995; Ericson et al., 1996; Dale et al., 1997; Dale et al., 1999).

Changes in expression of other members of the Gli family might also contribute to

the patterning of the telencephalon. Gli2 is expressed in the developing telencephalon, mainly ventrally, and has been shown to function as an activator of the Shh signalling pathway in the spinal cord and limb (Mo et al., 1997; Ruiz i Altaba, 1999; Sasaki et al., 1999; Jacob and Briscoe, 2003). Studies in chick and mouse provide evidence that the activator function of Gli2 and Gli3 partially overlap downstream of Shh signalling in patterning and cell fate specification in the spinal cord (Motoyama et al., 2003; Lei et al., 2004) and in skeletal formation (Mo et al., 1997). In fact, results from the Gli3 protein analysis show that a high level of the cleaved isoform forms in the dorsal telencephalon, which is severely affected by the loss of Gli3. In the ventral telencephalon, where there is more full length Gli3, Gli2 might function as an activator to compensate for the loss of Gli3 activity and that might account for the lack of severe phenotypic defects.

8.2 Gli3 and Wnt and Bmp signalling in forebrain patterning

One extreme requirement for Gli3 is in the dorsal midline area of the telencephalon. Studies have shown that the dorso-medial telencephalic wall fails to invaginate and midline structures, including the cortical hem, hippocampus and choroid plexus in the lateral ventricles, are lost in the *Gli3*$^{Xt/Xt}$ mutant embryos from very early stages (Grove et al., 1998; Theil et al., 1999). The expression of *Wnt* and *Bmp* genes is lost specifically from these regions (Grove et al., 1998; Theil et al., 1999). In this study, loss of *Wnt8b* expression from the *Gli3*$^{Xt/Xt}$ mutant telencephalon already at E9 (Chapter 5.2.5), indicates a more extensive loss of the dorsal tissue, including the dorso-medial telencephalon and part of the dorsal telencephalon. It is still unknown whether the loss of dorsal tissue or the loss of Wnt/Bmp is the primary defect in *Gli3*$^{Xt/Xt}$ mutants. The fact that *Wnt* and *Bmp* expression is lost specifically from the telencephalon might indicate that the loss of dorsal tissue is the primary defect. However, it is possible that the interactions between Gli3 and Wnt/Bmp in the

telencephalon are different from other regions of the developing nervous system.

Wnt and Bmp signalling might also be responsible for DV patterning in the *Gli3*$^{Xt/Xt}$ mutant telencephalon. Wnt and Bmp signalling have been shown to regulate *Emx1* and *Emx2* expression in the dorsal telencephalon, and loss of *Wnt* and *Bmp* expression might correlate with the severe reduction and/or loss of *Emx1* and *Emx2* in the dorsal telencephalon of *Gli3*$^{Xt/Xt}$ mutants (Tole et al., 2000a; Ohkubo et al., 2002; Theil et al., 2002a). The loss of Wnt and Bmp genes from the dorso-medial telencephalon might also be involved in the expansion of *Gli3*$^{Xt/Xt}$ ventral telencephalon (Chapter 5.2.6). Wnt3a can induce dorsal cell fate, including Pax6 and Ngn2 expression, and repress ventral cell fate (Gunhaga et al., 2003). It is possible that the loss of Wnt and Bmp signalling in the *Gli3*$^{Xt/Xt}$ mutant embryos relieves that repression leading to the expansion of the ventral telencephalon.

The Wnts and their inhibitor SFRP2 (secreted frizzled related protein-2) (Rattner et al., 1997; Dennis et al., 1999; Ladher et al., 2000) expressed in the pallial-subpallial boundary (PSB) and eminentia thalami, may also influence telencephalic patterning. Wnts and SFRP2 expression at these sites is negatively regulated by Pax6 (Kim et al., 2001). In addition, starting at E10.5, eminentia thalami cells can be detected in the *Gli3*$^{Xt/Xt}$ mutant neocortex (Fotaki et al., 2006). It would not be surprising if Wnt signalling is increased in the diencephalon of *Gli3*$^{Xt/Xt}$ mutants, and Wnts and SFRP2 from the eminentia thalami affect dorsal telencephalic patterning in the mutants. However, more experiments need to be carried out to test this.

8.3 Gli3 and Fgf signalling in forebrain patterning

Fgf8 has been shown to induce ventral cell fate and repress dorsal cell fate in dorsal telencephalic explants (Kuschel et al., 2003). It has been hypothesized that Fgf8

induces ventral markers' expression in *Gli3*$^{Xt/Xt}$ mutants, because *Fgf8* expression is expanded in the rostral telencephalon of *Gli3*$^{Xt/Xt}$ mutants (Theil et al., 1999; Aoto et al., 2002; Kuschel et al., 2003). In this thesis, detailed morphological studies of the *Gli3*$^{Xt/Xt}$ mutant telencephalon strongly suggest that the mutant septum is enlarged (Chapter 5.2.8). *Fgf8* null mutants die during gastrulation, whereas the *Fgf8* hypomorphic and telencephalic conditional *Fgf8* knock-out mutants survive until birth. These mutants show an increase in dorsal telencephalic gene expression, such as *Pax6*, *Emx2* and *Tbr1*, and they do not have septal structures (Meyers et al., 1998; Sun et al., 1999; Garel et al., 2003; Storm et al., 2003; Storm et al., 2006). These results further indicate the interactions between Gli3 and Fgf8 in ventral telencephalic formation. Whether Fgf8 is directly responsible for the expansion of rostro-ventral fate in the *Gli3*$^{Xt/Xt}$ mutants has been tested in this thesis (Chapter 6), but the results have not been conclusive.

Fgf8 has also been implicated in dorsal telencephalic development, specifically, by regulating *Emx2* expression. Studies have shown that exogenous Fgf8 can repress *Emx2* expression (Crossley et al., 2001; Storm et al., 2003), and *Emx2* expression is increased in *Fgf8* mutants (hypomorphic and telencephalic conditional knock-out embryos) (Garel et al., 2003; Storm et al., 2003; Storm et al., 2006). *Emx2* expression is largely lost in the *Gli3*$^{Xt/Xt}$ mutants (Theil et al., 1999; Tole et al., 2000a; Theil et al., 2002a), which could also be the result of an increase in Fgf8 signalling.

Other members of the Fgf family might also influence forebrain patterning, for example, *Fgf17* and *Fgf18*. *Fgf8*, *Fgf17* and *Fgf18* are expressed in the anterior telencephalon (ANR) and the isthmus during early development (Maruoka et al., 1998; Xu et al., 1999; Shinya et al., 2001), and they have similar receptor specificity and ability to induce proliferation (Xu et al., 1999; Xu et al., 2000). Furthermore, a study in cerebellum development has shown an overlap in function between Fgf8 and

Fgf17 (Xu et al., 2000). A more recent study has pointed out the importance of Fgf17 in telencephalic patterning (Cholfin and Rubenstein, 2007). In new born mice, the loss of Fgf17 selectively reduces the size of dorso-rostral telencephalon, whereas the ventral part appears normal (Cholfin and Rubenstein, 2007). Whether *Fgf17* expression is expanded in the *Gli3*$^{Xt/Xt}$ mutant telencephalon, and whether it is responsible for the loss of dorsal cell fate in the *Gli3*$^{Xt/Xt}$ mutants, needs to be examined.

8.4 Gli3 and Retinoic acid signalling

Gli3 is highly expressed in the developing dorsal telencephalon (Chapter 3.2), and the loss of Gli3 results in partial loss of the dorsal telencephalon, lack of lamination and formation of rosette-like structures (Chapter 4.2.6 and 5.2.3-5). The fact that not all the dorsal telencephalon is lost in *Gli3*$^{Xt/Xt}$ mutants suggests that some other factors might contribute to promote dorsal telencephalic fate. Pax6, which is highly expressed in the dorsal telencephalon in a ^{high}lateral-to-^{low}medial fashion, is largely unchanged in the *Gli3*$^{Xt/Xt}$ mutants, and the highest Pax6 expression site, the lateral cortex, is still observed in the *Gli3*$^{Xt/Xt}$ mutants. *Pax6* expression in the dorsal telencephalon is partially regulated by Wnt signalling (Gunhaga et al., 2003). However, *Wnt* expression is lost from the *Gli3*$^{Xt/Xt}$ mutant dorsal telencephalon, suggesting there might be other signals responsible for the Pax6 expression in the lateral cortex of *Gli3*$^{Xt/Xt}$ mutants. RA signalling has been shown to be responsible for telencephalic intermediate fates, including Pax6 expression in the lateral cortex and dorsal LGE (Marklund et al., 2004). A study has shown that RA-dependent gene expression is absent in the *Gli3*$^{Xt/Xt}$ mutant forebrain (LaMantia, 1999). In addition, it has been proposed that RA signalling might contribute to the rescue of LGE fates in *Shh*$^{-/-}$*;Gli3*$^{-/-}$ double mutants (Rallu et al., 2002b). However, how RA signalling affects the development of the *Gli3*$^{Xt/Xt}$ mutant telencephalon has not been thoroughly

studied.

8.5 Interactions between signalling centres in forebrain development

Accumulating data from studies in telencephalic development have implied that the signalling centres interact to regulate one another. There is evidence that Fgf from the ANR antagonizes the Bmp/Wnt in the dorsal midline area (Fukuchi-Shimogori and Grove, 2001; Shimogori et al., 2004). In chick, Fgf8 expression is downregulated by Bmp4 in the anterior telencephalon (Ohkubo et al., 2002), and in mouse, noggin can induce ectopic *Fgf8* expression in the cortical neuroepithelium (Shimogori et al., 2004). In mice lacking chordin and having only one copy of noggin, Bmp activity is increased and *Fgf8* expression is lost from the ANR (Anderson et al., 2002). These findings suggest that Bmp represses *Fgf8* expression in the ANR.

Wnt signalling is required to generate dorsal telencephalic cells in chick embryos, including *Pax6*, *Ngn2* and *Emx1* positive cells (Gunhaga et al., 2003). Wnts can induce dorsal cell fate in ventral telencephalic cells, and suppress ventral cell fate (Gunhaga et al., 2003). Fgf8 has been shown to be necessary for the generation of *Emx1* and *Emx2* positive cells in the dorsal telencephalon (Crossley et al., 2001; Gunhaga et al., 2003; Storm et al., 2003), but not *Pax6* or *Ngn2* positive cells (Gunhaga et al., 2003). Furthermore, the increase of Fgf8 in the ANR leads to a reduction of *Wnt3a* expression in the cortical hem (Shimogori et al., 2004). This evidence highlights the importance of the interactions between Wnt and Fgf signalling in dorsal telencephalic development.

In the $Gli3^{Xt/Xt}$ telencephalon, *Fgf8* expression is expanded rostrally, whereas *Bmp* and *Wnt* genes are lost specifically from the dorsal midline area (Grove et al., 1998; Theil et al., 1999; Tole et al., 2000a; Aoto et al., 2002). These results suggest that

Gli3 might function upstream of Wnt, Bmp and Fgf8 signalling in telencephalic development in three possible ways:

1. Gli3 negatively regulates *Fgf8* directly and loss of Gli3 increases *Fgf8* expression in the ANR, which in turn suppresses *Wnts* and *Bmps* in the dorsal midline.

2. Loss of Gli3 leads to loss of *Wnts* and *Bmps* expression in the dorsal midline, which in turn relieves the inhibition of *Fgf8*.

3. Gli3 regulates these pathways in parallel.

Both Shh and Fgf8 signalling are required to generate ventral telencephalic fate, but the interaction between them is still largely unknown. Studies from $Shh^{-/-};Gli3^{-/-}$ double mutants (Aoto et al., 2002; Rallu et al., 2002b) and mutants for Fgf receptors (Gutin et al., 2006) have suggested that Shh and Fgf signalling work in parallel to generate ventral precursors. In the rostral telencephalon, Shh is shown to be necessary to maintain *Fgf8* expression (Ohkubo et al., 2002). In the $Shh^{-/-}$ mutants, *Fgf8* expression is lost from the ANR (Ohkubo et al., 2002), which may be due to an activation of the repressor form of Gli3 (Chapter 6). By contrast, *Fgf8* expression is expanded in the $Gli3^{Xt/Xt}$ mutants (Theil et al., 1999; Aoto et al., 2002; Kuschel et al., 2003). In $Shh^{-/-};Gli3^{-/-}$ double mutants, where Gli3 no longer exists, *Fgf8* expression is still expanded (Aoto et al., 2002). These results suggest that Shh regulates *Fgf8* expression indirectly, by repressing Gli3 activity.

8.6 Gli3 and cell proliferation and cell differentiation

Gli3 is mainly expressed in proliferating cells (Chapter 3.2), which suggests that Gli3 might play a role in cell proliferation. However, the study of cell cycle parameters,

including the duration of S-phase and cell cycle in the *Gli3*$^{Xt/Xt}$ mutants, revealed no significant defects (Chapter 5.2.2). The only difference detected was in the labelling index in the E10.5 *Gli3*$^{Xt/Xt}$ mutant dorsal telencephalon, but not ventrally (Chapter 5.2.2), nor at later ages (E12.5 and E13.5, Chapter 4.2.7) (Theil et al., 1999). An increase in labelling index would be expected to result in an overgrowth of tissue at later stages. However, at E12.5, the dorsal telencephalon of the *Gli3*$^{Xt/Xt}$ mutants is smaller compared to that of wild types (Chapter 4.2.3). These results are quite hard to interpret without further analysis and can not exclude the possibility that Gli3 may regulate other aspects of the cell cycle. Gli3 seems to regulate cell differentiation in a specific region at a specific time (Chapter 5.2.3). However, the exact role of Gli3 in cell differentiation needs to be further studied, for example, the fraction of daughter cells which leave the cell cycle (Q fraction).

8.7 Gli3 and cell survival

Several lines of evidence have indicated a role of Gli3 in regulating cell survival. Aoto et al. (2002) have reported that cell death is lost from the *Gli3*$^{Xt/Xt}$ mutant dorso-medial telencephalon. *In vitro* studies have shown that telencephalic cells of E14.5 and E15.5 *Gli3*$^{Xt/Xt}$ mutant embryos survive better than those of wild types, and are more resistant to cell death induced by exogenous factors (Zaki et al., 2005). In this thesis, increased apoptosis has been observed in the ventral midline, as well as a reduction in the dorsal midline of the *Gli3*$^{Xt/Xt}$ mutant telencephalon at E10.5 (Chapter 5.2.4). The loss of apoptotic cells in the dorsal midline might actually reflect a tissue loss in the *Gli3*$^{Xt/Xt}$ mutant embryos. However, the results from the analysis of the ventral telencephalon show an increase of apoptotic cells in E10.5 *Gli3*$^{Xt/Xt}$ mutants, suggesting that Gli3 might inhibit cell death at a specific place and time point during early embryogenesis.

In vitro studies have shown that exogenous Bmp2 and Bmp4 can induce cell death in telencephalic explant cultures (Furuta et al., 1997; Ohkubo et al., 2002), and the Bmp antagonist noggin has been shown to inhibit apoptosis in limb (Bastida et al., 2004), suggesting Bmp signalling is important for cell survival. *Shh*$^{-/-}$ mutants exhibit ectopic cell death in spinal cord and an increase in *Bmp* and *Msx* expression (Chiang et al., 1996; Litingtung and Chiang, 2000; Ohkubo et al., 2002). However, since *Bmp* expression is lost from the *Gli3*$^{Xt/Xt}$ mutant telencephalon, this is less likely to be the apoptotic inducer.

In the telencephalon, loss or increase of *Fgf8* expression can induce cell death, and a reduced level of *Fgf8* expression promotes cell survival (Ohkubo et al., 2002; Storm et al., 2003). Perhaps, the increased level of *Fgf8* is responsible for the increase in cell death in the *Gli3*$^{Xt/Xt}$ mutant ventral telencephalon.

SUMMARY

The present study re-examined the forebrain defects of the *Gli3*$^{Xt/Xt}$ mutants. These results shed light into the function of Gli3 in the developing mouse forebrain. Gli3 seems to be involved in many aspects of forebrain development, such as, establishing the dorso-medial telencephalon, establishing the dorsal and ventral boundary between the telencephalon and the diencephalon, repressing ventral telencephalic fate, regulating the size and shape of the telencephalon and the diencephalon, and regulating cell death in the ventral telencephalon in both dorso-ventral and rostro-caudal axis. Accumulating data suggest that Gli3 regulates the expression of and the response to morphogenetic signals. It would be important to identify the direct and indirect downstream targets of Gli3 and investigate the exact interactions between Gli3 and these signalling molecules in order to explore further their functions in the forebrain.

BIBLIOGRAPHY

Abbott LC, Jacobowitz DM (1999) Developmental expression of calretinin-immunoreactivity in the thalamic eminence of the fetal mouse. Int J Dev Neurosci 17:331-345.

Alcantara S, Ruiz M, D'Arcangelo G, Ezan F, de Lecea L, Curran T, Sotelo C, Soriano E (1998) Regional and cellular patterns of reelin mRNA expression in the forebrain of the developing and adult mouse. J Neurosci 18:7779-7799.

Anderson RM, Lawrence AR, Stottmann RW, Bachiller D, Klingensmith J (2002) Chordin and noggin promote organizing centers of forebrain development in the mouse. Development 129:4975-4987.

Aoto K, Nishimura T, Eto K, Motoyama J (2002) Mouse GLI3 regulates Fgf8 expression and apoptosis in the developing neural tube, face, and limb bud. Dev Biol 251:320-332.

Aza-Blanc P, Lin HY, Ruiz i Altaba A, Kornberg TB (2000) Expression of the vertebrate Gli proteins in Drosophila reveals a distribution of activator and repressor activities. Development 127:4293-4301.

Bachiller D, Klingensmith J, Kemp C, Belo JA, Anderson RM, May SR, McMahon JA, McMahon AP, Harland RM, Rossant J, De Robertis EM (2000) The organizer factors Chordin and Noggin are required for mouse forebrain development. Nature 403:658-661.

Bachler M, Neubuser A (2001) Expression of members of the Fgf family and their receptors during midfacial development. Mech Dev 100:313-316.

Barnes EA, Kong M, Ollendorff V, Donoghue DJ (2001) Patched1 interacts with cyclin B1 to regulate cell cycle progression. Embo J 20:2214-2223.

Basler K, Struhl G (1994) Compartment boundaries and the control of Drosophila limb pattern by hedgehog protein. Nature 368:208-214.

Bastida MF, Delgado MD, Wang B, Fallon JF, Fernandez-Teran M, Ros MA (2004) Levels of Gli3 repressor correlate with Bmp4 expression and apoptosis during limb development. Dev Dyn 231:148-160.

Bear MarkF., Barry W. Connors, and Michael A. Paradiso. Neuroscience: Exploring the Brain. 2nd ed. Baltimore, Md.:Lippincott Williams &Wilkins, 2001. ISBN: 0683305964.

Bishop KM, Goudreau G, O'Leary DD (2000) Regulation of area identity in the mammalian neocortex by Emx2 and Pax6. Science 288:344-349.

Blunt AG, Lawshe A, Cunningham ML, Seto ML, Ornitz DM, MacArthur CA (1997) Overlapping expression and redundant activation of mesenchymal fibroblast growth factor (FGF) receptors by alternatively spliced FGF-8 ligands. J Biol Chem 272:3733-3738.

Briscoe J, Ericson J (1999) The specification of neuronal identity by graded Sonic Hedgehog signalling. Semin Cell Dev Biol 10:353-362.

Bumcrot DA, Takada R, McMahon AP (1995) Proteolytic processing yields two secreted forms of sonic hedgehog. Mol Cell Biol 15:2294-2303.

Buscher D, Grotewold L, Ruther U (1998) The XtJ allele generates a Gli3 fusion transcript. Mamm Genome 9:676-678.

Buscher D, Bosse B, Heymer J, Ruther U (1997) Evidence for genetic control of Sonic hedgehog by

Gli3 in mouse limb development. Mech Dev 62:175-182.

Campbell K (2003) Dorsal-ventral patterning in the mammalian telencephalon. Curr Opin Neurobiol 13:50-56.

Caric D, Gooday D, Hill RE, McConnell SK, Price DJ (1997) Determination of the migratory capacity of embryonic cortical cells lacking the transcription factor Pax-6. Development 124:5087-5096.

Casarosa S, Fode C, Guillemot F (1999) Mash1 regulates neurogenesis in the ventral telencephalon. Development 126:525-534.

Caviness VS, Jr. (1982) Development of neocortical afferent systems: studies in the reeler mouse. Neurosci Res Program Bull 20:560-569.

Caviness VS, Jr., Takahashi T, Nowakowski RS (1995) Numbers, time and neocortical neuronogenesis: a general developmental and evolutionary model. Trends Neurosci 18:379-383.

Chen Y, Knezevic V, Ervin V, Hutson R, Ward Y, Mackem S (2004) Direct interaction with Hoxd proteins reverses Gli3-repressor function to promote digit formation downstream of Shh. Development 131:2339-2347.

Chiang C, Litingtung Y, Lee E, Young KE, Corden JL, Westphal H, Beachy PA (1996) Cyclopia and defective axial patterning in mice lacking Sonic hedgehog gene function. Nature 383:407-413.

Chizhikov VV, Millen KJ (2004) Mechanisms of roof plate formation in the vertebrate CNS. Nat Rev Neurosci 5:808-812.

Cholfin JA, Rubenstein JL (2007) Patterning of frontal cortex subdivisions by Fgf17. Proc Natl Acad Sci U S A.

Cockroft DL (1991) Culture media for postimplantation embryos. Reprod Toxicol 5:223-228.

Corbin JG, Rutlin M, Gaiano N, Fishell G (2003) Combinatorial function of the homeodomain proteins Nkx2.1 and Gsh2 in ventral telencephalic patterning. Development 130:4895-4906.

Corbin JG, Gaiano N, Machold RP, Langston A, Fishell G (2000) The Gsh2 homeodomain gene controls multiple aspects of telencephalic development. Development 127:5007-5020.

Costa C, Harding B, Copp AJ (2001) Neuronal migration defects in the Dreher (Lmx1a) mutant mouse: role of disorders of the glial limiting membrane. Cereb Cortex 11:498-505.

Crossley PH, Martin GR (1995) The mouse Fgf8 gene encodes a family of polypeptides and is expressed in regions that direct outgrowth and patterning in the developing embryo. Development 121:439-451.

Crossley PH, Martinez S, Ohkubo Y, Rubenstein JL (2001) Coordinate expression of Fgf8, Otx2, Bmp4, and Shh in the rostral prosencephalon during development of the telencephalic and optic vesicles. Neuroscience 108:183-206.

Dahlstrand J, Lardelli M, Lendahl U (1995) Nestin mRNA expression correlates with the central nervous system progenitor cell state in many, but not all, regions of developing central nervous system. Brain Res Dev Brain Res 84:109-129.

Dahmane N, Sanchez P, Gitton Y, Palma V, Sun T, Beyna M, Weiner H, Ruiz i Altaba A (2001) The Sonic Hedgehog-Gli pathway regulates dorsal brain growth and tumorigenesis. Development 128:5201-5212.

Dai P, Akimaru H, Tanaka Y, Maekawa T, Nakafuku M, Ishii S (1999) Sonic Hedgehog-induced

activation of the Gli1 promoter is mediated by GLI3. J Biol Chem 274:8143-8152.

Dale JK, Vesque C, Lints TJ, Sampath TK, Furley A, Dodd J, Placzek M (1997) Cooperation of BMP7 and SHH in the induction of forebrain ventral midline cells by prechordal mesoderm. Cell 90:257-269.

Dale K, Sattar N, Heemskerk J, Clarke JD, Placzek M, Dodd J (1999) Differential patterning of ventral midline cells by axial mesoderm is regulated by BMP7 and chordin. Development 126:397-408.

Davies JE, Miller RH (2001) Local sonic hedgehog signaling regulates oligodendrocyte precursor appearance in multiple ventricular zone domains in the chick metencephalon. Dev Biol 233:513-525.

Davila JC, Real MA, Olmos L, Legaz I, Medina L, Guirado S (2005) Embryonic and postnatal development of GABA, calbindin, calretinin, and parvalbumin in the mouse claustral complex. J Comp Neurol 481:42-57.

del Rio JA, Martinez A, Fonseca M, Auladell C, Soriano E (1995) Glutamate-like immunoreactivity and fate of Cajal-Retzius cells in the murine cortex as identified with calretinin antibody. Cereb Cortex 5:13-21.

Dennis S, Aikawa M, Szeto W, d'Amore PA, Papkoff J (1999) A secreted frizzled related protein, FrzA, selectively associates with Wnt-1 protein and regulates wnt-1 signaling. J Cell Sci 112 (Pt 21):3815-3820.

Diez del Corral R, Olivera-Martinez I, Goriely A, Gale E, Maden M, Storey K (2003) Opposing FGF and retinoid pathways control ventral neural pattern, neuronal differentiation, and segmentation during body axis extension. Neuron 40:65-79.

Ding Q, Motoyama J, Gasca S, Mo R, Sasaki H, Rossant J, Hui CC (1998) Diminished Sonic hedgehog signaling and lack of floor plate differentiation in Gli2 mutant mice. Development 125:2533-2543.

Donoghue MJ, Rakic P (1999) Molecular gradients and compartments in the embryonic primate cerebral cortex. Cereb Cortex 9:586-600.

Dou CL, Li S, Lai E (1999) Dual role of brain factor-1 in regulating growth and patterning of the cerebral hemispheres. Cereb Cortex 9:543-550.

Echelard Y, Epstein DJ, St-Jacques B, Shen L, Mohler J, McMahon JA, McMahon AP (1993) Sonic hedgehog, a member of a family of putative signaling molecules, is implicated in the regulation of CNS polarity. Cell 75:1417-1430.

Echevarria D, Vieira C, Gimeno L, Martinez S (2003) Neuroepithelial secondary organizers and cell fate specification in the developing brain. Brain Res Brain Res Rev 43:179-191.

Eisenstat DD, Liu JK, Mione M, Zhong W, Yu G, Anderson SA, Ghattas I, Puelles L, Rubenstein JL (1999) DLX-1, DLX-2, and DLX-5 expression define distinct stages of basal forebrain differentiation. J Comp Neurol 414:217-237.

Ekker SC, Ungar AR, Greenstein P, von Kessler DP, Porter JA, Moon RT, Beachy PA (1995) Patterning activities of vertebrate hedgehog proteins in the developing eye and brain. Curr Biol 5:944-955.

Elson E, Perveen R, Donnai D, Wall S, Black GC (2002) De novo GLI3 mutation in acrocallosal syndrome: broadening the phenotypic spectrum of GLI3 defects and overlap with murine models. J Med Genet 39:804-806.

Englund C, Fink A, Lau C, Pham D, Daza RA, Bulfone A, Kowalczyk T, Hevner RF (2005) Pax6, Tbr2, and Tbr1 are expressed sequentially by radial glia, intermediate progenitor cells, and postmitotic neurons in developing neocortex. J Neurosci 25:247-251.

Ericson J, Muhr J, Jessell TM, Edlund T (1995a) Sonic hedgehog: a common signal for ventral patterning along the rostrocaudal axis of the neural tube. Int J Dev Biol 39:809-816.

Ericson J, Morton S, Kawakami A, Roelink H, Jessell TM (1996) Two critical periods of Sonic Hedgehog signaling required for the specification of motor neuron identity. Cell 87:661-673.

Ericson J, Muhr J, Placzek M, Lints T, Jessell TM, Edlund T (1995b) Sonic hedgehog induces the differentiation of ventral forebrain neurons: a common signal for ventral patterning within the neural tube. Cell 81:747-756.

Erter CE, Wilm TP, Basler N, Wright CV, Solnica-Krezel L (2001) Wnt8 is required in lateral mesendodermal precursors for neural posteriorization in vivo. Development 128:3571-3583.

Fekany-Lee K, Gonzalez E, Miller-Bertoglio V, Solnica-Krezel L (2000) The homeobox gene bozozok promotes anterior neuroectoderm formation in zebrafish through negative regulation of BMP2/4 and Wnt pathways. Development 127:2333-2345.

Fekany K, Yamanaka Y, Leung T, Sirotkin HI, Topczewski J, Gates MA, Hibi M, Renucci A, Stemple D, Radbill A, Schier AF, Driever W, Hirano T, Talbot WS, Solnica-Krezel L (1999) The zebrafish bozozok locus encodes Dharma, a homeodomain protein essential for induction of gastrula organizer and dorsoanterior embryonic structures. Development 126:1427-1438.

Fietz MJ, Concordet JP, Barbosa R, Johnson R, Krauss S, McMahon AP, Tabin C, Ingham PW (1994) The hedgehog gene family in Drosophila and vertebrate development. Dev Suppl:43-51.

Figdor MC, Stern CD (1993) Segmental organization of embryonic diencephalon. Nature 363:630-634.

Fode C, Ma Q, Casarosa S, Ang SL, Anderson DJ, Guillemot F (2000) A role for neural determination genes in specifying the dorsoventral identity of telencephalic neurons. Genes Dev 14:67-80.

Foley AC, Skromne I, Stern CD (2000) Reconciling different models of forebrain induction and patterning: a dual role for the hypoblast. Development 127:3839-3854.

Fotaki V, Yu T, Zaki PA, Mason JO, Price DJ (2006) Abnormal positioning of diencephalic cell types in neocortical tissue in the dorsal telencephalon of mice lacking functional Gli3. J Neurosci 26:9282-9292.

Franz T (1994) Extra-toes (Xt) homozygous mutant mice demonstrate a role for the Gli-3 gene in the development of the forebrain. Acta Anat (Basel) 150:38-44.

Fuccillo M, Rutlin M, Fishell G (2006) Removal of Pax6 partially rescues the loss of ventral structures in Shh null mice. Cereb Cortex 16 Suppl 1:i96-102.

Fuccillo M, Rallu M, McMahon AP, Fishell G (2004) Temporal requirement for hedgehog signaling in ventral telencephalic patterning. Development 131:5031-5040.

Fukuchi-Shimogori T, Grove EA (2001) Neocortex patterning by the secreted signaling molecule FGF8. Science 294:1071-1074.

Fukuchi-Shimogori T, Grove EA (2003) Emx2 patterns the neocortex by regulating FGF positional signaling. Nat Neurosci 6:825-831.

Furuta Y, Piston DW, Hogan BL (1997) Bone morphogenetic proteins (BMPs) as regulators of dorsal forebrain development. Development 124:2203-2212.

Galceran J, Miyashita-Lin EM, Devaney E, Rubenstein JL, Grosschedl R (2000) Hippocampus development and generation of dentate gyrus granule cells is regulated by LEF1. Development 127:469-482.

Garel S, Huffman KJ, Rubenstein JL (2003) Molecular regionalization of the neocortex is disrupted in Fgf8 hypomorphic mutants. Development 130:1903-1914.

Glinka A, Wu W, Delius H, Monaghan AP, Blumenstock C, Niehrs C (1998) Dickkopf-1 is a member of a new family of secreted proteins and functions in head induction. Nature 391:357-362.

Gokhan S, Marin-Husstege M, Yung SY, Fontanez D, Casaccia-Bonnefil P, Mehler MF (2005) Combinatorial profiles of oligodendrocyte-selective classes of transcriptional regulators differentially modulate myelin basic protein gene expression. J Neurosci 25:8311-8321.

Goodrich LV, Milenkovic L, Higgins KM, Scott MP (1997) Altered neural cell fates and medulloblastoma in mouse patched mutants. Science 277:1109-1113.

Gradwohl G, Fode C, Guillemot F (1996) Restricted expression of a novel murine atonal-related bHLH protein in undifferentiated neural precursors. Dev Biol 180:227-241.

Gratzner HG (1982) Monoclonal antibody to 5-bromo- and 5-iododeoxyuridine: A new reagent for detection of DNA replication. Science 218:474-475.

Grove EA, Tole S (1999) Patterning events and specification signals in the developing hippocampus. Cereb Cortex 9:551-561.

Grove EA, Fukuchi-Shimogori T (2003) Generating the cerebral cortical area map. Annu Rev Neurosci 26:355-380.

Grove EA, Tole S, Limon J, Yip L, Ragsdale CW (1998) The hem of the embryonic cerebral cortex is defined by the expression of multiple Wnt genes and is compromised in Gli3-deficient mice. Development 125:2315-2325.

Guillemot F, Joyner AL (1993) Dynamic expression of the murine Achaete-Scute homologue Mash-1 in the developing nervous system. Mech Dev 42:171-185.

Gulacsi A, Anderson SA (2006) Shh maintains Nkx2.1 in the MGE by a Gli3-independent mechanism. Cereb Cortex 16 Suppl 1:i89-95.

Gulisano M, Broccoli V, Pardini C, Boncinelli E (1996) Emx1 and Emx2 show different patterns of expression during proliferation and differentiation of the developing cerebral cortex in the mouse. Eur J Neurosci 8:1037-1050.

Gunhaga L, Jessell TM, Edlund T (2000) Sonic hedgehog signaling at gastrula stages specifies ventral telencephalic cells in the chick embryo. Development 127:3283-3293.

Gunhaga L, Marklund M, Sjodal M, Hsieh JC, Jessell TM, Edlund T (2003) Specification of dorsal telencephalic character by sequential Wnt and FGF signaling. Nat Neurosci 6:701-707.

Gutin G, Fernandes M, Palazzolo L, Paek H, Yu K, Ornitz DM, McConnell SK, Hebert JM (2006) FGF signalling generates ventral telencephalic cells independently of SHH. Development 133:2937-2946.

Hammerschmidt M, Brook A, McMahon AP (1997) The world according to hedgehog. Trends Genet 13:14-21.

Hanashima C, Shen L, Li SC, Lai E (2002) Brain factor-1 controls the proliferation and differentiation of neocortical progenitor cells through independent mechanisms. J Neurosci 22:6526-6536.

Hanashima C, Li SC, Shen L, Lai E, Fishell G (2004) Foxg1 suppresses early cortical cell fate. Science 303:56-59.

Hashimoto-Torii K, Motoyama J, Hui CC, Kuroiwa A, Nakafuku M, Shimamura K (2003) Differential activities of Sonic hedgehog mediated by Gli transcription factors define distinct neuronal subtypes in the dorsal thalamus. Mech Dev 120:1097-1111.

Hashimoto H, Itoh M, Yamanaka Y, Yamashita S, Shimizu T, Solnica-Krezel L, Hibi M, Hirano T (2000) Zebrafish Dkk1 functions in forebrain specification and axial mesendoderm formation. Dev Biol 217:138-152.

Hebert JM, McConnell SK (2000) Targeting of cre to the Foxg1 (BF-1) locus mediates loxP recombination in the telencephalon and other developing head structures. Dev Biol 222:296-306.

Hebert JM, Mishina Y, McConnell SK (2002) BMP signaling is required locally to pattern the dorsal telencephalic midline. Neuron 35:1029-1041.

Hevner RF, Neogi T, Englund C, Daza RA, Fink A (2003) Cajal-Retzius cells in the mouse: transcription factors, neurotransmitters, and birthdays suggest a pallial origin. Brain Res Dev Brain Res 141:39-53.

Hevner RF, Shi L, Justice N, Hsueh Y, Sheng M, Smiga S, Bulfone A, Goffinet AM, Campagnoni AT, Rubenstein JL (2001) Tbr1 regulates differentiation of the preplate and layer 6. Neuron 29:353-366.

Hooper JE, Scott MP (2005) Communicating with Hedgehogs. Nat Rev Mol Cell Biol 6:306-317.

Horton S, Meredith A, Richardson JA, Johnson JE (1999) Correct coordination of neuronal differentiation events in ventral forebrain requires the bHLH factor MASH1. Mol Cell Neurosci 14:355-369.

Houart C, Westerfield M, Wilson SW (1998) A small population of anterior cells patterns the forebrain during zebrafish gastrulation. Nature 391:788-792.

Houart C, Caneparo L, Heisenberg C, Barth K, Take-Uchi M, Wilson S (2002) Establishment of the telencephalon during gastrulation by local antagonism of Wnt signaling. Neuron 35:255-265.

Hsieh-Li HM, Witte DP, Szucsik JC, Weinstein M, Li H, Potter SS (1995) Gsh-2, a murine homeobox gene expressed in the developing brain. Mech Dev 50:177-186.

Huh S, Hatini V, Marcus RC, Li SC, Lai E (1999) Dorsal-ventral patterning defects in the eye of BF-1-deficient mice associated with a restricted loss of shh expression. Dev Biol 211:53-63.

Hui CC, Joyner AL (1993) A mouse model of greig cephalopolysyndactyly syndrome: the extra-toesJ mutation contains an intragenic deletion of the Gli3 gene. Nat Genet 3:241-246.

Hui CC, Slusarski D, Platt KA, Holmgren R, Joyner AL (1994) Expression of three mouse homologs of the Drosophila segment polarity gene cubitus interruptus, Gli, Gli-2, and Gli-3, in ectoderm- and mesoderm-derived tissues suggests multiple roles during postimplantation development. Dev Biol 162:402-413.

Ingham PW, McMahon AP (2001) Hedgehog signaling in animal development: paradigms and principles. Genes Dev 15:3059-3087.

Ishibashi M, McMahon AP (2002) A sonic hedgehog-dependent signaling relay regulates growth of diencephalic and mesencephalic primordia in the early mouse embryo. Development 129:4807-4819.

Ishibashi M, Saitsu H, Komada M, Shiota K (2005) Signaling cascade coordinating growth of dorsal and ventral tissues of the vertebrate brain, with special reference to the involvement of Sonic Hedgehog signaling. Anat Sci Int 80:30-36.

Jacob J, Briscoe J (2003) Gli proteins and the control of spinal-cord patterning. EMBO Rep 4:761-765.

Jimenez D, Rivera R, Lopez-Mascaraque L, De Carlos JA (2003) Origin of the cortical layer I in rodents. Dev Neurosci 25:105-115.

Johnson DR (1967) Extra-toes: anew mutant gene causing multiple abnormalities in the mouse. J Embryol Exp Morphol 17:543-581.

Kang S, Graham JM, Jr., Olney AH, Biesecker LG (1997) GLI3 frameshift mutations cause autosomal dominant Pallister-Hall syndrome. Nat Genet 15:266-268.

Kenney AM, Rowitch DH (2000) Sonic hedgehog promotes G(1) cyclin expression and sustained cell cycle progression in mammalian neuronal precursors. Mol Cell Biol 20:9055-9067.

Kerr JF, Wyllie AH, Currie AR (1972) Apoptosis: a basic biological phenomenon with wide-ranging implications in tissue kinetics. Br J Cancer 26:239-257.

Kiecker C, Lumsden A (2004) Hedgehog signaling from the ZLI regulates diencephalic regional identity. Nat Neurosci 7:1242-1249.

Kim AS, Anderson SA, Rubenstein JL, Lowenstein DH, Pleasure SJ (2001) Pax-6 regulates expression of SFRP-2 and Wnt-7b in the developing CNS. J Neurosci 21:RC132.

Klezovitch O, Fernandez TE, Tapscott SJ, Vasioukhin V (2004) Loss of cell polarity causes severe brain dysplasia in Lgl1 knockout mice. Genes Dev 18:559-571.

Knoetgen H, Teichmann U, Kessel M (1999) Head-organizing activities of endodermal tissues in vertebrates. Cell Mol Biol (Noisy-le-grand) 45:481-492.

Kohtz JD, Baker DP, Corte G, Fishell G (1998) Regionalization within the mammalian telencephalon is mediated by changes in responsiveness to Sonic Hedgehog. Development 125:5079-5089.

Kohtz JD, Lee HY, Gaiano N, Segal J, Ng E, Larson T, Baker DP, Garber EA, Williams KP, Fishell G (2001) N-terminal fatty-acylation of sonic hedgehog enhances the induction of rodent ventral forebrain neurons. Development 128:2351-2363.

Koos DS, Ho RK (1999) The nieuwkoid/dharma homeobox gene is essential for bmp2b repression in the zebrafish pregastrula. Dev Biol 215:190-207.

Krauss S, Concordet JP, Ingham PW (1993) A functionally conserved homolog of the Drosophila segment polarity gene hh is expressed in tissues with polarizing activity in zebrafish embryos. Cell 75:1431-1444.

Kuschel S, Ruther U, Theil T (2003) A disrupted balance between Bmp/Wnt and Fgf signaling underlies the ventralization of the Gli3 mutant telencephalon. Dev Biol 260:484-495.

Ladher RK, Church VL, Allen S, Robson L, Abdelfattah A, Brown NA, Hattersley G, Rosen V, Luyten FP, Dale L, Francis-West PH (2000) Cloning and expression of the Wnt antagonists Sfrp-2 and Frzb during chick development. Dev Biol 218:183-198.

Lako M, Lindsay S, Bullen P, Wilson DI, Robson SC, Strachan T (1998) A novel mammalian wnt gene, WNT8B, shows brain-restricted expression in early development, with sharply delimited expression boundaries in the developing forebrain. Hum Mol Genet 7:813-822.

LaMantia AS (1999) Forebrain induction, retinoic acid, and vulnerability to schizophrenia: insights from molecular and genetic analysis in developing mice. Biol Psychiatry 46:19-30.

Lee KJ, Jessell TM (1999) The specification of dorsal cell fates in the vertebrate central nervous system. Annu Rev Neurosci 22:261-294.

Lee MK, Tuttle JB, Rebhun LI, Cleveland DW, Frankfurter A (1990) The expression and

posttranslational modification of a neuron-specific beta-tubulin isotype during chick embryogenesis. Cell Motil Cytoskeleton 17:118-132.

Lee SM, Danielian PS, Fritzsch B, McMahon AP (1997) Evidence that FGF8 signalling from the midbrain-hindbrain junction regulates growth and polarity in the developing midbrain. Development 124:959-969.

Lee SM, Tole S, Grove E, McMahon AP (2000) A local Wnt-3a signal is required for development of the mammalian hippocampus. Development 127:457-467.

Lei Q, Zelman AK, Kuang E, Li S, Matise MP (2004) Transduction of graded Hedgehog signaling by a combination of Gli2 and Gli3 activator functions in the developing spinal cord. Development 131:3593-3604.

Lekven AC, Thorpe CJ, Waxman JS, Moon RT (2001) Zebrafish wnt8 encodes two wnt8 proteins on a bicistronic transcript and is required for mesoderm and neurectoderm patterning. Dev Cell 1:103-114.

Lewis PM, Dunn MP, McMahon JA, Logan M, Martin JF, St-Jacques B, McMahon AP (2001) Cholesterol modification of sonic hedgehog is required for long-range signaling activity and effective modulation of signaling by Ptc1. Cell 105:599-612.

Li HS, Wang D, Shen Q, Schonemann MD, Gorski JA, Jones KR, Temple S, Jan LY, Jan YN (2003) Inactivation of Numb and Numblike in embryonic dorsal forebrain impairs neurogenesis and disrupts cortical morphogenesis. Neuron 40:1105-1118.

Ligon KL, Echelard Y, Assimacopoulos S, Danielian PS, Kaing S, Grove EA, McMahon AP, Rowitch DH (2003) Loss of Emx2 function leads to ectopic expression of Wnt1 in the developing telencephalon and cortical dysplasia. Development 130:2275-2287.

Litingtung Y, Chiang C (2000) Specification of ventral neuron types is mediated by an antagonistic interaction between Shh and Gli3. Nat Neurosci 3:979-985.

Litingtung Y, Dahn RD, Li Y, Fallon JF, Chiang C (2002) Shh and Gli3 are dispensable for limb skeleton formation but regulate digit number and identity. Nature 418:979-983.

Liu A, Joyner AL (2001) EN and GBX2 play essential roles downstream of FGF8 in patterning the mouse mid/hindbrain region. Development 128:181-191.

Liu A, Losos K, Joyner AL (1999) FGF8 can activate Gbx2 and transform regions of the rostral mouse brain into a hindbrain fate. Development 126:4827-4838.

Lo LC, Johnson JE, Wuenschell CW, Saito T, Anderson DJ (1991) Mammalian achaete-scute homolog 1 is transiently expressed by spatially restricted subsets of early neuroepithelial and neural crest cells. Genes Dev 5:1524-1537.

Lu QR, Yuk D, Alberta JA, Zhu Z, Pawlitzky I, Chan J, McMahon AP, Stiles CD, Rowitch DH (2000) Sonic hedgehog--regulated oligodendrocyte lineage genes encoding bHLH proteins in the mammalian central nervous system. Neuron 25:317-329.

Ma Q, Sommer L, Cserjesi P, Anderson DJ (1997) Mash1 and neurogenin1 expression patterns define complementary domains of neuroepithelium in the developing CNS and are correlated with regions expressing notch ligands. J Neurosci 17:3644-3652.

MacArthur CA, Lawshe A, Shankar DB, Heikinheimo M, Shackleford GM (1995a) FGF-8 isoforms differ in NIH3T3 cell transforming potential. Cell Growth Differ 6:817-825.

MacArthur CA, Lawshe A, Xu J, Santos-Ocampo S, Heikinheimo M, Chellaiah AT, Ornitz DM (1995b) FGF-8 isoforms activate receptor splice forms that are expressed in mesenchymal

regions of mouse development. Development 121:3603-3613.

Machold R, Hayashi S, Rutlin M, Muzumdar MD, Nery S, Corbin JG, Gritli-Linde A, Dellovade T, Porter JA, Rubin LL, Dudek H, McMahon AP, Fishell G (2003) Sonic hedgehog is required for progenitor cell maintenance in telencephalic stem cell niches. Neuron 39:937-950.

Maden M, Gale E, Zile M (1998) The role of vitamin A in the development of the central nervous system. J Nutr 128:471S-475S.

Marigo V, Johnson RL, Vortkamp A, Tabin CJ (1996) Sonic hedgehog differentially regulates expression of GLI and GLI3 during limb development. Dev Biol 180:273-283.

Marin O, Anderson SA, Rubenstein JL (2000) Origin and molecular specification of striatal interneurons. J Neurosci 20:6063-6076.

Marklund M, Sjodal M, Beehler BC, Jessell TM, Edlund T, Gunhaga L (2004) Retinoic acid signalling specifies intermediate character in the developing telencephalon. Development 131:4323-4332.

Marti E, Bumcrot DA, Takada R, McMahon AP (1995a) Requirement of 19K form of Sonic hedgehog for induction of distinct ventral cell types in CNS explants. Nature 375:322-325.

Marti E, Takada R, Bumcrot DA, Sasaki H, McMahon AP (1995b) Distribution of Sonic hedgehog peptides in the developing chick and mouse embryo. Development 121:2537-2547.

Martinez S, Crossley PH, Cobos I, Rubenstein JL, Martin GR (1999) FGF8 induces formation of an ectopic isthmic organizer and isthmocerebellar development via a repressive effect on Otx2 expression. Development 126:1189-1200.

Martynoga B, Morrison H, Price DJ, Mason JO (2005) Foxg1 is required for specification of ventral telencephalon and region-specific regulation of dorsal telencephalic precursor proliferation and apoptosis. Dev Biol 283:113-127.

Maruoka Y, Ohbayashi N, Hoshikawa M, Itoh N, Hogan BL, Furuta Y (1998) Comparison of the expression of three highly related genes, Fgf8, Fgf17 and Fgf18, in the mouse embryo. Mech Dev 74:175-177.

Mastick GS, Davis NM, Andrew GL, Easter SS, Jr. (1997) Pax-6 functions in boundary formation and axon guidance in the embryonic mouse forebrain. Development 124:1985-1997.

Masuya H, Sagai T, Moriwaki K, Shiroishi T (1997) Multigenic control of the localization of the zone of polarizing activity in limb morphogenesis in the mouse. Dev Biol 182:42-51.

Masuya H, Sagai T, Wakana S, Moriwaki K, Shiroishi T (1995) A duplicated zone of polarizing activity in polydactylous mouse mutants. Genes Dev 9:1645-1653.

Matise MP, Epstein DJ, Park HL, Platt KA, Joyner AL (1998) Gli2 is required for induction of floor plate and adjacent cells, but not most ventral neurons in the mouse central nervous system. Development 125:2759-2770.

Maynard TM, Jain MD, Balmer CW, LaMantia AS (2002) High-resolution mapping of the Gli3 mutation extra-toes reveals a 51.5-kb deletion. Mamm Genome 13:58-61.

Menezes JR, Luskin MB (1994) Expression of neuron-specific tubulin defines a novel population in the proliferative layers of the developing telencephalon. J Neurosci 14:5399-5416.

Methot N, Basler K (1999) Hedgehog controls limb development by regulating the activities of distinct transcriptional activator and repressor forms of Cubitus interruptus. Cell 96:819-831.

Meyer G, Perez-Garcia CG, Abraham H, Caput D (2002) Expression of p73 and Reelin in the developing human cortex. J Neurosci 22:4973-4986.

Meyer NP, Roelink H (2003) The amino-terminal region of Gli3 antagonizes the Shh response and acts in dorsoventral fate specification in the developing spinal cord. Dev Biol 257:343-355.

Meyers EN, Lewandoski M, Martin GR (1998) An Fgf8 mutant allelic series generated by Cre- and Flp-mediated recombination. Nat Genet 18:136-141.

Miller RH (1996) Oligodendrocyte origins. Trends Neurosci 19:92-96.

Miller RH, Hayes JE, Dyer KL, Sussman CR (1999) Mechanisms of oligodendrocyte commitment in the vertebrate CNS. Int J Dev Neurosci 17:753-763.

Mo R, Freer AM, Zinyk DL, Crackower MA, Michaud J, Heng HH, Chik KW, Shi XM, Tsui LC, Cheng SH, Joyner AL, Hui C (1997) Specific and redundant functions of Gli2 and Gli3 zinc finger genes in skeletal patterning and development. Development 124:113-123.

Mohler J (1988) Requirements for hedgehod, a segmental polarity gene, in patterning larval and adult cuticle of Drosophila. Genetics 120:1061-1072.

Monuki ES, Walsh CA (2001) Mechanisms of cerebral cortical patterning in mice and humans. Nat Neurosci 4 Suppl:1199-1206.

Monuki ES, Porter FD, Walsh CA (2001) Patterning of the dorsal telencephalon and cerebral cortex by a roof plate-Lhx2 pathway. Neuron 32:591-604.

Moore-Scott BA, Gordon J, Blackburn CC, Condie BG, Manley NR (2003) New serum-free in vitro culture technique for midgestation mouse embryos. Genesis 35:164-168.

Motoyama J, Milenkovic L, Iwama M, Shikata Y, Scott MP, Hui CC (2003) Differential requirement for Gli2 and Gli3 in ventral neural cell fate specification. Dev Biol 259:150-161.

Mukhopadhyay M, Shtrom S, Rodriguez-Esteban C, Chen L, Tsukui T, Gomer L, Dorward DW, Glinka A, Grinberg A, Huang SP, Niehrs C, Belmonte JC, Westphal H (2001) Dickkopf1 is required for embryonic head induction and limb morphogenesis in the mouse. Dev Cell 1:423-434.

Murone M, Rosenthal A, de Sauvage FJ (1999) Sonic hedgehog signaling by the patched-smoothened receptor complex. Curr Biol 9:76-84.

Nery S, Wichterle H, Fishell G (2001) Sonic hedgehog contributes to oligodendrocyte specification in the mammalian forebrain. Development 128:527-540.

Niehrs C (1999) Head in the WNT: the molecular nature of Spemann's head organizer. Trends Genet 15:314-319.

Nieto MA, Patel K, Wilkinson DG (1996) In situ hybridization analysis of chick embryos in whole mount and tissue sections. Methods Cell Biol 51:219-235.

Nornes HO, Dressler GR, Knapik EW, Deutsch U, Gruss P (1990) Spatially and temporally restricted expression of Pax2 during murine neurogenesis. Development 109:797-809.

Novitch BG, Wichterle H, Jessell TM, Sockanathan S (2003) A requirement for retinoic acid-mediated transcriptional activation in ventral neural patterning and motor neuron specification. Neuron 40:81-95.

Nusslein-Volhard C, Wieschaus E (1980) Mutations affecting segment number and polarity in Drosophila. Nature 287:795-801.

O'Leary DD, Nakagawa Y (2002) Patterning centers, regulatory genes and extrinsic mechanisms controlling arealization of the neocortex. Curr Opin Neurobiol 12:14-25.

Ohkubo Y, Chiang C, Rubenstein JL (2002) Coordinate regulation and synergistic actions of BMP4, SHH and FGF8 in the rostral prosencephalon regulate morphogenesis of the telencephalic

and optic vesicles. Neuroscience 111:1-17.

Olivier C, Cobos I, Perez Villegas EM, Spassky N, Zalc B, Martinez S, Thomas JL (2001) Monofocal origin of telencephalic oligodendrocytes in the anterior entopeduncular area of the chick embryo. Development 128:1757-1769.

Olsen SK, Li JY, Bromleigh C, Eliseenkova AV, Ibrahimi OA, Lao Z, Zhang F, Linhardt RJ, Joyner AL, Mohammadi M (2006) Structural basis by which alternative splicing modulates the organizer activity of FGF8 in the brain. Genes Dev 20:185-198.

Oppenheim RW (1991) Cell death during development of the nervous system. Annu Rev Neurosci 14:453-501.

Orentas DM, Hayes JE, Dyer KL, Miller RH (1999) Sonic hedgehog signaling is required during the appearance of spinal cord oligodendrocyte precursors. Development 126:2419-2429.

Panchision DM, Pickel JM, Studer L, Lee SH, Turner PA, Hazel TG, McKay RD (2001) Sequential actions of BMP receptors control neural precursor cell production and fate. Genes Dev 15:2094-2110.

Parr BA, Shea MJ, Vassileva G, McMahon AP (1993) Mouse Wnt genes exhibit discrete domains of expression in the early embryonic CNS and limb buds. Development 119:247-261.

Parras CM, Hunt C, Sugimori M, Nakafuku M, Rowitch D, Guillemot F (2007) The proneural gene Mash1 specifies an early population of telencephalic oligodendrocytes. J Neurosci 27:4233-4242.

Patapoutian A, Reichardt LF (2000) Roles of Wnt proteins in neural development and maintenance. Curr Opin Neurobiol 10:392-399.

Persson M, Stamataki D, te Welscher P, Andersson E, Bose J, Ruther U, Ericson J, Briscoe J (2002) Dorsal-ventral patterning of the spinal cord requires Gli3 transcriptional repressor activity. Genes Dev 16:2865-2878.

Piccolo S, Agius E, Leyns L, Bhattacharyya S, Grunz H, Bouwmeester T, De Robertis EM (1999) The head inducer Cerberus is a multifunctional antagonist of Nodal, BMP and Wnt signals. Nature 397:707-710.

Pierani A, Brenner-Morton S, Chiang C, Jessell TM (1999) A sonic hedgehog-independent, retinoid-activated pathway of neurogenesis in the ventral spinal cord. Cell 97:903-915.

Poncet C, Soula C, Trousse F, Kan P, Hirsinger E, Pourquie O, Duprat AM, Cochard P (1996) Induction of oligodendrocyte progenitors in the trunk neural tube by ventralizing signals: effects of notochord and floor plate grafts, and of sonic hedgehog. Mech Dev 60:13-32.

Porter JA, von Kessler DP, Ekker SC, Young KE, Lee JJ, Moses K, Beachy PA (1995) The product of hedgehog autoproteolytic cleavage active in local and long-range signalling. Nature 374:363-366.

Porteus MH, Bulfone A, Liu JK, Puelles L, Lo LC, Rubenstein JL (1994) DLX-2, MASH-1, and MAP-2 expression and bromodeoxyuridine incorporation define molecularly distinct cell populations in the embryonic mouse forebrain. J Neurosci 14:6370-6383.

Pringle NP, Yu WP, Guthrie S, Roelink H, Lumsden A, Peterson AC, Richardson WD (1996) Determination of neuroepithelial cell fate: induction of the oligodendrocyte lineage by ventral midline cells and sonic hedgehog. Dev Biol 177:30-42.

Puelles L, Rubenstein JL (2003) Forebrain gene expression domains and the evolving prosomeric model. Trends Neurosci 26:469-476.

Puelles L, Kuwana E, Puelles E, Rubenstein JL (1999) Comparison of the mammalian and avian telencephalon from the perspective of gene expression data. Eur J Morphol 37:139-150.

Puelles L, Kuwana E, Puelles E, Bulfone A, Shimamura K, Keleher J, Smiga S, Rubenstein JL (2000) Pallial and subpallial derivatives in the embryonic chick and mouse telencephalon, traced by the expression of the genes Dlx-2, Emx-1, Nkx-2.1, Pax-6, and Tbr-1. J Comp Neurol 424:409-438.

Puschel AW, Westerfield M, Dressler GR (1992) Comparative analysis of Pax-2 protein distributions during neurulation in mice and zebrafish. Mech Dev 38:197-208.

Radhakrishna U, Wild A, Grzeschik KH, Antonarakis SE (1997) Mutation in GLI3 in postaxial polydactyly type A. Nat Genet 17:269-271.

Ragsdale CW, Grove EA (2001) Patterning the mammalian cerebral cortex. Curr Opin Neurobiol 11:50-58.

Rallu M, Corbin JG, Fishell G (2002a) Parsing the prosencephalon. Nat Rev Neurosci 3:943-951.

Rallu M, Machold R, Gaiano N, Corbin JG, McMahon AP, Fishell G (2002b) Dorsoventral patterning is established in the telencephalon of mutants lacking both Gli3 and Hedgehog signaling. Development 129:4963-4974.

Rattner A, Hsieh JC, Smallwood PM, Gilbert DJ, Copeland NG, Jenkins NA, Nathans J (1997) A family of secreted proteins contains homology to the cysteine-rich ligand-binding domain of frizzled receptors. Proc Natl Acad Sci U S A 94:2859-2863.

Richardson M, Redmond D, Watson CJ, Mason JO (1999) Mouse Wnt8B is expressed in the developing forebrain and maps to chromosome 19. Mamm Genome 10:923-925.

Richardson WD, Smith HK, Sun T, Pringle NP, Hall A, Woodruff R (2000) Oligodendrocyte lineage and the motor neuron connection. Glia 29:136-142.

Riddle RD, Johnson RL, Laufer E, Tabin C (1993) Sonic hedgehog mediates the polarizing activity of the ZPA. Cell 75:1401-1416.

Roelink H, Porter JA, Chiang C, Tanabe Y, Chang DT, Beachy PA, Jessell TM (1995) Floor plate and motor neuron induction by different concentrations of the amino-terminal cleavage product of sonic hedgehog autoproteolysis. Cell 81:445-455.

Roelink H, Augsburger A, Heemskerk J, Korzh V, Norlin S, Ruiz i Altaba A, Tanabe Y, Placzek M, Edlund T, Jessell TM, et al. (1994) Floor plate and motor neuron induction by vhh-1, a vertebrate homolog of hedgehog expressed by the notochord. Cell 76:761-775.

Roessler E, Belloni E, Gaudenz K, Vargas F, Scherer SW, Tsui LC, Muenke M (1997) Mutations in the C-terminal domain of Sonic Hedgehog cause holoprosencephaly. Hum Mol Genet 6:1847-1853.

Roessler E, Belloni E, Gaudenz K, Jay P, Berta P, Scherer SW, Tsui LC, Muenke M (1996) Mutations in the human Sonic Hedgehog gene cause holoprosencephaly. Nat Genet 14:357-360.

Rowitch DH, B SJ, Lee SM, Flax JD, Snyder EY, McMahon AP (1999) Sonic hedgehog regulates proliferation and inhibits differentiation of CNS precursor cells. J Neurosci 19:8954-8965.

Rubenstein JL, Beachy PA (1998) Patterning of the embryonic forebrain. Curr Opin Neurobiol 8:18-26.

Rubenstein JL, Shimamura K, Martinez S, Puelles L (1998) Regionalization of the prosencephalic neural plate. Annu Rev Neurosci 21:445-477.

Rubenstein JL, Anderson S, Shi L, Miyashita-Lin E, Bulfone A, Hevner R (1999) Genetic control of

cortical regionalization and connectivity. Cereb Cortex 9:524-532.

Ruiz i Altaba A (1998) Combinatorial Gli gene function in floor plate and neuronal inductions by Sonic hedgehog. Development 125:2203-2212.

Ruiz i Altaba A (1999) Gli proteins encode context-dependent positive and negative functions: implications for development and disease. Development 126:3205-3216.

Ruiz i Altaba A, Palma V, Dahmane N (2002a) Hedgehog-Gli signalling and the growth of the brain. Nat Rev Neurosci 3:24-33.

Ruiz i Altaba A, Sanchez P, Dahmane N (2002b) Gli and hedgehog in cancer: tumours, embryos and stem cells. Nat Rev Cancer 2:361-372.

Ruiz i Altaba A, Nguyen V, Palma V (2003) The emergent design of the neural tube: prepattern, SHH morphogen and GLI code. Curr Opin Genet Dev 13:513-521.

Ruppert JM, Vogelstein B, Arheden K, Kinzler KW (1990) GLI3 encodes a 190-kilodalton protein with multiple regions of GLI similarity. Mol Cell Biol 10:5408-5415.

Sasai Y, De Robertis EM (1997) Ectodermal patterning in vertebrate embryos. Dev Biol 182:5-20.

Sasaki H, Nishizaki Y, Hui C, Nakafuku M, Kondoh H (1999) Regulation of Gli2 and Gli3 activities by an amino-terminal repression domain: implication of Gli2 and Gli3 as primary mediators of Shh signaling. Development 126:3915-3924.

Sato T, Nakamura H (2004) The Fgf8 signal causes cerebellar differentiation by activating the Ras-ERK signaling pathway. Development 131:4275-4285.

Sato T, Araki I, Nakamura H (2001) Inductive signal and tissue responsiveness defining the tectum and the cerebellum. Development 128:2461-2469.

Schimmang T, Lemaistre M, Vortkamp A, Ruther U (1992) Expression of the zinc finger gene Gli3 is affected in the morphogenetic mouse mutant extra-toes (Xt). Development 116:799-804.

Schneider RA, Hu D, Rubenstein JL, Maden M, Helms JA (2001) Local retinoid signaling coordinates forebrain and facial morphogenesis by maintaining FGF8 and SHH. Development 128:2755-2767.

Schuurmans C, Guillemot F (2002) Molecular mechanisms underlying cell fate specification in the developing telencephalon. Curr Opin Neurobiol 12:26-34.

Shanmugalingam S, Houart C, Picker A, Reifers F, Macdonald R, Barth A, Griffin K, Brand M, Wilson SW (2000) Ace/Fgf8 is required for forebrain commissure formation and patterning of the telencephalon. Development 127:2549-2561.

Sharpe J, Ahlgren U, Perry P, Hill B, Ross A, Hecksher-Sorensen J, Baldock R, Davidson D (2002) Optical projection tomography as a tool for 3D microscopy and gene expression studies. Science 296:541-545.

Sheng HZ, Bertuzzi S, Chiang C, Shawlot W, Taira M, Dawid I, Westphal H (1997) Expression of murine Lhx5 suggests a role in specifying the forebrain. Dev Dyn 208:266-277.

Sherr CJ, Roberts JM (1999) CDK inhibitors: positive and negative regulators of G1-phase progression. Genes Dev 13:1501-1512.

Sheth AN, Bhide PG (1997) Concurrent cellular output from two proliferative populations in the early embryonic mouse corpus striatum. J Comp Neurol 383:220-230.

Shibui S, Hoshino T, Vanderlaan M, Gray JW (1989) Double labeling with iodo- and bromodeoxyuridine for cell kinetics studies. J Histochem Cytochem 37:1007-1011.

Shimamura K, Rubenstein JL (1997) Inductive interactions direct early regionalization of the mouse

forebrain. Development 124:2709-2718.

Shimamura K, Martinez S, Puelles L, Rubenstein JL (1997) Patterns of gene expression in the neural plate and neural tube subdivide the embryonic forebrain into transverse and longitudinal domains. Dev Neurosci 19:88-96.

Shimamura K, Hartigan DJ, Martinez S, Puelles L, Rubenstein JL (1995) Longitudinal organization of the anterior neural plate and neural tube. Development 121:3923-3933.

Shimogori T, Banuchi V, Ng HY, Strauss JB, Grove EA (2004) Embryonic signaling centers expressing BMP, WNT and FGF proteins interact to pattern the cerebral cortex. Development 131:5639-5647.

Shin SH, Kogerman P, Lindstrom E, Toftgard R, Biesecker LG (1999) GLI3 mutations in human disorders mimic Drosophila cubitus interruptus protein functions and localization. Proc Natl Acad Sci U S A 96:2880-2884.

Shinya M, Koshida S, Sawada A, Kuroiwa A, Takeda H (2001) Fgf signalling through MAPK cascade is required for development of the subpallial telencephalon in zebrafish embryos. Development 128:4153-4164.

Simeone A, Gulisano M, Acampora D, Stornaiuolo A, Rambaldi M, Boncinelli E (1992) Two vertebrate homeobox genes related to the Drosophila empty spiracles gene are expressed in the embryonic cerebral cortex. Embo J 11:2541-2550.

Smith D, Wagner E, Koul O, McCaffery P, Drager UC (2001) Retinoic acid synthesis for the developing telencephalon. Cereb Cortex 11:894-905.

Smith SM, Cartwright MM (1997) Spatial visualization of apoptosis using a whole-mount in situ DNA end-labeling technique. Biotechniques 22:832-834.

Sommer L, Ma Q, Anderson DJ (1996) neurogenins, a novel family of atonal-related bHLH transcription factors, are putative mammalian neuronal determination genes that reveal progenitor cell heterogeneity in the developing CNS and PNS. Mol Cell Neurosci 8:221-241.

Spassky N, Olivier C, Perez-Villegas E, Goujet-Zalc C, Martinez S, Thomas J, Zalc B (2000) Single or multiple oligodendroglial lineages: a controversy. Glia 29:143-148.

Stamataki D, Ulloa F, Tsoni SV, Mynett A, Briscoe J (2005) A gradient of Gli activity mediates graded Sonic Hedgehog signaling in the neural tube. Genes Dev 19:626-641.

Stenman J, Yu RT, Evans RM, Campbell K (2003) Tlx and Pax6 co-operate genetically to establish the pallio-subpallial boundary in the embryonic mouse telencephalon. Development 130:1113-1122.

Storm EE, Rubenstein JL, Martin GR (2003) Dosage of Fgf8 determines whether cell survival is positively or negatively regulated in the developing forebrain. Proc Natl Acad Sci U S A 100:1757-1762.

Storm EE, Garel S, Borello U, Hebert JM, Martinez S, McConnell SK, Martin GR, Rubenstein JL (2006) Dose-dependent functions of Fgf8 in regulating telencephalic patterning centers. Development 133:1831-1844.

Stoykova A, Gruss P (1994) Roles of Pax-genes in developing and adult brain as suggested by expression patterns. J Neurosci 14:1395-1412.

Stoykova A, Fritsch R, Walther C, Gruss P (1996) Forebrain patterning defects in Small eye mutant mice. Development 122:3453-3465.

Stoykova A, Treichel D, Hallonet M, Gruss P (2000) Pax6 modulates the dorsoventral patterning of

the mammalian telencephalon. J Neurosci 20:8042-8050.

Sun X, Meyers EN, Lewandoski M, Martin GR (1999) Targeted disruption of Fgf8 causes failure of cell migration in the gastrulating mouse embryo. Genes Dev 13:1834-1846.

Super H, Soriano E, Uylings HB (1998) The functions of the preplate in development and evolution of the neocortex and hippocampus. Brain Res Brain Res Rev 27:40-64.

Sussel L, Marin O, Kimura S, Rubenstein JL (1999) Loss of Nkx2.1 homeobox gene function results in a ventral to dorsal molecular respecification within the basal telencephalon: evidence for a transformation of the pallidum into the striatum. Development 126:3359-3370.

Szucsik JC, Witte DP, Li H, Pixley SK, Small KM, Potter SS (1997) Altered forebrain and hindbrain development in mice mutant for the Gsh-2 homeobox gene. Dev Biol 191:230-242.

Tabata T, Eaton S, Kornberg TB (1992) The Drosophila hedgehog gene is expressed specifically in posterior compartment cells and is a target of engrailed regulation. Genes Dev 6:2635-2645.

Takahashi T, Nowakowski RS, Caviness VS, Jr. (1995a) Early ontogeny of the secondary proliferative population of the embryonic murine cerebral wall. J Neurosci 15:6058-6068.

Takahashi T, Nowakowski RS, Caviness VS, Jr. (1995b) The cell cycle of the pseudostratified ventricular epithelium of the embryonic murine cerebral wall. J Neurosci 15:6046-6057.

Takebayashi H, Ohtsuki T, Uchida T, Kawamoto S, Okubo K, Ikenaka K, Takeichi M, Chisaka O, Nabeshima Y (2002) Non-overlapping expression of Olig3 and Olig2 in the embryonic neural tube. Mech Dev 113:169-174.

Takiguchi-Hayashi K, Sekiguchi M, Ashigaki S, Takamatsu M, Hasegawa H, Suzuki-Migishima R, Yokoyama M, Nakanishi S, Tanabe Y (2004) Generation of reelin-positive marginal zone cells from the caudomedial wall of telencephalic vesicles. J Neurosci 24:2286-2295.

Tao W, Lai E (1992) Telencephalon-restricted expression of BF-1, a new member of the HNF-3/fork head gene family, in the developing rat brain. Neuron 8:957-966.

Tekki-Kessaris N, Woodruff R, Hall AC, Gaffield W, Kimura S, Stiles CD, Rowitch DH, Richardson WD (2001) Hedgehog-dependent oligodendrocyte lineage specification in the telencephalon. Development 128:2545-2554.

Theil T (2005) Gli3 is required for the specification and differentiation of preplate neurons. Dev Biol 286:559-571.

Theil T, Alvarez-Bolado G, Walter A, Ruther U (1999) Gli3 is required for Emx gene expression during dorsal telencephalon development. Development 126:3561-3571.

Theil T, Aydin S, Koch S, Grotewold L, Ruther U (2002a) Wnt and Bmp signalling cooperatively regulate graded Emx2 expression in the dorsal telencephalon. Development 129:3045-3054.

Theil T, Ariza-McNaughton L, Manzanares M, Brodie J, Krumlauf R, Wilkinson DG (2002b) Requirement for downregulation of kreisler during late patterning of the hindbrain. Development 129:1477-1485.

Tole S, Christian C, Grove EA (1997) Early specification and autonomous development of cortical fields in the mouse hippocampus. Development 124:4959-4970.

Tole S, Ragsdale CW, Grove EA (2000a) Dorsoventral patterning of the telencephalon is disrupted in the mouse mutant extra-toes(J). Dev Biol 217:254-265.

Tole S, Goudreau G, Assimacopoulos S, Grove EA (2000b) Emx2 is required for growth of the hippocampus but not for hippocampal field specification. J Neurosci 20:2618-2625.

Tomioka N, Osumi N, Sato Y, Inoue T, Nakamura S, Fujisawa H, Hirata T (2000) Neocortical origin

and tangential migration of guidepost neurons in the lateral olfactory tract. J Neurosci 20:5802-5812.

Toresson H, Potter SS, Campbell K (2000) Genetic control of dorsal-ventral identity in the telencephalon: opposing roles for Pax6 and Gsh2. Development 127:4361-4371.

Toresson H, Mata de Urquiza A, Fagerstrom C, Perlmann T, Campbell K (1999) Retinoids are produced by glia in the lateral ganglionic eminence and regulate striatal neuron differentiation. Development 126:1317-1326.

Trousse F, Marti E, Gruss P, Torres M, Bovolenta P (2001) Control of retinal ganglion cell axon growth: a new role for Sonic hedgehog. Development 128:3927-3936.

Truett GE, Heeger P, Mynatt RL, Truett AA, Walker JA, Warman ML (2000) Preparation of PCR-quality mouse genomic DNA with hot sodium hydroxide and tris (HotSHOT). Biotechniques 29:52, 54.

Van Maele-Fabry G, Picard JJ, Attenon P, Berthet P, Delhaise F, Govers MJ, Peters PW, Piersma AH, Schmid BP, Stadler J, et al. (1991) Interlaboratory evaluation of three culture media for postimplantation rodent embryos. Reprod Toxicol 5:417-426.

Varga ZM, Wegner J, Westerfield M (1999) Anterior movement of ventral diencephalic precursors separates the primordial eye field in the neural plate and requires cyclops. Development 126:5533-5546.

Vaux DL, Korsmeyer SJ (1999) Cell death in development. Cell 96:245-254.

Vieira C, Garda AL, Shimamura K, Martinez S (2005) Thalamic development induced by Shh in the chick embryo. Dev Biol 284:351-363.

von Mering C, Basler K (1999) Distinct and regulated activities of human Gli proteins in Drosophila. Curr Biol 9:1319-1322.

Walther C, Gruss P (1991) Pax-6, a murine paired box gene, is expressed in the developing CNS. Development 113:1435-1449.

Wang B, Fallon JF, Beachy PA (2000) Hedgehog-regulated processing of Gli3 produces an anterior/posterior repressor gradient in the developing vertebrate limb. Cell 100:423-434.

Wang C, Ruther U, Wang B (2007) The Shh-independent activator function of the full-length Gli3 protein and its role in vertebrate limb digit patterning. Dev Biol.

Wang HF, Liu FC (2001) Developmental restriction of the LIM homeodomain transcription factor Islet-1 expression to cholinergic neurons in the rat striatum. Neuroscience 103:999-1016.

Warren N, Caric D, Pratt T, Clausen JA, Asavaritikrai P, Mason JO, Hill RE, Price DJ (1999) The transcription factor, Pax6, is required for cell proliferation and differentiation in the developing cerebral cortex. Cereb Cortex 9:627-635.

Whitlock KE, Westerfield M (2000) The olfactory placodes of the zebrafish form by convergence of cellular fields at the edge of the neural plate. Development 127:3645-3653.

Wijgerde M, McMahon JA, Rule M, McMahon AP (2002) A direct requirement for Hedgehog signaling for normal specification of all ventral progenitor domains in the presumptive mammalian spinal cord. Genes Dev 16:2849-2864.

Wilson SI, Edlund T (2001) Neural induction: toward a unifying mechanism. Nat Neurosci 4 Suppl:1161-1168.

Wilson SW, Rubenstein JL (2000) Induction and dorsoventral patterning of the telencephalon. Neuron 28:641-651.

Xu J, Liu Z, Ornitz DM (2000) Temporal and spatial gradients of Fgf8 and Fgf17 regulate proliferation and differentiation of midline cerebellar structures. Development 127:1833-1843.

Xu J, Lawshe A, MacArthur CA, Ornitz DM (1999) Genomic structure, mapping, activity and expression of fibroblast growth factor 17. Mech Dev 83:165-178.

Xuan S, Baptista CA, Balas G, Tao W, Soares VC, Lai E (1995) Winged helix transcription factor BF-1 is essential for the development of the cerebral hemispheres. Neuron 14:1141-1152.

Yamaguchi TP (2001) Heads or tails: Wnts and anterior-posterior patterning. Curr Biol 11:R713-724.

Yamazaki H, Sekiguchi M, Takamatsu M, Tanabe Y, Nakanishi S (2004) Distinct ontogenic and regional expressions of newly identified Cajal-Retzius cell-specific genes during neocorticogenesis. Proc Natl Acad Sci U S A 101:14509-14514.

Yang A, Walker N, Bronson R, Kaghad M, Oosterwegel M, Bonnin J, Vagner C, Bonnet H, Dikkes P, Sharpe A, McKeon F, Caput D (2000) p73-deficient mice have neurological, pheromonal and inflammatory defects but lack spontaneous tumours. Nature 404:99-103.

Ye W, Shimamura K, Rubenstein JL, Hynes MA, Rosenthal A (1998) FGF and Shh signals control dopaminergic and serotonergic cell fate in the anterior neural plate. Cell 93:755-766.

Yun K, Potter S, Rubenstein JL (2001) Gsh2 and Pax6 play complementary roles in dorsoventral patterning of the mammalian telencephalon. Development 128:193-205.

Zaki PA, Quinn JC, Price DJ (2003) Mouse models of telencephalic development. Curr Opin Genet Dev 13:423-437.

Zaki PA, Martynoga B, Delafield-Butt JT, Fotaki V, Yu T, Price DJ (2005) Loss of Gli3 enhances the viability of embryonic telencephalic cells in vitro. Eur J Neurosci 22:1547-1551.

Zeltser LM (2005) Shh-dependent formation of the ZLI is opposed by signals from the dorsal diencephalon. Development 132:2023-2033.

Zhang XM, Ramalho-Santos M, McMahon AP (2001) Smoothened mutants reveal redundant roles for Shh and Ihh signaling including regulation of L/R asymmetry by the mouse node. Cell 105:781-792.

Zhao H, Tian Y, Breedveld G, Huang S, Zou Y, Y J, Chai J, Li H, Li M, Oostra BA, Lo WH, Heutink P (2002) Postaxial polydactyly type A/B (PAP-A/B) is linked to chromosome 19p13.1-13.2 in a Chinese kindred. Eur J Hum Genet 10:162-166.

Zhou Q, Wang S, Anderson DJ (2000) Identification of a novel family of oligodendrocyte lineage-specific basic helix-loop-helix transcription factors. Neuron 25:331-343.